STUDIES IN HIGH SPEED GAS CHROMATOGRAPHY

by

Lilian McLaren, B.Sc.

Thesis for the Degree of Doctor of Philosophy

University of Edinburgh May, 1965.

To My Parents

TABLE OF CONTENTS

Page

SECTION II: THE DETERMINATION OF D_g AND γ

CHAPTER I: THE MEASUREMENT OF DIFFUSION COEFFICIENTS OF GASES AND VAPOURS.

CHAPTER II: THE MEASUREMENT AND INTERPRETATION OF γ.

Page

SECTION III: THE COATING OF CAPILLARY COLUMNS AND THE PROPERTIES OF THE PHOTO-IONISATION DETECTOR

CHAPTER I: THE PREPARATION OF CAPILLARY COLUMNS.

CHAPTER II: AN INVESTIGATION OF A PHOTO-IONISATION DETECTOR.

SECTION IV: THE APPENDIX

ACKNOWLEDGMENTS

The author would like to thank Professor Sir Edmund L. Hirst and Professor T.L. Cottrell for the provision of library, technical and laboratory facilities. Thanks are also due to British Petroleum Ltd. for the provision of a maintenance grant.

The author is indebted to the Electronics Division of Bruce Peebles Ltd. Edinburgh, for the provision of the electronic equipment. It was a great pleasure to be part of such an enthusiastic team and she would like to thank her colleagues for ready assistance on many occasions. Thanks are also extended to Mr. David J.A. Carswell, the Manager, for his kind interest and encouragement.

Above all, it is a great pleasure to thank Dr. John H. Knox for the interest he has shown in this research. His lively comments and fertile brain have provided a valuable stimulus without which this work could not have been achieved.

Finally, appreciation is extended to the many other members of the Department who have helped to make this work a most pleasant experience.

"If we tie the gas chromatograph to other pieces of laboratory equipment we have the possibility of almost the automatic chemist. We can separate a substance on the gas chromatograph, we can take every column that is reasonable in turn, and substances as they run from the column can go directly to various instruments such as NMR, ultra-violet, visible and infra-red spectroscopy, and we can have a mass spectrograph working as well. Here you have the uniting instrument of the gas chromatograph in the centre with its slaves clustered around. The calculating machine in the background will have the records of all previous substances separated on its magnetic drums and it will come out with a sheet typed at the end with the name of the compound and the weight percent in the mixture. We may even get it to the stage where it will work out the structure too."

Martin 1957

INTRODUCTION

The idea of using a gas as carrier fluid in a chromatogram first occurred as a few lines in a general paper on liquid-liquid chromatography (1). This idea gave birth to a technique which has, in the space of a few years, through its simplicity, sensitivity and speed of analysis, established itself as the most efficient method for the analysis of all gases, nearly all organic liquids and many solids.

(i) Definitions

Like distillation, chromatography is a process of repeated equilibrations in which a solute is partitioned repeatedly between a mobile and a fixed phase. The different migration velocities of components through the column arise from selective retention. Following the recommendation of the Hydrocarbon Research Group of the Institute of Petroleum (2) the term gas chromatography (GC) is used for those chromatographic techniques in which an inert gas phase carries the substances to be separated through a stationary phase which has a high surface to volume ratio and which is packed into a suitable container. The technique is called gas-solid chromatography (GSC) when the stationary phase is a solid adsorbent and gas-liquid chromatography (GLC) when the stationary phase is an absorbent liquid supported by inert material.

(ii) Historical Outline

The formal development of chromatography dates from approximately 1900 when Tswett (3) separated organic compounds of botanical interest. His major contribution was the use of a solvent often different from the original solvent of the organic material, and the realisation that the separation was due only to selective adsorption. Others like Kvitka (4) and Day (5) fractionated petroleum by simple filtration through porous media, but it is not clear whether they appreciated the underlying principles. Tswett's work was not taken up until 25 years later by Kuhn et al.(6) who separated plant pigments by liquid-solid chromatography using an elution technique. Thereafter the method gained widespread recognition.

In 1941 Martin and Synge (1) developed a liquid-liquid system. They replaced the column by a strip of paper and so invented paper chromatography. In their original paper they suggested that it should be possible to achieve separation on

the basis of partition and development in the gaseous state, but at that time the detection of small amounts of foreign vapours in the carrier gas presented a considerable difficulty. The basic method nevertheless is of long standing for Ramsay (7) used it in 1905 to separate mixtures of gases and vapours. The suggestion was finally taken up ten years later, and the technique of elution GLC was demonstrated practically by Martin and James (8) when they described the qualitative and quantitative analysis of mixtures of fatty acids by par-:tition between nitrogen and a silicone oil supported by a diatomaceous earth. In the intervening period Claesson (9,10), Clough (11), Turner (12), Turkel' taub (13) and Phillips (14) had all made contributions to the frontal and dis-:placement methods of GC, pioneered for liquid-solid chromatography by Tiselius (15), but for reasons discussed below the methods never became widely used.

From 1952 onwards interest centred on the elution technique and so began the rapid development of GC. Prominent in the field of GSC were Cremer and Mueller (16), Turkel'taub and Zhukhovitskii (17), Janak (18), Ray (19) and Patton et al.(20), while in the field of GLC important contributions came from James and Martin (21), James and Phillips (22), Ray (19) and Glueckauf (23), Knox and Purnell (24) used GLC as an analytical tool in kinetic studies in 1953 but this work was never published.

(iii)Reasons for the Rapid Development

Figure 1 shows the literature growth in the field as compiled by Ettre (25). The reasons for this phenomenal development are many. Because of the low viscosity and high diffusivity of gases, one can work with very long columns at high flow rates and so obtain efficient high-speed analysis. The apparatus is basically simple requiring only four units, a carrier gas supply, a sample inlet, a column and a detector. It is generally desirable to thermostat the column and record the detector signal on a suitable recorder. The columns may be used many hundreds of times before the stationary phase is stripped off and the analysed material may be recovered and used for further study if required. Results are highly reproducible, to about 1%, and with the introduction of ionisation detectors the sensitivity has reached the parts per billion level.

(iv) Methods of Operating Columns

Differences in the partition coefficients of substances can be utilised for

their separation in three ways, by elution analysis, frontal analysis and displacement development (Figures 2 and 3). In elution analysis the sample introduced as a sharp band at the beginning of a column containing the stationary phase is passed through the column by the inert carrier gas. The sample constituents travel through the column at different rates according to their respective distribution coefficients between the gas and fixed phases and so emerge in the gas stream at different times after the introduction of sample.

In frontal analysis the mixture is carried continuously onto a column of an adsorbent and at constant concentration in the carrier gas. The component which is least strongly adsorbed leaves the column first and each succeeding component leaves the column mixed with the preceding components.

With displacement development the mixture to be separated is adsorbed upon a column of adsorbent, and the constituents are displaced from the adsorbent by a displacer vapour which is carried continuously onto the column at constant concentration in the gas stream. The displacer is chosen so that it is more strongly adsorbed than any of the constituents of the sample to be analysed. Each component emerges from the column substantially pure except for a small overlap fraction between each band. This technique leaves the column saturated with the displacer after an analysis. The column must then be repacked or the displacer desorbed by heating before the column is available for another analysis. Although frontal analysis has been used for the study of the symmetry of peaks (26, 27) and for the measurement of adsorption isotherms (28, 29), elution analysis is the favoured method for analysis. At present GLC is used in most analyses apart from those of mixtures of the permanent gases; for these GSC is often used.

S E C T I O N I

CHROMATOGRAPHIC THEORY

CHAPTER I

PRINCIPLES GOVERNING THE ELUTION OF SUBSTANCES THROUGH CHROMATOGRAPHIC COLUMNS

In the early papers on the subject complex mathematical systems were developed as seen in the papers of Walter (30) and Thomas (31). They gave little or no guidance to practical workers, and since at that time such spectacular results could be obtained with little or no knowledge of the underlying theory, practice tended to be divorced from theory. For more difficult separations, however, some familiarity with the fundamentals at least became essential, and the mathematical rigour has been slowly compromised by the need and desire for simplified theories of practical applicability. Gradually the gap between theory and experiment is being bridged and any further development of GC depends largely upon the application and development of theory.

I. Distinction Between Column Efficiency and the Separation Factor

The aim of any chromatograph is ultimately to obtain the best resolution in the minimum time. Resolution, as seen from Figure 4, is achieved by attention to two factors, disengagement of the centres of gravity of peaks and compactness or narrowness of peaks. The degree of disengagement is related to the thermodynamics of the chromatographic process and the compactness is related to the kinetics of the process. The degree of disengagement of two substances can be measured as the separation factor or relative retention times of the two substances while the peak width is commonly measured in terms of the HETP. Column resolution may be defined as suggested by Martin et al.(32) and Jones and Kieselbach (33), as the separation of the peak maxima divided by the average peak width. Since for the analysis of complex mixtures an increase in resolution can in general be obtained only by increasing peak sharpness, far more effort has been devoted to understanding and elucidating the kinetics rather than the thermodynamics of the process. The present work is concerned with one aspect of the kinetics, namely the kinetics of processes occurring in the mobile phase.

II. Classification of the Theories of Chromatography and their Application to GLC

"If I say theory I do not mean sheaf after sheaf of mathematical discussion... By gas chromatographic theory I mean rather an intimate understanding of the partitioning process, something that we should be able to discuss with words only."

Golay 1960.

Following the approach of Van Deemter et al.(34) and Hardy and Pollard (35) the simpler theories of chromatography may be classified according to (i) the type of distribution isotherm that the solutes obey and (ii) the ideality or non-ideality of the conditions.

(i) In 'linear' chromatography the distribution coefficient (the amount of material in the stationary phase to the amount in the mobile phase) is independent of the concentration of the solute. (The distribution isotherm is linear.) In 'non-linear' chromatography the distribution coefficient is dependent on the concentration of the solute and the isotherm is non-linear.

(ii) In 'ideal' chromatography the flow of the mobile phase is considered uniform, the column is uniformly packed, all conceivable paths in the column are of equal length, equilibrium between the two phases is instantaneous and longitudinal diffusion in either liquid or gas phases does not occur, a contradiction to the preceding condition. In 'non-ideal' chromatography which includes all real chromatography these conditions cannot be met.

The 4 possible types are illustrated in Figure 2 (36).

1. Linear Ideal Chromatography: The shape of the band remains unchanged during the elutions. Mixtures of solutes behave independently, and the requirements for individual bands to be separated depend only on the initial band widths and can be calculated by simple mathematics (37).

2. Non-Linear Ideal Chromatography: This was first treated by Wilson (37) and later by De Vault (38) for a single solute but solutes can affect the behaviour of each other and rigorous treatment is not possible (39).

3. Non-Linear Non-Ideal Chromatography: This has been discussed by

Klinkenberg and Sjenitzer (40). Since GSC is the main type of chromatography concerned and the mathematical treatment becomes very involved it will not be considered further.

4. Linear Non-Ideal Chromatography: Since the assumption of a linear isotherm is a good approximation for the low concentrations of vapour usually encountered in GC, this type is of particular importance for the treatment of LC and GC.

In what follows consideration is restricted to linear non-ideal chromatography which is the simplest form to which real systems approximate reasonably well and which can be approached very closely, particularly in GLC.

III. Summary of Different Approaches to the Theory

Chromatography is a process of differential molecular movement; the displacement steps of any substance down a column resulting from flow, diffusion and sorption-desorption processes. The mutual interaction of the nature and flow rate of the carrier gas; the form, amount and packing density of the solid support; the pressure gradient along the column; the viscosity and flow profile of the carrier gas; the viscosity and film thickness of the liquid phase; the geometry of the liquid phase and the relative times spent in the liquid phase and in the carrier gas is so complex that a vast amount of theoretical and experimental work has been devoted to the quantitative elucidation of the relationships between them. Any adequate physical concept of the process is of necessity an idealization and its acceptability has to be checked experimentally.

The basic approaches to the theory are described in this section. The process has also been considered by analogy with the transmission of electricity along a wire as in the Golay treatment (41). Cremer and Mueller (16) thought of it as analogous to boats drifting down a river while Chmitov and Filatova (42) gave a hydrodynamic model of a sorption column and illustrated the principal cases of chromatogram formation under different kinetic and hydrodynamic conditions. In his treatment Bosanquet (26) considered only single fronts as a means of investi-:gating peak spreading during elution.

IV. The 'Plate' and 'Rate' Theories

The theory can be considered to have been dealt with in two ways. (1) By the 'plate' theory in which a linear isotherm is considered. The column is regarded as a discontinuous medium analogous to a distillation column in which a small finite volume of solute is equilibrated successively with a large number of equal solvent quantities (theoretical plates). The efficiency of the column is measured by the height equivalent to a theoretical plate, HETP, which is the length of the column divided by the number of plates $(\frac{L}{N})$. This concept was introduced into chromatography by Martin and Synge (6) and applied to GC by Martin and James (8). According to the plate theory the peak spread is related to HETP by $H = \frac{\sigma^2}{L}$ where σ^2 is the variance of the gaussian peak. It was re-examined by Mayer and Tompkins (43) who expanded the theory so as to render possible a calculation of the number of theoretical plates needed to obtain a required purity of the separated products.

Whereas the step-by-step equilibration leads to a binomial distribution, a flow model in which mass transfer is a continuous process leads to a distribution of the Poisson type. This approach due to Glueckauf (44) also enables N to be calculated from the S-shaped breakthrough curves characteristic of frontal and displacement analysis. Although for a sufficiently large number of equilibrations both distributions approximate to Gaussian curves, Klinkenberg and Sjenitzer (40) have shown that their widths are different. These authors point out that many mechanisms will account for the gaussian distribution and many experiments are needed before any one mechanism can be accepted. The most useful function of the plate model has been the provision of the parameter H.

The plate theory has been critised by Giddings for several reasons. It cannot accurately predict column performance. Exact theories have shown that the simplest possible sorption-desorption process leads to a distribution much more complex than Poisson though all distributions approach the Gaussian under practical conditions. Most important of all, it sidesteps the kinetic processes that make chromatography what it is. It assumes that the plate effluent is in equilibrium with the stationary phase in that plate. With perhaps the trivial exceptions of the precise centre of the zone, such gas-liquid equilibrium

does not exist anywhere in the column and in fact it is shown later that this non-equilibrium constitutes the most important source of zone spread-:ing.

Knox disagrees with the above criticism of the plate theory. The plate theory never suggested that a real column was made up of a number of plates. The starting point of the theory is a model, made up of a number of plates, which resembles the chromatographic column in giving rise to Gaussian elution peaks, etc. By its very nature it says nothing about how equilibrium is achieved, how fast it is achieved and whether the height EQUIVALENT to a theoretical plate is a constant or a variable in any real column; further-:more the assumption that the effluent is in equilibrium with the stationary phase in the middle of the plate actually defines a degree of non-equilibrium (see Chapter II, (III).

(2) By the 'rate' theory in which a linear non-ideal system is considered, the column is regarded as a continuous medium and the HETP is brought into relation with the actual phenomena occurring in the column which lead to band broadening.

Lapidus and Amundsen (45) deduced a general equation for the band broaden-:ing which resulted both from a finite rate of mass transfer and from longitud-:inal diffusion. Tunitskii (46) introduced the further possibility of eddy diffusion and diffusion within a solid particle, but it was Glueckauf and his associates (47-49) who first showed how such factors as particle size, particle diffusion, and diffusion in the film around the particle could be related to the HETP. This theory was then extended and generalized by Klinkenberg and Sjenitzer (40) and more specifically by van Deemter, Zuiderweg and Klinkenberg (34) who worked out the material balance in each of the phases to give the 'rate' equation.

$$H = 2\lambda d_p + 2\frac{\gamma D_g}{u} + \frac{8}{\pi^2}\,\frac{k}{(1+k)^2}\,\frac{d_f^2}{D_{liq.}}\,u$$

Eddy Diffusion — Molecular Diffusion — Resistance to Mass Transfer

(symbols are defined in Appendix VI)

Band broadening was considered to result from 3 independent mechanisms which contribute additively to H.

1. Eddy Diffusion. Turbulence is not implied by the name but rather the formal analogy with true eddy diffusion is meant. Because of the presence of the packing gas molecules travel through the column along many paths of different lengths, cross-sections and directions. A dispersion of speeds is also caused by fluctuations in the value of k in different interstices. This leads to the depletion and widening of a solute band to an extent depending on the size and shape of the particles and the mode of packing.

2. Molecular Diffusion of the solute in the gas phase. This is superimposed on its movement along the column.

3. Resistance to mass transfer in the liquid phase. Instantaneous equi-:librium would require an infinite rate of mass transfer between the two phases. For the high rates of flow operative in GC the finite rate of mass transfer in practice makes an important contribution to H even although the high dispersion of the liquid phase is a very effective means of enhancing the establishment of equilibrium. As a result of the finite rate of mass transfer molecules either fail to go into solution and then travel slightly ahead of the band, or are slow in getting into the moving phase and so lag behind the band. If F_g and F_l are the fractional plate volumes occupied by gas and liquid respectively, u_c is the carrier gas velocity and $\bar{\alpha}$ the mass transfer coefficient, the material balances per unit cross-sectional area are

$$F_g\left(\frac{dc_g}{dt}\right) = -F_g u_c \left(\frac{dc_g}{dt}\right) + \bar{\alpha}\,(c_l' - Kc_g)$$

Gain Solute in Gas Phase of Plate — Loss by Convection — Gain from Liquid

and, in terms of the liquid phase,

$$F_l \frac{dc_l}{dt} = \bar{\alpha}(Kc_g - c_l')$$

Gain in Solute in Liquid Phase of Plate — Gain from Gas

(c_l' is the out of equilibrium value of c_l; $K = c_l/c_g$)

Van Deemter et al. showed that the general solution obtained by Lapidus and Amundsen for these equations may be simplified to a Gaussian distribution, provided the column contains a sufficient number of plates, which is directly comparable with a corresponding formula of the plate theory and the value for H can be obtained.

Keulemans (50, 39) has reviewed the combination of 'rate' and 'plate' theories. He pointed out that the variation of H with carrier velocity followed a hyperbolic equation, viz. : $H = A + B/u + Cu$ where A, B and C are constants referring to 1, 2 and 3 respectively (Figure 5). This is a hyperbola with a minimum $H_{,} (2\sqrt{BC} + A)$, at an optimum value of $u_{,} (\sqrt{B/C})$. As a result of the compressibility of the gas phase (see Appendix III) only a small section of the column can operate at maximum efficiency. Although there is no doubt that much of the experimental data can be fitted to such an equation numerous corrections and extensions have been found necessary to explain observed results quantitatively.

Giddings criticised the early theories on the grounds that they did not express the most useful combination of exactness (as a limit for a fairly long but practical time period) and simplicity (in the form of Gaussian, plate height or effective diffusion concepts). In 1957, prompted by a paper outside of chromatography dealing with migration within an electric field (51), Giddings accomplished this for a simple reversible adsorption-desorption reaction (52). In 1958 Golay (41) gave an exact treatment of the diffusion controlled sorption and desorption of solute within an open, uniformly coated capillary column. In 1959 Giddings started the development of a generalized non-equilibrium theory of chromatography for the purpose of calculating the influence of any complex combination of sorption and desorption steps, whether controlled by diffusion or single-step reactions (53). In subsequent papers this theory was applied to a wide range of chromatographic problems, from GSC to the influence of flow patterns in large-scale preparative columns.

In this way the theories of chromatography have reached a compromise between the excessive rigour of the early theories which enabled only the simplest cases to be treated, and over-simplification which led to non-quantitative results. The area of compromise is now being widened so that more and more complex systems can be treated in a way which is useful to practical workers in the field.

CHAPTER II

LATER APPROACHES TO COLUMN THEORY

There have been two successful approaches to the formulation of approxi-:mate theories which are asymptotically correct for long columns with a large number of theoretical plates. Both have been developed mainly by Giddings, the stochastic or random-walk theories and the non-equilibrium theories. Of these the random-walk theory is the simpler but also the less exact. It is of most value when applied to the most complex band broadening processes such as those occurring in the mobile phase.

I. The Simplified Stochastic Theory

The stochastic theory is concerned with the movement of a single molecule through a chromatographic column. It obtains data on the movement of bands by a statistical averaging process. The treatment of Beynon et al.(54), an ex-:tension of the work of Giddings and Eyring (55) is very mathematical but the approach of Giddings (56) gives the same result in a simpler way. This model provides the simplest and most direct approximate theory of zone dispersion.

It is well known in statistics that a group of identical objects (molecules in this case) controlled by random forces develop a Gaussian distribution, the mean behaviour determining the centre of gravity of the group while the number and size of fluctuations about the mean determine the spread of the group. The random-walk model shows that $\sigma = ln^{\frac{1}{2}}$ where σ is the standard deviation of the gaussian distribution, l is the distance a molecule is displaced with respect to the mean in a single random event, and n is the number of these displacements. In general any increase in column length L, keeping all other parameters constant will increase n in the same proportion; hence $\sigma \propto n^{\frac{1}{2}} \propto L^{\frac{1}{2}}$, or the variance $\sigma^2 = HL$ where H the constant of proportionality may now be defined as a measure of the generation of variance per unit length. Another law, used throughout the rate theory, is that for a group of independent statistical processes occurring simultaneously the total variance is the sum of the individual variances while the mean is the sum of the individual means. Thus $\sigma^2 = \sum \sigma_i^2$ and each of the

terms can then be divided by L to relate them to H ie. $H = \sum H_i$. This is equivalent to the assumption made by van Deemter et al. (34) that the plate height contributions were additive.

It is well known (57) that the spreading due to ordinary molecular diffusion is given by $\sigma = \sqrt{2Dt}$. Thus chromatography may be described as a random walk process generating a value of $\sigma = \ln^{\frac{1}{2}}$ or formally as a diffusion process with an effective coefficient $D_{eff.} = \sigma^2/2t$. The plate height can then be expressed as $H = \sigma^2/L = 2D_{eff.}\, t/L = 2\, D_{eff.}/u_b$.

Using this basis the contribution to H for various effects may be readily evaluated. If t_1 and t_2 are the mean times spent in the gas and liquid phases respectively and $\bar{u}_c$ is the carrier gas velocity, then $\bar{u}_b$ the average solute band velocity, is given by $\bar{u}_b = \bar{u}_c \frac{t_1}{t_1 + t_2}$. This relation was first obtained by Le Rosen (58).

If there are ϵ sorptions during an elution there must also be ϵ desorptions,

$\therefore$ 2ϵ = total number of steps = n.

Measuring the standard deviation in time units and replacing the step length l by the duration of a step, $\triangle t$, gives $\sigma_t = \triangle t \sqrt{2\epsilon}$ and $\sigma = \bar{u}_b \times \sigma_t$. If k_1 is the number of sorptions per second and k_2 is the rate for the desorption process, then before elution, $\epsilon = k_1 t_1 = k_2 t_2$ and $\triangle t$, the average desorption time, $= 1/k_2$

$$\sigma_t = \frac{(2k_1 t_1)^{\frac{1}{2}}}{k_2} \quad \text{or,} \quad \sigma_t^2 = \frac{2k_1 t_1}{k_2^2} ; \quad \sigma^2 = \bar{u}_b^2 \times \frac{2k_1 t_1}{k_2^2}$$

The zone spreading is thus related to the rates of the kinetic processes.

$$\sigma_t^2 = \frac{2k_1 t_1}{k_2^2} . \qquad \text{Since } t_1 = \frac{L}{\bar{u}_c} ; \quad \bar{u}_b = \bar{u}_c \frac{t_1}{t_1 + t_2} = \bar{u}_c \frac{k_2}{k_1 + k_2} ; \quad t_2 k_2 = t_1 k_1$$

$$\sigma_t^2 \bar{u}_b^2 = \sigma^2 = \frac{2L\, k_1 \bar{u}_b}{k_2^2} \left(\frac{t_1}{t_1 + t_2}\right) = \frac{2L\, k_1 \bar{u}_c}{(k_1 + k_2)^2}$$

$$\therefore \quad H = \frac{2k_1 \bar{u}_c}{(k_1 + k_2)^2} \quad \text{and} \quad D_{eff.} = \frac{\sigma^2}{2(t_1 + t_2)} = \bar{u}_b^2 \frac{k_1}{k_2^2} \frac{t_1}{(t_1 + t_2)} = \bar{u}_c^2 \frac{k_1 k_2}{(k_1 + k_2)^3}$$

The equivalence of this expression to the van Deemter c term is readily shown.

$$H = \frac{2\bar{u}_c (t_2 / t_1)}{k_2 (1 + t_2/t_1)^2} = \frac{2k\bar{u}_c}{k_2 (1 + k)^2} \text{ since } \frac{t_2}{t_1} = k$$

$\triangle t$ may be taken as the time for the solute molecule to traverse half the solvent film thickness in both directions, ie. a distance df.

By the Einstein equation, $l^2 = d_f^2 = 2D_l \triangle t$

$$\text{whence} \quad \triangle t = \frac{1}{k_2} = \frac{d_f^2}{2D_l}$$

$$\therefore H = \frac{k\bar{u}_c}{(1+k)^2} \cdot \frac{d_f^2}{D_l}$$

in agreement with van Deemter, except for the constant $\frac{8}{\pi^2}$

In treatment of longitudinal diffusion molecules diffuse in the mobile phase only over a time t_1. The longitudinal spread is given by the Einstein equation, $\sigma^2 = 2D_g t_1 = 2D_g \frac{L}{\bar{u}_c}$ since $t_1 = \frac{L}{\bar{u}_c}$

$$\therefore H = 2D_g/\bar{u}_c$$

The tortuosity factor, δ, is absent or is assumed equal to unity.

In the treatment of eddy diffusion $\triangle t$ is taken as $dp/\bar{u}_c$ and $n = L/dp$

$$\therefore \sigma_t^2 = Ldp/\bar{u}_c^2 \qquad \text{and } \sigma^2 = Ldp$$

Thus, H = dp, giving $\lambda = 0.5$ which was the minimum value expected by Glueckauf.

More correctly, $\triangle t$ is the time taken to move, say, λ^1 particle diameters in the gas phase, ie. $\triangle t = \lambda^1 dp/\bar{u}_c$. This gives $\sigma^2 = \lambda^{12} Ldp$ and $H = \lambda^{12} dp = 2\lambda dp$ in the van Deemter treatment.

The final result of the simplest approach is thus

$$H = dp + \frac{2Dg}{\bar{u}_c} + \frac{k\bar{u}_c}{(1+k)^2} \cdot \frac{d_f^2}{D_l}$$

II. The Rigorous Stochastic Theory

This theory was developed by Giddings and Eyring (55,62) for determining the effects on zone structure of the random sorption-desorption processes of chromatography. It has recently been extended by McQuarrie (59). The theory has notbeen applied to diffusion-controlled processes as these are not indepen-:dent of time or of the molecules history. Even for a single-stage process the theory is difficult to apply and the following complicated elution profile was obtained as a function of time.

$$P = \left(\frac{k_a k_d t^o}{t}\right)^{\frac{1}{2}} \sum_{r=o}^{\infty} \frac{(k_a k_d t^o t)^{2r+1}}{r!\,(r+1)!} \exp.(-k_a t^o - k_d t)$$

t^o is the retention time for an unretained peak, k_a and k_d sorption constants and r a running index. Since this theory leads to the same conclusions as the random-walk model the rigorous stochastic approach is useful only when the long-time assumption of the generalised non-equilibrium theory cannot be made. Due to the length and complexity of the mathematical derivation it will not be discussed here.

III. Kinetic Interpretation of the Theoretical Plate Model

Giddings (60) has related the empirical parameter H to the kinetic parameters. The HETP is the length of the cell whose mean concentration (concentration at its mid-point) is in equilibrium with its own effluent.

If the concentration c_i of a chemical species A is perturbed slightly from its equilibrium value it will return to equilibrium according to a first order process, that is by exponential relaxation. The relaxation time, t_R, has been shown to be (61) $t_R = \frac{c_1 - c_1^*}{-dc_1/dt}$ where c_1^* is the equilibrium concentration of A,

When an equilibrium is disturbed by movement of one phase over another as in a chromatographic column, a small volume element in the mobile phase must be in equilibrium with a corresponding element in the fixed phase crossed a time t_R previously. If the flow velocity in the column is $\bar{u}_c$, this equilibrium point is the distance $\bar{u}_c t_R$ upstream. By the definition of a theoretical plate this is the

distance between the end of the cell and its mid-point, that is

$$\bar{u}_c t_R = \frac{HETP}{2} \quad \text{and } N = \frac{L}{H} = \frac{t}{2t_R} \quad \text{where } t = \frac{L}{\bar{u}_c}$$

For the kinetic model $A \underset{k_2}{\overset{k_1}{\rightleftarrows}} B$ $\quad t_R = \dfrac{1}{k_1 + k_2}$

$$\text{Hence HETP} = 2\bar{u}_c/(k_1 + k_2)$$

It has been assumed that the volume element is unmodified by incoming fluid during the movement. This is equivalent to the discontinuous flow model of Mayer and Tompkins (43). For the continuous flow model the concept of concentration displacement is introduced. For the distance $\bar{u}_c t_R$ the overall concentration displacement is approximately given by $R\bar{u}_c t_R$. In this case the distance from the mid-point to the end of the cell is $\bar{u}_c t_R(1 - R)$

Thus $HETP/2 = \bar{u}_c t_R (1 - R)$. For the $A \underset{k_2}{\overset{k_1}{\rightleftarrows}} B$ model, $R = \dfrac{k_2}{k_1 + k_2}$

and $HETP = 2k_1\bar{u}_c / (k_1 + k_2)^2$ in agreement with the stochastic theory.

IV. The Theory of the Capillary Column

"...so we should be able to work from the milligram down to the microgram scale. Of course, that will imply that we decrease the diameter of our column correspondingly. We shall have columns only two tenths of a millimetre in diameter and these will carry, I believe, advantages of their own..."

Martin 1956.

This idea was realised in theory and practice by Golay in 1957 (41, 63-66). In the early theories packed columns were regarded as bundles of long capillaries. Golay showed that the passage of a concentration pulse along a column could be considered in the corresponding mathematical terms as that of an electrical pulse along a series of resistances and condensers. He applied the analogy first to a packed column considered as a system of parallel capillaries of internal diameter approximately equal to particle size and he concluded on theoretical grounds

that the HETP of the latter should be roughly the same as the particle size. He found that, in practice, packed columns behaved as if they were character-:ised by two granule sizes, the first, about ten times the particle size, determined the HETP, the second, about one tenth of the particle size, deter-:mined the resistance to gas flow. This 100:1 ratio meant a viscous resis-:tance to flow 10^4 greater than an ideal capillary column having the same HETP. Golay also noted that air peaks in packed columns were ten times broader than expected from a capillary theory. This led Golay to consider well-defined capillary tubes of circular and rectangular cross-section coated internally with a very thin film of the stationary liquid.

Golay's somewhat mathematical treatment is based on the general laws of diffusion. Although it is simplified by the absence of tortuosity and laby-:rinth effects, the derivation is still lengthy and involved and only his conclusions are stated. Not long after Golay's paper Aris (67) published a similar work.

Golay considered (1) dispersion resulting from viscous flow in an uncoated tube and then (2) dispersion in the presence of a stationary phase with both instantaneous and non-instantaneous equilibration.

The first problem was first considered by Taylor (68, 69) for cylindrical tubes, and later by Aris (70) for tubes of arbitrary cross-section. In a circular pipe of radius r, the velocity u at a distance x from the central line is $u = u_o(1 - x^2/r^2)$ where u_o is the maximum velocity at the axis. In a small bore tube the vapour spreads out under the combined action of molecular diffusion and the variation of velocity across the cross-section. An initially planar concentration contour (see Figure 6) in the absence of diffusion is distorted by viscous flow into a paraboloid. While the low velocity near the wall will help equilibration between phases, molecules in the centre will pass through the column much more rapidly than those at the wall unless there is rapid exchange of positions by lateral diffusion as indicated by the arrows. The lateral diffusion thus limits the spread of the band caused by velocity gradients. Taylor and later Golay showed that the dispersion for cylindrical tubes of radius r was $\sigma^2_{(x)} = r^2ux/24Dg$ where u is the average flow rate. The dynamic diffusion coefficient is then $D_{eff.} = \sigma^2/2t = r^2u^2/48Dg$

In the ideal case of instantaneous equilibrium in a coated capillary the variance produced was $\sigma^2(x) = \frac{1 + 6k + 11k^2}{(1 + k)^2} \frac{r^2 ux}{24Dg}$

When $k = 0$, $\sigma^2(x) \longrightarrow \frac{r^2 ux}{24\ Dg}$, the Taylor expression and

when $k = \infty$ $\sigma^2(x) \longrightarrow \frac{11 r_o^2\ ux}{24\ Dg}$, the velocity-profile contribution in a wetted wall distillation column derived by Westhaver (71).

The additional variance introduced for slow diffusion in the stationary phase was $\sigma^2(x) = \frac{k^3}{6(1 + k)^2} \frac{r^2\ ux}{K^2\ D_l} = \frac{2}{3} \frac{k}{(1 + k)^2} \frac{d_F^2\ ux}{D_L}$

The equation for the HETP of an open tube can thus be written as $H = B/u + C_g u + C_l u$. Golay suggested that in a packed column C_l was probably less important than C_g while in a capillary column the reverse was probably true.

(i) Refinements of Capillary Column Theory

1. Column Pressure Drop

Golay assumed that all the parameters were constant throughout the length of the column but due to gas compressibility and the dependence of D_g on pressure this is not strictly correct. Giddings et al. (75,76) have derived equations for the pressure corrections and their results have been extensively verified for capillary and packed columns by Haarhoff and Pretorius (77) and de Ford et al. (188).

2. Interfacial Adsorption

The solute may be adsorbed at the gas-liquid and liquid-solid interfaces (78). This is indicated by an increase in the retention volume and the dependence of k on the amount of liquid phase. Giddings (107) has used the non-equilibrium method to calculate the plate height contributions from such processes.

3. Slow Mass-Transfer Across the Interface

Golay assumed that once any diffusing molecule struck the gas-liquid interface it entered the solution without any resistance. Khan (80, 81)

has elaborated Golay's theory by deriving an expression for interfacial resistance to mass transfer and has shown that the term is significant only if the fraction of colliding molecules which stick to the surface and condense, the 'accommodation coefficient', is 10^{-4} or less. Measurements of gas adsorption rates (82) have given contradictory values of accommodation coefficients, but the recent work of Goodridge et al. (83) indicates that they are generally near unity. If so the contribution of interfacial resistance to mass transfer is likely to be negligible. Jones and Krige and Pretorius have also proposed a similar term (79, 84). Scott and Hazeldean (98) concluded that interfacial resistance was not significant for the n-heptane-argon-dinonyl phthalate system. In most recent paper on the subject it is concluded that this effect is negligible in practical laboratory columns (99).

4. Non-Uniformity of the Liquid Film

A more serious error lies in the assumption of a uniform liquid film on a smooth, geometrically-true, wall surface. In reality wall roughness is of the same magnitude as the film thickness and Giddings (85) has calculated that even a variation of a few parts in 10^5 in radius of curvature would influence liquid accumulation through capillarity. Indeed it is the surface irregularities which hold the liquid through capillarity and any film deposited on a perfectly smooth surface would be unstable. One could therefore argue that the experimental evidence for an interfacial term in fact indicated simply non-uniformity of the liquid film.

(ii) A Comparison between Packed and Capillary Columns

Capillary columns couple very high plate numbers with a relatively short analysis time. Zlatkis and Kaufman (86) and Scott (87) have reported efficiences of the order of one million theoretical plates for a nylon capillary column one mile long without an unduly high inlet pressure.

It is not the smallness but the openness of the capillary which is important(88). In a tubular column the size of the passage available for the carrier gas is several times the average distance over which the sample molecules must diffuse in order to strive for equilibrium between the moving and fixed phase. In a packed column the size of the free passages between the packing granules is only a fraction of the desired distance; also in a range of particle sizes the small ones will tend to determine the size of the passages while the large ones will determine the

diffusion distance. In ordinary separations C_l, C_g and B are comparable to those for packed volumes if a value approximately equal to d_p is substituted for r in the Golay equation.

Purnell (89-91) has cationed that care must be used in relating the large number of plates to actual separating power and has shown (92) that a capillary and a packed column operated under identical conditions of pressure drop with the same value of C and at the same velocity could, in certain instances, carry out the same separation equally rapidly. Smith (93) has advanced a similar view. The capillary column has the advantage that small values of k can be used without fear of adsorption effects and it is excellent for exceedingly demanding separations. With a packed column the requirements for high-speed analysis, viz. longer columns and increased flow rates, give rise to high average pressures and a correspondingly detrimental increase in C_g. This is prevented by the lower flow resistance of the capillary.

V. Non-Equilibrium and Zone Spreading

In the generalised non-equilibrium theory the velocity divergence due to increased and decreased concentration of molecules in the mobile phase ahead and behind of zone centre respectively, is given quantitative meaning. The degree of non-equilibrium is first calculated in terms of the sorption-desorption rates and the concentration changes accompanying the moving gradients of the zone. Next the velocity increase ahead of zone centre is written in terms of an excess forward flux of solute through a typical cross-section. To the rear the forward flux is calculated to be deficient in amount. The theory shows that the excess, or deficiency, of solute flux is proportional to the negative concentration gradient, analogous to a diffusion process. The rate of zone spreading can thus be described by an effective diffusion coefficient from which H can be calculated directly. In contrast to the single-molecule approach of the stochastic theory, the non-equilibrium approach is concerned with the gross processes of mass transfer and the theory has been developed for the higher flow region where non-equilibrium is significant (60, 53, 100-102).

(i) Non-Equilibrium Kinetics Applied to Chromatography

Each of the various kinetic steps in chromatography can be represented by $A_i \underset{k_{ji}}{\overset{k_{ij}}{\rightleftharpoons}} A_j$ where A_i and A_j represent different states of the solute molecule A (sorbed, desorbed, hydrogen-bonded, etc.). k_{ij} and k_{ji} are the first order rate constants for the transitions. The concentration of the ith state of A c_i, per unit volume of the overall column material, at a fixed location in the column, is constantly changing due to the simultaneous processes of reaction, mass flow and diffusion. We consider the kinetics of the reaction near equilibrium.

Let the net rate of production by reaction of species A in state i be r_i.

Then $r_i = dc_i/dt_{\text{reaction}} = \sum_j k_{ji} c_j - c_i \sum_j k_{ij}$

At equilibrium $r_i = 0$ and the concentration in each state is its equilibrium value c_i^*. In this case the c_i's are obtained from the n equations

$$\sum c_i = c \qquad r_i = 0 \quad i = 1, 2 \ldots\ldots n-1.$$

where c is the total concentration of A in all states per unit volume of column.

When equilibrium is not established it is convenient to define an 'equil-:ibrium departure' term ϵ for each state i: $c_i = c_i^* (1 + \epsilon_i)$. We assume $r_i \cong r_i^*$ where r_i^* is the value of r_i for a concentration c_i^*.

The equations to be solved are

$$\begin{cases} \sum c_i^* (1 + \epsilon_i) = c \\ r_i^* = \sum k_{ji} c_j^* (1 + \epsilon_j) - c_i^* (1 + \epsilon_i) \sum_j k_{ij} \quad i = 1,2 \ldots\ldots n-1. \end{cases}$$

and these simplify to

$$\begin{cases} \sum c_i^* \epsilon_i = 0 \\ r_i^* = \sum_j k_{ji} c_j^* \epsilon_j - c_i^* \epsilon_i \sum_j k_{ij} \end{cases}$$

Since at equilibrium $k_{ji} c_j^* = k_{ij} c_i^*$, substitution gives

$$\begin{cases} \sum c_i^* \epsilon_i = 0 \\ r_i^* = c_i^* \sum_j k_{ij} (\epsilon_j - \epsilon_i) \qquad i = 1, 2 \ldots\ldots n-1 \end{cases}$$

i.e. n algebraic equations which are linear in the ϵ's which can be solved for by applying Cramer's rule.

To obtain the r* values we form the material conservation equation for the ith species, viz.

$$\partial c_i/\partial t = r_i - u_i (\partial c_i/\partial z) + D_i (\partial^2 c_i/\partial z^2$$

reaction mass flow diffusion

Molecules in the ith state diffuse in the z direction with a diffusion coefficient D_i and are simultaneously carried along by mass flow at a velocity u_i. Since the system is close to equilibrium $\partial c_i/\partial z$, etc., can be replaced by $\partial c_i^*/\partial z$, etc. Each term thus obtained will have a fractional error ϵ. The ratio $c_i/c = x_i$, the mole fraction. It can be shown that the last term is ordinarily negligible.

Hence $r_i \cong \partial c_i^*/\partial t + u_i \partial c_i^*/\partial z$

Since c_i^* is a constant fraction of c, namely x_i^*,

$$r_i/c_i^* \cong \partial \ln c/\partial t + u_i \partial \ln c/\partial z$$

and since $\partial c/\partial t \cong - \bar{u}_b \partial c/\partial z$ where $\bar{u}_b$ is the average velocity of the solute zone, to a good approximation, $r_i/c_i^* = (u_i - \bar{u}_b) \partial \ln c/\partial z$ and the equations for the value of ϵ become $\sum c_i^* \epsilon_i = 0$

and $(u_i - \bar{u}_b) \partial \ln c/\partial z = \sum k_{ij} (\epsilon_j - \epsilon_i)$

From these n equations the ratios $\epsilon i/(\partial \ln c/\partial z$ can be obtained in terms of c_i^* and k_{ij}'s. These quantities are all in theory calculable either from thermodynamics or rate theory, and if the isotherms are linear

(ie. the equilibrium mole fractions x_i^* are independent of c) the equations reveal that $\epsilon_i/(\mathrm{d}\ln c/\mathrm{d}z)$ is independent of both position in the column and total concentration.

The flux of material through a unit cross-section of the column is given by

$$q = \sum c_i u_i = \sum c_i^* (1 + \epsilon_i) u_i \quad \text{and since } c_i^* = x_i^* c$$

$$q = c\sum x_i^* u_i + c\sum x_i^* \epsilon_i u_i$$

The first summation is the average velocity $\bar{u}_b$ of the solute zone.

$$\therefore q = c\bar{u}_b + c\sum x_i^* \epsilon_i u_i$$

The second term is equivalent to a diffusion term. Equating this term to $-D_c\ \partial c/\partial z$ we obtain for D_c, the effective diffusion coefficient

$$D_c = -\sum x_i^* \epsilon_i u_i / (\partial \ln c/\partial z) = -\sum x_i^* u_i\ (\epsilon_i/\mathrm{d}\ln c/\mathrm{d}z)$$

Since x_i^*, u_i and $(\epsilon_i/\mathrm{d}\ln c/\mathrm{d}z)$ are all independent of position in the column or total concentration, D_c is a true constant for any species A. This expression is directly related to H by $H = 2Dc/Ru = 2Dc/\bar{u}_b$

R is the equilibrium fraction of molecules in the mobile phase and equals $\sum_{\text{mobile}} x_i^*$ ie. $\bar{u}_b = Ru_i = Ru$. Since for the stationary phase

$u_i = 0$, $\sum x_i \epsilon_i u_i = \sum_{\text{mobile phase}} x_i \epsilon_i u = \epsilon . uR$ (mobile)

thus $H = -2\,\bar{\epsilon}_{\text{mobile}} / \partial \ln c/\partial z$

where $\bar{\epsilon}$ is the average value of ϵ in the mobile phase. Thus a measureable value for H can be calculated once the ϵ_i values have been obtained.

The assumptions made are

1. The kinetic processes are sufficiently rapid that the departure from local equilibrium remains small, ie. $\epsilon_i \ll 1$.
2. The u_i terms are independent of concentration, the kinetics are linear and reactions are first order.

(3) Longitudinal diffusion terms are neglected.

(4) In the application of the equation to mass transfer processes involving both stepwise kinetics and diffusion processes, it is assumed that the various terms are additive. Thus, for non-competitive mechanisms,

$$H = \sum_{i=1}^{m} H(k_i, \infty) + \sum_{i=1}^{n} H(D_i, \infty)$$

where each term is the plate height calculated with its particular rate parameter intact and with all other rate parameters at infinity.

Note: The approach to kinetics from the equilibrium point of view has been used extensively by Hirshfelder and co-workers in the theoretical analysis of flame properties (94), and Giddings and Shin have used this method to predict departure from the steady state in complex reactions (96).

(ii) Application to 1-Site Adsorption Kinetics

The simplest scheme is

$$A_1 \underset{k21}{\overset{k12}{\rightleftarrows}} A_2$$

where subscript 1 refers to mobile phase and 2 to the fixed phase. This may be described by the equations,

$$c_1^* \epsilon_1 + c_2^* \epsilon_2 = 0$$

$$k_{12}(\epsilon_2 - \epsilon_1) = r_1^*/c_1^* = (1 - R)\, u\, (\partial \ln c/\partial z)$$

It was shown that $r_1^*/c_1^* = (1 - R)\, u\, (\partial \ln c/\partial z)$ in section (i). Solving for ϵ_i we obtain

$$\epsilon_i = -(1 - R)/k_{12} \cdot u \cdot \partial \ln c/\partial z \cdot c_2^*/(c_1^* + c_2^*)$$

$$= -(1 - R)^2/k_{12} \cdot u \cdot \partial \ln c/\partial z$$

$$\therefore D_c = -u \sum_{\text{mobile}} x_i^* \epsilon_i / (\partial \ln c/\partial z)$$

Since $R = \sum_{\text{mobile}} x_i^*$, $D_c = \left[R(1 - R)^2 u^2 \right] / k_{12}$

$$\text{Since } R = x_1^* \; k_{21}/(k_{21} + k_{12})$$

$$(1 - R) = x_2^* = k_{12}/(k_{21} + k_{12})$$

$$\text{Then, } D_c = k_{12}\, k_{21}\, u^2/(k_{12} + k_{21})^3$$

From the stochastic theory,

$$H = 2k_1 u/(k_1 + k_2)^2 = 2Dt/L$$

$$\therefore D = 2k_1 u/(k_1 + k_2)^2 . \quad L/2t = k_1 k_2 u^2/(k_1 + k_2)^3$$

$$\text{Since } L/t = \bar{u}_b = k_2 u/(k_1 + k_2)$$

thereby showing the equivalence of the two approaches for a simple process.

VI. The Generalised Diffusion Theory

Although it was first developed for rate processes involving discrete kinetic steps, Giddings has applied the non-equilibrium method to diffusion controlled processes which lead to local non-equilibrium in the form of lateral concentration gradients. Since the departure from equilibrium is generally small, the same approximations as before can be made.

The rate of accumulation by reaction r_i is then replaced by the rate of solute accumulation s_i due to lateral diffusion and this is given, from the overall mass balance equation, by,

$$s_i = (u_i - \bar{u}_b)\; \partial c_i / \partial z$$

This is formally similar to Fick's first law (see section II), and so by analogy to the second law, $dn/dt = D(d^2n/dl^2)$ we can also write $s_i = D_i \nabla^2 c_i$ where the operator ∇^2 is to be applied only to local concentration gradients. Again, $c_i = c_i^* (1 + \epsilon_i)$ and since c_i^* is locally invariant, $s_i = c_i^* D_i \nabla^2 \epsilon_i$ Elimination of s_i gives $\nabla^2 \epsilon_i = (u_i - \bar{u}_b)\; 1/D_i \; \partial \ln c / \partial z$ from which the ϵ values may be obtained. The integration constants are evaluated through the use of certain boundary conditions. These include

1. $\sum c_i^* \epsilon_i = \sum x_i^* \epsilon_i = 0$
2. At a closed surface $\partial \epsilon_i' / \partial w = 0$ where w is the distance normal to the interface.
3. At an interface $\epsilon_i' = \epsilon_j'$
4. At planes, lines and points of symmetry $\partial \epsilon_i' / \partial w = 0$ expressing the fact that there is no solute transport through such places.

5. Since the solute transport must be equal on the two sides of a connecting interface,

$$D_i \left(\partial \in_i 1 / \partial w \right) = D_j \left(c_j^{*\prime} / c_i^{*\prime} \right) \left(\partial \in_j{}' / \partial W \right)$$

The flux of material through a unit area A normal to the flow direction is given by

$$q = \sum_i \int c_i u_i dA_i$$

Thus $q = \sum_i \int c_i^* \; u_i dA_i \; + \sum_i \int c_i^* \in_i u_i dA_i$

The last term is responsible for all local non-equilibrium effects and can be equated to $-D_c \, \partial c / \partial z$.

Thus $D_c = -\sum_i \int c_i^* \in_i u_i dA_i / \partial \ln c / \partial z$

Since the ϵ_i terms are proportional to $\partial \ln c / \partial z$, D_c is independent of position and concentration.

As before $H_c = 2D_c / \bar{u}_b$.

(i) <u>The Significance of the Generalised Diffusion Theory</u>

The general theory just outlined has many applications to both stationary and mobile phases (95, 103 - 112) Giddings has used this approach to confirm the results of Golay and van Deemter showing that the theory of gas chromatography is basically sound. He has worked out contributions to H resulting from multi-site adsorption, adsorption in partition chromatography, reversible chemical changes, etc. The generalised non-equilibrium theory has given us every C_1 term now known except for a uniform liquid film. In the general combination law the dispersion is written as a sum of terms each referring to a small isolated region of comparatively simple geometry, and the differential equation of the Poisson type applicable to each such unit is formed and solved with the aid of the boundary conditions.

C_1 is given as $C_1 = \sum q_i F_i R \, (1 - R) \, d_i^2 / D_1$, and where F_i is the fraction of total liquid in unit i, d_i is the depth of liquid in unit i, q_i is a configuration factor which can be shown to be 2/3 for a uniform film, 1/4 for rod-shaped liquid units, 2/15 for spherical droplets and 1/12 for the liquid ring

around the contact point between glass beads. Application of the theory to narrow pores allows many practical equations to be derived. The cross-sectional area of many units may be approximated by a=const.(thickness)^n where n is the taper factor. q is then found to be given by $\frac{2}{(n+1)(n+3)}$ in agreement with the above values for n from 0 to 3 respectively. Plate height calculations can thus be made which realistically reflect the complex nature of the solid and liquid phases and absolute plate height values have been predicted to within 20 to 50% of experimental data for glass bead columns.

The main difficulty now lies in knowing the manner in which neighbouring regions combine in their overall contribution to the dispersion and the exact geometry and configuration of these units. The current bottleneck on GC theory is the development of really accurate models for the support structure. Adsorption and condensation theory, the science of porous materials, micro-:scopic observations and mercury penetration have all been used to elucidate structure.

Unfortunately no simplifying method comparable to the combination law has been found for the mobile phase and the treatment of this is still far from complete. Where the mass transfer occurs by a combined process of diffusion and stepwise kinetics one can consider either the non-equilibrium in every part of the system simultaneously, a complex approach, or use the more straightforward additive law.

VII. Modifications, Extensions and Corrections to the van Deemter Equation

(i) Resistance to Mass Transfer in the Gas Phase

The earliest theories of non-equilibrium effects in the mobile phase centred around a diffusion film in an ion-exchange column (113). The first quantitative discussion of mass transfer in the gas phase was given by van Deemter et al. (34). They assumed the transfer occurred in a channel of the order of one-fifth particle diameter and since gaseous diffusion is 10^5 faster than liquid diffusion they ignored it. This may be justified if the liquid inhabits deep and narrow pores, but if the thickness of the liquid layer is reduced to 1/100 of the distance across the gas channel, the relax-:ation times for diffusion in the 2 phases become comparable. Thus Jones (114) found that liquid diffusion was not dominant in his experiments and

presented an equation of the form $H = B/u + Eu$ where E reflects gas phase mass transfer effects. He and van Deemter were later reconciled at a Discussion Group meeting (115) which resulted in Jones adding a second gas diffusion term to the now extended van Deemter equation,

thus $H = A + B/u + c_1u + (Dg + Eg)u$.

Golay (41) derived 'dynamic diffusion' terms for his open tubes as discussed earlier. He pointed out that in a packed column the air peak, which should be unaffected by the liquid phase, is of the same relative width as the sample peaks and he suggested that C_g may well be comparable or even greater than C_1. Giddings also considered transverse gaseous diffusion in so far as it affected the A term (116).

(ii) The Jones Extended HETP Equation

Jones (117) encouraged by experimental evidence (118-119),(84) produced a highly technical random-walk model which may be considered to be the Golay equivalent for a packed column. Jones identified unknown constants in his final equations by equating them to the Golay term assuming that dp^2 was equivalent to r^2. The Giddings coupling equation was considered as a limit to the velocity distribution term. The complete equation is :

$$HETP = 2\lambda dp + 2\gamma Dg/u + 2/3\left[\frac{k}{(1+k)^2}\right](d_1^2/D_1)u$$
$$+ c_1\left[\frac{k^2}{(1+k)^2}\right](dg^2/Dg)u + c_2(dp^2/Dg)u + 2\rho(c_1c_2)^{\frac{1}{2}}\left[\frac{k}{1+k}\right](dp\ dg/Dg)u$$

which can be written as $H = A + B/u + (C_1 + C_1 + C_2 + C_3)u$.

C_1u is the resistance to mass transfer in the gas phase, C_2u is the velocity distribution term and C_3u is a term accounting for the correlation between the C_1 and C_2 terms.

Using the statistical approach, $\sigma^2 = nl^2$, $k = t_1/t_g$ and $t_g = L/u$.

The frame of reference was chosen to move with the centre of the peak being considered. Thus the gas moves forward with a velocity $ku/1 + k = Ru$ and the liquid moves back with a velocity $u/1 + k = (1 - R)u$. The distance travelled per step is equal to the time per step multiplied by the relative velocity of the phase with respect to the peak.

The C1 Term: Assuming a molecule has on average to migrate laterally a distance α dg in order to arrive at the liquid surface, the process of broadening by mass transfer can be regarded as a series of random-walk steps in which the step length is the distance traversed in a time

$$\tau = \alpha^2 dg^2 / 2Dg$$

The number of such steps is

$$n = L/u\tau = (2Dg/\alpha^2 dg^2)\ L/u$$

The length of each step is the length relative to the moving band and is given by

$$l = \tau\,(k/1+k)u = \alpha^2 dg^2/2Dg \cdot (k/1+k)u$$

Hence

$$H = \sigma^2/L = nl^2/L = (k/1+k)^2\ \alpha^2\ dg^2/2Dg \cdot u$$
$$= c_1\,(k/1+k)^2 \cdot dg^2/Dg \cdot u \text{ where } c_1 = \alpha^2/2$$
$$= C_1 u$$

The factor $(k/1+k)^2$ in the c_1 term increases with k to a limiting value of 1 whereas the $K/(1+k)^2$ factor in the c_1 term approaches zero with increasing k. Thus for large k values the c_1 term will predominate but both vanish for k = 0.

The C2 Term: In packed columns there will be a large velocity difference between the gas in the relatively stagnant interior of the porous packing and that in the regions between the particles. The diffusion paths will be of the order of the particle diameter and as before, the time to diffuse this distance

$$\tau = \beta^2 dp^2 / 2Dg$$

$$\therefore\ n = L/u\tau = (2Dg/\beta^2 dp^2) \cdot L/u \text{ and } l = (\beta^2 dp^2/2Dg) \cdot u$$

$$\therefore\ H = c_2\,(dp^2/Dg)\,u = C_2 u$$

The term derived by Giddings for the velocity dependence of the A term, viz. $H = 2\lambda\, dp/(1 + 4\lambda\, Dg/\beta^2 d_p u)$ reduces to the C_2 term at low velocities.

Thus $H = (\beta^2 dp^2/2Dg)\,u$ if β^2 the geometric constant $= 2c_2$.

The C3 Term: A molecule which stays closer than average to the walls will spend shorter times in the gas phase and travel at a lower average velocity and vice versa. Thus c_1 and c_2 are interdependent and the correlation is $c_3 u$. Unfortunately the correlation coefficient ρ cannot be calculated

exactly and there is not sufficient experimental verification of this term to warrant discussion, though Jones does consider the correlation to be fairly strong.

When applied to capillary columns, $dp = dg = r$ and $A = 0$ and

$$H = \frac{2Dg}{u} + \frac{2}{3}\left(\frac{k}{(1+k)^2}\right)\left(\frac{d_1^2}{D_1}\right)u + \frac{(c' + c''k + c'''k^2)}{(1+k)^2}\left(\frac{r^2}{Dg}\right)u$$

where $c' = c_2$

$$c'' = 2c_2 + 2\rho\,(c_1c_2)^{\frac{1}{2}}$$

$$c''' = c_1 + c_2 + 2\rho\,(c_1c_2)^{\frac{1}{2}}$$

On comparison with Golay's C_g term,

$$c_1 = \frac{1}{4}, \quad c_2 = \frac{1}{24}, \rho = \left(\frac{2}{3}\right)^{\frac{1}{2}} = 0.817$$

and when $k = 0$ the mass transfer term reduces to

$H = (r^2/24Dg)\,u$ as in the Golay equation.

In common with other random-walk models, the Jones theory cannot distinguish single-channel flow and interacting multi-channel flow and thus cannot be used to correlate plate height values with support structure.

(iii) <u>The Giddings Approach to the Nature of Gas Phase Mass Transfer</u>

Before rigorous calculations can be made the complex packing geometry and the resulting intricate flow pattern must be quantitatively understood. Giddings in an approximate treatment lists five contributions to C_g. These involve

1. Diffusion across the narrow channels between particles.
2. Diffusion through the particles.
3. Diffusion between unequal flow channels.
4. Diffusion between long-range inhomogeneities.
5. Diffusion across the column.

1. Calculation of the trans-channel contribution is based on a uniform capillary and the plate height can probably be calculated within a factor of 2 or 3 and this effect contributes less than 2% of the total.

2. In calculating the trans-particle effect it is assumed that the velocity of any mobile phase within the support particles is essentially zero. Since flow velocity is approximately proportional to channel size squared intraparticle channels 1/3 of interparticle size for instance, may well carry 10% or so of flow. Approximations have to be made concerning particle geometry and obstructive factor and the plate height can be calculated to only about 50% accuracy. However, when applicable this effect may contribute about 10%.
3. The short-range inter-channel effect occurs in the bridged space between close-packed islands. The size of the channels depends on the density of packing and intimacy of contact of the particles. From Figure 7 showing two packing structures, the diameters of the inscribed circles are in (a) 15% and in (b) 41% of the constituent spheres and this factor of 2.7 in the interstitial aperture leads to about a 7.5 fold velocity increase. It may be that the bridged 'channels' are too isolated to permit such increased flow but it is felt that a large velocity bias still exists because of the extensive interconnections between flow channels and perhaps between bridged regions themselves.
4. The long-range interchannel effect refers to flow inequalities over a distance of about 10 particle diameters due to long-range random variations in permeab-:ility and porosity. This effect is extremely difficult to assess but because of coupling is probably less important than (3) which can be calculated within a factor of 2 or 3. Giddings considers that (3) and (4) together make the principal contribution to plate height.
5. The trans-column effect is a manifestation of column-wide differences which arise from
   a. Variations in particle diameter and porosity over the column cross-section.
   b. The 'wall' effect. (a) and (b) will be discussed later.
   c. The bending or coiling of a column. This introduces a velocity gain at the inside of the bend and a velocity lag at the outside because these paths have different lengths with the same pressure drop. The velocity profile is given by the ratio of the local carrier velocity u and the velocity at the centre u viz. $u/\tilde{u} = Ro/(Ro + r \sin \theta)$ where Ro is the radius of curvature, r is the distance from the tube centre and θ is the angle with respect to a line extending through the tube centre parallel to the coil axis (95, 104, 111).

The five effects are illustrated in Figure 8.

The probable consequences of column inhomogeneities were first treated in some theoretical detail by Golay (120). He showed that $Cg = \omega\, dp^2/Dg$ but he identified ω only in the broadest terms. By applying first the random-walk treatment and then the non-equilibrium approach, Giddings has given a precise definition of ω. In the random-walk treatment each of the five categories of flow inequalities are characterised by an S value, the persistence of velocity span, which is related to H by $H = \omega_\beta^2 S$. S is given by ut_e where t_e the 'exchange time' equals $\omega_\alpha^2 dp^2/2Dm$. $\omega\alpha$ is the distance of exchange per particle diameter and ω_β the ratio of the velocity bias from the mean to the average velocity.

$$\text{Thus } H = \frac{\sigma^2}{L} = \frac{l^2 n}{L} = \frac{\omega_\beta^2 (ut_e)^2}{L} \cdot \frac{L}{ut_e} = \omega_\beta^2 ut_e = \frac{(\omega_\alpha^2 \omega_\beta^2)}{2} \left(\frac{dp^2 u}{Dm}\right)$$

For a given effect i, $H = \omega_i (dp^2 u/Dm)$ where $\sum \omega_i = \omega$

Before the generalised non-equilibrium theory can be applied a model must be postulated which reproduces the main feature of the erratic flow profile. Giddings considered the model in Figure 9. The outer annulus corresponds to the tightly packed particles while the 'inner-cone' is the high velocity region. The detailed calculations are fully described in the literature (103). For the small-range interchannel diffusion ω is given as $\omega = 0.70 (1 - 0.15 R)$ for porous materials

and $\omega = 0.62 (1 - 0.3 R)$ for non-porous supports.

Although the above model is rather crude it has not been possible to do even this for the long-range inter-channel effect. The total value of ω for a porous and non-porous support may be summarised approximately by

$$\omega \cong 0.82 - 0.20 R$$

and $\omega \cong 0.63 - 0.20 R$ respectively.

Here the R dependence of plate height is only moderate. While H is reduced by about 15 to 30% on going from a highly retained solute to a non-partitioning one, the gas phase term for a capillary column would be correspondingly reduced by a factor of 11 emphasising again the inadequacy of the early treatments of packed columns as bundles of non-interacting capillaries.

(iv) Experimental Evaluation of ω

Giddings has calculated ω from published results. His results are shown in Table (i).

ω	R	k	Support	Reference
0.45	0.09	10	F.B.	75
- 1.0	0 - 1	0 - ∞	C.S.	84
1.12	0.1	10	S.O.C.	121
0.33	1	0	C.S.	122
0.79	1	0	C.S.	123
1.62	0	∞	C.S.	123

Table (i). Empirical ω values for Porous Supports

Dal Nogare and Chiu obtained hyperbolic H - u plots for air samples (k = 0) and strongly sorbed substances ($C_1 = 0$) (123). The observed C term under these conditions is due entirely to slow gas phase processes. Perrett and Purnell (124) have examined ω in detail. If Giddings' view is correct a plot of C_g or $\omega /(1 + k)^{-1}$ should be linear. Although Perrett and Purnell do obtain straight line plots of ω against $(1 + k)^{-1}$ they are nowhere near the theoretical line. They concluded that flow processes alone cannot account for the whole of C_g which might better be given by a contribution of the form

$$Cgu = \left[0.5 - \frac{0.2}{(1 + k)} + f_3 (V_1)\right] \frac{d_p^2 u}{Dg}$$

where $f_3 (V_1)$ represents a maldistribution function associated with the liquid phase but not necessarily explicitly defined in terms of V_1.

Giddings does say that, due to the very wide range of experimental systems and the approximations made, etc., a 2 or 3 fold error is to be expected and any closer agreement is fortuitous.

CHAPTER III

AN EXPERIMENTAL STUDY OF THE RATE EQUATION

I. The Eddy Diffusion Term A

The existence of a velocity independent contribution to H was first demonstrated by Kramers and Alberda (125) and subsequently by Klinkenberg and Sjenitzer (40). Later treatments have come to a similar conclusion (126, 56). It is generally assumed that λ is a constant of order unity and is independent of all non-geometrical parameters. There is no exact theory of eddy diffusion or the complex geometry of the packed bed and the A term has been the subject of much speculation and controversy. Giddings has given an excellent review of the subject (127, 128).

(i) Experimental Anomalies

Experiments to determine A show many anomalies which include the following:

1. A values which are nearly zero or negative

Bohemen and Purnell (129) found λ = 0.3 for 20-30 and 30-40 mesh columns but obtained negative values with finer particles and mixed mesh columns. Littlewood (130) using uniform glass beads found values of A between zero and 0.1 mm. Giddings (75) has also found apparent negative values of A and recent publications have tended to assume A = 0 (122, 131-133).

2. Variation of λ with Particle Size

λ is generally found to increase almost linearly with decrease in particle size (34, 133-137). This was explained by relatively coarse materials packing more regularly than fine particles. Thus Klinkenburg and Sjenitzer (40) found λ to be 8, 3 and 1 for 200-400, 50-100 and 20-40 mesh respectively. The increase in λ was outweighted by the decrease in dp and λ was found to decrease with decrease in particle size. Many other workers (34, 50, 131, 136, 137) have shown that the A values are independent of particle size.

3. Variation of A with Flow Velocity

The variation is inconsistent. Glueckauf (136) found a rapid increase

of A with velocity followed perhaps by a slight decrease. The curves obtained varied only moderately with the size and method of packing. In a later experiment (138) no evidence was found for this variation. Purnell et al. (129, 139) found that the A term combined with the B term and had an inverse dependence on flow velocity.

4. Variation of A with Retention Volume

Kieselbach (133, 140) and Littlewood (130) have shown that light gases tend to have a larger A value than more highly retained components.

5. Variations of A with Solute, etc.

Variations of A with solute (134, 141), with liquid loading (135) and with pressure and diffusivity of the carrier gas (142) have also been reported whereas in theory A should be a property of the column geometry only.

(ii) Origin of Anomalies

Possible sources may include failure to correct the plate height expression for the column pressure drop, failure to include mass transfer in the gas phase, errors of graphical methods and equipment errors. Giddings et al. (75) and Littlewood (130) have shown that the use of pressure correction terms can change the apparent eddy diffusion contribution from a very small positive value to a slightly negative one. Ayers et al. (131) have found a substantial intercept of the limiting tangent in an H - u plot even when eddy diffusion is absent.

The effect of a finite time constant for the injector or detector would be to add a finite width to any peak such that at higher gas velocities an increasing proportion of the total peak width would be due to the time constant of the apparatus. Values of H at high flow rates would be too large and the dependence of H upon u too steep. The intercept of the limiting tangent in this case would yield a negative value of A and this effect would be most serious for early peaks.

Although Glueckauf (136) considers that λ must always be at least 0.5 the view is now becoming general that over the usual range of operating conditions the A term can be made negligible by careful column construction and its presence can usually be attributed to some instrumental artifact. Littlewood and Kieselbach (130, 133) have shown for instance that positive

values of A can arise from a finite sample volume and from bad geometry of the sample introduction system or detector. Tests with dyes in an aqueous system showed that severe channelling can occur in the glass wool plugs conventionally used to retain the column packing. Kieselbach showed that improved peak symmetry resulted when the glass wool plugs were replaced by nickel screens and at the same time the A term dropped from 0.02 to 0.004 cms. Dead volumes throughout the system will also cause tailing particularly noticeable for faster moving peaks and this would explain why the early peaks in a chromatogram are usually skewed.

(iii). The Coupling Theory of Eddy Diffusion

As a result of the failure of experimental results to conform to the classical eddy diffusion concept, Giddings put forward the 'Coupling Theory of Eddy Diffusion' which predicts the net contribution of eddy diffusion to be a function of flow velocity (100, 116, 143) viz.

$$H_c = \frac{1}{(2\lambda d_p)^{-1} + (Cgu)^{-1}}$$

where H_c is the mobile phase contribution to H apart from longitudinal diffusion.

$$\text{As} \quad u \longrightarrow 0 \qquad A \longrightarrow 0$$

$$\text{as} \quad u \longrightarrow \infty \qquad A \longrightarrow 2\lambda dp$$

The Cgu term does not include the contribution of stagnant gas which contributes a separate additive term to H. This theory has been criticised by Klinkenberg and Sjenitzer (198). Thus when u is low the term $2\lambda dp$ may well contribute practically nothing to H. The coupling equation arose from considering the fact that in a packed column, unlike a capillary column, the velocity of a molecule can be changed both by movement along a single stream path which passes through regions of a wide spectrum of velocities (eddy diffusion), or by transverse diffusion across stream paths (transverse mass transfer). Thus a low velocity may be caused by the nearness of the streamline to a particle boundary or by the presence of a predominating lateral component of the velocity. At low velocities there may be time for several lateral diffusional transfers and so a velocity bias

for an individual molecule may not persist for an entire particle diameter. According to Giddings this would cause a proportional reduction in the co-:efficient of eddy diffusion with the result that the latter effect would no longer contribute a velocity independent term to the plate height.

In the 3 - dimensional packing structure the flow regions are intimately connected by a network of lateral diffusion paths. Since both lateral dif-:fusion and the effective exchange of streamlines act together to re-establish equilibrium, and since the smallness of the plate height is a measure of how rapidly molecules exchange their positions, the two mechanisms should be com-:pounded as resistances in parallel rather than in series; hence the coupling equation (see Figure 10). By the random-walk treatment, the velocity per-:sistance span, S, may be written as L/n since n spans make up the total migration distance L. The number n is the sum of the two independent processes due to the flow mechanism, n_f, and the diffusion mechanism, n_D. Thus

$$S = \frac{L}{(n_f + n_D)}$$

Assuming that a stream-path must proceed a distance $\omega_\gamma dp$ to complete a step and diffusion must take a molecule the distance

ω_α dp to complete a step, $n_D = \dfrac{2 LD_g}{\omega_\alpha^2 d_p^2 u}$ and $n_f = \dfrac{L}{\omega_\gamma dp}$

where u is the average velocity of the mobile phase.

Thus $H = \dfrac{\omega_\beta^2 L}{(n_f + n_D)} = \dfrac{1}{1/2\,\lambda_i dp + D/\omega_i u dp^2}$

where ω_i has been submitted for $\omega_\alpha^2\ \omega_\beta^2/2$ (see chapter II (I and VII)) and λ_i for $\omega_\gamma \omega_\beta^2/2$.

The actual situation is more complicated because the processes may not compete throughout. The effective exchange of streamlines will operate more rapidly in the higher velocity regions since to a first approximation a new velocity is assumed after the passage of a constant distance, the particle diameter. Consequently a situation can exist in which lateral diffusion controls the equilibration rate in the slow moving regions and the exchange of streamlines predominates in the faster moving regions. In its most recent

form coupling is written as a sum of terms,

$$H_c = \sum \frac{1}{1/2\,\lambda_i d_p + 1/c_{gi} u}$$

where the summation is over five terms, one for each type of structural feature mentioned in chapter II (III).

(iv) Experimental Evidence for the Coupling Theory

Published results are not conclusive. Glueckauf (136, 144) obtained values of λ ranging from 0.5 to 3 with increasing velocity. Bohemen and Purnell (129) plotted the difference in plate height against 1/u for H_2 and N_2 as carrier gas. Since only the B term is affected the plot should be a straight line through the origin. They obtained a curve which intercepted the 1/u axis. More recently Perrett and Purnell (124) concluded from their data that the classical theory is valid. One difficulty is that the C_1 term either swamps or obscures the others. For this reason non-sorbing column-solute systems (122, 145, 155) appear the best hope for determining the relevance and importance of coupling.

II. The Molecular Diffusion Term B

The significance of A is discussed in detail in section III of this thesis. Diffusion is influenced by the choice of carrier gas, the pressure and the temperature. For low molecular weight hydrocarbons values of B equal to 0.2 to 0.5 cm^2/sec in H_2 and 0.05 to 0.1 cm^2/sec in N_2 at about atmospheric pressure have been reported (50, 146). Bohemen and Purnell (129) found that the values of B varied in a haphazard way with change of particle size. Littlewood (130) has pointed out that one should also consider the volume in the column connections to the injector and detector in which diffusion contributing to B will occur. Scott (147) has demonstrated that at gas flow rates below the optimum a plot of peak width against time gives a straight line and for a series of homologous hydrocarbons a series of straight lines are obtained whose slopes are in proportion to the molecular weights. With a single hydrocarbon at a series of temperatures the slope approximately relates to the square root of the absolute temperature supporting the theory of molecular diffusion (see section II). B is generally written as $2\gamma D_g$ where experimental values of γ range from 0.5 to unity in support of the theoretical view that the B/u term represents a partially obstructed longitudinal diffusion.

III. The Liquid Mass Transfer Term C_l

Although this research never graduated to using a liquid phase I shall include a brief note on C_l for completeness. Liquid diffusion occurs by a process in which diffusing molecules push through an energy barrier formed by the cage of surrounding molecules. The larger the diffusing molecule the more energy is required and the smaller is its diffusion coefficient. C_l is thus made small by a uniform thin film of a low molecular weight non-polar liquid.

The expression for C_l is clearly a simplification for packed columns since a uniform film cannot possibly be present (148, 103, 85). The theory of the intermolecular forces responsible for the selective retard-:ation is very complex (149 and the choice of liquid is still semi-empirical. Liquid diffusion coefficients are still largely unpredictable (150, 151) and direct measurements of D_l from GLC data are very rare (151, 105) and likely to be inaccurate. The interaction between the liquid phase and solid support is also important since the liquid must wet the solid and if the forces extend into the liquid phase they may influence selectivity. Giddings has given a detailed theoretical treatment of the C_l term (106).

(i) The Relative Importance of the C_l and C_g Terms

Depending on the support structure the majority of conventional packed column show a C_l term in the range from 3×10^{-4} to 3×10^{-2} seconds, with 10^{-3} to 10^{-2} seconds being most common. Assuming typical values for d_p and D_g of 0.02 cm (60–80 mesh) and 0.4 cm^2/sec respectively, with ω of the order of unity, C_g is about 10^{-3} seconds. Thus packed columns are well balanced with respect to the C terms. With glass bead columns, the only detailed work (106) has suggested that C_l may totally dominate C_g, due to the relatively large values of d_f compared to those for porous supports of high surface area. Giddings has given an excellent account of the measure-:ment and interpretation of the C terms (152).

IV. The Packed Column 1964: Conclusion

It thus appears that the plate height of a packed column may be most realistically described by an equation of the form:

$$H = \sum_i \frac{1}{\frac{1}{2\lambda_i dp} + \frac{Dg}{\omega_i dp^2 u}} + \frac{2\gamma Dg}{u} + \sum q_i \left(\frac{Vi}{V_l}\right) R\,(1-R)\,\frac{di^2 u}{D_l} + \frac{\omega_i' dp^2 u}{Dg} + H_{tc}$$

$$= \sum \frac{1}{\frac{1}{A_i} + \frac{1}{C_{gi} u}} + \frac{B}{u} + \sum C_{li} u + C_g' u + H_{tc}$$

This expression does not include contributions less than 1% or terms describing interfacial solute adsorption, nor does it contain contributions from the equipment, finite sample size and non-linear isotherms. Table (ii) gives the compilation of terms (108).

Table (ii). Compilation of Terms

(a) Ordinary Longitudinal Diffusion
1. Gas Phase
2. Liquid Phase < 1%
3. Gas-Liquid Interface<1%
4. Gas-Solid Interface < 1%

(b) Liquid Phase Mass Transfer
1. Capillary Pools
2. Adsorbed Films <1%

(c) Gas Phase Mass Transfer
1. Trans-Particle
2. Trans-Channel < 1%
3. Short-Range Channel Interaction
4. Long-Range " "
5. Tube-Bending (trans-column effect)
6. Particle-Size Variation (trans-column effect)
7. Wall Effect (trans-column effect)

(d) Interfacial Adsorption and Mass Transfer
1. Gas-Liquid Interface
2. Liquid-Solid Interface
3. Gas-Solid Interface (non-wetting systems)< 1%

Conclusion: While we are still a long way from the ultimate objective of bridging the gap between theory and experiment, we have now progressed far beyond the uniform film and capillary bundle models of the last decade. No small part of this development can be attributed to Giddings whose con-:tributions indeed fill the major portion of this work, and it is fitting to end on his words:

"Although we must still invent models, average out details, compart-mentalize the interrelated, rely on inadequate data, ignore the tenuous... we are well along the track of new concepts and refinements, which, in yielding independent plate height calculations, show immense potential in selecting promising and yet unborn columns and in bringing chromatography into the realm of a controlled and quantitative science."

V. The Aim of the Research

The introduction constitutes a review of relevant literature up to the middle of 1964. When this research was started in 1961 the theory was in a much more disordered state than it is to-day. A current point of interest was then the size of the eddy diffusion term A. Since then it has become clear that A can be made negligible by careful column construction. Theor-:etically λ is very difficult to evaluate but if the Giddings coupling theory of eddy diffusion holds this term would be ineffective over the usual range of operating velocities. Reported values of λ vary from + 8 to -0.5. Until very recently there was little conclusive experimental data in support of coupling and if, as the theory predicts, it does become important at higher velocities relative to the optimum, the gas phase contribution to H ought to reach a velocity independent maximum. If so, this would greatly influence the conditions required for high-speed analysis. Thus an import-:ant aim of the work at its inception was the determination of the eddy diffusion parameter A. As it became apparent that eddy diffusion and mass transfer processes should be considered as coupled, the aim shifted to the investigation of the role, relevance and importance of this concept, and we became particularly interested in the behaviour of H versus u plots at relatively high velocities.

In order to eliminate contributions from liquid phase processes, we studied the spreading of air peaks on uncoated glass beads (153, 154) first used in a study of column performance by Littlewood (130). With uniform spherical beads it is possible to prepare a column whose geometrical characteristics are known. In order to increase the upper limit of the effective velocity range larger beads were used and a systematic study of the effect of bead to column diameter on column efficiency was carried out to separate any such effect from that of particle size alone. This led to the observation that the column to particle diameter ratio had a major influence on the plate height. This discovery was made concurrently with a similar discovery by Sternberg and Poulson (155).

From the introduction it is seen that for discussion purposes the HETP equation could be written

$$H = A + B/u + (1/A' + 1/C_g u)^{-1} + C_1 u$$

incorporating both 'classical' and 'coupled' eddy diffusion concepts. For unsorbed substances C_1 is zero and the pressure dependent quantities u and D_g appear only as the pressure independent ratio u/Dg. The study of air peaks may thus be fully described by the simplified equation of

$$H = A + 2\gamma D_g^o/u_o + (1/A' + D_g^o/(\omega d_p^2 u_o))^{-1}$$

when $A' = \infty$, $H = A + B/u + C_g u$ ——(1). This equation may be cast into a reduced form, $h = v^{-1} + \alpha + v$ where $h = H/(BC)^{\frac{1}{2}}$. $v = u(C/B)^{\frac{1}{2}}$ and $\alpha = A/(BC)^{\frac{1}{2}}$. A series of plots of log h against log v are shown in Figure 11. The curves are symmetrical about the log v axis with minima at $h = 2 + \alpha$ and $v = 1$. The asymptotes to all the curves are the same and if equation (1) is obeyed it should be possible to determine α by curve fitting. The critical region for determining α is clearly that around the minimum.

When A = 0 the equation becomes $H = B/u + (1/A' + 1/C_g u)^{-1}$ the form favoured by Giddings. Writing $\alpha' = A'/(BC)^{\frac{1}{2}}$ and h and v as before, the reduced form of this equation is $h = v^{-1} + (1/\alpha' + 1/v)^{-1}$. Plots of log h against log v for different values of α' are given in Figure 12.

The curves now show inflection points only for $\alpha' > 1$. The minimum is then at $h = 2 - 1/\alpha'$, $v = (1 - 1/\alpha')^{-1}$. In this case the asymmetry of the curve can be used to determine α'. While this method of plotting data, suggested by Knox, provides a general method for the determination of A and A' given the theoretical curves for all possible combinations of α and α', a reasonable estimate of these values can be obtained by examining the minimum and the asymmetry of the curve respectively.

The aim of the research described in this section was thus to clarify the inter-relationship of eddy diffusion and gas phase mass transfer, and determine their respective contributions to the HETP of unsorbed peaks in columns packed with glass beads.

CHAPTER IV

EXPERIMENTAL : GENERAL CONSIDERATIONS

I. Essential Requirements

The block diagram of the basic GC apparatus is shown in Figure 13. Although the essential requirements are extraordinarily simple a thorough understanding of the properties and mechanisms of the component parts is essential for the attainment of maximum system performance. The study of air peaks of widths down to less than a second places stringent demands on the equipment (122, 145, 155, 156). In order to isolate effects due to column geometry alone, any solute spreading in the rest of the apparatus must be minimised and any adsorption on the solid support eliminated. This is the art of GC.

II. The Injector

Ideally it was required automatically and instantaneously to inject a sharp pulse of about one microlitre of gas (157-159). In 1961 no such commercial injector was available. After some initial investigation a "hammer" type injector was constructed after Scott (160) (Figure 14). The injector chamber was continuously purged with ethylene, the sample gas. The ethylene pressure was maintained slightly below the column inlet pressure by mounting the rubber bladder containing the ethylene inside a glass bulb itself held at a pressure slightly below that of the column by a slow leak through it from the column inlet to the atmosphere. All connections to and from the injector were of nylon. An injection of about 1 mm^3 was achieved by energising the solenoid which worked the hammer and sent a pulse of gas into the column. Because the column inlet pressure was always greater than the injector chamber pressure, the tube from the injector to the column was continuously purged with pure carrier gas, resulting in a 'plug' of sample with no tailing. It was found, however, that the time constant of this injector was of the order of 0.2 seconds and it was difficult to control the sample size especially when the inlet pressure was altered.

As a result the injector shwon in Figure 15 was built. This model gave reproducible, instantaneous plug-type injection. It consisted of a 3/16 inch diameter steel rod with two transversely drilled holes as shown. The rod could move inside a closely fitting teflon sleeve which was itself tightly held in the steel tube. The holes were drilled such that sample gas could be passed through one hole while carrier gas passed through the other. On activating the solenoid the sample hole was brought into the carrier gas line and a sample injected. The main difficulty was leakage of sample into the column at low column pressures. The problem of leakage was finally solved by thermostatting the whole injector by a closely fitting waterjacket. One of the main causes of wear was the different coefficient of expansion of the PTFE and the brass. Repeated use caused the spindle to tighten in the sleeve and eventually the spindle became worn and loose.

III. The Detector

The differential detector measures some property related to the concentration of components in the carrier gas stream and the resulting chromatogram is a series of peaks. At least 24 different detectors have been reported for use in GC (356-7). Detectors suitable for submicrogram analysis include the thermionic ionisation detector (162), spark gap detector (163, 351), glow discharge detector (164, 347-350), radiofrequency glow detector (165, 354), radiological detector (166, 342-3), electron-affinity detector (167, 344), electron mobility detector (345-6), radioactivity detector (168), coulometer (169), infra-red absorption detector (170, 338-341), and mass spectrometer (171). Of the detectors employing combustion in a flame, viz. hydrogen-flame detector (172), the emissivity detector (173) and the flame-ionisation detector (174-176, 352-3), the latter has the greatest potential for low level analysis and was the detector used throughout this work.

There have been numerous detailed studies of this detector (177-181). Our design with the basic circuitry, is shown in Figure 17 after Desty (178). The detector base, chamber and lid were of brass. A porous stainless steel disc (Metal and Plastic Components Ltd., Birmingham) was fitted into the base to provide a uniform flow of air to the flame chamber. The air, which also serves to remove water vapour, passed out of the chamber through a series of small holes bored in the detector lid.

The upper electrode was a brass rod 0.09 inches in diameter mounted directly above the jet which formed the other electrode. The jet had a tip of platinum, to prevent thermionic emission of electrons, and an internal diameter of 0.0135 inches. Platinum is also favoured by its chemical inertness. It has been shown (182) that electrodes consisting of loops, wires, gauze or plates have similar efficiencies, although a slightly increased ionisation efficiency was obtained with the design in Figure 17b. In his detailed study Sternberg used a 5 mm diameter platinum ring as collector 5 mm above the tip of the jet and for this reason a platinum 'hat' was fitted to the brass electrode as shown. Onkienong, however, showed that electron capture is complete in any circumstances by finding that a probe electrode placed above the collector gave no signal, while the collector gave no signal when the probe was placed below it.

McWilliam and Dewar in their original description used the jet as the anode at a potential of about 200 v. Many workers have since shown that the upper electrode should be the anode since this confers sensitivity and stab-:ility, possibly a result of the shorter travel for the slower moving positive ions thereby minimising recombination. It is generally agreed that 200 volts represents saturation conditions for a variety of detector designs with the electrode spacing as small as is consistent with stability. It is interesting to note that Novak and Janak (183) placed the electrode in the flame at varying distances from the orifice. Condon et al. (184) found that the use of a heavy-walled jet reduced the noise probably through the metal acting as a heat sink and reducing flame temperature.

The linearity of the detector has been shown to extend over 7 orders of magnitude up to about 0.5 to 1% by volume of the total flame gas (185). With hydrocarbons the sensitivity of the detector is roughly proportional to the carbon content of the solute (181, 186-7). The basic circuity is shown in Figure 17.

This detector was used throughout the research. It has many advantages over the argon detector which was tried at the start but discarded. It gave no trouble apart from corrosion of the collector electrode which was occasion-:ally cleaned and polished. It did not require thermostatting and the response was effectively insensitive to burner gas composition and flow rate.

The noise level (355) and background current could not be detected on the most sensitive range of the amplifier. The background current in a very stable and clean flame has been found to be 5×10^{-14} amp (184). Without adequate air filtration this value rises to about 10^{-12} amp. The very small effective volume of a few microlitres, its very fast response, its sensitivity and stability made it ideal for our studies. The flow rates used were 25 ml/min for hydrogen and 900 ml/min for air. An excessive air supply can cause turbulence in the flame zone with resultant noise. The one great disadvantage was its lack of response to inert gases which prevented the use of air in the study of 'air' peaks. As a result ethylene was used as solute. The mechanism of response is discussed in the Appendix.

IV. The Electronic Equipment

The block diagram of the electronic equipment supplied by Bruce Peebles Limited, Edinburgh, is shown in Figure 18. This is self-explanatory. The machine was christened 'Sir Frederick'. The most sensitive range of the amplifier, of time constant 0.01 secs, gave 5 volts per 10^{-10} amp input. The signal was fed to an integrator (standard 'C-Scope') and peak-holding unit which stopped an electronic timer, started by an electrical impulse from the solenoid. Thus for each injection, retention time (secs), peak height (volts) and peak area (volt secs) were recorded. Peak symmetry was checked on a $\frac{1}{4}$-second Honeywell-Brown recorder at a chart speed of 12 inches a minute. A typical 'air' peak shown in Figure 19 illustrates the high degree of symmetry achieved.

V. Columns and Packing Materials

The columns were straight lengths of pyrex, soda glass or stainless steel. The capillary columns, which were coiled, were of nylon. The column internal diameter was measured by filling the column with water or mercury and weighing the liquid. It was checked with a micrometer gauge.

In the column efficiency studies the packing was spherical beads of glass, polyvinylchloride or stainless steel. The beads were cleaned by washing with

various organic solvents. The diameters of the beads were measured by aligning them in a right-angled groove in a length of brass so that they touched and noting the length and number. The diameters of the largest beads were measured with a micrometer screw gauge.

The columns were filled vertically through a filter funnel. They were tapped and vibrated until the level of the beads did not change with further tapping. The column connections are shown in Figure 16. The nylon could be drawn down by stretching to ensure tightness of fit. The packed columns were terminated with fine copper gauge screens instead of the usual glass or cotton wool plugs, to avoid an undesirably large instrumental spread and peak asymmetry. Particular care was taken to eliminate any unswept dead volumes in the direct line between the injector and detector.

VI. Calculation of Results

Plate heights were evaluated from the peak width W and the retention time t_R. The peak width W was defined as Integral/Peak Height. Since the integrator recorded 1.20 volt for every volt sec input,

$$W_{(sec)} = \frac{\text{Integral}}{\text{Peak Height}} = \frac{\text{Peak Area}}{1.20 \times \text{Peak Height}}$$

For a gaussian curve, area/height = $\sqrt{2\pi} \times \sigma_t$

Hence $W = \frac{\sqrt{2\pi}}{1.20} \times \sigma_t$. The observed plate height is then

$\hat{H} = L(\sigma_t / t_R)^2 = 1.44/2\pi W^2 \bar{u}^2/L$ where $t_R = L/\bar{u}$ Thus $\hat{H} = 0.232\, W^2\bar{u}^2/L$

With the improved version of the integrator the response was 0.96 volt sec per volt sec input and $\hat{H}$ was given by

$$\hat{H} = 0.350\, W^2 \bar{u}^2/L$$

In the figures and tables $\hat{H}$ is given as H. In the later column work the peak height was taken from the recorder chart as the peak height unit became irreproducible. The integral was also read on the recorder to keep the error as small as possible.

VII. Method of Allowance for Extra-Column Spreading

Although care was taken to minimise extra-column spreading the use of a short column packed in the same manner as the longer column makes it possible to subtract out all end effects, including that of the detection and injection systems (127). Since the total spreading due to a number of independent or consecutive processes is given by

$$\sigma^2 = \sigma_1^2 + \sigma_2^2 + \sigma_3^2 + \ldots\ldots\ldots$$

the spreading due to the column alone may be obtained from the total spreading and that due to the apparatus from the formula

$$W^2_{\text{column}} = W^2_{\text{total}} - W^2_{\text{apparatus}}$$

VIII. Pressure Corrections

The observed plate height,

$$\hat{H} = L/(\sigma_t/t_R)^2 = \sigma_t^2 \bar{u}^2/L$$

as shown in the appendix is slightly different from the local plate height H_g^o due to the effects of the pressure drop along the column. However in all our experiments the correction was negligible and we have taken $H_g^o \equiv \hat{H}$. Thus,

$$\hat{H} = \sigma_t^2 \bar{u}^2/L \equiv H_g^o = 2\gamma D_g^o/u_o + f(dp, D_g^o, u_o),$$

and for the evaluation of the dependence of H_g^o on various parameters we have plotted $\log_{10} \hat{H}$ against $\log_{10} u_o$ where u_o is calculated (see appendix) from $\bar{u} = L/t_R$ and the inlet/outlet pressure ratio.

CHAPTER V

THE SPREADING OF UNSORBED PEAKS IN CAPILLARY AND PACKED COLUMNS

I. Experiments with the 'Hammer' Injector

Two columns were studied a) an open tube of length 1664 cm and id. 0.88 mm and b) a packed column consisting of 4 x 150 cm lengths of 3.80 mm diameter tubing packed with 0.50 mm diameter glass beads. The packing was retained by fine gauze screens and the 4 lengths were connected together by short lengths of 2 mm id. tubing used to retain the screens. The short columns consisted of a 40 cm length of capillary and 4 x 10 cm lengths of packed column joined in the same way as the longer lengths. With the short columns the peak widths tended to a constant value with increasing velocity, suggesting that the time constant of the injector was too high. At the highest gas velocities $W^2_{apparatus}$ accounted for as much as 20% of W^2_{total} showing the necessity for the extra-column spreading correction (chapter IV.(VII.), Figures 20, 21, Tables 1, 2). The logarithmic plots of HETP against outlet linear gas velocity are shown in Figures 22 and 23 (Tables 1 and 2). The derived experimental parameters are given in Table 3.

For the capillary column the Golay equation predicts a minimum HETP of $r/1.732 = 0.26$ mm, somewhat lower than the experimental value of 0.34 mm and $u_{opt} = \sqrt{48}\, Dg/r = 26$ cm.sec^{-1} from which $Dg = 0.16$ cm^2 sec^{-1}. This agrees well with published data (see later).

For the packed column the best fit of the experimental and theoretical curves yields $\alpha_{max.} = 0.5$ giving $A < 0.14$ mm $= 0.28$ dp and the van Deemter constant $\lambda < 0.14$. There is no evidence of asymmetry in the plot, therefore $\alpha' \geqslant 10$ and may be infinite. The values of δ and ω depend on the values taken for α and α' and various reasonable combinations are shown in Table 3.

If $\alpha' = \infty$, $H_{min.} = (2 + \alpha)\ (2\ \delta\omega)^{\frac{1}{2}} dp$, and

if $\alpha = 0$, $H_{min.} = (2 - 1/\alpha')\ (2\ \delta\omega)^{\frac{1}{2}}\ dp$.

The δ values 0.75 are in reasonable agreement with published data (130, 134).

For inter-channel diffusion the generalised non-equilibrium theory predicts a value of ω of about 0.3 for unsorbed solutes (R = 1). Our value of about 0.3 for the packed column is in reasonable agreement with that deduced by Giddings from Norem's data (103, 122). The value ω =0.3 implies that the solute molecule must diffuse about half a particle dia-:meter within the time constant of the equilibrium process. Using the Kozeny-Carman equation (189) Knox calculated that a column of randomly packed spheres has the same linear flow resistance as a capillary whose radius is 0.135 times the particle diameter. The value of the Cg term calculated on the basis of the Golay equation for a tube of this radius and for k = 0 is $dp^2/1300\ Dg$ giving $\omega = 1/1300$. Thus ω is some 400 times larger in the packed column than in an open tube of the same resis-:tance to flow. It is the high specific permeability of the capillary with a correspondingly low mass transfer coefficient which makes it so suitable for high speed analysis.

II. Experiments with the Improved Injector and Electronics

Before investigating the effects of column/particle diameter ratio, the experiments carried out with the 'hammer' injector were repeated along with additional checks on the new equipment.

The reproducibility of the improved equipment is shown in Figures 24 and 25 for 3 ranges of the amplifier, i.e. 5 volts for 10^{-8}, 3×10^{-9} and 10^{-9}amp. It can be seen that the peak width for a given integral value increases slightly as the range (i.e. sample size) increases, showing a small dependence of H on sample size (190). All further measurements were made on the 3×10^{-9} amp range giving a maximum systematic error in W of 2% and in H of 4%. The reproducibility of H was about 5%.

Experiments with both long and short packed columns were repeated and two capillary columns differing greatly in length and internal diameter were investigated. For both columns experiments with short lengths showed that the spreading in the rest of the apparatus was negligible. The data were more consistent than those obtained in the original experiments, and are given in Figures 26 and 27 and Tables 4 - 6. The derived column parameters are listed in Tables 7 and 8. There is excellent agreement between the

experimental and theoretical values of H_{min} for the open tubes (Table 7). This agreement showed that the performance of the apparatus as a whole was satisfactory and that it did not introduce any extraneous peak broadening. The smallness of the short column corrections was also an independent indication that dead volumes and time constants were sufficiently small.

Table 8 gives the parameters for the packed column. It can be seen that these have changed considerably. γ and ω are now 0.6 and 0.06 respectively. Although α' is still ≥ 10, α is > 1 and is about 1.2. This however gives the same value for A as found previously, namely A = 0.15 mm = 0.3 dp and λ = 0.15.

i. Conclusion

The classical eddy diffusion term is evidently not zero although it is much smaller than unity, the value predicted by the classical theory. Although at the maximum gas velocity used there was no evidence for coupling, which would show up as a flattening of the curve, the coupling theory has not been disproved. Coupling may still become significant at higher velocities relative to $u_{optimum}$.

III. Particle-to-Column Diameter Ratio Effect

i. Introduction

As a result of the above work it was decided to increase the upper limit of the effective velocity range by using larger glass beads. Although it has generally been assumed that in packed columns the lowest H is obtained with the smallest particles and that the column diameter (dc) has little influence on H on the analytical scale, recent studies (155, 191-2) have indicated that unexpectedly good performance is obtained when particles larger than 1/8 of the column diameter are used. It was therefore necessary to carry out a systematic study of the effect of bead-to-column diameter ratio (dp/dc) on column efficiency in order to separate any such effects from those of particle size alone. During the course of the present work Sternberg and Poulson (155) published a study of the same effect which showed clearly the importance of column/particle diameter ratio on column efficiency. Our more comprehensive data is in good agreement with their results.

ii. Experimental

The columns used in this part of the work were straight lengths of stainless steel of internal diameters 2.40 mm (I), 4.52 mm (II) and 6.12 mm (III). Glass beads of the following mean diameters were used: 2.08, 1,32, 0.97, 0.85, 0.62 and 0.50 mm. Ball-bearings (id. = 3.97 and 5.55 mm) were also used for column III. As before, nitrogen was the carrier gas and ethylene the sample gas. The performance of the system had already been shown to be satisfactory by the experiments on open tubes. Experiments with short packed columns again showed that the extraneous spreading was negligible.

The column performance was measured over a wide range of particle-to-column diameter ratio. For each column the following parameters were measured over a range of carrier gas velocities: retention time, peak height, peak area, inlet pressure, outlet pressure and colume flow rate.

Runs were first carried out with an 'uncut' length (L = 468 cm) of 6.12 mm id. packed tube (column IV). This column was difficult to manip-:ulate and being too long to be filled vertically in the laboratory it was packed at the head of the department stairs, but it was then difficult to tap. Columns I, II and III could be clamped vertically in the laboratory with the top just missing the ceiling.

iii. Results and Discussion

The data for columns I, II, III and IV are given in Tables 9-12, 13-16, 17-20 and 21-27 respectively. The main derived column parameters are given in Tables 28 and 29. The data is plotted in Figures 28-32. The log H/log u_o curves for column IV (Figure 32) are above the corresponding curves for column III (Figure 31). This must be attributed to bad packing and shows the importance of this in determining column efficiency. Apart from experiments with dp = 4.96 mm data for column LV will not be considered in the discussion which follows. They will, however, be discussed later in connection with turbulence. The main features of the results are given in the next paragraph.

In agreement with Sternberg and Poulson it was found that with only 3 exceptions, all for column III, $H_{min} \leq dp$. Figure 28, (Table 9), shows a plot

of W against t_R for various dp for column I. The curves are almost parallel and for a given t_R value (= 50 secs), W increases almost linearly with dp (Figure 33a); however from the plot of log H_{min} against dp in Figure 33b the dependence of H on dp can be seen to decrease with increasing particle diameter.

The dependence of H_{min}/dp on dp/dc is shown in Figure 34 (Table 28), H_{min}/dp is seen to decrease sharply with increasing dp/dc indicating that for a fixed diameter column, the price paid in plate height for using larger particles in order to diminish pressure drop is not as severe as would be expected on the assumption that H_{min}/dp was independent of dp/dc. The value obtained with the glass column (L = 593 cm) studied previously is seen to fit the curve as does the point (dp/dc = 0.81) obtained with column IV.

The van Deemter coefficients are given in Tables A, B and C and were deter-:mined by curve fitting but, due to lack of points, a considerable range of parameters gave an acceptable fit. The values given in the table must there-:fore be regarded as approximate.

Plots of A/dp and A/dp against dp/dc are shown in Figures 35a and 35b. Although curve fitting is often hindered by the lack of points the plots of the deduced A values do show a definite trend. For a given particle size A is seen to increase with increasing column diameter. A/dp is seen to decrease rapidly with increasing dp/dc ratio as found with the H_{min}/dp plot (Figure 34). In all cases A lies between zero and 0.5 dp which disagrees with Sternberg and Poulson who found that in all cases A was negligible within experimental error.

The variation in γ is small (Table 29). Taking $D_g = 0.165\ cm^2\ sec^{-1}$, for dp/dc equal to 0.26, 0.35 and 0.55 on column I, γ is 0.69, 0.74 and 0.83 res-:pectively for respective porosities of 0.49, 0.60 and 0.72. These points are marked on Figure 57 supporting the validity of the theoretical approach to γ discussed in section II. It is interesting to note that on the whole my values for γ are about 10% greater than those obtained by Sternberg and Poulson for glass beads. γ is however more accurately determined using the arrested elution technique described in section II.

The ω values are all smaller than those predicted from the theory of Giddings. From the plot of ω against dp/dc (Figure 36) it can be seen that for the wider diameter columns ω is strongly dependent upon the ratio dp/dc but

this dependence is much less for column I. The values of ω are in reasonable agreement with those obtained by Sternberg. As would be expected, ω decreases with increase in porosity, i.e. as the packed column approaches the capillary column.

The curves in Figures 29-32 show varying degrees of asymmetry which implies either coupling or turbulence or both (see later) since the asymmetry cannot be due to experimental error. Unfortunately, because of the lack of points at high velocities, the constants for the coupled form cannot be determined with any degree of precision. Because of the irreproducibility of the right hand sides of the plots turbulence is probably occurring in the flattest cases. This is supported by the liquid studies of Knox who has shown that tortuosity comes in at lowest Re values for smallest dp/dc values. This is discussed in detail later but it is interesting to note that for column I the asymmetry increases with decreasing dp/dc values (Figure 29).

Due to the high pressure drop across the connection to the detector for the wider bore columns with associated greater volume flow rates, the ϵ values are only reliable for column I and these are given in Table 29. Porosity as a function of dp/dc for column I is shown in Figure 37. The pressure drop is very sensitive to the porosity, an increase in porosity from 0.4 to 0.6 increasing the specific permeability (defined as $B_o = \eta L F_o P_o / A_c \Delta_p \bar{p}$ and given for a packed column by the Kozeny-Carman equation as $B_o = \epsilon/180\ dp^2 (\epsilon/1-\epsilon)^2$), nearly 8-fold. Since capillary columns with a porosity of unity can give good plate heights there should be no reason why an increase of porosity of packed columns should lead to impaired performance and this is seen to be the case. For dp/dc = 0.40, ϵ = 0.6 and dp/dc = 0.2, ϵ = 0.48, in reasonable agreement with Sternberg and Poulson though in general my ϵ values are higher than his for the same dp/dc value. The porosity of randomly packed spheres dp/dc < 0.1 is usually about 0.4. The porosity was given by $\epsilon = {}^{t}R(air)\ F_o P_o / A_c L \bar{P}$ where A_c and L are the column cross-sectional area and length respectively. With the largest beads it was found that the pressure drop across the column was considerably greater than expected due to the flow being obstructed by the packing. This, of course, is avoided in the drawn-down glass-capillary columns of Halasz where the flow channel is kept open by the particles sticking to the walls.

Table 1 (Figures 20, 22)

Capillary Column Data: d_c = 0.088 cm. T = 18°C. p_o = 76.0 cm.

L_1 = 1664 cm.				L_2 = 38.0 cm.		L_3 = 1664 cm.			
W	$\bar{u}$	W	$\bar{u}$	W	$\bar{u}$	log $\bar{u}$	1+log H_{mm}	log $\bar{u}$	1+log H_{mm}
0.33	71.0	1.19	14.5	1.00	5.9	1.852	0.64	1.162	0.57
0.34	68.5	1.37	13.5	1.28	5.2	1.836	0.65	1.130	0.64
0.39	65.0	1.51	12.2	1.65	4.3	1.813	0.79	1.087	0.64
0.42	62.5	1.75	11.2	2.55	3.4	1.796	0.85	1.050	0.70
0.43	59.7	2.08	10.3	3.50	3.0	1.776	0.84	1.013	0.79
0.45	53.5	2.10	9.7	3.20	3.2	1.729	0.78	0.986	0.74
0.43	49.3	2.53	8.5	0.47	11.0	1.694	0.67	0.930	0.79
0.44	46.0	0.41	49.2	0.44	12.8	1.663	0.63	1.692	0.62
0.46	43.0	0.39	45.9	0.43	13.7	1.634	0.62	1.620	0.55
0.49	39.1	0.42	39.9	0.39	15.7	1.592	0.60	1.590	0.53
0.52	35.5	0.44	41.7	0.33	18.3	1.550	0.58	1.260	0.53
0.55	32.6	0.51	35.0	0.34	19.9	1.514	0.56	1.114	0.60
0.61	28.2	0.70	24.5	0.31	24.4	1.450	0.53	0.790	0.96
0.68	24.3	0.93	18.2	0.28	27.1	1.386	0.49	0.712	0.98
0.77	22.9	1.35	13.0	0.27	30.3	1.360	0.56	1.017	0.68
0.75	24.8	2.50	8.30	0.25	32.7	1.394	0.62	1.045	0.68
0.68	25.8	4.20	6.15	0.23	35.0	1.412	0.55	0.810	0.89
0.76	24.1	5.30	5.03	0.23	38.5	1.382	0.60	1.702	0.67
0.78	22.5	1.85	10.4	0.23	43.0	1.352	0.57	1.754	0.72
0.85	20.3	1.72	11.1	0.22	52.5	1.308	0.54	1.882	0.74
0.87	19.2	2.55	8.5	0.22	75.0	1.284	0.52	1.868	0.76
0.95	17.9	3.80	6.32	0.20	113.0	1.253	0.54	1.731	0.75
1.00	16.9	0.43	50.0	0.22	126.0	1.228	0.54	1.200	0.57
1.09	15.8	0.41	56.6	0.22	108.0				
1.10	15.8	0.37	66.4	0.22	63.0				
0.43	53.8	0.35	73.8	0.23	46.5				
		0.46	43.1						

Table 2 (Figures 21, 23)

Packed Column Data: dp = 0.050 cm. T = 18°C. p_o = 76.0 cm.

L_1 = 593.0 cm.		L_2 = 28.0 cm.		L = 593.0 cm.	
W	$\bar{u}$	W	$\bar{u}$	log u_o	1 + log H_{mm}
1.54	9.4	0.31	18.2	0.975	0.87
1.16	12.3	0.30	20.5	1.089	0.85
0.94	15.5	0.28	21.4	1.189	0.87
0.86	17.2	0.25	25.3	1.236	0.88
0.80	19.9	0.23	29.9	1.299	0.95
0.73	21.8	0.22	34.0	1.339	0.94
0.52	35.3	0.20	45.5	1.548	1.06
6.30	2.8	0.16	81.8	0.452	1.07
5.62	3.2	0.83	6.9	0.998	1.06
3.80	4.3	1.00	5.9	0.628	0.97
2.75	5.6	1.15	4.4	0.751	0.93
1.95	7.5	0.35	15.0	0.872	0.86
2.11	6.8	0.42	12.1	0.835	0.85
2.30	6.4	0.64	7.4	0.806	0.88
1.88	7.8	2.00	2.6	0.994	0.88
1.68	8.6	0.45	12.4	0.937	0.86
1.54	9.5	0.51	10.2	0.975	0.87
1.33	10.8	0.61	8.7	1.033	0.86
3.00	5.2	1.44	3.8	0.715	0.95
3.56	4.7	2.75	2.8	0.675	1.01
4.32	3.9	3.80	2.2	0.601	1.04
5.28	3.4	1.30	3.8	0.526	1.07
5.82	3.0	1.06	4.8	0.474	1.05
0.62	28.6	0.88	5.9	1.456	1.02
0.67	26.8	1.74	3.0	1.420	1.04
0.70	24.4	1.52	3.4	1.344	0.98
0.75	22.1	2.30	2.3		

Table 3

Experimental Parameters Obtained Using 'Hammer' Injector

	Packed			Capillary
H_{min}	0.071 cm			0.034 cm
u_{opt}	11 cm sec^{-1}			26 cm sec^{-1}
α	< 0.5			Zero
α'	> 10			Infinite
D_g (C_2H_4 in N_2)				0.16 $cm^2 sec^{-1}$
Tortuosity γ	$\alpha = 0$	$\alpha' = \infty$	0.85	
	$\alpha = 0.5$	$\alpha' = \infty$	0.70	
	$\alpha = 0$	$\alpha' = 10$	0.75	
ω	$\alpha = 0$	$\alpha' = \infty$	0.30	
	$\alpha = 0.5$	$\alpha' = \infty$	0.23	
	$\alpha = 0$	$\alpha' = 10$	0.36	
A and A'	< 0.014 cm		> 0.35 cm	
A/dp and A'/dp	< 0.28		> 7	
$(BC)^{\frac{1}{2}}$	0.035 cm			0.017 cm
H_{min}/dp and $H_{min}/2r$	1.42			0.39

Table 4 (Figure 26)

Glass Bead Column: L = 593 cm. dp = 0.05 cm. Po = 74.0 cm. T = 20°C

ΔP_{cm}	f_1	u_o	log u_o	H_{mm}	1 + log H
12.3	0.924	16.6	1.220	0.47	0.671
14.3	0.911	18.4	1.264	0.49	0.690
16.9	0.895	23.5	1.371	0.52	0.713
20.4	0.877	29.1	1.464	0.55	0.738
24.4	0.858	35.4	1.549	0.55	0.738
28.8	0.838	42.8	1.631	0.60	0.775
10.9	0.927	14.2	1.151	0.50	0.653
9.8	0.938	12.8	1.106	0.46	0.660
8.5	0.947	11.3	1.054	0.46	0.659
8.0	0.948	10.3	1.013	0.46	0.667
6.4	0.956	8.2	0.912	0.49	0.689
7.1	0.956	9.1	0.958	0.47	0.674
5.9	0.961	7.6	0.878	0.53	0.727
4.5	0.971	5.7	0.756	0.57	0.757
3.4	0.980	4.2	0.620	0.75	0.874
13.8	0.911	18.7	1.271	0.45	0.652
11.5	0.926	15.4	1.188	0.44	0.646
11.0	0.927	14.7	1.167	0.45	0.650
12.7	0.920	17.2	1.235	0.43	0.637
17.0	0.895	23.7	1.375	0.48	0.683
5.8	0.961	7.4	0.867	0.52	0.716
4.6	0.975	6.2	0.789	0.57	0.754
26.5	0.848	39.0	1.591	0.61	0.786
22.5	0.865	32.2	1.507	0.52	0.717
18.7	0.890	26.2	1.418	0.49	0.694
14.5	0.910	19.9	1.299	0.45	0.650
11.8	0.937	15.8	1.200	0.43	0.635
10.5	0.933	14.0	1.146	0.45	0.656
4.3	0.975	5.3	0.723	0.60	0.781
3.5	0.980	4.5	0.651	0.67	0.828
3.2	0.980	4.0	0.602	0.73	0.864

Table 5 (Figure 27)

Capillary Column Data: L = 3970 cm d_o = 0.088 cm p_o = 74.0 cm. T = 20°C

Δp_{cm}	f_1	u_o	log u_o	H_{mm}	1 + log H
9.5	0.938	94.7	1.976	0.52	0.717
10.4	0.933	105.6	2.024	0.55	0.743
12.3	0.924	127.7	2.082	0.62	0.795
8.5	0.945	86.1	1.935	0.46	0.658
7.7	0.947	76.7	1.885	0.42	0.627
6.4	0.956	63.0	1.299	0.36	0.559
5.4	0.966	52.0	1.716	0.33	0.520
4.6	0.971	43.0	1.634	0.29	0.460
3.8	0.975	35.6	1.551	0.29	0.455
2.5	0.985	22.9	1.360	0.26	0.415
2.1	0.985	18.7	1.272	0.26	0.421
1.7	0.990	14.6	1.165	0.31	0.495
1.4	0.990	12.0	1.078	0.34	0.529
1.1	0.990	10.0	1.000	0.42	0.622
0.8	0.995	7.25	0.860	0.56	0.748
0.9	0.995	8.0	0.903	0.50	0.701
1.1	0.990	10.3	1.014	0.39	0.594
3.2	0.980	27.9	1.446	0.26	0.416
1.5	0.990	12.8	1.055	0.36	0.552
1.2	0.990	10.5	1.019	0.39	0.587
1.0	0.990	9.33	0.970	0.42	0.625
0.9	0.995	8.37	0.923	0.49	0.688
0.8	0.995	7.47	0.873	0.50	0.695
0.8	0.995	7.47	0.873	0.53	0.723

Table 6 (Figure 27)

Capillary Column Data: L = 635 cm. d_c = 0.288 cm. p_o = 74.0 cm. T = 20°C

Δ p cm	f_1	u_o	log u_o	H mm	1 + log H
1.0	0.990	21.0	1.321	1.30	1.113
1.2	0.990	22.5	1.351	1.36	1.134
1.4	0.990	27.1	1.433	1.59	1.202
1.6	0.990	31.7	1.500	1.79	1.252
1.7	0.990	34.0	1.532	1.88	1.273
2.0	0.985	38.3	1.583	2.13	1.328
2.2	0.985	41.8	1.621	2.20	1.343
2.4	0.985	45.8	1.660	2.53	1.403
2.5	0.985	50.1	1.700	2.73	1.436
3.4	0.980	56.8	1.754	3.13	1.496
3.9	0.975	60.8	1.784	3.18	1.503
4.3	0.972	68.5	1.836	3.71	1.569
1.1	0.990	19.9	1.299	1.24	1.092
1.0	0.990	18.3	1.261	1.15	1.062
0.9	0.993	15.6	1.192	1.05	1.021
0.7	0.995	13.5	1.130	0.99	0.996
0.6	1.000	11.8	1.073	0.97	0.985
0.6	1.000	10.3	1.012	0.95	0.977

Table 7.

Experimental Parameters for the Capillary Columns.

	I	II
Length	3970 cm.	635 cm.
Diameter	0.088 cm.	0.288 cm.
H min	0.25 mm.	0.84 mm.
r/1.732	0.25 mm.	0.83 mm.
Dg	0.17 $cm^2 sec^{-1}$	0.17 $cm^2 sec^{-1}$

Table 8.

Experimental Parameters for the Packed Column.

Length	593 cm.
Tube Diameter d_c	0.38 cm.
Bead Diameter d_p	0.50 mm.
α	1.2
A/d_p	0.3
γ	0.6
H min	0.43 mm.
H min/d_p	0.86
d_p/d_c	1.31
α'	$>10.$
A'/d_p	>7
Cg	9.3 x 10-4
ω	0.06

Table 9 (Figure 28)

Data for Column I: Variation of W with Residence Time (RT) for different d_p.

Column empty		dp = 0.50 mm.		dp = 0.62 mm.		dp = 0.85 mm.		dp. = 1.32 mm	
RT	W	RT	W	RT	W	RT	W	RT	W
14.5	0.67	13.4	0.35	21.5	0.64	14.5	0.56	16.5	0.86
19.4	0.81	16.4	0.43	30.3	0.91	18.6	0.68	12.3	0.70
30.2	1.18	22.5	0.58	47.4	1.57	32.2	1.15	28.0	1.26
50.6	2.03	27.2	0.75	61.4	2.20	54.5	2.05	46.0	2.03
85.5	4.13	43.2	1.31	100.0	4.60	12.7	6.43	64.4	2.93
25.0	1.00	59.4	2.04	23.4	0.69	67.6	2.72	83.0	4.08
40.0	1.58	95.0	4.50	14.7	0.44	86.0	3.76	20.0	0.98
64.0	2.75	20.0	0.52	12.9	0.38	25.0	0.75	34.0	1.50
57.5	2.38	35.0	1.00	9.5	0.29	45.0	1.63	40.0	1.75
		52.5	1.70	25.0	0.75	63.5	2.50		
		69.0	2.50	40.0	1.25	75.0	3.13		
				55.0	1.90				
				71.0	2.70				

Table 10 (Figure 29)

Data for Column I (d_c = 2.40 mm) L = 310 cm. T = 20°C

Unpacked Column p_o = 76.0 cm.

△ p cm	f_1	u_o	log u_o	H mm	1 + log H
		21.3	1.328	0.97	0.985
		15.9	1.201	0.79	0.897
		10.2	1.009	0.69	0.841
		6.1	0.785	0.73	0.865
		3.6	0.556	1.09	1.037
		12.3	1.090	0.72	0.859
		7.7	0.887	0.70	0.844
		4.8	0.683	0.83	0.921
		5.4	0.729	0.77	0.887

Particle Diameter = 0.50 mm p_o = 75.5 cm.

△ p cm	f_1	u_o	log u_o	H mm	1 + log H
18.4	0.890	26.0	1.414	0.31	0.485
14.9	0910	20.9	1.320	0.31	0.490
11.0	0933	14.8	1.170	0.30	0.480
8.6	0947	12.1	1.081	0.34	0.536
5.7	0961	7.5	0.874	0.42	0.619
4.1	0975	5.4	0.728	0.53	0.727
2.6	0985	3.3	0.521	0.86	0.935
11.7	0929	16.7	1.223	0.31	0.486
7.2	0952	9.3	0.969	0.37	0.569
5.0	0971	6.2	0.791	0.47	0.676
3.3	0980	4.6	0.661	0.60	0.776

Table 11 (Figure 29)

Data for Column I (d_c = 2.40 mm) L = 310 cm. T = 20°C

Particle Diameter = 0.62 mm p_o = 76.0 cm

△ p cm	f_1	u_o	log u_o	H mm	1 + log H
7.1	0.956	15.1	1.179	0.41	0.610
5.2	0.966	10.6	1.025	0.41	0.614
3.4	0.980	6.7	0.825	0.50	0.697
2.5	0.985	5.1	0.710	0.58	0.764
1.6	0.990	3.1	0.497	0.98	0.991
6.5	0.956	13.9	1.142	0.39	0.593
10.4	0.933	22.6	1.354	0.40	0.601
12.0	0.924	26.0	1.415	0.40	0.600
16.1	0.902	36.2	1.559	0.42	0.625
6.0	0.961	12.9	1.111	0.41	0.610
4.0	0.973	8.0	0.902	0.44	0.645
2.4	0.983	5.6	0.760	0.54	0.733
2.0	0.985	4.4	0.647	0.66	0.817

Particle Diameter = 0.85 mm p_o = 75.5 cm.

△ p cm	f_1	u_o	log u_o	H mm	1 + log H
5.7	0.961	22.3	1.348	0.68	0.833
4.5	0.971	17.2	1.236	0.60	0.781
2.5	0.985	9.8	0.990	0.57	0.757
1.4	0.990	5.7	0.759	0.64	0.805
0.6	0.995	2.5	0.389	1.08	1.035
1.2	0.990	4.6	0.667	0.73	0.866
0.9	0.995	3.6	0.560	0.88	0.944
3.0	0.980	12.7	1.102	0.56	0.746
2.0	0.987	7.0	0.845	0.39	0.771
1.6	0.990	4.9	0.694	0.70	0.847
1.0	0.993	4.2	0.620	0.79	0.892

Table 12 (Figure 29)

Data for Column I (d_c = 2.40 mm) L = 310 cm. T = 20°C

Particle Diameter 0.97 mm p_o = 76.0 cm

△ p cm	f_1	u_o	log u_o	H mm	1 + log H
5.0	0.966	23.4	1.369	0.72	0.860
4.0	0.975	18.8	1.274	0.66	0.817
2.6	0.980	12.7	1.104	0.60	0.783
1.4	0.990	6.95	0.842	0.64	0.805
1.0	0.995	4.98	0.697	0.75	0.876
0.8	0.995	4.03	0.605	0.79	0.900
0.5	0.995	2.63	0.520	1.29	1.109
0.6	0.995	3.52	0.547	0.97	0.988
1.8	0.985	8.85	0.947	0.64	0.803
0.8	0.995	4.08	0.611	0.90	0.956

Particle Diameter = 1.32 mm p_o = 76.0 cm.

△ p cm	f_1	u_o	log u_o	H mm	1 + log H
2.1	0.985	19.1	1.281	1.25	1.097
3.2	0.980	25.8	1.412	1.47	1.167
0.7	0.995	6.78	0.831	0.88	0.944
0.5	0.995	4.85	0.686	0.94	0.974
0.4	0.995	3.76	0.575	1.10	1.040
1.3	0.990	11.2	1.049	0.92	0.962
2.4	0.985	15.8	1.197	1.08	1.032
1.2	0.990	9.22	0.960	0.88	0.946
1.0	0.995	7.80	0.889	0.87	0.939

Table 13 (Figure 30)

Data for Column II(d_c 4.52 mm) L = 388 cm. T = 20°C

Unpacked Column p_o = 74.7 cm

△ p cm	f_1	u_o	log u_o	H mm	1 + log H
2.0	0.990	6.45	0.810	1.60	1.205
2.6	0.985	8.35	0.922	1.50	1.177
3.6	0.980	11.0	1.040	1.74	1.241
4.7	0.975	13.9	1.142	2.12	1.327
5.9	0.970	16.5	1.218	2.56	1.409
7.8	0.961	21.5	1.332	3.12	1.494
9.8	0.947	25.8	1.412	3.89	1.590
11.7	0.937	29.6	1.471	4.43	1.646
16.0	0.920	38.0	1.580	5.78	1.762
1.8	0.990	5.49	0.740	1.67	1.223
1.6	0.995	4.54	0.657	1.80	1.256
4.6	0.975	14.0	1.145	2.12	1.326
6.0	0.965	17.5	1.243	2.51	1.400
3.9	0.980	11.9	1.076	1.90	1.278
3.3	0.980	10.3	1.013	1.74	1.240
2.7	0.985	8.50	0.929	1.57	1.195
2.1	0.990	6.75	0.829	1.58	1.198

Particle Diameter = 0.50 mm p_o = 76.5 cm.

△ p	f_1	u_o	log u_o	H mm	1 + log H
22.9	0.865	20.0	1.300	0.48	0.679
20.9	0.877	19.0	1.278	0.50	0.701
17.9	0.894	15.9	1.201	0.48	0.685
14.7	0.911	13.1	1.118	0.49	0.692
11.3	0.929	9.85	0.993	0.51	0.707
8.9	0.942	7.63	0.883	0.54	0.734
6.8	0.956	5.75	0.760	0.58	0.764
5.0	0.966	4.14	0.617	0.69	0.839
2.6	0.980	2.50	0.398	1.02	1.010
5.2	0.966	3.54	0.549	0.75	0.876

Table 14 (Figure 30)

Data for Column II (d_c = 4.52 mm) L = 388 cm.

Particle Diameter = 0.62 mm p_o = 75.5 cm. T = 20° C.

Δ p cm	f_1	u_o	log u_o	H mm	1 + log H
18.8	0.885	24.9	1.396	0.66	0.820
16.2	0.898	21.6	1.335	0.65	0.810
12.5	0.920	16.5	1.218	0.63	0.797
9.4	0.938	12.2	1.085	0.61	0.784
7.0	0.956	8.73	0.941	0.59	0.774
5.3	0.966	6.62	0.821	0.65	0.812
4.1	0.975	4.97	0.696	0.68	0.832
2.2	0.985	2.70	0.431	1.08	1.032
6.3	0.960	8.18	0.913	0.60	0.781
2.3	0.985	4.03	0.605	0.86	0.935
2.9	0.980	3.61	0.557	0.88	0.942

Particle Diameter = 0.85 mm p_o = 75.7 cm.

Δ p	f_1	u_o	log u_o	H mm	1 + log H
9.6	0.938	21.2	1.326	0.64	0.808
7.4	0.952	16.3	1.211	0.62	0.789
5.7	0.966	12.2	1.086	0.60	0.781
3.9	0.975	8.35	0.922	0.59	0.774
2.4	0.985	5.32	0.726	0.69	0.837
1.8	0.990	4.02	0.604	0.79	0.898
3.0	0.980	6.60	0.820	0.63	0.800

Table 15 (Figure 30)

Data for Column II (d_o 4.52 mm) L = 388 cm. T = 20°C

Particle Diameter = 0.97 mm p_o = 76.5 cm.

△ p cm	f_1	u_o	log u_o	H mm	1 + log H
11.2	0.929	27.2	1.435	1.09	1.038
9.8	0.938	23.1	1.364	1.06	1.026
8.1	0.947	19.3	1.286	1.04	1.015
6.1	0.961	14.5	1.161	0.98	0.992
4.2	0.971	10.2	1.009	0.93	0.968
2.8	0.980	6.85	0.836	0.89	0.950
1.9	0.990	5.04	0.702	0.94	0.971
1.1	0.995	2.69	0.430	1.22	1.087
1.7	0.990	4.38	0.642	0.96	0.982

The column was emptied and repacked p_o = 75.7 cm.

△ p	f_1	u_o	log u_o	H mm	1 + log H
8.0	0.952	19.6	1.292	0.90	0.953
6.0	0.961	14.9	1.173	0.84	0.925
4.3	0.971	10.4	1.017	0.82	0.913
2.5	0.985	6.35	0.803	0.81	0.907
1.8	0.990	4.60	0.663	0.84	0.926

Particle Diameter = 1.32 mm p_o 76.0 cm.

△ p	f_1	u_o	log u_o	H mm	1 + log H
6.8	0.956	24.1	1.382	0.94	0.973
6.1	0.961	22.1	1.344	0.93	0.969
5.1	0.966	18.4	1.265	0.89	0.947
4.1	0.975	15.0	1.175	0.83	0.920
3.1	0.980	11.8	1.070	0.82	0.915
1.9	0.990	7.93	0.899	0.79	0.900
1.3	0.990	5.45	0.736	0.88	0.945
1.0	0.995	3.89	0.590	0.99	0.996

Table 16 (Figure 30)

Data for Column II (d_j = 4.52 mm) L = 388 cm.

Particle Diameter 2.08 mm. p_o = 76. 2 cm. T = 20°C.

$\triangle$ p cm	f_1	u_o	log u_o	H mm	1 + log H
6.1	0.961	26.5	1.423	2.11	1.325
5.1	0.966	23.2	1.366	1.94	1.287
4.1	0.975	19.3	1.284	1.74	1.241
3.2	0.980	15.4	1.186	1.51	1.179
2.1	0.985	11.0	1.041	1.34	1.126
1.4	0.990	7.38	0.868	1.13	1.054
1.0	0.995	5.30	0.724	1.10	1.041
0.7	0.995	4.13	0.616	1.15	1.062
0.4	1.00	2.59	0.413	1.34	1.128

Table 17 (Figure 31)

Data for Column III (d_c = 6.12 mm) L = 366 cm.

Unpacked Column p_o = 76.0 cm. T = 20°C

△p cm	f_1	u_o	log u_o	H mm	1 + log H
17.1	0.894	21.0	1.321	5.22	1.718
14.7	0.911	18.4	1.264	4.60	1.663
13.0	0.920	16.2	1.210	4.12	1.615
10.6	0.933	13.8	1.141	3.74	1.573
8.6	0.947	10.5	1.021	3.04	1.483
6.4	0.961	9.17	0.962	2.50	1.397
5.1	0.966	7.65	0.884	2.14	1.331
3.7	0.975	5.83	0.766	1.85	1.267
2.3	0.985	4.05	0.608	1.74	1.241
1.6	0.990	3.04	0.483	1.67	1.222

Particle Diameter = 0.50 mm. p_o = 75.7 cm.

△p cm	f_1	u_o	log u_o	H mm	1 + log H
36.5	0.797	28.4	1.453	0.78	0.889
30.6	0.826	23.2	1.366	0.71	0.851
25.2	0.853	19.0	1.279	0.72	0.855
20.7	0.877	15.5	1.190	0.63	0.797
15.7	0.902	11.1	1.045	0.63	0.797
11.8	0.924	8.23	0.915	0.62	0.789
6.6	0.956	5.81	0.764	0.65	0.810
6.1	0.961	4.00	0.602	0.78	0.894
5.1	0.966	3.38	0.529	0.85	0.931
3.5	0.975	2.27	0.356	1.11	1.046

Table 18 (Figure 31)

Data for Column III (d_c = 6.12 mm) L = 366 cm.

Particle Diameter = 0.62 mm. p_o = 74.0 cm. T = 20°C

Δp cm	f_1	u_o	log u_o	H mm	1 + log H
19.0	0.881	21.2	1.326	0.80	0.901
15.4	0.902	16.7	1.223	0.75	0.873
12.1	0.924	13.2	1.121	0.74	0.867
8.9	0.942	9.72	0.988	0.72	0.857
6.3	0.956	7.00	0.845	0.75	0.872
4.1	0.971	4.45	0.648	0.79	0.897
2.4	0.985	2.55	0.407	1.10	1.043

Particle Diameter = 0.85mm p_o = 74.5 cm.

Δp	f_1	u_o	log u_o	H mm	1 + log H
14.1	0.911	23.1	1.363	1.14	1.055
11.1	0.929	18.4	1.266	1.08	1.032
8.2	0.947	13.6	1.323	1.02	1.010
5.1	0.966	8.60	0.935	0.94	0.975
3.7	0.975	6.08	0.784	0.95	0.977
2.3	0.985	3.97	0.599	1.03	1.012
1.4	0.990	2.56	0.408	1.30	1.113

Particle Diameter = 0.97 mm p_o = 75.7 cm

Δp	f_1	u_o	log u_o	H mm	1 + log H
12.3	0.924	22.1	1.343	0.89	0.947
10.3	0.933	19.2	1.282	0.84	0.924
8.2	0.947	15.3	1.185	0.83	0.918
6.6	0.956	12.3	1.089	0.82	0.912
4.7	0.971	8.85	0.947	0.79	0.896
3.3	0.890	6.48	0.812	0.81	0.906
2.3	0.985	4.52	0.655	0.85	0.929
1.3	0.990	3.14	0.497	0.95	0.979

Table 19 (Figure 31)

Data for Columns III (d_c = 6.12 mm) L = 366 cm.

Particle Diameter = 1.32 mm p_o = 74.0 cm. T = 20°C

△ p cm	f_1	u_o	log u_o	H mm	1 + log H
9.3	0.938	21.7	1.337	1.08	1.034
7.8	0.947	18.3	1.261	0.98	0.990
6.0	0.961	14.7	1.166	0.97	0.988
4.5	0.971	11.1	1.045	0.91	0.961
3.3	0.975	8.70	0.940	0.90	0.953
2.4	0.985	6.57	0.818	0.89	0.950
1.6	0.990	4.70	0.672	0.98	0.993
1.2	0.990	3.34	0.524	1.03	1.013

Particle Diameter = 3.97 mm. p_o = 76.0 cm.

△ p	f_1	u_o	log u_o	H mm	1 + log H
38.5	0.786	15.5	1.190	6.55	1.816
24.4	0.857	12.6	1.099	5.75	1.760
13.2	0.920	6.35	0.803	2.81	1.449
15.8	0.902	14.9	1.173	6.58	1.818
9.6	0.938	9.30	0.969	4.04	1.606
7.4	0.952	7.10	0.851	3.25	1.512
2.9	0.980	2.87	0.458	2.19	0.341
3.7	0.975	3.66	0.564	2.21	0.345

Particle Diameter = 5.55 mm. p_o = 76.0 cm.

△ p	f_1	u_o	log u_o	H mm	1 + log H
32.8	0.815	18.1	1.257	2.29	1.360
20.2	0.877	11.1	1.045	1.80	1.255
15.4	0.907	8.40	0.924	1.60	1.204
11.9	0.924	6.48	0.812	1.42	1.151
8.4	0.947	4.53	0.656	1.50	1.176
5.9	0.961	3.08	0.471	1.71	1.233
10.4	0.933	5.62	0.750	1.42	1.153

Table 20 (Figure 31)

Data for Column III (d_c = 6.12 mm) L = 366 cm

Particle Diameter = 2.08 mm. p_o = 74.0 cm. T. 20°C.

△p cm	f_1	u_o	log u_o	H mm	1 + log H
15.2	0.902	33.3	1.522	2.90	1.462
13.5	0.915	29.2	1.465	2.79	1.445
11.5	0.924	26.1	1.417	2.70	1.431
9.4	0.938	22.2	1.346	2.60	1.414
7.2	0.952	17.8	1.250	2.41	1.382
5.7	0.961	14.2	1.152	2.34	1.369
4.1	0.971	10.8	1.032	2.12	1.326
2.8	0.980	8.12	0.910	1.94	1.288
1.9	0.985	5.93	0.773	1.69	1.227
1.4	0.990	4.13	0.616	1.65	1.218
1.0	0.990	3.14	0.497	1.67	1.223

The Column was emptied and repacked p_o = 75.2 cm

△p cm	f_1	u_o	log u_o	H mm	1 + log H
16.7	0.890	32.4	1.511	2.49	1.396
9.8	0.938	20.4	1.310	2.23	1.349
7.4	0.952	16.0	1.204	2.10	1.322
5.1	0.966	11.2	1.047	1.92	1.283
3.3	0.975	7.50	0.875	1.66	1.221
2.3	0.985	5.70	0.756	1.54	1.186
1.6	0.990	3.94	0.596	1.54	1.186
1.2	0.990	3.03	0.481	1.48	1.169

Table 21 (Figure 32)

Data for Column IV (d_c = 6.12 mm) L = 468 cm

Particle Diameter = 0.50 mm p_o = 75.0 cm. T = 20°C.

$\triangle p_{cm}$	f_1	u_o	log u_o	H mm	1 + log H
18.8	0.987	12.4	1.092	1.38	1.139
21.4	0.870	16.1	1.207	1.42	1.152
26.4	0.845	20.2	1.305	1.49	1.173
31.0	0.818	24.0	1.380	1.61	1.208
36.1	0.797	28.0	1.447	1.61	1.206
41.4	0.772	32.8	1.516	1.65	1.217
48.3	0.743	39.0	1.591	1.68	1.226
20.0	0.881	14.7	1.166	1.36	1.134
16.3	0.898	11.9	1.077	1.33	1.125
14.0	0.915	10.1	1.004	1.32	1.122
11.6	0.933	8.25	0.917	1.32	1.119
9.4	0.938	6.62	0.821	1.27	1.102
7.1	0.956	4.82	0.683	1.28	1.070

Table 22 (Figure 32)

Data for Column IV (d_c = 6.12 mm) L = 468 cm.

Particle Diameter = 0.62 mm p_o = 76.0 cm T = 20°C.

△ p cm	f_1	u_o	log u_o	H mm	1 + log H
13.1	0.920	13.7	1.137	2.14	1.330
11.1	0.929	11.4	1.055	2.04	1.309
9.4	0.942	9.55	0.980	1.93	1.285
7.7	0.952	7.78	0.891	1.80	1.256
5.7	0.960	5.63	0.751	1.65	1.217
5.7	0.960	5.63	0.751	1.59	1.201
6.1	0.956	6.95	0.842	1.76	1.246
4.7	0.971	4.70	0.672	1.63	1.212
4.3	0.972	4.18	0.621	1.62	1.209
3.6	0.975	3.45	0.538	1.75	1.244
3.6	0.975	3.48	0.542	1.69	1.228
14.0	0.915	14.5	1.161	2.14	1.330
15.5	0.907	16.2	1.210	2.27	1.356
16.9	0.898	17.6	1.246	2.31	1.364
19.6	0.881	20.7	1.316	2.44	1.387
21.5	0.873	22.6	1.354	2.42	1.383
23.6	0.861	24.5	1.389	2.41	1.382
29.5	0.837	31.2	1.494	2.37	1.375
33.6	0.818	35.3	1.548	2.34	1.369

Table 23 (Figure 32)

Data for Column IV (d_c = 6.12 mm) L = 468 cm.

Particle Diameter = 0.85 mm. p_o = 76.0 cm. T = 20° C.

Δp cm	f_1	u_o	log u_o	H mm	1 + log H
9.3	0.947	15.1	1.179	1.92	1.283
10.9	0.938	17.6	1.249	2.04	1.309
12.4	0.929	20.0	1.301	2.05	1.312
14.0	0.920	22.3	1.348	2.12	1.326
15.8	0.911	25.3	1.402	2.24	1.350
17.9	0.898	28.2	1.450	2.14	1.330
19.6	0.890	30.2	1.480	2.10	1.322
21.3	0.877	33.1	1.520	2.18	1.339
22.9	0.869	35.8	1.554	2.09	1.321
24.8	0.861	38.5	1.589	2.13	1.328
27.0	0.849	41.2	1.615	2.09	1.321
29.1	0.837	45.0	1.653	2.09	1.321
9.6	0.947	15.3	1.183	1.72	1.235
8.8	0.952	14.0	1.145	1.68	1.226
7.8	0.956	12.5	1.097	1.69	1.228
6.6	0.966	10.5	1.021	1.71	1.232
5.6	0.971	8.83	0.946	1.66	1.220
4.5	0.980	7.18	0.856	1.63	1.213
3.7	0.985	5.82	0.765	1.70	1.231
3.0	0.990	4.85	0.686	1.65	1.218
2.3	0.995	3.65	0.562	1.85	1.267
1.8	0.995	2.87	0.458	1.89	1.277

Table 24 (Figure 32)

Data for Column IV (d_c = 6.12 mm) L = 468 cm.

Particle Diameter = 2.08 mm. p_o = 77.0 cm. T = 20°C.

△ p cm	f_1	u_o	log u_o	H mm	1 + log H
2.3	0.985	9.05	0.957	7.18	1.856
3.1	0.980	11.3	1.051	8.36	1.922
4.7	0.971	14.6	1.165	9.42	1.974
5.3	0.966	17.7	1.247	10.1	2.004
6.7	0.960	21.1	1.323	10.5	2.023
7.9	0.952	24.6	1.391	11.2	2.050
9.1	0.942	27.9	1.445	11.6	2.063
10.8	0.933	31.3	1.496	11.7	2.069
11.4	0.929	34.3	1.535	11.5	2.059
12.9	0.920	38.7	1.588	12.3	2.091
14.9	0.911	42.9	1.633	11.8	2.073
1.9	0.985	7.57	0.879	6.53	1.815
1.5	0.990	5.87	0.769	6.31	1.800
0.9	0.995	3.49	0.543	5.77	1.761
1.2	0.992	4.81	0.682	5.90	1.771

Table 25 (Figure 32)

Data for Column IV (d_c = 6.12 mm) L = 468 cm.

Particle Diameter = 3.97 mm p_o = 77.0 cm. T = 20^0 C.

$\triangle p_{cm}$	f_1	u_o	log u_o	H mm	1 + log H
7.9	0.952	9.22	0.965	4.56	1.659
10.9	0.933	12.7	1.104	6.10	1.785
11.7	0.929	13.8	1.138	6.49	1.812
13.4	0.915	15.7	1.196	7.30	1.863
14.7	0.911	17.1	1.232	7.59	1.880
16.5	0.902	18.7	1.272	8.11	1.909
18.8	0.885	21.6	1.333	9.02	1.955
20.5	0.877	23.1	1.364	8.93	1.951
22.5	0.869	25.5	1.407	9.53	1.979
23.5	0.861	27.8	1.444	9.46	1.976
23.5	0.861	27.8	1.444	9.84	1.993
9.6	0.938	10.4	1.015	4.78	1.679
8.3	0.947	8.77	0.943	4.06	1.609
6.3	0.961	7.60	0.881	3.89	1.590
4.8	0.971	5.77	0.761	2.91	1.464
3.8	0.975	4.50	0.653	3.03	1.482

Table 26 (Figure 32)

Data for Column IV (d_o = 6.12 mm) L = 468 cm.

Particle Diameter = 4.96 mm. p_o = 76.5 cm. T = 20°C.

△ p cm	f_1	u_o	log u_o	H mm	1 + log H
5.5	0.966	6.95	0.842	2.31	1.364
6.9	0.956	8.78	0.944	2.64	1.421
7.8	0.952	9.82	0.992	2.74	1.438
8.5	0.947	10.7	1.031	2.99	1.475
9.4	0.942	11.8	1.073	3.16	1.500
10.4	0.933	13.2	1.121	3.38	1.529
11.8	0.924	15.0	1.175	3.74	1.573
12.8	0.920	16.2	1.210	3.98	1.600
14.4	0.911	18.0	1.255	4.36	1.639
19.1	0.885	23.3	1.367	5.45	1.736
21.5	0.873	25.9	1.413	5.86	1.768
25.5	0.853	30.0	1.476	6.41	1.807
28.2	0.837	33.5	1.525	6.86	1.836
31.4	0.823	36.0	1.556	7.02	1.846
5.3	0.966	6.55	0.816	2.18	1.338
4.7	0.971	5.78	0.762	2.01	1.304
4.0	0.975	4.92	0.692	1.86	1.269
3.5	0.975	4.36	0.640	1.92	1.283
2.8	0.980	3.47	0.540	1.20	1.310

Table 27 (Figure 32)

Data for Column IV (d_c = 6.12 mm) L = 468 cm.

Particle Diameter = 5.55 mm p_o = 75.5 cm T = 20°C.

Δp_{cm}	f_1	u_o	log u_o	H mm	1 + log H
11.2	0.929	12.5	1.095	2.87	1.458
12.7	0.920	15.5	1.190	3.18	1.502
14.5	0.911	18.9	1.275	3.43	1.535
16.5	0.898	22.6	1.354	3.66	1.563
18.0	0.890	26.2	1.418	3.85	1.585
20.1	0.881	29.2	1.465	3.82	1.582
22.6	0.865	33.8	1.529	3.99	1.601
24.4	0.857	37.5	1.574	4.12	1.615
28.6	0.833	44.2	1.654	4.37	1.640
8.15	0.947	8.17	0.912	2.84	1.454
6.05	0.961	5.98	0.777	2.59	1.413
4.20	0.975	3.99	0.601	2.88	1.459
9.60	0.938	10.5	1.021	2.77	1.443
17.1	0.894	23.9	1.378	3.93	1.594

Table 28.

Experimental Parameters for Stainless Steel Columns.

dc mm	dp mm	$dp/_{dc}$	H min	$Hmin/_{dp}$	α	A mm	$A/_{dp}$
2.40	0.50	0.21	0.30	0.60			
	0.62	0.26	0.40	0.64	0.5	0.08	0.13
	0.85	0.35	0.56	0.66	0.4	0.09	0.11
	0.97	0.40	0.60	0.62	0.4	0.10	0.10
	1.32	0.55	0.87	0.66	0.4	0.15	0.11
	Empty		0.86	$(x/\sqrt{3} = 0.70)$			
5.52	0.50	0.11	0.48	0.96	1.0	0.16	0.32
	0.62	0.14	0.59	0.95	1.5	0.25	0.47
	0.85	0.19	0.59	0.70	1.6	0.26	0.31
	0.97	0.22	0.79	0.82	2.0	0.40	0.41
	1.32	0.29	0.79	0.60	1.0	0.26	0.20
	2.08	0.46	1.10	0.53	1.0	0.37	0.18
	Empty		1.58	$(x/\sqrt{3} = 1.31)$			
3.80	0.50	0.13	0.43	0.86	1.2	0.15	0.30
6.12	0.50	0.08	0.62	1.24	1.2	0.24	0.47
	0.62	0.10	0.72	1.17	1.5	0.31	0.50
	0.85	0.14	0.93	1.10	1.5	0.40	0.47
	0.97	0.16	0.79	0.82	1.8	0.37	0.39
	1.32	0.22	0.89	0.67	1.7	0.41	0.31
	2.08	0.34	1.48	0.71			
	3.97	0.65	2.14	0.54			
	5.55	0.91	1.45	0.26	1.0	0.08	0.09
	4.96	0.81	1.88	0.38			
	Empty		1.66	$(x/\sqrt{3} = 1.76)$			

Table 29.

Experimental Parameters for Stainless Steel Columns.

dc mm	dp mm	$dp/_{dc}$	B	γ	C_g	ω	$\rho=\frac{dc}{dp}$	ϵ
2.40	0.50	0.21					4.80	0.48
	0.62	0.26	0.229	0.69	1.12	0.05	3.87	0.49
	0.85	0.35	0.245	0.74	2.14	0.05	2.83	0.59
	0.97	0.40					2.48	0.61
	1.32	0.55	0.275	0.83	5.13	0.05	1.82	0.74
4.52	0.50	0.11	0.186	0.56	1.59	0.11	9.04	
	0.62	0.14	0.186	0.56	1.59	0.07	7.30	
	0.85	0.19	0.170	0.52	1.62	0.04	5.32	
	0.97	0.22	0.178	0.54	2.75	0.05	4.67	
	1.32	0.29	0.240	0.73	2.95	0.03	3.42	
	2.08	0.46	0.209	0.63	2.63	0.01	2.17	
6.12	0.50	0.08	0.199	0.61	1.86	0.12	12.2	
	0.62	0.10	0.186	0.56	1.70	0.07	9.88	
	0.85	0.14	0.200	0.62	3.5	0.08	7.20	
	0.97	0.16	0.186	0.56	2.5	0.04	6.30	
	1.32	0.22	0.178	0.55	3.2	0.03	4.64	
	2.08	0.34					2.94	
	3.97	0.65					1.54	
	5.55	0.91					1.12	

IV. General Discussion

I should like now to consider the concept of turbulence in chromatographic flow for both gas and liquid systems to show how this can give rise to an apparent 'coupling' effect. I should then like to consider the nature of the gas phase mass transfer process in the light of my own results and those obtained recently by Knox and Littlewood.

i. Turbulence

In streamline or laminar flow the resistance to flow is entirely due to viscous drag or internal friction. As the velocity is increased the regular pattern of streamline flow becomes unstable and gives way to a regime in which innumerable small, randomly distributed local eddies form spontaneously. There is no exact theory of turbulence even in flow through straight tubes. The degree of turbulence is usually given by the Reynold's number which is $Re = \rho udp/\eta$.

For the development of turbulence Collins (193) gives a transition range from R_e 1 to 10 while Perkins and Johnson (194) indicate that a full transition is obtained only when $R_e > 10^3$. For chromatographic purposes the probable range is 1 to 100. Whereas in straight tubes turbulent flow occurs suddenly as R_e exceeds 2100, in the packed column where many widely varying flow channels are involved turbulence is envisaged as gradually spreading into progressively smaller channels as R_e increases.

There is no unanimous agreement that turbulence begins at R_e 1 to 100. Scheideggar (195) believes that R_e is not always an adequate criterion of turbulence but Muskat (196) points out that the irregularity of the packing structure would be conducive to turbulence which can actually be observed with a stream of fluorescin in a packed column. Turbulence also occurs around a bend in a tube sooner than it does in a straight portion of the same tube.

ii. Turbulence and Chromatography

Besides the increase in mass transfer rate resulting from erratic shifts in the entire flow stream 'turbulent diffusion', turbulence also exerts a

velocity-equalisation effect. Due to the resulting increased resistance to flow the flow rate in the larger channels caused by bridging, etc. will be reduced. It has been shown that $V_T = V_L^{\frac{1}{4}}$ where V_T and V_L are the ratios of velocity extremes under laminar and turbulent conditions. Thus in the short-range interchannel effect where V_L is about 7, V_T would be about 1.6 and this would greatly reduce zone spreading.

The mathematics of turbulent diffusion is far from complete even for non-porous materials. Both longitudinal and lateral transport are enhanced by turbulent diffusion. In the turbulent state D_m becomes proportional to velocity and so the mobile phase terms, $H_m = B/u + C_m u$ become $H_m = H_t$, a constant independent of velocity in agreement with the coupling theory. It has generally been assumed that $H_t = dp$ though Giddings feels that this assumption does not adequately account for long-range non-uniformities and that $H_t > dp$. The effects of turbulence are limited by the associated very high pressure drop.

Sternberg and Poulson applied the equation developed by Carman (189) for turbulent flow, viz.

$$\bar{p} \triangle p/u_o = \frac{\eta L \epsilon}{B_o f_m} p_o + b \frac{ML}{t_R} p_o^2 \left(\frac{\epsilon}{f_m}\right)^2 u_o$$

where the b coefficient determines the contribution due to turbulence. For laminar flow $\bar{p} \triangle p/u_o$ against u_o should be constant. Sternberg found that $p_m \triangle p/u_o$ varied linearly with linear velocity. Plots for some of my data are shown in Figure 38 and Tables 30-32. In agreement with Sternberg the 'turbulence' contribution in general increases as the particle diameter decreases, at constant column diameter, while the turbulence contribution increases as the column diameter increases. The plot for the 2 capillary columns and column I for all dp values are horizontal.

Logically R_e represents the ratio of inertial and viscous forces. Inertial effects (proportional to ρu^2) are known to become important in curved tubes or in very short tubes where the end effects are important and the flow may still be laminar eventhough $\triangle p$ and flow rate are no longer linearly related, i.e.

Table 30 (Figure 38)

Check of Darcy's Law

Column I: d_c = 2.40 mm. T = 20°C.

dp = 0.50 mm		dp = 0.62 mm		dp = 0.85 mm		dp = 1.32 mm	
u_o	$\Delta p\bar{p}/u_o$	u_o	$\Delta p\bar{p}/u_o$	u_o	$\Delta p\bar{p}/u_o$	u_o	$\Delta p\bar{p}/u_o$
26.0	60.1	15.1	37.3	78.5	20.0	19.1	8.5
20.9	59.0	10.6	38.6	77.8	20.8	25.8	7.6
14.8	60.2	6.7	39.4	76.8	19.6	6.8	7.9
12.1	57.0	5.1	37.9	76.2	18.7	4.9	7.9
7.5	59.5	3.1	39.6	75.8	18.2	3.8	8.1
5.4	59.0	13.9	37.1	76.1	19.8	11.2	8.9
3.3	60.5	22.6	37.4	76.0	19.0		
		26.0	37.8				
		36.2	37.3				

Column II: d_c = 4.52 mm. T = 20°C.

dp = 0.50 mm		dp = 0.85 mm		dp = 0.62 mm		dp = 2.08 mm	
u_o	$\Delta p\bar{p}/u_o$	u_o	$\Delta p\bar{p}/u_o$	u_o	$\Delta p\bar{p}/u_o$	u_o	$\Delta p\bar{p}/u_o$
2.5	81.0	21.2	36.6	24.9	64.4	26.5	18.2
19.0	96.0	16.3	36.3	21.6	63.0	23.2	17.3
15.9	96.0	12.2	36.9	16.5	62.3	19.3	16.6
13.1	94.0	8.4	36.3	12.2	62.5	15.4	16.1
9.9	94.0	5.3	34.7	8.7	63.3	11.0	14.7
7.6	94.5	4.0	34.3	6.6	62.6	7.4	14.6
5.8	94.5			5.0	64.0	5.3	14.4
4.1	95.0			2.7	62.4	4.1	13.0
				8.2	60.7	2.6	11.6

Table 31 (Figure 38)

Check of Darcy's Law

Col II empty		Col. IV empty		Col. IV dp = 4.96 mm.		Capillary id. 0.88 mm.		Capillary id. 2.88 mm.	
u_o	$\Delta p\bar{p}/u_o$	u_o	$\Delta p\bar{p}/u_o$	u_o	$\Delta p\bar{p}/u_o$	u_o	$\Delta p\bar{p}/u_o$	u_o	$\Delta p\bar{p}/u_o$
6.5	23.9	7.5	41.2	7.0	62.3	94.7	7.9	21.0	3.5
8.4	24.1	8.3	42.5	8.8	62.5	105.6	7.8	22.5	3.8
11.0	25.1	9.7	44.0	9.8	63.5	120.7	8.2	27.1	3.9
13.9	26.5	10.9	44.2	10.7	63.8	86.1	7.7	31.7	3.8
16.5	28.2	18.3	50.0	11.8	64.3	76.7	7.8	34.0	3.7
21.5	29.0	20.0	52.3	13.2	64.0	52.0	8.0	38.3	3.8
25.8	30.7	22.1	54.5	15.0	64.5	43.0	8.2	41.8	3.9
29.6	32.2	4.6	40.3	16.2	65.0	35.6	8.1	45.8	3.9
38.0	35.2	3.6	38.5	18.0	66.7	22.9	8.2	50.1	3.8
5.5	25.2	3.0	38.6	23.3	70.0	18.7	8.5	56.8	4.5
4.5	27.0	15.9	48.5	25.9	72.0	14.6	8.7	60.8	4.8
14.0	25.7	14.3	46.8	30.0	75.5	12.0	8.7	68.5	4.7
17.5	27.0	6.8	41.5	33.5	75.7			19.9	4.1
11.9	25.6	12.4	45.6	36.0	80.0			18.3	4.1
10.3	24.9	8.0	42.2						
8.5	24.6	4.8	35.8						
6.8	24.0								

Table 32 (Figure 38)

Check of Darcy's Law

Col. III empty		Col. III dp = 0.5 mm		Col. III dp = 0.62 mm		Col. III dp = 0.85 mm	
u_o	$\Delta p\bar{p}/u_o$	u_o	$\Delta p\bar{p}/u_o$	u_o	$\Delta p\bar{p}/u_o$	u_o	$\Delta p\bar{p}/u_o$
21.0	69.0	16.1	115.0	20.5	82.0	17.9	49.7
18.4	66.5	20.2	116.5	22.5	82.5	20.1	50.7
16.2	66.2	24.0	118.5	24.2	85.5	22.4	51.8
13.8	62.5	28.0	121.0	26.5	86.0	28.4	53.5
10.5	65.7	32.8	122.0	31.2	86.0	30.4	55.3
9.2	55.2	39.0	124.0	35.3	88.5	33.2	55.5
7.7	53.0			38.8	90.0	35.9	55.8
5.8	49.3			17.6	81.0	38.6	56.8
4.1	43.8					41.2	58.7
3.1	40.2					45.1	58.5

Glass Column L = 593 cm. dp = 0.5 mm.		Glass Column L = 267 cm. dc = 6.5 mm dp = 0.5 mm.	
u_o	$\Delta p\bar{p}/u_o$	u_o	$\Delta p\bar{p}/u_o$
16.6	59.3	5.9	77.5
18.4	63.2	7.6	77.3
23.5	59.3	9.5	78.0
29.1	59.0	11.7	79.3
35.4	59.5	15.3	79.3
42.8	59.6	17.5	80.0
14.2	51.0	20.2	81.5

Darcy's law is no longer valid. A predominant wall effect can also cause Darcy's law to break down. The first change of flow occurs when the inertia effects in laminar flow become important, caused by curved flow channels, etc., and the second change occurs when true turbulence sets in, the R_e value at which non-linearity sets in being determined by the particular system and not by a 'universal' number.

Since the column connections consisted in each case of 0.88 mm id. nylon tubing the 'end' effects would be most marked in the case of column III. For this reason tapered connections were used (Figure 16). The same data was also plotted for a glass column (dc = 6.5 mm, dp = 0.50 mm, L = 267 cm). The ends were drawn down so that the nylon capillary was a tight fit. This gives about the smoothest possible change in diameter but the slope of the line is still considerable. For an absolute comparison, of course, all the columns should be of the same length.

iii. The Equivalence of Gas and Liquid Chromatography

The laws of fluid dynamics show that gas and liquid systems can be scaled one into the other so that the combined effect of flow and diffusion is the same. Since D_m is about 10^4 times lower for a liquid than a gas, a slowly flowing liquid system can be used to attain the very high flow region where gas chromatographic data is not available.

Giddings (199-201) has shown the GC and LC equivalent in the mobile phase when the reduced velocity $\nu = dpu/D_m$ is the same and the reduced plate height $h = H/dp$ is essentially equal for the 2 methods since structural factors are nearly the same for any random packing of granules. A plot of h versus ν should then, to a first approximation, yield a universal curve after the equation

$$h = 2\gamma/\nu + \sum \frac{1}{1/2\lambda_i + 1/\omega_i \nu}$$

$$\cong 2\gamma/\nu + \frac{1}{1/2\lambda + 1/\omega\nu}$$

The corresponding classical expression is

$$h = 2\lambda + 2\gamma/\nu + \omega\nu$$

iv. Turbulence and Coupling

The relative importance of turbulence and coupling which both flatten the HETP plate at high velocities, may be given by the ratio of R_e to the reduced velocity, i.e.

$$\frac{\nu}{R_e} = \frac{\eta}{D_m \rho}$$

This ratio is about 10^3 for liquids and unity for gases. A reduced velocity of 1 corresponds to about 10 cm per sec. for gases and 10^{-4} cm per sec. for liquids. Giddings has calculated that for the short-range interchannel effect, coupling reaches half its effectiveness at $\nu_{\frac{1}{2}}$ of about 2. If $Re_{\frac{1}{2}}$ is taken as about 10, coupling will be very approximately achieved about 5 times more readily than turbulence for gases and 5000 times more readily for liquids. A liquid system must thus be used in order to separate the 2 effects completely.

Terry et al. (201) were the first to compile results obtained by a number of investigators on inert columns using liquid carriers. In nearly every case h approached a constant value at high velocities proving the validity of the coupling theory of eddy diffusion.

Using a 10 per cent aqueous solution of potassium nitrate as the mobile phase Knox (202) recently studied the spreading of bands of potassium permanganate in columns packed with glass beads using a photometer cell detector. Some of his results are given in Figure 39 along with my data for the same ρ values Tables 33-35). Knox found that his data could only be explained by the coupling theory. He also found that at reduced velocities above about 5000, H/dp first became constant and then declined. This decrease can only be explained by the onset of turbulence which was also observed to be taking place. This corresponds to an Re value of about 5 proving that turbulence must become important in gases at low reduced velocities as discussed above, thereby masking the coupling effect.

Although the liquid studies have provided nearly conclusive evidence against the classical theory, the small but constant A term, of magnitude less than dp, must still be explained.

Table 33 (Figures 39, 43)

Variation of log h with log ν for different dp values

$\log \nu = \log u_o \, dp/0.165 = \log u_o + \log Y$
$\log h = \log H/dp = \log H - \log dp = \log H + X$

dp	0.50	0.62	0.85	0.97	1.32	2.08	3.97
Y	0.303	0.376	0.515	0.588	0.800	1.26	2.41
log Y	-0.519	-0.425	-0.288	-0.231	-0.097	0.100	0.382
X	0.301	0.208	0.071	0.132	-0.121	-0.318	-0.599

Col I: dp = 0.50				Col I: dp = 0.62			
1 + log H	1 + log h	log u_o	log ν	1 + log H	1 + log h	log u_o	log ν
0.485	0.786	1.414	0.896	0.610	0.818	1.179	0.754
0.490	0.791	1.320	0.802	0.614	0.821	1.025	0.601
0.480	0.781	1.170	0.652	0.697	0.905	0.825	0.400
0.536	0.837	1.081	0.562	0.764	0.972	0.710	0.285
0.619	0.920	0.874	0.355	0.991	1.198	0.497	0.072
0.727	1.028	0.728	0.210	0.593	0.801	1.142	0.717
0.935	1.261	0.521	0.003	0.601	0.809	1.354	0.929
0.486	0.787	1.222	0.704	0.600	0.808	1.415	0.990
0.569	0.870	0.969	0.450	0.625	0.832	1.559	1.134
0.676	0.977	0.791	0.272	0.610	0.817	1.111	0.686
0.776	1.077	0.661	0.142	0.645	0.853	0.902	0.477
				0.733	0.941	0.960	0.335
				0.817	1.025	0.647	0.223

Table 34 (Figures 39, 43)

Variation of log h with log ν for different dp values

Col II: dp = 1.32				Col III: dp = 0.50			
1 + log H	1 + log h	log u_o	log ν	1 + log H	1 + log h	log u_o	log ν
0.973	0.852	1.382	1.285	0.889	1.190	1.453	0.935
0.969	0.848	1.344	1.248	0.851	1.152	1.366	0.847
0.947	0.826	1.265	1.168	0.855	1.156	1.279	0.760
0.920	0.800	1.175	1.078	0.797	1.098	1.190	0.671
0.915	0.795	1.070	0.973	0.797	1.098	1.045	0.527
0.900	0.780	0.899	0.802	0.789	1.090	0.915	0.397
0.945	0.824	0.736	0.640	0.810	1.111	0.764	0.246
0.996	0.875	0.590	0.493	0.894	1.195	0.602	0.084
				0.931	1.232	0.529	0.010

Col III: dp=1.32				Col III: dp = 0.97			
1 + log H	1+ log h	log u_o	log ν	1 + log H	1 + log h	log u_o	log ν
1.034	0.913	1.337	1.240	0.947	0.960	1.343	1.113
0.990	0.869	1.261	1.164	0.924	0.938	1.282	1.052
0.988	0.867	1.166	1.069	0.918	0.931	1.185	0.954
0.961	0.840	1.045	0.948	0.912	0.925	1.089	0.858
0.953	0.833	0.940	0.843	0.896	0.909	0.947	0.716
0.950	0.830	0.818	0.721	0.906	0.920	0.812	0.581
0.993	0.872	0.672	0.575	0.929	0.943	0.655	0.425
1.013	0.892	0.524	0.427	0.979	0.992	0.497	0.266

Col III: dp = 0.62

1 + log H	1 + log h	log u_o	log ν
0.901	1.109	1.326	0.902
0.873	1.080	1.223	0.798
0.869	1.075	1.121	0.696
0.857	1.065	0.988	0.563
0.872	1.079	0.845	0.420
0.897	1.104	0.648	0.224

Table 35 (Figures 39, 43)

Variation of log h with log ν for different dp values

Col I: dp = 0.97				Col II: dp = 0.50			
1 + log H	1 + log h	log u_o	log ν	1 + log H	1 + log h	log u_o	log ν
0.860	0.874	1.369	1.139	0.679	0.980	1.300	0.781
0.817	0.830	1.274	1.044	0.701	1.002	1.278	0.759
0.783	0.796	1.104	0.873	0.685	0.986	1.201	0.683
0.805	0.818	0.842	0.611	0.692	0.993	1.118	0.600
0.900	0.913	0.605	0.375	0.707	1.008	0.993	0.475
1.109	1.122	0.420	0.189	0.734	1.035	0.883	0.364
0.988	1.001	0.547	0.316	0.764	1.065	0.760	0.241
0.803	0.816	0.947	0.716	0.839	1.140	0.617	0.098
0.956	0.970	0.611	0.380				

Col II: dp = 0.62				Col II: dp = 0.85			
1 + log H	1 + log h	log u_o	log ν	1 + log H	1 + log h	log u_o	log ν
0.820	1.027	1.396	0.971	0.808	0.870	1.326	1.038
0.810	1.017	1.335	0.910	0.789	0.860	1.211	0.923
0.797	1.005	1.218	0.793	0.781	0.852	1.086	0.798
0.834	0.991	1.085	0.660	0.774	0.845	0.922	0.634
0.774	0.982	0.941	0.516	0.837	0.908	0.726	0.438
0.812	1.020	0.821	0.396	0.898	0.969	0.604	0.316
0.832	1.040	0.696	0.272	0.800	0.871	0.820	0.531
1.032	1.239	0.431	0.007				
0.781	0.989	0.913	0.488				
0.935	1.142	0.605	0.181				

Giddings (203) has explained the origin of this term by considering the differing behaviour of the terms in the summation of the coupling expression, i.e.

$$H_{(ED)} = \sum \frac{1}{1/2\lambda_i dp + 1/C_{gi}u}$$

In single interstitial channels the Cgi contribution would be small, while a long range interaction, on account of the large equilibration distance, would yield large Cgi terms. While the former situation would give $H = C_{gi}u$, the latter would yield $H = 2\lambda_i dp$ over most of the experimental range and such terms as this may well explain the observed A values. Thus over a relatively narrow range of velocities, experiments may well fit the approximate equation

$$H = 2\ dp + \frac{1}{1/2\lambda' dp + 1/C_g' u} + C_g u$$

as suggested by Knox and McLaren (197).

v. The Irreproducibility of the Packing Process

"Description of Column Packing is no substitute for Experience"

Ambrose and Ambrose.

Before considering the nature of the Cg term I should like to comment briefly on the difficulty in reproducibly packing a column. The same column on being emptied and refilled in apparently the same way with the same batch of beads gives a different HETP plot. This is seen in Figure 30 where the curves for dp values of 0.62 and 0.85 were repeated with the column repacked. In all the HETP curves shown there may thus be an uncertainty of as much as 0.1 mm in H_{min}. Sternberg's results are more consistent than mine and he does not appear to have had this difficulty. Knox, however, experienced the same thing with his liquid studies but the effect was less marked. The influence of packing is even more pronounced in data for column IV (Figure 32) where the HETP curves for the same dp/dc value, though of the same general shape as for column III, lie much higher on the graph. This column was known to be packed less carefully, but even so the difference is surprisingly large.

Figure 40 shows a plot of BS mesh against particle size. It can be seen that the 20-30 and 30-40 mesh ranges cover a larger particle size range than the 80-100 one and it is difficult to reduce this range to increase particle size uniformity. Sieving has the additional disadvantage of separating in 2 dimensions only so that 'rugby-ball' shaped beads can also pass through the mesh. Examination of the finest beads under the microscope revealed that many of them are indeed 'rugby-ball' shaped, but the larger-sized ones used in this work appeared uniformly spherical.

There are many recipes in the literature concerning the packing method, especially with regard to prep-scale columns (204-5) but they all lack experimental data. Pypker (206) using coloured models of different mesh sizes, usually studied the effects of vibration, tapping, rotation, etc., but he was unable to form a homogeneous mixture in the column. He found that segregation occurred at the very start in the separating funnel. Higgins and Smith (207) found, on the contrary, that several quite distinct methods of column packing each gave reproducible results. These were descriptively classified into 'bulk', 'snow', 'snow-storm' and 'mountain' packing. It is interesting that the last method, 'mountain-packing', was found to give the most efficient columns for 60/70 mesh support though this method had been previously condemned by Giddings and Fuller (208). How to pack columns reproducibly with maximum efficiency is still an unsolved problem, and requires further investigation. The indications from this work and that of Knox in liquid chromatography are that much more attention should be paid both to packing uniformity and particle size distribution.

vi. <u>The Nature of the Trans-Column Effect</u>

For straight columns the trans-column inhomogeneity may be due to a 'size-separation effect' and the 'wall effect' (208, 209). Giddings and Fuller (208) observed that the larger particles moved preferentially to the outside as a stream of particles impacted at the centre of a large tube. As a result of their larger terminal velocity the large particles rebound more upon impact with the bulk material than do small particles, thus giving a differential distribution. The flow velocity will thus vary widely over the column cross-section.

Where wall and packing meet the flow channels are different from the normal interstitial channels due to the lack of over-lapping particles. Golay (210)

postulated that this 'wall effect' leads to a velocity about 5 times higher than average within half a particle diameter from the wall. Schwartz and Smith (211) found that the maximum velocity occurred one particle diameter from the wall and based on this work Hupe (212) derived an expression for the velocity profile relating H and column diameter. He then succeeded in eliminating the wall effect by inserting 'pre-calculated' discs.

The trans-column flow pattern is known to be of great importance in large-scale chromatography. Carle and Johns (213) obtained a 20-fold increase in H when scaling up columns from 5 to 75 mm diameter, but this work is open to question since Huyten (214) obtained H values of 2 mm with columns up to 100 mm in diameter. Huyten et al found a 12-fold increase in flow velocity within a $\frac{1}{2}$ - particle diameter of the wall was necessary to explain the velocity variation on the basis of wall effects. In contrast, the work of Benenati and Brosilow (215) showed that the average porosity of a wall layer $dp/_2$ thick is about 0.44 which would result in a velocity increase of less than 50% in the layer. They found that the outside to inside flow velocity ratio was about 1.25 and 1.44 in the tapped and untapped chromosorb columns respectively. Many investigators however (195) have found a decreased rather than an increased velocity within a $\frac{1}{2}$-particle diameter of the wall due to the flattening of irregular particles against the wall.

The 'wall effect' was also demonstrated by Frisone (216) who drew air through a column saturated with hexane. The hexane could be seen evaporating away from the walls quicker than from the centre.

Novem (217) put forward the view that the wall effect is a misnomer. He suggested that a continuously varying velocity profile is due to some systematic packing inhomogeneity rather than to a narrow annular space around the wall which, although increasing in area as the column diameter increases, becomes a smaller fraction of the total area. This was supported by Hudy (218) who thought the effect may not be a 'wall effect' at all but a manifestation of some non-linear flow pattern through the column. Giddings and Fuller concluded that particle size variation alone could easily explain the full velocity variation of Huyten, and that the wall effect can only account for a small fraction, if any, of the observed result. However, the centre and wall regions of the tube are never equivalent and thus cannot be subjected to the same influences and forces. The proximity of a wall must always influence packing structure. A suggested band profile as a result of the 'wall effect' is shown in Figure 41.

vii. The Importance of the Trans-Column Effect

Using the random-walk approach, Giddings has calculated approximate values for the separate λ_i and ω_i terms associated with each of the 5 types of flow inequality. These are given in Table (iii). The curves in Figure 42 are constructed with the parameters for a straight column. Curve 5a is plotted for a column with a diameter of 12 dp (i.e. m = 12) giving $\omega = 0.14$ and $\lambda = 2.8$. This is the one curve which varies widely from column to column firstly because the values of ω and λ vary

Table (iii)

Type of Velocity Inequality	ω_i	λ_i	$\nu_{\frac{1}{2}}$
1. Trans-Channel	0.01	0.5	10^2
2. Trans-Particle	0.1	10^4	2×10^5
3. Short-Range Interchannel	0.5	0.5	2
4. Long-Range Interchannel	2	0.1	0.1
5a. Trans-Column	0.02 - 10	0.4 - 200	40
5b. Trans-column (coiled)	$0 - 10^2$	$0 - 10^3$	40

$$\nu_{\frac{1}{2}} = 2\lambda_i/\omega_i$$

with m^2 and secondly because these parameters will be a sensitive function of the method of packing the column and the uniformity of the support particles.

It is interesting to compare the form of these curves with those in Figure 39 for gases and liquids. Although the curves obtained by Knox for liquids are all slightly lower than the corresponding curves for gases, the fit is reasonably satisfactory. This difference could be perhaps an indication of more uniform packing. It can be seen that the curves for different values of ρ are very nearly parallel and Knox expresses H in the form

$$H/dp = g_1(\rho) \times g_2(\nu) \times h_o$$

showing that all contributions to H contain the same dependence on column to particle diameter ratio. Figure 43 (Table 36) shows a plot of log h/log ρ at

Table 36 (Figure 43)

Variation of log h with log ρ at constant ν (63)

d_o	dp	ρ	log ρ	1 + log h
2.40	0.50	4.80	0.681	0.79
	0.62	3.87	0.588	0.81
	0.97	3.48	0.394	0.79
4.52	0.50	9.04	0.956	1.00
	0.62	7.30	0.863	1.01
	0.85	5.32	0.726	0.85
	1.32	3.42	0.534	0.78
6.12	0.50	12.24	1.088	1.14
	0.62	9.88	0.995	1.08
	0.97	6.30	0.799	0.91
	1.32	4.64	0.667	0.83

a fixed value of ν, 300 for liquids and 6.3 for gases, which again illustrates the equivalence of the 2 systems and confirms the importance of column-to-particle diameter ratio.

From the liquid studies Knox concluded that at reduced velocities above about 20 trans-column processes are the only ones which are important. This conclusion is contrary to the view of Giddings but is confirmed by the present data. The efficiency was greatly decreased by looser packing giving a greater void space and greater irregularity of flow profile. The departure from Darcy's law increased in order of increasing diameter irrespective of the pack-:ing. The A term also increased with column diameter, i.e. with increase in trans-column effects as stated by Giddings. For a given dp value, ω increased with increase in column diameter indicating an increase in equilibration dis-:tance, i.e. ω results from a trans-column interaction. The importance of the trans-column effect was most elegantly illustrated in theory and practice by Littlewood (219) at the recent Brighton symposium.

Using the generalised non-equilibrium theory, Littlewood calculated plate height contributions corresponding to different kinds of velocity profiles and showed that the factor which increased Hg more than anything else was the exis-:tence of widely separated points with different gas speeds. H was shown to be very sensitive to the value of the column diameter.

Littlewood prepared columns so as to exaggerate the flow profile, i.e. of different porosity in the middle and outside, and found that in the more unevenly packed column the Cg term was dominant, the order of the C values being also the order of the diffusion coefficients. The agreement with within 10% of the calculated value. He calculated the effect of small-scale flow variations extending over the order of one particle diameter and found values much less than the observed ones but in agreement with Kieselbach's data on glass-bead columns (145).

From the relation $u \propto \frac{\epsilon^3}{(1-\epsilon)^2}$ a 15% change in u is produced by a 3% change in voidage ϵ. He suggested that fluctuations in packing density across the column contribute largely to Cg. This is also supported by the irreproduc-:ibility of the filling procedure. Thus Kieselbach obtained values of Cg differing by 50% from 'identical' chromosorb columns. This was discussed

earlier and it is far more probable that this change results from small differences in large-scale fluctuations rather than large differences in small-scale fluctuations.

Littlewood illustrated his theory with cresol-red impregnated columns through which he passed alternately acid and alkali vapours. He found that the colour change was very sharp, no broader than one particle diameter. The surface of colour change represents a surface of constant concentration at which the pH attains a particular value. Usually the line of change was inclined across the width of the column as in Figure 44. Thus the large-scale unevenness producing a very large Cg term must be attributed to the profile. In contrast to Perrett and Purnell (124) Littlewood found no dependence of Cg with K.

At the symposium Giddings was not completely convinced by this work and commented that Littlewood had underestimated the 'long-range' interchannel effect and non-uniformities over 3, 4 or 5 particle diameters could have a considerable effect. In many of the columns which I have considered there are, however, only about this number of particles across the column section thus the long-range interchannel and the trans-column effects are often equivalent. The final word on the matter came from Giddings; appropriately it was "Greater calculation is required" !

V. Conclusion

Although this work has helped to clarify the inter-relationship and magnitude of eddy diffusion and mass transfer, and the coupling theory has been conclusively proved by the liquid studies of Knox and others, the theory of the chromatographic process is still far from complete and none of the results exactly fit the theoretical equations of Giddings. It is therefore concluded that the present theories must be revised in order to accommodate the growing experimental data.

SECTION II

THE DETERMINATION OF D_g AND χ

CHAPTER I

THE MEASUREMENT OF DIFFUSION COEFFICIENTS OF GASES AND VAPOURS.

I. Introduction

i. Definition and Historical

When a gas contains two or more different kinds of molesules whose relative concentrations vary from point to point, a process called diffusion is observed to occur in such a way as to diminish the inequalities of composition. The net flow of each kind of molecule will obviously occur in the opposite direction to its concentration gradient. Besides its importance in many practical applications where the mixing-time by diffusion may be rate-determining, accurate knowledge of the molecular diffusion coefficients of gases and their temperature dependence is important in studies of laminar flame propagation and structure and is useful in obtaining fundamental information on forces between unlike molecules.

Early experimenters in the field include Priestley (220) in 1786, Dalton (221) in 1803 and Berthollet (222) in 1809. Grahame (223) showed that the rates of diffusion of two gases are inversely proportional to the square roots of the densities. The general law of diffusion was first stated by Fick (224) and relates the number of molecules (dN/dt) crossing a plane in time t to the area A and the concentration gradient dn/dl, i.e. $dN/dt = -DA\,(dn/dl)$; or for a plane of unit area, $dN/dt = -D(dn/dl)$ D is the diffusion coefficient or diffusivity. The negative sign shows that diffusion occurs in the direction of diminishing concentration. Fick's second law relates the rate of increase of concentration (dn/dt) in a given element of volume. For diffusion in three directions, Fick's second law gives

$$dn/dt = D(\partial^2 n/\partial x^2 + \partial^2 n/\partial y^2 + \partial^2 n/\partial z^2)$$

For 1-dimensional diffusion of interest in gas chromatography, this becomes $dn/dt = D(d^2n/dl^2)$. Fick's laws describe diffusion in regions

which are fixed in the medium. For a flowing fluid the effects due to flow transport through each cross-section must be added and the second law, as used in the generalised non-equilibrium theory, becomes

$$dn/dt = -Ru \ dn/dl + D\,(d^2n/dl^2)$$

ii. The General Equation for Diffusion

An acceptable solution to Fick's second law, $dn/dt = D\,(d^2n/dl^2)$ is $n = A/t^{\frac{1}{2}}.e^{-l^2/4Dt}$(225). If we write $y^2 = l^2/4Dt$,

$$dl = 2(Dt)^{\frac{1}{2}}dy \quad \text{and} \quad n = A/t^{\frac{1}{2}}.e^{-y^2}$$

The total quantity of diffusing material m, is $m = \int_{-\infty}^{\infty} n\,dl$

$$\text{Thus } m = 2AD^{\frac{1}{2}}\int_{-\infty}^{\infty} e^{-y^2}dy \qquad \text{i.e. } m = 2A\,(\pi D)^{\frac{1}{2}}$$

$$\therefore \ A = m/2\,(\pi D)^{\frac{1}{2}} \quad \text{and} \quad n = m/2(\pi D)^{\frac{1}{2}}.e^{-l^2/4Dt}$$

This equation represents a gaussian distribution (see Appendix I)

$$n_{max} = m/2\,(\pi Dt)^{\frac{1}{2}}$$

Hence $n = n_{max}e^{-l^2/4Dt}$. Writing $n = n_{max}/e$, $l_e^{\,2} = 4Dt$ where l_e represents the $\frac{1}{2}$-band-width at 1/eth of the height and is related to the standard deviation σ by $l_e = \sqrt{2}\,\sigma$ where σ is the $\frac{1}{2}$-band-width at the inflexion point.

$$\text{Thus } \sigma^2 = l_e^{\,2}/2 = 2Dt$$

This is the Einstein equation and gives the 'width' of the concentration profile for a given diffusivity as a function of time.

II. The Experimental Measurement of Diffusion Coefficients

Most experimental and theoretical studies of diffusion in gases have been concerned with very simple systems, e.g. He in N_2, and there is a strong need

for more extensive diffusion coefficient date (226-229) particularly on organic molecules. Current methods (229-231) involving a Loschmidt-type apparatus or the point-source method of Walker and Westenburg (229, 232) are time-consuming while the faster methods of Waldman (233) appear to be less precise. The precision ranges from 0.4% for the best Loschmidt-type determination to 5% for other types. The most widely used method for the measurement of vapour diffusion coefficients is that of Stefan (227, 234-240). The precision is poor for vapours of liquids of very high or very low vapour pressures and the method is thus limited to a rather narrow temperature range. No measurement whatever can be made above the boiling-point of the liquid and each determination requires a relatively large quantity of liquid and a period of several hours.

The general theories of band spreading in chromatographic columns are founded on the basic theory of diffusion, and in particular the molecular diffusion and gas mass transfer terms are strongly dependent on Dg. Several workers (134, 241-245) have shown that diffusion coefficients can be measured rapidly and accurately by variations of an elution method involving an empty tube. Only trace amounts of sample are required. The Golay equation (41) for an open tube with no liquid phase reduces to

$$H = 2D_g/u_o + (r^2/24\ D_g)u_o .$$

Thus it should only be necessary to measure H and obtain Dg from a single experiment since

$$D_g = u_o/4\ (H \pm \sqrt{H^2 - r^2/3})$$

One is not restricted to very low flow rates and the associated difficulties of back diffusion, detector instability, etc., are eliminated. The precision has been given as 1% by Giddings et al. (242-245). Each measured value of H gives two values of Dg which become equal at $u = \sqrt{48D_g}/r$ and one works either well before or well after this critical velocity.

Alternatively for low velocities, the straight-line plot of Hu against u^2 gives an intercept of 2Dg. Using this method Bohemen and Purnell obtained an experimental to literature ratio for Dg of 0.97 - 1.03, an excellent agreement. Scott and Hazeldean on the other hand (246) working with a coated capillery calculated Dg both from the B and Cg terms and obtained widely differing values differing widely from the calculated value. Desty and Goldup (72) found a similar result. These anomalies could perhaps be explained by the non-uniform-:ity of the liquid film but the situation is not a happy one. Carberry and

Bretton, indeed (247, 248), ignored the existance of γ at very low velocities and assumed that the product Hu yielded Dg, thereby introducing an error of 10 to 40% ! What is required is a general method for gases and vapours which is rapid and has an accuracy of about 1% .

i. The Arrested Elution Method

By Einstein's equation, the concentration profile of a spike of gas spreading by diffusion into another gas is Gaussian after a finite time t and the rate of spreading is given by the equation, $d\sigma_x^2/dt = 2Dg$ where σ_x is the standard deviation of the Gaussian concentration profile measured as a distance and Dg is the binary diffusion coefficient. In practice in any quasi-chromatographic method the time variance σ_t^2 of the eluted band is measured rather than σ_x^2. If the spreading band moves slowly down the column at a constant linear velocity u, longitudinal diffusion will occur at the same rate as if the band were static. In an empty tube, if u is sufficiently low, other sources of spreading may be neglected and diffusional spreading is given by $d\sigma_t^2/dt = 2D_g/u^2$ since $\sigma x/\sigma t = u$. The arrested elution method is a development of the continuous elution method. A sharp band of an unsorbed gas B is injected into the column and eluted at a controlled and measurable velocity. When the band is about half-way down the column the gas flow is arrested for a time t, during which spreading can occur only by diffusion. Finally the band is eluted from the column and its concentration profile and standard deviation determined by the detector. Provided that B is not sorbed by the column, the above equation holds for the additional variance produced by diffusion during the delay period if u is taken as the outlet elution velocity u_o. The variance produced by the injector, column connections, detector and elution along the column are now the same whatever the delay and can accordingly be subtracted out. Thus a plot of σ_t^2 against delay should be a straight line of gradient $2D_g/u_o^2$ with the intercept at zero delay the variance introduced by the standard procedure.

The method has 3 major advantages over the continuous method. Extra-column spreading and spreading within the column due to processes other than longitudinal diffusion are allowed for. Quite a short column can be

used whose diameter can be made uniform. Non-uniformity would clearly introduce an error into the band width. It is unnecessary to maintain a low flow rate constant over a long period of time, say ten minutes, so that most of the experimental difficulties met with in the continuous elution method are avoided.

III. The Theoretical Estimation of Dg

Dg can be calculated from theory with different degrees of precision. Early equations were based on the elementary kinetic theory of gases which regarded molecules as hard spheres, but later theories considered more realistic models. There have been several reviews, the most recent being that of Giddings and Fuller (150, 249-252).

Meyer's formula (253) gave Dg as composition dependent, a fact not found in practice for low concentrations. In terms of mole fractions x, it is $D_{12} = 1/2\ X_1\ \bar{c}_2\ \lambda_2 + 1/2\ X_2\ \bar{c}_1\ \lambda_1$ Maxwell (254) postulated that diffusion was not hindered by collisions of molecules of the same kind. The Stefan-Maxwell equation is:

$$D_{12} = \frac{\alpha}{(n_1 + n_2)\ \sigma_{12}^2} \left[\frac{8\ RT}{\pi} \left(\frac{1}{M_1} + \frac{1}{M_2} \right) \right]^{\frac{1}{2}}$$

where the constant α is variously given as $1/3\pi$, 1/8, $1/2\pi$ and 3/32 (150, 255). Although based on the hard sphere model this equation does represent the behaviour of gases fairly well. It follows from the above equation that

$D_{12} = D_{12}^{o} \left(\frac{T}{T_o} \right)^{m'} \frac{p_o}{p}$ where m' = 1.50. The temperature dependence has been found to vary from system to system and m' does not always have the value of 1.50 (241).

In the Gilliland equation (256) the σ_{12} values, for which only limited data are available, were replaced by more accessible molar volume terms.

$$D_{12} = 0.0043\ T^{3/2} \sqrt{1/M_1 + 1/M_2}\ /\ (V_1^{1/3} + V_2^{1/3})^2\ p$$

This followed the approach of Arnold (257). He adopted the Sutherland

temperature function (258) and the temperature dependence of Dg was changed to $T^{5/2}$.

The diffusion equation was further developed by Hirschfelder, Bird and Spotz (259, 260). Following the rigorous Chapman-Enskog kinetic approach (255) the equation is

$$D_{12} = \frac{0.001858\ T^{3/2}\ (1/M_1 + 1/M_2)^{\frac{1}{2}}}{p\ \sigma_{12}^{2}\ \Omega_{D,\,12}}$$

$\Omega_{D,12}$ is a dimensionless function of the temperature and of the intermolecular potential field. This potential field may be approximated by the Lennard-Jones function with inverse-sixth power attractive terms and inverse-twelfth power repulsive terms, viz.

$$\phi_{12}(r) = 4\epsilon_{12}\left[\left(\frac{\sigma_{12}}{r}\right)^{12} - \left(\frac{\sigma_{12}}{r}\right)^{6}\right]$$

Ω_D evaluated as a function of $(kT/\epsilon)_{12}$ is listed in tables (150, 252). The values of the Lennard-Jones force constants for each component are best obtained from viscosity data, and for non-polar, non-reacting molecule pairs they may be combined empirically, thus (261, 262)

$$\sigma_{12} = 1/2\ (\sigma_1 + \sigma_2)$$

$$\epsilon_{12} = (\epsilon_1\ \epsilon_2)^{\frac{1}{2}}$$

Although the equation was derived for monatomic, non-polar gases, it has been found to work well for polyatomic and non-polar gases as well. Chen and othmer (263) further developed this to eliminate the need to use collision integrals from tables but the method is very involved.

Wilke and Lee (264) reduced the average error to 4% from 7% by introducing the empirical function $0.00214 - 0.000492\ (1/M_1 + 1/M_2)^{\frac{1}{2}}$ where the force constants were obtained from viscosity data. The diffusion equation has since been developed further by Slattery and Bird (265) and Othmer and Chen (266).

A comparison of experimental and calculated results (249, 251) shows that the Gilliland equation incurs the largest errors and is the most erratic. The error is of the order of -50% for helium as the main component and -12% for the heavier gases. The best overall agreement is obtained with the Wilke and Lee

modification of the Hirschfelder, Bird and Spotz equation. Diffusion co-efficients are difficult to measure accorately as evidenced by the dis-agreement among different experimental values for the same gas pair and the experimental methods are apt to give too large values for Dg because of convection.

IV. A test of the Arrested Elution Method

i. Aim of the Research

Ten diffusion coefficients were measured using the arrested elution technique and the values obtained were compared with those calculated from the Wilke and Lee version of the diffusion equation.

ii. Experimental Procedure

The first experiments were carried out with nylon capillary tubing of internal diameter 0.88 and 1.48 mm at different flow rates of carrier gas (columns I - III). A typical experiment was as follows: The ethylene sample was injected and eluted as usual and the time spent in the column calculated from the observed time and the volumes of the column and the ancillary tubing, the latter being always less than 3% of the former. Pressure corrections were always less than 2%. The values of u_o were checked by direct measurement of the volume flow rates and the gas phase volumes of the column. The latter were determined by filling the tubes with mercury and weighing the liquid. In the case of the C_5 liquids, samples were obtained by bubbling nitrogen through a 5% solution of the hydrocarbon in dinonylphthalate. The resulting contaminated stream was then used as the sample gas.

To study the static spreading in the column the band of ethylene was eluted about half-way along the column at the linear flow rate used in the continuous elution experiment. The flow was then switched to a dummy column of exactly equal resistance by turning the two-way tap T as shown in Figure 13. After a delay of 1 to 20 minutes the flow was reconnected to the column and the peak eluted. A plot of w^2 against t was then drawn up.

By using nitrogen slightly contaminated with pentane as the carrier gas the recorder deflection was proportional to the flow and it was found that with

large pressure drops across the column the gas velocity did not reach its stationary value before the peak was eluted. A typical trace is shown in Figure 45a. This led to an excessively high Dg value because the assumed value of u in the equation $d\sigma_t^2/dt = 2D_g/u_o^2$ (see below) was higher than the actual value. With a pressure drop of the order of 2 cm of mercury the deflection reached at least 99% of its stationary value before the peak was eluted as shown in Figure 45b and the error was negligible.

The apparatus was then improved. The nylon tube was replaced by a five foot length of glass tubing of internal diameter 1.56 mm. This was silanised with dichlorodimethylsilane (see later). Column connections were reduced to an absolute minimum. The column and injector were surrounded by water jackets and thermostatted at 20°C. The diffusion coefficients of a selection of pure hydrocarbons, supplied by B.H.C. Ltd. and B.P. Ltd., were then measured.

iii. Calculation of Results

Since the expression for diffusional spreading in an empty tube,

$$d\sigma_t^2/dt = 2D_g/u^2$$

holds for the additional variance produced by diffusion during the delay period if u is taken as u_o, a plot of σ_t^2 against delay gives a straight line of gradient $2D_g/u_o^2$ from which Dg may be determined. The intercept at zero delay is the variance produced by extra-column spreading processes. In practice w^2 is plotted against delay time and σ_t is obtained from the relationship,

$$w = \frac{\text{Integral}}{\text{Peak Height}} = \frac{\sqrt{2\pi}}{0.96} \cdot \sigma_t$$

$$\text{Hence} \qquad D_g = \frac{dw^2}{dt} \frac{(0.96)^2}{2\pi} \frac{u_o^2}{2}$$

Since u_o occurs to the second power in the above expression it must be measured as accurately as possible. With the present apparatus the accuracy of the method cannot be claimed to be any better than 2%

iv. Results and Discussion

The experimental parameters and run data are given in Tables 37-40. The straight-line plots are shown in Figures 46-49. The agreement between the measured and calculated values for the paraffin-type molecules (Table 41) which may be linear or crumpled in the gas phase, is good, considering the assumptions that the molecular interaction can be described in terms of a Lennard-Jones potential and that the force constants between unlike molecules may be taken as the average of the force constants between like molecules evaluated from viscosity data. The excellent agreement for systems involving ethane or butane must mean that at room temperature the molecules are effect-:ively spherically symmetrical in their interaction with other molecules.

In each case the value for the iso-paraffin is about 2% lower than that for the normal isomer. This might be expected from structural considerations though the branched isomer has been reported as having a higher diffusion co-:efficient than the straight-chain one (267-268). The decreased value may be interpreted as meaning that the collision diameter for iso-butane is slightly larger than that for normal butane.

The diffusion coefficient falls off rapidly with increasing molecular size and more slowly with increasing molecular weight. Figure 50 (Table 42) shows the proportionality of D to the inverse square root of the molecular weight, i.e. density, as originally noticed by Grahame (223). The linearity of the plot is surprisingly good considering that all the other parameters entering into the expression for D have been ignored.

The largest error between calculated and experimental is found with the pentanes. The experimental values are however consistent among themselves, and it is to be expected that the agreement between calculated and experi-:mental will fall off with increasing molecular complexity.

There is also a slight discrepancy between my values calculated from the parameters in Table 42 and those reported in the literature (251, 249). Thus D = 0.163 ($T = 298^{\circ}C$) has been reported for ethylene, and cyclohexane, calculated by me as 0.0780, has been reported as 0.0764 ($T = 289^{\circ}C$). This discrepancy could easily be in the method of calculation.

Table 37.

Experimental Parameters and Data for the Nylon Tubing.

$T = 18^{\circ}C.$ $p_o = 75.0$ cm.

	I	II	III
Length cm	1640	834	693
d_{mm}	0.88	0.88	1.48
Δp_{cm}	2.80	1.40	1.30
f_1	0.982	0.990	0.992
u_o cm.sec^{-1}	28.8	26.2	15.4
D_g cm^{2}sec-1	0.164	0.166	0.164

Table 38 (Figures 46 and 47)

Individual Run Data.

Column I			Column II			Column III		
Residence Time(mins)	W	W^2	Residence Time(mins)	W	W^2	Residence Time(mins)	W	W^2
0.97	0.60	0.36	0.53	0.48	0.23	0.88	1.67	2.80
2.54	0.88	0.78	1.27	0.64	0.41	2.45	1.81	3.26
3.54	0.90	0.81	2.27	0.74	0.54	3.45	2.14	4.75
4.54	0.98	0.96	3.29	0.88	0.77	4.45	2.34	5.47
5.54	1.07	1.15	4.29	0.99	0.99	5.45	2.51	6.30
6.54	1.14	1.31	5.28	1.10	1.20	6.45	2.66	7.10
7.54	1.21	1.46	6.29	1.17	1.37	7.45	2.78	7.70
9.54	1.34	1.79	7.30	1.27	1.62	8.45	2.92	8.52
10.54	1.38	1.90	8.30	1.33	1.78	9.45	3.08	9.47
12.57	1.48	2.20	9.30	1.40	1.96			
14.75	1.63	2.67	10.29	1.43	2.05			
16.58	1.72	2.95	11.30	1.55	2.40			
			13.35	1.64	2.70			
			15.28	1.71	2.94			
			16.63	1.86	3.47			
			17.30	1.86	3.46			
			19.32	1.94	3.78			

Table 39. (Figures 48 and 49)

Experimental Data for Open Tube for Different Sample Cases

$T = 20^{\circ}C$. p_o = Atmospheric. $p_i = 0.40$ cm H_g

METHANE			ETHYLENE			ETHANE			PROPANE			ISO-BUTENE		
Residence Time(mins)	W	W^2	Residence Time(mins)	W	W^2	Residence Time(mins)	W	W^2	Residence Time(mins)	W	W^2	Residence Time(mins)	W	W^2
0.38	1.33	1.75	0.35	1.09	1.119	0.41	1.33	1.77	0.40	1.17	1.36	0.39	1.01	1.02
1.20	2.20	4.83	1.20	1.83	3.33	1.22	2.09	4.35	1.20	1.80	3.24	1.20	1.57	2.45
2.20	2.99	9.80	2.20	2.47	6.10	2.22	2.79	7.77	2.45	2.48	6.15	2.26	2.04	4.18
3.20	3.55	12.7	3.20	2.92	8.53	3.22	3.39	11.5	3.21	2.79	7.80	3.20	2.38	5.65
4.20	4.03	16.2	4.20	3.31	10.95	4.22	3.82	14.6	3.20	10.2	4.24	4.24	2.83	8.00
5.20	4.55	20.7	5.20	3.69	13.6	5.24	4.28	18.3	5.21	3.49	12.2	5.21	3.06	9.35
6.21	5.00	25.0	6.20	4.03	16.2	6.23	4.62	21.3	6.80	3.97	15.8	6.20	3.34	11.2
7.21	5.36	28.7	7.28	4.36	19.0	7.23	4.93	24.3	7.21	4.17	17.4	7.20	3.56	12.7
8.23	5.73	32.9	8.20	4.62	21.3	8.24	5.28	27.8	9.21	4.64	21.5	8.21	3.80	14.4
$u_o = 6.77$ cm.sec^{-1}			$u_o = 7.27$ cm.sec^{-1}			$u_o = 6.17$ cm.sec^{-1}			$u_o = 6.44$ cm.sec^{-1}			$u_o = 6.67$ cm. sec.$^{-1}$		

Table 40 (Figure 49)

Experimental Data for Open Tube for Different Sample Gases

$T = 20^{\circ}C$. p_o = Atmospheric. p_i = 0.40 cm. H_g

N-BUTANE			ISO-BUTANE			2-PENTENE			N-PENTANE			ISO-PENTANE		
Residence Time(Mins)	W	W^2	Residence Time(Mins)	W	W^2	Residence Time(Mins)	W	W^2	Residence Time(Mins)	W	W^2	Residence Time(Mins)	W	W^2
0.42	1.11	1.22	0.42	1.10	1.22	0.39	1.05	1.09	0.39	1.05	1.10	0.39	1.04	1.08
1.21	1.69	2.85	1.24	1.70	2.87	1.20	1.53	2.32	1.20	1.52	2.28	1.20	1.50	2.27
2.23	2.23	4.97	2.23	2.19	4.80	2.20	1.92	3.68	2.20	1.93	3.72	2.22	1.99	3.95
3.23	2.63	6.92	3.23	2.57	6.63	3.20	2.25	5.08	3.20	2.28	5.20	3.20	2.31	5.35
4.23	3.00	9.00	4.23	2.93	8.57	4.21	2.60	6.75	4.20	2.58	6.67	4.19	2.58	6.64
5.23	3.28	10.8	5.23	3.20	10.3	5.21	2.90	8.40	5.20	2.86	8.20	5.20	2.89	8.34
6.23	3.60	12.9	6.23	3.52	12.4	6.21	3.12	9.70	6.21	3.12	9.75	6.20	3.08	9.48
7.24	3.80	14.4				7.21	3.37	11.4	7.29	3.42	11.7	7.22	3.35	11.2
8.24	4.10	16.8				8.22	3.63	13.2	8.22	3.66	13.4	8.21	3.53	12.5
u_o = 6.19 cm.sec^{-1}			u_o = 6.23 cm.sec^{-1}			u_o = 6.57 cm.sec^{-1}			u_o = 6.57 cm.sec^{-1}			u_o = 6.57 cm.sec^{-1}		

Table 41.

Comparison of Experimental and Theoretical Results. T = 20°C. p = 76.0 cm.

Gas	D_g (Exp)	D_g (Cal)	% Error
CH_4	0.224	0.223	+ 0.4
C_2H_4	0.165 *(0.163)	0.166	- 0.6
C_2H_6	0.154 *(0.145)	0.151	+ 2
C_3H_8	0.116	0.117	-1
ISO-C_4H_8	0.0939	-	-
N-C_4H_{10}	0.0930 *(0.0960)	-	-
ISO-C_4H_{10}	0.0913 *(0.0908)	0.0904	+ 1
2-C_5H_{10}	0.0793	-	-
N-C_5H_{12}	0.0797	0.0879	-10.3
ISO-C_5H_{12}	0.0778	-	-

* Values obtained by Boyd et al (226)

$$\% \text{ Error} = \left(\frac{\text{Exp} - \text{cal.}}{\text{Exp}}\right) \times 100$$

Table 42 (Figure 50)

Intermolecular Force Parameters

Gas	M	σ (Å)	$\epsilon/k(\sigma_K)$	$1/\sqrt{M}$
N_2	28.02	3.681	91.5	
CH_4	16.04	3.822	137	0.250
C_2H_4	28.05	4.232	205	0.189
C_2H_6	30.07	4.418	230	0.182
C_3H_8	44.09	5.061	254	0.151
ISO-C_4H_{10}	58.12	5.341	313	0.131
N-C_5H_{12}	72.15	5.769	345	0.118

v. Conclusion

The arrested elution technique provides a rapid, precise method of determining diffusion coefficients. Its applicability to higher molecular weight compounds has still to be investigated.

CHAPTER II

THE MEASUREMENT AND INTERPRETATION OF γ

I. Introduction

1. The Measurement of γ

Although it is generally agreed that the tortuosity of a packed bed is given by $(Le/L)^2$ where Le and L are the tortuous and straight path lengths, respectively, there is a considerable difference of opinion on the value to be accepted for this factor. While Bartell and Osterhof (269) adopted $(Le/L)^2 = \pi/2 = 1.57$ the ratio between diameter and semi-circumference of a circle, Carman (270), from the motion of a coloured streamline through a bed of large glass spheres, found that it appeared to adopt an average angle θ of 45° to the direction of flow and hence used $Le/L = 1/\cos 45^\circ = \sqrt{2} = 1.41$ Fowler and Hertel (271) pointed out that θ cannot have a constant value but varies from point to point along the path. The correct average for $(Le/L)^2$ should be $(\cos^2\theta)_{av.}$ taken over all values of θ, but the distribution of θ cannot be determined. By their method every streamline followed a course parallel to the surface nearest to it and from the diagram (Figure 51) $\theta = 90-\phi$, ϕ being the angle between the normal to the surface of a solid particle and the direction of flow. Thus $(\cos^2\theta)_{av.} = (\sin^2\phi)_{av.}$ This gives a tortuosity value of 1.5 for a bed of spheres, but the relationship between θ and ϕ is a doubtful one. Thus a theoretical treatment is extremely difficult and the above approaches have ignored intra-particle porosity.

In the van Deemter equation $B = 2\gamma D_g$ where γ is the so-called 'tortuosity factor'. Early workers with packed columns and an elution method (50, 56, 129, 130, 137-8, 146) determined γ from the simplified van Deemter equation, but for more precise data the extended rate equation should be used. By working with unsorbed solutes at very low velocities of the order of 1 cm/sec, the gas phase mass transfer contribution may be ignored and γD_g may be determined directly from a plot of $H/1/u$ (121, 134). More generally γD_g can be found by calculation (122, 129, 140), by obtaining the best fit between the experimental data and the HETP equation. γ is then obtained by assuming a

theoretical value of Dg. The results tend to fall into 2 groups. While Littlewood (130) and Kieselbach (133) found γ to lie between 0.5 and 0.65, Glueckauf (136) and Purnell et al. (129) found γ to lie between 0.8 and 1. This disagreement may be attributed to uncertainties in the HETP equation and experimental method at low flow rates and to the inaccuracy of diffusion coefficient data.

ii. The Electrophoretic Approach to γ

γ has been interpreted as a correction on the appropriate velocity to be used (134) or as a correction factor modifying the diffusion coefficient (188). This term "tortuosity" was first criticised by Barrer (272) who suggested the name 'Structure Factor' was more appropriate since γ is undoubtedly a function of support structure. However no attempt was made to predict the magnitude of γ or its relationship to structure.

In the field of electrophoresis two concepts have been proposed to account for the hindrance of ionic migration in the network of semi-permeable obstructions. The 'barrier' theory of McDonald (273) considered the supporting medium to be composed of randomly distributed obstructions which slow the migrant by collision or by mechanical restriction of the free pathways. The 'tortuous path' concept of Kurkel and Tiselius (274-5) predicted a lowered mobility because of the increased path length around fibres and the decreased electric field strength acting along this path. The paper was represented by a bundle of tortuous capillary channels each of uniform cross-section and the ratio of the observed to free solution mobility was given by $(l/l')^2$ where l' was the effective length of the tortuous path and l the length of the direct straight-line path.

The erratically changing size of the migration channel and the attendant difficulty in diffusion through a constriction have been shown by Owen (276) and especially by Boyack and Giddings (277-279) to contribute a 'constriction factor' C approximately equal in importance to the tortuosity factor T. Giddings (108) suggested that this approach should be applicable to γ which, by analogy to electrophoresis, should be called the 'obstructive' factor and should be given by $\gamma = CT^{-2}$.

iii. The Aim of the Research

We have tried to give a more precise interpretation of γ by showing that the electrophoretic approach does indeed provide a theoretical foundation to the heretofore empirical parameter. The arrested elution method was used as this bypasses most of the experimental difficulties associated with continuous elution methods based upon HETP measurements and it is of intrinsically higher precision.

II. The Interpretation of γ

The longitudinal diffusion of solute is best envisaged by assuming all flow has ceased. According to Boyack and Giddings, diffusion through static gas will be hindered (1) by the tortuosity which prevents diffusion of molecules along the shortest, most direct path and (2) by channel constrictions which create 'bottlenecks' at random points. These are illustrated in Figure 52.

i. Theory of Tortuosity

As before the diffusion profile of a solute spike is given by $\sigma_x^2 = 2Dt$ with D the apparent diffusion coefficient and σ_x the spread along the axis of the column. Due to tortuosity, the diffusion path is $lT/l = T$ times longer than the axial path where T is the tortuosity. The actual displacement is thus $T\sigma_x$ instead of σ_x giving $(T\sigma_x)^2 = 2D_g t$ where Dg is the molecular diffusion coefficient. Thus $D/D_g = T^{-2} = \gamma$.

ii. Theory of Constriction

By Fick's first law the solute flux J_c through a cross-section of a constricted but straight channel is $J_c = -D_g (dc/dz)A$ where A, the channel cross-section is variable due to the constrictions. Thus $dc/dz = -J_c/D_g A$ and integration over the length l of the channel gives

$$\Delta c = -(J_c/D_g) \int_0^l dz/A \quad / \quad -(J_c/D_g)(\overline{1/A})l$$ where Δc is the concentration difference over the length l. In the steady state the same flux must pass each cross-section along the segment, i.e. J_c is constant.

If D is the effective diffusion coefficient and $\bar{A}$ the mean cross-sectional area,

$$Jc = - D(\Delta c/l)\ \bar{A}$$

$$\therefore \Delta C = - (Jc/D)\ (1/\bar{A})l$$

$$\therefore D/D_g = \delta = 1/\bar{A}\ (\ \overline{1/A}\ ) = C$$

Then, by Boyack and Giddings, $\delta = CT^{-2}$

In reality there are no channels with clearly defined walls in a 3-dimensional packed structure and with porous materials there is the possibility of intra-particle diffusion so that if the above theory is to be tested simple regular models must be devised and so we investigated models based on spheres of equal size.

iii. Models used in the Calculation of δ

Boyack and Giddings applied this theory to a variety of particle types. The model they considered for spheres of equal size is shown in Figure 53a, viz. a regular array of spheres in cubical boxes, each box containing a single sphere. When the spheres are touching this arrangement has a minimum porosity of 0.477 compared with the accepted values of 0.26 for closest packing and 0.38 for random packing of spheres and this model is probably too 'open' for most closely packed structures. For this reason we studied the model shown in Figure 53b containing a single row of touching spheres of radius r in a round tube of radius R. This arrangement shows a minimum porosity of 0.333 when r = R in which configuration however the model is impervious to gas. Although this model deviates from the real situation it can nevertheless be used to test predictions quantitatively since it can be precisely constructed. The last model to be considered is shown in Figure 53c. With 5 or 6 hemispheres arrang-:ed around the central row in a porosity range 0.35 to 0.45 a reasonable approximation to a randomly packed bed is obtained.

III. The Calculation of T and C

The basic premise of the method used by Boyack and Giddings was that the porous medium and an average cell having the same void fraction and containing a single particle behave approximately the same. This was justified by the

independence of C and T on a particle size for a constant porosity. In the model C and T are independent of the position of the particle within the cell thus allowing for a certain degree of randomness. The particle is still restricted to the volume within the cell boundaries and the realistic structure is extremely difficult to treat.

Tortuosity: The model used by Giddings and Boyack is shown in Figure 54. Those lines which pass through the area A_2 proceed straight across the cell. Any path which intercepts the A_1 plane which is the axial projection of the particle profile on the wall of the box, proceeds straight to the surface of the particle and then follows the shortest route on the particle surface around to its original trajectory. It then follows this straight line through to the opposite face. The tortuosity is then the length of these lines averaged over the whole cell. This procedure overestimates the length of the lines originating inside A_1 since curvature actually begins long before the particle is reached, and underestimates the length of lines originating within A_2 since such paths are never straight with the result that the errors tend to cancel out and the approximation probably gives quite a good measure of T. The tortuosity is found to have the same functional form for every shape of particle and is given by $T = 1 + a\,\theta$ where θ is the occupancy of the medium ($\theta = 1 - \epsilon$) and a is a constant for any given particle type.

In a random packing all the paths are more or less tortuous and the factor 0.178 is almost certainly too small. In model (Figure 55) representing close-packed spheres through which there are no straight paths, the shortest and longest paths as shown have tortuosities of 1.19 and 1.33 respectively. Assuming a linear relationship between tortuosity and occupancy which for this arrangement is 0.74, the equations for the two extreme cases are $T = 1 + 0.26\,\theta$ and $T = 1 + 0.45\,\theta$. The equation $T = 1 + 0.33\,\theta$ was arbitrarily selected.

Constriction: $$C = 1 \left[\bar{A} \int_0^1 dx/Ax \right]^{-1}$$

where $\bar{A}$ is the mean cross-sectional area of the column and A_x is a variable cross-section.

Giddings has plotted the various obstructive factors against porosity and his graphs are shown in Figure 56 along with the data for models 53B and 53C.

In model 53B the unoccupied cross-sectional area, a distance x from the centre of any sphere in the central row, is

$$A_x = \pi (R^2 - y^2) = \pi (R^2 - r^2 + x^2)$$, and the mean area is $$\bar{A} = \pi (R^2 - 2r^2/3)$$. Inserting this value in the above equation for C and integrating from 0 to r gives

$$C = \frac{\sqrt{\rho^2 - 1}}{(\rho^2 - 2/3)\tan^{-1}\sqrt{\rho^2 - 1}}$$

where $\rho = R/r$. The values of C, T^{-2} and CT^{-2} for various values of ρ are shown in Figure 57; values as a function of porosity are shown in Figure 56.

For model 53C with n hemispheres around the central row, the free cross-sectional area, a distance x from any point of contact on the axis, and the average area are, respectively,

$$A_x = \pi \left[R^2 - n/2 \cdot r^2 + 1/2 \cdot (n + 2)\, x^2 - 2rx\right]$$

$$\bar{A} = \pi \left[R^2 - 1/3 \cdot (n + 2)\, r^2\right]$$

For 5 and 6 beads around the central row the integrated expressions for C are respectively,

$$C = \left(\frac{7}{2}\right)^{\frac{1}{2}} \frac{\sqrt{\rho^2 - 39/14}}{\rho^2 - 7/3} \left\{ \arctan \frac{(2/7)^{\frac{1}{2}}}{\sqrt{\rho^2 - 39/14}} + \arctan \frac{2.5\,(2/7)^{\frac{1}{2}}}{\sqrt{\rho^2 - 39/14}} \right\}^{-1}$$

and $$C = \frac{2\sqrt{\rho^2 - 13/4}}{\rho^2 - 8/3} \left\{ \arctan \frac{1}{2\sqrt{\rho^2 - 13/4}} + \arctan \frac{3}{2\sqrt{\rho^2 - 13/4}} \right\}^{-1}$$

For porosities above 0.36 there is little to choose between the calculated values. For $\epsilon = 0.38$ the predicted value of δ is 0.63.

IV. Experimental

The experimental procedure was the same as that used in the determination of diffusion coefficients with the capillary column replaced by a packed column with end connections as before (Figure 16). Packings used were glass beads, firebrick (Molar Products, Colchester, Fosalsil No.6) and Celite (Gas Chroma - :tography Limited). For model 2B experiments steel ball bearings and polyvinyl- :chloride spheres were used.

The volume of the empty tubes were determined by filling with mercury or water and weighing the liquid. The total porosities of the packed columns were determined with a Toepler pump using ethylene and nitrogen. Identical values of ϵ with the 2 gases were taken to indicate absence of residual adsorption.

i. Deactivation of the Support

With celite and firebrick it was necessary to eliminate adsorption by the support. There appear to be at least two different types of active sites on the surface of the support. One type is acidic and may be caused by mineral impurities (Si - OH); the other may involve hydrogen-bonding (Si - O - Si) (280 - 286). The two basic approaches in deactivation are to remove the active sites by washing with acid (286 - 288) or by reaction with the silanol group, or to cover them by coating the support with a liquid or solid (290 - 292).

Reaction with the Silanol Group: Deactivation with dimethyldichlorosilane (DMDCS) has been used with varying degrees of success by several workers, (291, 293, 294). Following Holmes and Stack (295) I used the DMDCS in toluene solution and washed with methanol. Bohemen et al. (29) suggest the following mechanism for the reaction:

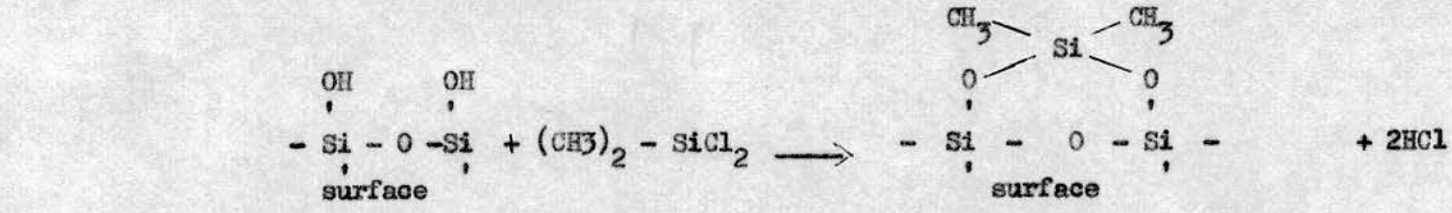

Two adjacent OH groups are required before the reaction goes to completion. With a single OH group the following reaction might proceed:

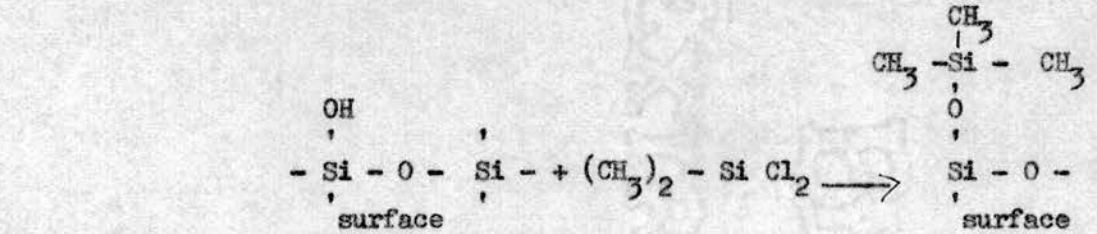

However the Si - Cl group can hydrolyse to give Si - OH again. Both reactions probably proceed simultaneously. The HCl is removed by the methanol wash.

Bohemen et al. also reported the use of hexamethyldisilazone (HMPS). The reaction is:

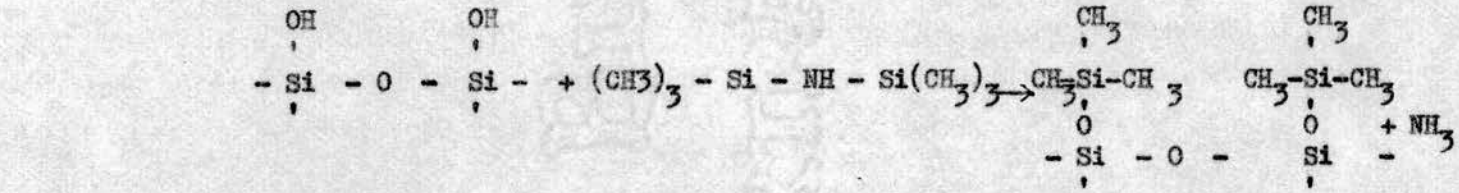

Any residual adsorption is then removed by the addition of 0.1 percent by weight of polyethylene glycol 400. While treated celite is fairly inert Perrett and Purnell (286) found that HMDS-treated firebrick was comparable to the untreated white celite (296, 297). In this case the treatment with DMDCS proved to be entirely satisfactory from retention time measurements and the perfect peak symmetry. A small quantity of firebrick was also treated with 20% w/w of urea formaldehyde resin polymerized in situ.

V. Results and Discussion

i. Calculation of Results

Where diffusion is hindered by obstructing but non-sorbing material, the rate of band spreading is given by the equation $d\sigma_x^2/dt = 2\gamma D_g$ and as before $d\sigma_t^2/dt = 2\gamma D_g/u_o^2$. Thus a plot of σ_t^2 against delay gives a straight line of gradient $2\gamma D_g/u_o^2$, the intercept at zero delay representing the variance introduced by the standard procedure. This plot gives the apparent diffusion coefficient from which γ can be obtained knowing D_g (real) from empty tube studies. In all these experiments the pressure drop was sufficiently small to ensure that the gas velocity had reached its stationary value before the peak was eluted.

ii. Results

The data for the glass bead, firebrick and celite columns are given in Tables 43-45, Figures 58 and 59. The data and experimental parameters for the model 53B experiments are given in Tables 46-48, Figures 57 and 60. The plots are very reproducible and the error in γ is about 2%. The value of $\gamma = 0.60 \pm 0.02$ for 2 sizes of beads in different diameter columns agrees with the value obtained from the HETP measurements on air peaks in glass bead

columns. The γ values for firebrick and celite were 0.46 $\pm$ 0.01 and 0.74 $\pm$ 0.02 respectively. These are in reasonable agreement with published data (123, 124, 130, 133, 134, 138, 140, 298). Bohemen and Purnell (134) have suggested that γ is approximately unity when the carrier gas velocity computed as the ratio of the volume flow rate to the inter-particle cross-sectional area is used instead of the velocity of an unretained component. Sternberg and Poulson (155), however, have pointed out that if the best overall curve is drawn the results for non-sorbed peaks on glass bead and chromosorb columns no longer support this theory. Berge and Pretorius (299) have also criticised Bohemen and Purnell. They obtained a value of γ of 0.6 by replacing the apparent inter-particle pore velocity by the effective linear velocity. Sternberg and Poulson found average values of 0.74 and 0.63 for glass beads and chromosorb respectively. Kieselbach's data also differs in that he finds essentially identical B values for beads and chromosorb and this is difficult to explain. (145).

iii. Discussion of Results

1. Non-Porous Glass Beads: The value of γ for glass beads (Figure 58, Table 43) is shown in Figure 56 along with the theoretical curves for the model 53C. The agreement is surprisingly good since the value for the tortuosity was arbitrarily selected and shows that both constriction and tortuosity effects must be considered in the evaluation of γ. The constriction effect is particularly evident in the studies on model 53B. The γ values (Figure 60, Tables 46-48) are plotted in Figure 57 and here the agreement between theory and practice is excellent and the difference in γ for different ρ values may be attributed almost entirely to the constriction effect. While the claims of Boyack and Giddings appear to have been verified for non-porous supports, the celite and firebrick results require a closer examination in order to explain the substantial difference in γ.

2. Comparison of Celite and Firebrick: Celite is made by calcining diatomaceous earth above 900^{0} in the presence of Na_2CO_3 as fluxing agent when the finer particles are fused into coarser aggregates and the iron oxide is converted to a colourless sodium iron silicate. Firebrick is made by first calcining diatomite without using fluxing agent to form an aggregate and then mixing it with clay and firing it to make brick. Again part of the silica becomes

Table 43 (Figure 58)

Data for Glass Bead Columns. $T = 18^{\circ}C$. $p_o = 75.0$ cm.

	Column I	Column II	Column III
Length cm	152	152	79
d_c mm	5.7	3.0	6.4
d_p mm	0.50	0.50	0.275
Δp cm	2.8	3.3	2.5
f_1	0.981	0.978	0.983
u_o	4.9	7.4	2.4
ϵ	0.38	0.38	0.38
γD_g	0.102	0.096	0.102
γ	0.62	0.58	0.62

Column I			Column II			Column III		
Residence Time(mins)	W	W^2	Residence Time(mins)	W	W^2	Residence Time(mins)	W	W^2
0.53	1.65	2.74	0.36	0.83	0.69	0.56	2.79	7.78
1.28	2.36	5.55	1.20	1.34	1.79	1.32	4.21	17.7
2.28	3.05	9.30	2.20	1.73	2.98	2.32	5.65	31.8
3.30	3.60	12.95	3.20	2.17	4.70	3.32	6.95	48.3
4.28	3.88	15.1	4.20	2.41	5.80	4.32	7.9	62.5
5.28	4.17	17.3	5.20	2.68	7.15	5.32	8.80	77.3
6.28	4.68	21.9	6.20	2.96	8.80	6.32	9.34	87.0
7.28	5.07	25.6	7.20	3.18	10.1	7.32	10.1	102
8.28	5.37	28.8	8.20	3.46	12.0	8.35	11.05	122
9.28	5.80	33.6	9.20	3.52	12.4	9.32	11.7	137
10.30	6.13	37.5	10.20	3.80	14.4	5.00	8.3	69
11.28	6.35	40.3	12.27	4.26	18.8	6.66	9.85	97
12.30	6.57	43.0				8.00	10.8	117
14.28	7.17	51.3				6.15	9.38	88
13.28	6.93	48.0						
18.3	8.0	6.40						
16.3	7.62	58.0						

Table 44 (Figure 59)

Data for Firebrick Columns. $T = 18^{\circ}C$. $p_o = 75.0$ cm.

	Column I	Column II	Column III
Length cm.	79	79	79
d_c mm.	6.4	6.4	6.4
$d_{p(ASTM)}^{(Mesh)}$	33.45	25.35	25.35
$\triangle p_{cm}$	3.6	2.8	2.4
f_1	0.977	0.982	0.984
u_o	2.87	3.63	3.65
ϵ	0.80	0.80	0.73
γD_g	0.075	0.077	0.073
γ	0.46	0.47	0.45
Pre-Treatment	Silanised with Dichlorodimethylsilane		20% (w/w)Urea Formaldehyde Resin

Column I			Column II			Column III		
Residence Time(mins)	W	W^2	Residence Time(mins)	W	W^2	Residence Time(mins)	W	W^2
0.47	2.22	4.93	0.37	1.89	3.57	0.37	1.89	3.56
1.25	3.20	10.2	1.20	2.69	7.23	1.20	2.64	6.97
2.25	4.20	17.6	2.00	3.27	10.7	2.20	3.36	11.3
3.25	4.97	24.7	2.22	3.50	12.25	3.20	3.99	15.9
4.25	5.62	31.5	2.50	3.66	13.4	4.20	4.42	19.5
5.25	6.35	40.2	3.00	4.02	16.1	5.20	4.98	24.8
6.25	7.18	51.5	3.22	4.21	17.7	6.20	5.46	29.8
7.29	7.52	56.5	3.50	4.12	17.0	7.20	5.80	33.5
8.25	7.96	63.3	4.20	4.55	20.7			
1.75	3.84	14.7	4.00	4.52	20.3			
2.75	4.70	22.0	4.50	4.76	22.7			
3.75	5.35	28.6	5.00	4.98	24.8			
			5.20	5.30	28.0			
			6.20	5.48	30.0			
			6.56	5.72	32.7			
			7.00	5.92	35.0			

Table 45 (Figure 59)

Data for Celite Columns.

Columns I and II were silanised with dichlorodimethylsilane and hexamethyldisalazane respectively. $T = 18^{\circ}C.$ $p_o = 75.0$ cm.

	Column I	Column II
Length cm.	72	74
d_c mm.	5.6	5.7
d_p (Mesh) (ASTM)	35-45	80-100
Δp_{cm}	3.9	5.2
f_1	0.975	0.966
u_o	3.46	1.80
ϵ	0.88	0.88
γD_g	0.125	0.119
γ	0.76	0.72

Column I			Column II		
Residence Time (mins)	W	W^2	Residence Time (mins)	W	W^2
0.35	1.80	3.23	0.70	4.53	20.6
1.19	3.23	10.4	1.36	6.40	40.8
2.19	4.35	18.95	2.36	8.36	70.0
3.19	5.30	28.0	5.36	4.03	16.3
5.19	6.70	45.0	6.36	4.38	19.1
7.19	7.90	62.3	1.80	7.45	55.5
1.66	3.74	14.0	2.86	9.37	87.7
8.19	8.80	77.7	3.86	10.9	119.0
2.70	4.82	23.2	4.86	11.8	139.0
3.70	5.65	32.0	5.86	13.5	182.0
4.70	6.27	39.3	3.36	9.95	99.0
3.00	5.07	25.6	4.36	11.3	128.0

Table 46 (Figure 6)

Individual Run Data for Model 53B Experiments.

Column 1			Column 2			Column 3			Column 4		
Residence Time(mins)	W	W^2	Residence Time(mins)	W	W^2	Residence Time(mins)	W	W^2	Residence Time(mins)	W	W^2
0.29	2.00	4.0	0.42	2.73	7.48	0.30	5.00	25.0	0.37	2.25	5.05
3.10	3.77	14.2	3.18	3.59	12.9	7.57	5.53	30.5	3.00	3.91	15.3
6.1	4.92	24.2	3.97	3.94	15.5	10.74	5.38	34.5	1.00	2.70	7.3
9.1	6.22	38.7	1.57	3.30	10.9	12.42	5.92	35.0	7.00	5.38	29.0
12.1	6.55	42.7	5.68	4.12	17.0	15.13	6.33	40.0	4.00	4.37	19.1
4.1	4.15	17.2	6.00	4.58	21.0	17.57	6.47	41.8	5.50	4.62	21.3
5.1	4.52	20.3	8.25	4.95	24.5	21.93	6.68	44.5	2.00	3.39	11.5
7.1	5.05	25.5	9.88	5.25	27.5	25.94	7.15	51.0	9.00	6.13	37.5
8.1	5.52	30.5	12.50	5.75	33.0	3.00	5.33	28.3	12.00	7.17	51.3
10.1	6.30	39.5	16.97	6.45	41.5	4.65	5.38	29.0	5.00	4.80	23.0
11.1	6.63	44.0	17.72	6.57	43.0	6.57	5.60	31.3	8.00	5.92	35.0
13.1	7.15	51.0	11.50	5.63	31.7	13.33	6.13	37.5	6.00	5.13	26.3
			19.70	7.05	49.5	20.10	6.68	44.5	10.00	6.43	41.3
			14.57	6.25	39.0	9.42	5.83	34.0	11.00	6.73	45.2
			18.0	6.70	45.0						
			22.3	7.42	55.0						
			29.7	7.75	60.0						

Table 47 (Figure 60)

Individual Run Data for Model 53B Experiments

Column 5			Column 6			Column 7			Column 8		
Residence Time(mins)	W	W^2	Residence Time(mins)	W	W^2	Residence Time(mins)	W	W^2	Residence Time(mins)	W	W^2
0.57	3.08	9.5	0.68	4.40	19.4	0.42	2.53	6.40	0.56	2.87	8.25
5.00	5.43	29.5	0.33	2.70	7.27	1.97	3.89	15.1	2.30	4.35	18.9
1.57	3.94	15.5	1.87	5.57	31.0	2.97	4.47	20.0	3.30	4.75	22.5
3.00	4.67	21.8	2.33	5.70	32.4	3.97	5.10	26.0	4.10	5.57	31.0
6.82	6.28	39.5	3.37	6.06	36.7	4.97	5.70	32.5	5.30	6.00	36.0
8.00	6.62	43.7	5.87	7.35	54.0	5.97	6.20	38.5	6.30	6.43	41.3
12.58	8.07	65.0	3.50	5.70	32.4	6.98	6.56	43.0	8.30	7.52	56.5
15.00	8.70	75.5	4.87	6.97	48.5	7.98	7.00	49.0	9.30	7.62	58.0
19.30	10.0	100.	6.37	7.65	58.3	8.98	7.52	56.5	10.10	8.18	67.0
17.00	9.38	88.	17.10	3.69	13.6	9.98	7.95	63.0	11.30	8.36	70.0
9.22	7.18	51.5	9.33	9.10	82.5				12.10	9.10	82.5
10.82	7.65	58.5	12.87	10.2	104.0				13.30	9.17	84.0
13.00	8.28	68.5	14.33	11.0	121.0				15.30	9.95	99.0
16.00	9.15	83.5							18.30	10.85	118.0
									22.10	12.05	145.0
									7.10	6.93	48.0

Table 48 (Figures 57 and 60)

Experimental Parameters for Model 53B Experiments. $T = 18^{\circ}C.$ $p_o = 75.0$ cm

Column	1	2	3	4	5	6	7	8
Length cm.	74	144	151	106	148	152	105	144
d_c mm.	4.16	6.28	5.20	6.28	6.75	5.90	6.75	6.28
d_p mm.	3.97	5.90	4.87	5.55	5.90	4.87	5.55	4.87
d_c/d_p	1.047	1.065	1.070	1.132	1.145	1.210	2.215	1.290
ϵ	0.392	0.413	0.417	0.479	0.491	0.537	0.552	0.598
Δp_{cm}	1.8	2.2	2.1	1.7	1.6	1.1	2.5	1.6
f_1	0.988	0.985	0.985	0.989	0.989	0.993	0.983	0.983
u_o	4.20	5.82	8.50	4.90	4.41	3.80	4.18	4.25
χD_g	0.078	0.088	0.088	0.110	0.113	0.126	0.125	0.134
χ	0.48	0.54	0.54	0.67	0.69	0.77	0.77	0.82
Material *	BB	PVC	PVC	BB	PVC	Glass	BB	PVC

*BB are steel ball bearings.

PVC are polyvinylchloride spheres of 2% diameter range.

crystalline cristobalite and the mineral impurities form complex oxides or silicates. It has been shown (300 - 303) that the pink and white forms differ considerably with respect to surface area, surface activity, pore volume and packing density. While the majority of the pores in firebrick are between 0.4 and 2 microndiameter with an average of about 1 micron, celite was found to have a wider pore size distribution with the average around 8 to 9 microns.

As a result of the difference in preparation, the firebrick in a relatively dense mass of diatomite with a relatively small amount of internal void space consisting of small pores which produce a high surface area. The particle is relatively hard. Celite on the other hand consists of a lightly fused mass with a very open structure of large internal void space. The particle is relatively weak and friable. This difference in the structure of the supports is reflected in the void space in the bed. A packed column of the uncoated celite is approximately 90% void space, firebrick is approximately 80% void. This difference in structure is illustrated in Figure 61.

3. Porous Supports: The values of $\delta = 0.74$ for celite and $\delta = 0.45$ for firebrick cannot be explained on the basis of the models considered since none of them predict such low values in the porosity range near 0.8 and although the porosity of firebrick is about twice that of glass beads o is much lower.

Consider the situation if Dg within the particles was restricted and hence much lower than Dg in the free gas. The rate of spreading would then be given by $d\sigma_t^2/dt = 2\,\delta\,Dg/(1 + k)u_o^2$ and δ' (measured) $= \delta / (1 + k)$. Since k would be approximately unity for firebrick or celite $\delta = 0.3$, much lower than the values found. Since the microstructure has many pores of dimensions greater than the gas mean free path at normal pressures (600 A in N_2), the diffusion coefficient within the porous particles should not differ from that outside and hence the above reasoning might be expected to be unsound.

It is interesting to consider two of the other models treated by Giddings and Boyack, namely cubes and fibres. If the particle is cubic both C and T depend upon the orientation of the particle. The two extreme cases (a) with the edge of the cube and (b) the diagonal of a face, parallel to the direction of the field were considered. In each case the C factor was within 3% agreement of the value for spheres for the same θ value, showing that the

treatment holds for particles of any simple geometry. The calculated tortuosities were (a) $T = 1 + 0.33\,\theta$ and (b) $T = 1 + 0.357\,\theta$ and $\gamma = 0.55$ at a porosity of 0.4. This reduced value was explained as a possible consequence of the fact that the abrupt changes in direction on a cubical surface depart significantly from the actual lines of force which change more continuously. If this is so, the same effect would be observed with any particles exhibiting sharp angles, e.g. firebrick.

For fibres, represented by an array of long cylinders with axes perpendicular to the direction of the impressed field γ was 0.35 for a porosity of 0.4. This significantly lower value was difficult to explain.

Smith (303) recently gave a paper on large-scale columns in which celite and firebrick were critically compared. "At a macroscopic level the column space in a packed column may be considered as a statistically distributed network of tubular pathways (inclined to the column axis at an angle $\pm\,\theta$) with sets enclosing the average particles." It then follows that $\gamma = \cos.\,\theta$, $\gamma_R = \sin\theta$ where γ_R is the radial contribution. Only tortuosity is considered. Tan θ is the radial: axial space anisotropy ratio of the packing and from this model is given by $\tan\theta = \sqrt{\frac{1}{\gamma^2} - 1}$.

In a perfectly isotropic packing $\tan\theta = 1$ whence $\gamma = 0.707$ which is close to both his and my value. From the description of its properties firebrick is anisotropic and $\tan\theta$ is large.

Comparison of two of the columns in Smith's paper, namely 1500 x 25/BP/T/N_2 and 1500 x 25/S/T/N_2, gives γ (firebrick) = 0.36 and 0.49 respectively, assuming γ (celite) = 0.71. Thus the difference between firebrick and celite might well be explained on the basis of anisotropy. The observed γ values are still rather high, however, and it may therefore be necessary to consider also the tortuosity in both inter- and intra-particle channels. Boyack and Giddings (304) have since derived a 'retardation factor' which is meant to account for a similar phenomenon in paper electrophoresis but as yet this has not been transferred to gas chromatography.

De Ford et al. (188) found that the B coefficient tended to decrease with liquid loading. If the interparticle porosity was the controlling factor

this and thus B would increase with increased liquid loading. De Ford concluded that diffusion both around and through the particles must be considered. Increased liquid loading would then decrease the diffusion through the particles and this would decrease the B term as observed.

Another approach is to try to eliminate the additional tortuosity due to the particle structure. From Figure 62 the overall tortuosity might be increased to $T = T_e \left[(1 - l_i) + T_i l_i \right] / l$ where T_e is the tortuosity of smooth paths through the bed, T_i the tortuosity of the paths within the particles, l_i the length of that part of a smooth path which passes through the particles (broken line) and l is the total length of a path as shown. Assuming interstitial and total porosities of 0.4 and 0.8 respectively, the porosity of the particles themselves is about 0.6 and $T_i = 1.11$. Assuming 60% of the total length of a diffusion path is through the particles and 40% outside, then $T = 1.20 \times 1.07 = 1.28$ and if the constriction is unaltered $\gamma = 0.55$. Thus the net effect of the particles being porous is to reduce γ by about 15%.

The values of $\gamma = 0.46$ and γ 0.74 for firebrick and celite may thus be explained: Firebrick is a hard, relatively compact mass characterised by very fine narrow pores tending to favour inter- to intra-particle diffusion. It is friable and jagged with sharp angles leading to anisotropy. The diffusion paths through the bed will thus tend to be inclined at a considerable angle to the axial direction. Celite, on the other hand, is a very open structure with wide unobstructing pores so that both intra- and inter-particle diffusion can take place with the minimum of deflection from the axial direction.

Since γ is essentially a structural constant it should be independent of the mobile phase. Giddings has suggested that there is very likely a slight velocity dependence to γ . When the reduced velocity ν exceeds unity (such that flow displacement exceeds diffusive displacement over a distance dp) the constriction effect is probably reduced in importance by virtue of the fact that solute is carried directly through the constrictions by the flow stream. It is difficult to say how the tortuosity would change. The theory of γ 's velocity dependence has not been worked out yet and at present the velocity effect is assumed negligible.

iv. Conclusion

The foregoing work has demonstated that δ can be accurately and simply measured and that both tortuosity and constriction effects must be considered in defining δ. So far the theory has been worked out only for simple regular models and more information is required before δ can be theoretically estimated for the complex structures characteristic of the popular support materials used in gas chromatography.

SECTION III

SOME NOTES ON THE COATING OF CAPILLARY COLUMNS AND THE PROPERTIES OF THE PHOTO - IONISATION DETECTOR

(The work described in this section was carried out at Bruce Peebles Limited, Edinburgh, and permission has been obtained to reproduce it here)

CHAPTER I

THE PREPARATION OF CAPILLARY COLUMNS

I. Introduction

From the results of investigations on nylon capillary columns (87, 305) it became apparent that there were two possible applications for the capillary system. The columns could be used to produce very high efficiencies with elution times of 10-60 minutes, or the high efficiencies could be sacrificed and chromatograms developed in a matter of seconds, with moderate efficiencies of perhaps 5000 or 10,000 plates. Under these conditions it was found that a chromatogram of a mixture boiling over a range of about 100 degrees centigrade could be developed in 60 seconds, the early peaks being eluted during a period of about a second. A high-speed recording system with time constants of the order of milliseconds would then be required. Such performance cannot be achieved by the normal potentiometric recorder, and the oscillo-:scope or the high speed photographic galvanometric recorder are the only attractive methods of presenting the chromatogram.

These ideas led the Electronics Division of Bruce Peebles Limited to design and produce a gas chromatograph, the 'C-Scope', which could be used for high speed repetitive analysis. The chromatograph employed an argon detector (166, 180, 184, 318 - 323) and a capillary column, the chromato-:gram being displayed on a high persistence cathode ray tube (306-7).

An automatic trigger signal started the analysis by activating both the injector and the time base of the CRT. After a sufficient time for elution of the sample (0.1 - 10 sec) the time base was reset and another sample injected automatically. The frequency of injection could be varied and the timing of CRT sweep could be altered by varying the sweep speed and the delay between injection and the start of the sweep. In this way any peak or part of the chromatogram could be expanded and displayed. One of the purely chromatographic problems was the production of reproduc-:ible columns of high efficiency.

II. The Coating Procedure

The loading of capillary columns is critical with respect to thickness and uniformity of coating. An excess of stationary phase damages efficiency through an increase in C_1 while a deficit tends to be removed by repeating sample overloading. Uneven distribution on the wall, caused by surface irregularity or poor wetting properties also leads to poor performance (308).

In practice reliable, reproducible and efficient columns are difficult to prepare and the coating procedure has been the subject of much controversy both in our department and elsewhere. Materials used include stainless steel (63), nylon (87), copper (310) and glass (73). Several coating procedures have been suggested (63, 72-74, 87, 309-312).

1. The column is completely filled with a 10% solution of the liquid phase in a suitable solvent by applying pressure at the front end of a small tube connected to the capillary and containing about 5 ml of the solution. After the solution is blown through the column the volatile solvent evaporates leaving a thin coating of liquid phase.
2. The capillary filled with a dilute solution of the oil is passed through a heated oven and the solvent is vaporised directly as it passes through the heated region.
3. The column is about one-third filled with the solution and the slug is passed down at a slow rate which has been shown to be critical.

Desty et al. (309) and Kreyenbuhl (313) developed a machine for making glass capillaries by drawing down heat-softened wider bore tubing. Although Averill (314) claims that non-polar liquid phases will only stick to glass if an additive of the proper type is added, Desty et al. appear to have experienced no difficulty in coating by method (3) for any flow rate of solution though they have only been concerned with non-polar liquid phases. Several workers have tried to roughen the inside of glass columns to decrease the contact angle (315).

It seems that there is quite a variation in the metal in any one batch and in the batches from different suppliers. The only way to check a column is to coat it and test it ! A general complaint is the difficulty in coating with polar stationary phases so as to obtain symmetrical peaks for polar solutes.

Stainless steel and copper are the favourite metals on account of their strength and excellent heat-transfer properties, though the oxidation of copper at high temperatures limits its usefulness. Smith (316) noticed that many metal capillaries as received from the manufacturers showed resolving power before any coating process probably due to a lining of lubricant used in the drawing process. On removing this layer severe tailing of polar solutes resulted. Perkin-Elmer found that copper cap-:illaries lined with silicone rubber before coating coupled higher effic-:iencies with a longer lifetime but this is open to question.

Nylon columns are cheap and thus good to experiment with. However most organic materials either soften the nylon or react with it and it cannot be used above 100°C. Method (3) was used and methylene blue was added to the 10% solution of dinonylphthalate or squalane in chloroform as a check on the uniformity of the liquid film. The uniformity of the film was most affected by the velocity at which the coating solution was passed through the column and in agreement with Scott and Hazeldean (246) the critical rate for maximum column efficiency was found to be 2-5 mm per second. In order to reduce the tendency for droplet formation which leads to a patchy, uneven coating, the spool on which the nylon capillary was wound was fixed to a vibrating motor. Lengths of nylon were attached before and after column to keep the flow in the latter as steady as possible. Miller (317) used an electrolytic cell to generate a constant flow of gas. By our method, a 20 ft length of 10 thou. nylon tubing coated with squalane (10% solution in chloroform) gave, for cyclohexane, a maximum number of plates of 8656 at a linear velocity of about 10 cm per second (H_{min} 0.7 mm). This column resolved seven components in BDH n-heptane. All my successful columns deteriorated on lying unused for several months.

I had no success in the many attempts to coat the metal capillaries made of cupro-nickel (Negretti and Zambra) and copper even with a non-polar liquid phase. During 1964 I visited the Ecole Polytechnique in Paris at the invitation of Dr. Guiochon. There Madame Landault and other had success-:fully coated thin-walled copper using the method recommended by Perkin-Elmer - method (1) (Figure 63). About 5 ml of solution (10% liquid phase in methylene chloride) was forced through the column under pressure at a slow bubbling rate seen in the pure solvent in the beaker. After it had blown out the column was

put into an oven and the temperature raised slowly, still with a slow flow rate of gas. This usually produced an efficient column. The column was regenerated by attaching it to the apparatus and washing with methylene chloride, followed by methyl alcohol to remove the methylene chloride, and water to remove the alcohol. The column was then cleaned with 20% nitric acid to remove the scales, followed by water, methyl alcohol and finally methylene chloride. Following Averill (314) 0.1% Alkaterge T was added to the solution as a surface-active agent to facilitate the wetting process. Although there is the chance that surface-active agents may be adsorbed on the surface of the capillary and reduce the solid-liquid adhesion, Alkaterge T seemed to be quite successful.

The two cupro-nickel capillaries which I took with me were coated with squalane and polyethylene glycol by this method. While the squalane column was first-class (about 100,000 plates for 50 feet of 20 thou. id.) the glycol column was less good. On the first day after its preparation it gave about twenty peaks for a sample of cognac but next day it had deteriorated to a mere few hundred plates. This appeared to be a common occurrence for polar phases, even on the thin-walled copper capillaries. Successful coating with a polar liquid phase has, however, been reported (325).

III. Conclusion

Although from the literature metal can be coated with any kind of liquid phase, I have only been successful with non-polar liquid phases.

CHAPTER II

AN INVESTIGATION OF A PHOTO-IONISATION DETECTOR

On behalf of Griffin and George Limited I was asked to investigate a photo-ionisation detector. Smith of NRPRA (324) had already done some work on the brass Griffin and George model and his results are compared with mine.

I. Introduction

The ideal detector for gas chromatography is one which measures a specific property of the eluted vapours and which gives virtually no signal when the carrier gas alone passes through it. Selective ionisation of eluted vapours may be achieved by means of high energy photons.

The properties of a gas discharge are determined to a large extent by the nature of the gas present. In the photo-ionisation detector first described by Lovelock (326) a suitable gas (He, A or H_2) enters the ionisation chamber through a hollow anode at a pressure of 5-10 mm Hg. A glow discharge is pro-:duced between the anode and a heavy ring cathode by means of high voltage. Photons of high energy arise in the discharge when excited atoms return to the unexcited condition or some intermediate level. The quantum of energy given up in the transition appears as a pulse of energy radiated on a wavelength appropriate to that particular quantum. The various possible transitions give the line spectrum which is characteristic of the particular gas.

The breakdown voltage (V_i) of a gap is that at which a self-sustaining discharge takes place. For a particular gas it varies with the pressure (p), and the electrode spacing (d) and is a function of the product p.d. (Figure 64). Some breakdown voltages, with associated wavelengths, are given below (Table (i)).

Table (i)

Gas	He	A	H	H_2	N_2
V_i	24.5	15.7	13.5	15.4	15.8
λ_i	506	790	915	905	784

The energy of the radiation quantum $h\nu = V$.

Since $\lambda = \frac{c}{\nu}$ ($\mathring{A} = 10^{-8}$ cm, $c = 3 \times 10^{10}$ cm/sec),

$$\lambda V = 3 \times 10^{18}\ h \quad (h = 4.13 \times 10^{-15} \text{ electron volt sec})$$

$$= 12{,}398 \quad (V \text{ is in electron volts})$$

Hence for ionisation $\lambda_i \leq 12{,}398/V_i$

Typical ionisation potentials are given in Table (ii).

Table (ii)

Typical Ionisation Potentials (I.P.)

Substance	I.P. ev	λ_i
Cyclohexane	9.2	
Benzene	9.5	1290
Ethyl Acetate	10.0	
n-Hexane	10.6	1170
Ethanol	10.6	
Methanol	10.9	
Water	12.8	967
Oxygen	13.6	
Methane	13.2	
Carbon Dioxide	14.4	
Nitrogen	15.5	

The photons not absorbed by the carrier gas pass down the tube and can ionise any eluted vapour which enters from the column through a hollow electrode at the opposite end of the ionisation chamber. The rate of photo-ionisation is determined by applying a potential of about 100 v between the inlet tube from the column and a cylindrical anode. Also photons falling on a surface may give rise to photo-electric emission.

Various gaseous components are ionised by electromagnetic radiation of different energies thus making it possible to ionise preferentially one component in a gaseous mixture in the presence of another component when the

two components have different ionisation potentials. Selective filters could be used for isolation of particular bands of radiation. Thus (327)

L_iF	transmits	from	0.105 to 6 u
S_rF	"	to	11 u
$Ca\ F_2$	"	from	0.125 to 9 u
Fused Silica	"	"	0.19 to 3.5 u

i. Ionisation by Radiation

The reaction of ionisation by radiation may be written as $M \longrightarrow M^{\oplus} + e^{\ominus}$. A plot of current against voltage in an ionisation chamber is shown in Figure 65. In (A) the magnitude of the current is determined by the concentration of charged particles and their speed of drift. At very small ion concentrations the speed of drift is proportional to the applied voltage and the gas obeys Ohm's Law. As the applied voltage and therefore ion current increases (B) the removal of ions by drift to the electrodes augments the removal of ions by other processes, so that the steady-state concentration of ions begins to fall. This causes the current to lag behind the Ohm's Law prediction. At a sufficiently intense field every ion formed is removed by conduction so that further increase in the applied voltage produces no further increase in current. A saturation plateau (BC) is reached. At still greater voltages, (D), electrons reach sufficient speeds in the course of their drift to ionise further molecules by collision and there is a sharp increase in current. This eventually leads to a spark discharge.

The steady-state ion concentration is a function of the intensity of the radiation. As this is increased the saturation region decreases while regions A and B increase and region D remains relatively steady. In a non-uniform field different parts of the gas between the electrodes would operate on different parts of the curve.

ii. The Photo-Ionisation Detector (P.I.D.)

The photo-ionisation detector was invented by Lovelock (326). It is illustrated in Figure 66. The detector was claimed to be stable over long periods and uninfluenced by contaminants. It was also insensitive to flow rate and operating pressure. The detector was highly sensitive and had a

background current of 10^{-10} amp which might possibly be due to the photo-electric emission of electrons from the surfaces of the measuring chamber.

In the presence of ionisable vapour a substantially linear response to vapour concentration was observed up to a signal current of 10^{-7} amp. The efficiency of ionisation of propane as a test substance was approx-:imately 0.01 per cent. The response of the detector appeared to be unaffected by gross contamination of its surfaces with dirt or decompos-:ition products and was stable over long periods and on repeated operation. It could probably be used for inert gases. Lovelock added that the design should not be considered as final but simply served to illustrate the potentialities of the method. The Griffin and George Design of the P.I.D. is illustrated in Figure 67.

iii. Smith's Investigation of the P.I.D.

Smith of NRPRA (324) using the Griffin and George model of the P.I.D. found that 1. Peak inversion occurred above quite small sample sizes.

2. The detector was non-linear. A typical plot of detector signal against sample concentration, together with typical 'peaks', is given in Figure 68.
3. There was no well-defined plateau in the output response/ collector voltage curve. This is essential to make detector performance uncritical with respect to working conditions. This is illustrated in Figure 69.

Dr. Smith argued that the exhaust from the detector was close enough to the discharge and ionisation regions to make it probable that at least a proportion of the ions produced away from the immediate vicinity of the collector electrodes will be swept out of the unit, making a stable equilibrium insensitive to pumping rate, difficult to achieve. He also felt that there must necess-:arily be some absorption of the photons before they reach the collector electrode region. This would again explain the apparently low sensitivity, non-Linearity and poor dynamic range.

With these points in mind Smith modified the geometry of the P.I.D. to the form shown in Figure 70. From work on this revised design Smith has shown a good plateau, less severe peak distortion with no peak inversion and improved

linearity. He also found that the background current was considerable. This was shown to be almost entirely due to photo-ionisation of the carrier gas by inserting a filter which would remove any ions produced by the discharge. Using a Ca F_2 plate (this transmits above 1250 A) paraffins could no longer be detected, branched hydrocarbons gave only a faint signal, while benzenoid compounds could be detected at about a hundredth of the sensitivity level without Ca F_2. Using Li F as a filter (this transmits up to 1050 A) they found full detector response to chemically almost everything. Thus photons with wavelengths between 1050 and 1250 A seem to be necessary for operation. The actual value for the optical transmission of the plates had still to be measured.

Unfortunately flat plates do not fit well into a circular chamber and the rectangular geometry of the collector chamber allows spreading of the sample into the corners of the detector with the production of badly-tailed peaks.

Changes in the arc discharge colour produce changes in the response of the detector to a pentane-isopentane mixture, with the Li F window in. This does not occur with the Li F window removed. Significant ionisation thus occurs by light not transmitted by the Li F window (i.e. wavelengths less than 1050 A).

At the moment Smith believes he has a detector with practically no back-:ground current, good linearity (up to 25% by volume) but with slightly lowered sensitivity, which does not make it so suitable for capillary column work.

II. Experimental

A block diagram of the system is given in Figure 71 and the injector is illustrated in Figure 72. The detector was evacuated with an oil pump to a pressure of 5 mm Hg. The column was a 25 ft. length of 10 thou. nylon coated with squalane. One end was drawn down slightly to be a tight fit in the collector electrode and the junction was sealed with araldite. The other end of the nylon column rested in an atmosphere of carrier gas as illustrated in Figure 72. When the relay operated the column end was moved rapidly down through the annular chamber into an atmosphere of sample gas. The column was therefore continually sucking either carrier or sample gas and the sample size

was proportional to the dwell time when the relay operated. The latter could be varied from 100 to 600 milliseconds.

The rate of generation of photons and their energy distribution is solely a function of the discharge current, for a fixed discharge voltage and given carrier gas. For this design the discharge voltage was about 300 v. Hydrogen was used as the discharge gas and nitrogen as the carrier.

III. Results and Discussion

Hutchison (328) varied the discharge current from 200 microamps to 1 milliamp. He found that while the background remained almost constant, the signal rose linearly and steeply and then began to level off. Also as the discharge current rose to 1 milliamp the discharge became much larger and diffused back into the discharge chamber. At the same time the cathode tip and inner rim of the annulus appeared to become hot and glow brightly, and afterwards the inside of the detector showed considerable signs of surface deterioration. It was decided to work at 0.5 mA.

With the original design plots of background current (BC) against collector volts (CV) cut the collector voltage axis at about + 20 v. These are shown in Figure 72 for 3 values of the discharge current (i_D).

The pattern was similar for each of the three detectors supplied for different positions of the discharge electrode. The cleanest, shiniest detector had a background current of 5×10^{-8} amp while the other two had a background current about 5×10^{-7} amp at zero collector volts.

The shape of the curves was explained by a photo-electric effect, the contribution to signal current due to electron emission by the collector electrodes being aided by a negative collector voltage and opposed by a positive collector voltage. The energy of the photons must be in excess of the work function of the collector electrodes material, which is of the order of 5 ev to cause any photo-electric effect contribution. Small flat pieces of a selection of different metals were fixed between the collector electrodes. The carrier gas inlet was blocked, and in all cases about + 40 collector volts were required to zero the background current. With the collector electrodes alone, the voltage required was + 26V. It was rather difficult to draw any conclusions from this since the work functions

of the metals used were all about 5 ev, but the constant increase of 14 volts could indicate the energy of the particles striking the metal. It is pro-:bably advantageous to keep the collector electrodes out of the direct beam of photons to reduce photo-electric contribution to background current.

It was noticed that with each injection of calor gas sample the shape of the discharge changed. There was also a perceptible flicker on the discharge current milliammeter. A partition should be inserted in the body of the detector to keep the discharge region quite separate from the collector elec-:trode region to reduce this apparent interaction.

The linearity of the detector was determined using a P.T.F.E. mixing vessel and stirrer after Lovelock (321). The sample was calor gas. Though the mixing vessel was later found to mix very inefficiently, the experiment did show that the detector was only about a hundredth as sensitive as the argon detector under the same conditions. Thus my results were in agreement with Smith's work.

The next step was to investigate the effect of progressive changes in detailed design to detector performance, at the same time trying to gain more information about the fundamental processes involved. Ionisation processes are virtually instantaneous and the reponse time of a detector which is based purely on ionisation processes is usually limited only by the detector volume and the carrier gas flow rate. The finite band width of the associated elec-:trical detector and amplifier circuits can be ignored.

i. Modifications Made to the Design

Several modifications were made to the design.

1. Discharge End: With the original electrode (Figure 73a) any discharge between the tube and the flat brass wall would be spread over an indeterminate area and this would tend to make the discharge irreproducible as well as of lowered concentration. The modified electrode is shown in Figure 73b.

The spherical discharge was very pressure dependent and at 5 mm pressure it was also tongue-shaped as shown in Figure 73b. A possible mechanism for this discharge is

$$H_2 \rightarrow H + H - 3 \text{ ev}$$

$$H \rightarrow H^+ + e - 13.5 \text{ ev}$$

The electrons produced will be largely attracted to the positive electrode leaving a concentration of positive ions as shown. Photons from the discharge may then liberate electrons from W which will be attracted to the positively charged ions. The recombination which takes place will be accompanied by a large emission of photons.

The final design of the discharge electrode is shown in Figure 73c. The discharge was now quite reproducible and much more concentrated than before. The end-on view is also illustrated in Figure 73c.

2. Collector Electrode Design: As a result of the design shown in Figure 74 peak tailing was greatly reduced.

Due to lack of workshop facilities no further modifications were made and the final design is shown in Figure 75.

ii. Summary of Detector Performance

Even with the modifications described above, there was still interference between the discharge and collector ends of the detector. The Li F filter eliminated this. Li F transmits from 1050 A upwards. This corresponds to about 11.6 v so that permanent gases are not ionised. It should also decrease the sensitivity towards aliphatic hydrocarbons. The background current was 2×10^{-9} amp with or without the Li F window. Without the Li F window double peaks were obtained with calor gas, viz. The initial sharp peak corresponded to a flicker on the discharge current ammeter. The flicker disappeared with reduced sample size. It could be explained by the initial surge of sample entering the discharge and partly quenching it. The rest of the sample would then be ionised by a less intense discharge. If this interference could be eliminated increased sinsitivity would result. It was found that, with calor gas,

1.8×10^{-6} moles $\equiv$ 0.04 ml calor gas $\simeq$ 10^{-7} amp.

With Li F window in 0.04 ml " " $\simeq$ 0.6×10^{-7} amp.

The response increased with the discharge current and was almost doubled at i_D = 0.9 mA. The response was noticeably less with parallel-plate collector electrodes and these were ignored. The sensitivity also increased slightly

with increasing collector voltage up to + 400 volts. With the argon detector.

4×10^{-6} ml propane gives a response of 2.5×10^{-10} A

i.e. 4×10^{-2} ml gives 2.5×10^{-6} A

Thus the P.I.D. is 1/25 as sensitive as the argon detector. Lovelock's paper does not state sensitivity but he does say that the ionisation efficiency of propane was 0.01%. The ionisation efficiency of the argon detector is 0.5%. Thus the P.I.D. will never be as good as the argon detector, even when it is up to Lovelock's standard. Our design appears to be better than Lovelock's one. The curve of background current/collector volts also now passes through the origin, with or without the Li F window (Figure 76).

With a glass detector made to Lovelock's specification, the background current was 2×10^{-9} amp with argon and 5×10^{-9} amp with hydrogen as discharge gas. Unfortunately the copper electrodes quickly blackened and the discharge became very irreproducible. Double peaks were always obtained and the incoming sample practically extinguished the discharge each time.

With hydrogen as discharge gas inert gases could not be detected and even with helium as discharge gas nitrogen was barely detectable and the background current was increased to 4×10^{-9} amp. Also with helium as discharge gas the detector noise was increased and sensitivity was reduced. The noise level was 2×10^{-11} A.

The detector was linear down to 10^{-7} amp. This was done using the bubbler technique. The mixing vessel is shown in Figure 77 and the method is fully described in the literature (329). On the assumption that the flame ionisation detector response was linear, the linearity of the P.I.D. response was determined at the same flow rate of scrubbing gas. Plots of log response/time were straight lines of identical slope.

The design could still be improved upon. Nicholls of Bruce Peebles Limited suggests a model of the form shown in Figure 78. The metal plates would be standing at suitable voltages to mop up stray electrons from the discharge, etc. thus ensuring that the detection mechanism was purely photo-ionisation and not a mixture of photo-ionisation and ionisation by electron impact.

Prof. Craggs (330) favoured the latter mechanism in Lovelock's design.

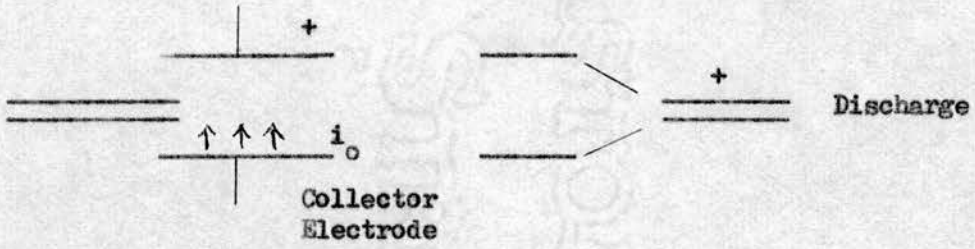

He thought that the standing current i_o would avalanche on the introduction of sample. He said that the exact mechanism of the discharge was difficult to predict as the conditions inside the detector were not known absolutely, but at the working pressure of 5 to 10 mm Hg he preferred the excitation (low pressure) mechanism to the radiation-recombination (high pressure) one, viz. $H^+ + e \longrightarrow H + h\nu$, though both processes are probably going on simultaneously due to the high discharge voltage involved. A spectrum of the discharge would help to clarify this.

He suggested experimenting with screens, etc., in a much simpler model than the brass body as this was very restricting. He was not in favour of a filter, such as lithium fluoride, as this was bound to reduce sensitivity. He did not think that the electrode material was very important, though platinum would probably be best because of its chemical inertness and relatively high work function. He thought, however, that the dimensions and the design might prove very critical for maximum sensitivity.

iii. Conclusion

My results do appear to agree with Smith's work. The detector has a low background current, is of good linearity, but is too insensitive for capillary column work. From a commercial point, however, other considerations, such as robustness, price and safety must also be taken into account, and the photo-ionisation detector is unlikely to become a great commercial success. A detector operating on similar principles to the P.I.D. has already been patented (331).

IV. The Photo-Ionisation Detector of Yamane

Since the above work another study of a photo-ionisation detector has

been published (332/4). Yamane's conclusions were similar to my own findings and his model was fitted with an earthed ion trap between the discharge, gap distance only 0.1 mm. The sensing chamber and the collector electrode were placed out of the direct beam of photons to eliminate photo-electric emission. Helium was used as both the discharge and carrier gas because, as shown by Hopfield (335) and Tanaka, Huffman et al. (336-7), the discharge in helium at the high pressures, at which this detector was operated, emits a continuum of radiation in the wavelength region ca 600 and 100 Å. The use of helium as carrier gas prevented the absorption of these high-energy photons by the carrier gas provided it was pure.

The background current - collector voltage plot was of the same form as Figure 76 but the background current was a factor of 10 lower. With increasing discharge gas flow the background current reached a maximum at about 50 ml per min and then decreased, showing that the photo-ionisation of impurities in carrier and discharge gas had not been eliminated in spite of purification. When the impurity traps were maintained at room temperature permanent gases were not removed from the discharge gases and absorbed UV light with a decrease in sensitivity; however with liquid nitrogen as coolant results were reproducible. The anode voltage was usually 100 v and the discharge current 30 - 60 uA.

With increasing gas flow the peak current increased at first, reached a maximum and then decreased as with the background current - gas flow variation. The discharge gas thus had two effects, namely increasing the number of photons and reducing the concentration of the sample gas in the sensing chamber. Peak inversion for low gas flow and large sample size was attributed to the diffusion of the sample gas into the discharge region with absorption of the ionising photons. The minimum detectable quantity for the inert gases was about 10^{-11} g/ml and the noise level was only 3×10^{-13} A. The detector was non-linear and this was attributed to the cell geometry.

V. Final Conclusion

With extremely pure gases and good cell geometry the photo-ionisation detector is a very sensitive detector, particularly useful for those substances which cannot be detected with the argon or flame ionisation detectors, but much more work regarding reproducibility, reliability and linearity is necessary before it can be used with confidence.

SECTION IV

THE APPENDIX

I. The Theoretical Plate Treatment

Consider the column to be made up of r plates in each of which equilibrium is established between the two phases. Consider the chromatographic process as taking place by the transfer of all the gas from one plate into the next plate where a new equilibrium is established with the fixed phase (358).

The probability p of a vapour molecule being in the gas phase during one of these transfer processes is $p = \frac{1}{1 + k}$. We then calculate the chance P_n^r of a molecule being in the r^{th} plate, i.e. just about to emerge from the column when n volumes of gas each equal to the volume of gas in one plate have passed, i.e. there were n transfer processes and the molecule will have been in the gas phase exactly r times. The problem is a standard one in statistics - the probability of picking out exactly r marked individuals in a sample of n, taken from a pop-:ulation in which the proportion of marked individuals is p.

$$P_n^r = \frac{n!}{r!(n-r)!} p^r (1-p)^{n-r}$$

This is the binomial distribution.

(1) $$\frac{P_n^r + 1}{P_n^r} = \frac{(n+1)(1-p)}{(n+1-r)}$$

If $P_n^r > P_{n+1}^r$, $(n+1)(1-p) < (n+1-r)$ and $n > (\frac{r}{p} - 1)$

If $P_n^r > P_{n-1}^r$, $n < \frac{r}{p}$

Thus for all practical purposes $n_{max} = \frac{r}{p}$

(2) When n, r, and n - r are all large the distribution may be simplified using Stirling's formula (359) to the normal distribution $P_n^r = \frac{1}{\sqrt{(2\pi npq)}} e - \frac{\delta^2}{2npq}$ where $q = 1 - p \cong 1$ and $\delta = p(n - n_{max})$
This may be written as $P_n^r = \frac{1}{\sqrt{(2\pi r)}} e^{-(\triangle r)^2/2r}$ which may in turn be simpli-:fied to $y = he^{-\triangle r^2/2N}$ where N is now the total number of plates in the column.

The ratio of the volumes of carrier gas required to elute a band of substance through N and $\triangle r$ plates, V_R and x respectively, may be given by $\frac{V_R}{x} = \frac{\phi N}{\phi x}$ where ϕ is constant for any given column.

$\therefore \frac{\triangle r^2}{2N} = \frac{x^2}{2\phi V_R}$ Thus $y = he^{-x^2/2\phi V_R}$ and may be compared with $y = he^{-x^2/6^2}$

where y is the peak ordinate at a distance x from the centre and x is now the distance from the peak maximum measured as a volume of carrier gas. This is the expression for a Gaussian distribution and

$$\sigma^2 = \phi V_R \text{ , } (\beta_e)^2 = 8\sigma^2 = 8\phi V_R$$

from the properties of a Gaussian distribution.

$$\therefore \quad N = \frac{V_R}{\phi} = 8\left(\frac{V_R}{\beta_e}\right)^2$$

II. The Calculation of N, the Number of Theoretical Plates

The number of plates in a column is found experimentally by measuring the peak width and the retention volume in the same units and applying one of the formulae (1, 2, 21, 49, 52, 132).

$$N = \left(\frac{V_R}{\sigma}\right)^2 = 8\left(\frac{V_R}{\beta_e}\right)^2 = 16\left(\frac{V_R}{W}\right)^2 = 5.54\left(\frac{V_R}{\beta_{\frac{1}{2}}}\right)^2 = 2\left(\frac{hV_R}{Area}\right)^2$$

(1) (2) (3) (4) (5)

Of the above methods (1) and (2) are slow and (5) involves the additional measurement of area. Since there is probably more personal error involved in the drawing of tangents than there is in measuring $\beta_{\frac{1}{2}}$ (4) is the pre-:ferred method, though (3) has been officially recommended (2). See Figure 19.

Note: $\beta_e = 2\sqrt{2}\,\sigma$

$\beta_{\frac{1}{2}} = 0.834\,\beta_e$

$W = 0.414\,\beta_e$

III. The Relation between the Average and the Outlet Column Pressure

The pressure gradient dp/dx and the linear velocity u in the column are related by $u = -Kdp/dx\eta$ where η is the gas viscosity and K is a constant, the 'column permeability' x is the distance from the column inlet. From Boyle's Law, $aup = au_o p_o = a\bar{u}\bar{p}$ where $\bar{u}$ and $\bar{p}$ are the values averaged over the column length.

$$\text{Then (360)} \quad dx = -\frac{Kdp}{\eta u} = -\frac{Kpdp}{\eta p_o u_o}$$

By definition,

$$\bar{p}\int_x^o dx = \int_x^o pdx \; ; \quad \bar{p}\int_{p_o}^{p_i} pdp = \int_{p_o}^{p_i} p^2 dp$$

$$\therefore \quad \bar{p}\,\frac{(p_i^2 - p_o^2)}{2} = \frac{p_i^3 - p_o^3}{3}$$

$$\therefore \quad \bar{p} = \frac{2}{3}\,\frac{(p_i^3 - p_o^3)}{(p_i^2 - p_o^2)} = \frac{2}{3}\,p_o\left(\frac{(p_i/p_o)^3 - 1}{(p_i/p_o)^2 - 1}\right)$$

$$\text{Thus} \quad u_o = \bar{u}\,\frac{\bar{p}}{p_o} = \bar{u}f_1 \quad \text{where} \quad f_1 = \left\{\frac{3}{2}\left(\frac{(p_i/p_o)^2 - 1}{(p_i/p_o)^3 - 1}\right)\right\}^{-1}$$

IV. The Influence of Gas Compressibility on Plate Height

Any gas packet within a column containing significant pressure gradients will physically expand as it passes down the column by an amount over and above that due to ordinary isostatic spreading (110, 361 - 365).

Consider the equation for HETP.

$$H(x) = A + \frac{B'D_{gx}}{u_x} + \frac{C_g' u_x}{D_{gx}} + C_1 u_x$$

$$u_x p_x = u_o p_o \; ; \qquad D_{gx} p_x = D_{go} p_o$$

$$\therefore H(x) = A + \frac{B'D_{go}}{u_o} + \frac{C_g' u_o}{D_{go}} + C_1 u_o \frac{p_o}{p_z}$$

$$= H_g^{\,o} + H_L^{\,o} \frac{p_o}{p_z}$$

$H_g^{\,o}$ is the sum of these terms which remain constant. The variance as a function of x, where x is the distance from the outlet, is $d\sigma^2(x) = -H(x)dx$. As the peak moves into regions of smaller pressure it expands. The dependence due to expansion may be written

$$\frac{\partial(\sigma^2(x))}{\partial(p^2)} = \frac{-\sigma^2(x)}{p^2} \quad \text{since } \sigma(x) \propto \frac{1}{p}$$

The total differential may be written as

$$-d\sigma^2(x) = H(x)dx + \frac{\sigma^2(x)}{p^2} \cdot dp^2$$

The experimental plate height is defined from the chromatographic record by the equation

$$\hat{H} = L\left(\frac{\sigma_t^2}{t_R}\right)^2 = \frac{1}{L}\,\sigma_t^2\,\bar{u}_b^2 \quad \text{since } \bar{u}_b = \frac{L}{t_R}$$

Since $\sigma_o = \sigma_t \times u_o$ (band), $\hat{H} = \frac{1}{L} \times \sigma_o^2 \frac{\bar{u}_b}{u_{ob}} \equiv \frac{1}{L} \times \sigma_o^2 \left(\frac{\bar{u}}{u_o}\right)^2 \equiv \frac{1}{L} \times \sigma_o^2 \left(\frac{p_o}{p_{av}}\right)^2$

By integration of the equation for $d\sigma^2(x)$ we obtain σ_o

Since $p^2 = p_o^2 + 2Ku_o p_o(x)$; x = distance from outlet

$dx = dp^2/2Ku_o p_o$

Hence, $$-d\sigma^2 = \left(\frac{H(x)}{2Ku_o p_o} + \frac{\sigma^2}{p^2}\right) dp^2$$

$$= \left(\frac{H_g^o}{2Ku_o p_o} + \frac{H_L^o}{2Ku_o p} + \frac{\sigma^2}{p^2}\right) dp^2$$

$$= \left(\frac{H_g^o p}{Ku_o p_o} + \frac{H_L^o}{Ku_o} + \frac{2\sigma^2}{p}\right) dp$$

This is of the form $dY + (AX + B + 2Y/X)\,dx = 0$

i.e. $dY/dx + 2/X \cdot Y = -AX - B$ where $\sigma^2 = Y$, $p = X$, $A = H_g^o/Ku_o p_o$ and $B = H_L^o/Ku_o$

The integrating factor for the equation of the general form $dy/dx + f(x)\,y = g(x)$ is $e^{\int f(dx)}$ which in this case is x^2 (339)

i.e. $dyx^2 + (Ax^3 + Bx^2 + 2yx)\,dx = 0$

This is the perfect differential of $(Ax^4/4 + Bx^3/3 + x^2y) = R$

Hence the solution is R = constant = c and replacing x, y, A and B gives

$$H_g^o/4Ku_o p_o \cdot p^4 + H_L^o/3Ku_o \cdot p^3 + p^2\sigma^2 = C$$

when $p = p_i$, $\sigma^2 = 0$

$$\therefore p_o^2\,\sigma_o^2 = \frac{H_g^o}{4ku_o p_o}(p_i^4 - p_o^4) + \frac{H_L^o}{3Ku_o}(p_i^3 - p_o^3)$$

$$\therefore \sigma_o^2 = \frac{H_g^o p_o}{4Ku_o}(P^4 - 1) + \frac{H_L^o P_o}{3Ku_o}(P^3 - 1) \text{ where } P = \frac{p_i}{p_o}$$

$$\therefore \frac{\sigma_o^2}{L} = 2\left(\frac{H_g^o/4\cdot(P^4-1) + H_L^o/3\cdot(P^3-1)}{(P^2-1)}\right)$$

since $L = \frac{1}{2}\left(\frac{p_i^2 - p_o^2}{Ku_o p_o}\right)$

$\therefore$ $\hat{H}$ = Observed Plate Height

$$= \frac{\sigma_o^2}{L} \times \left(\frac{p_o}{\bar{p}}\right)^2 = \frac{\sigma_o^2}{L} \cdot \frac{9(P^2-1)^2}{4(P^3-1)^2}$$

$$\therefore H = H_g^o \left\{\frac{9}{8}\frac{(P^4-1)(P^2-1)}{(P^3-1)^2}\right\} + H_L^o \left\{\frac{3}{2}\frac{(P^2-1)}{(P^3-1)}\right\}$$

In the present work we were concerned only with gas phase contributions to H, that is, the second term in the last equation is omitted.

The above expression may be written as $\hat{H} \cong H_g^{\circ} f_1 + H_L^{\circ} f_2$

where f_1 may be more simply written as $f_1 = \frac{(p)^2 \text{ mean}}{(\bar{p})^2}$

where (p^2) mean $= \frac{p_i^2 + p_o^2}{2}$ and $\bar{p} = \frac{2}{3} p_o \frac{(p^3 - 1)}{(p^2 - 1)}$

It was found that this correction was in fact negligible in all the log plots. In the other cases the irreproducibility of the data did not make this correction worth while. We therefore used the approximate form $H_g^{\circ} = B_o/u_o + f(A, C_o u_o)$.

Plots were accordingly made of log $\hat{H}$ against log u_o where u_o was calculated from $\bar{u}$ and the known inlet and outlet pressures.

V. Mechanism of Response of the Flame Ionisation Detector

Ionisation in flames is a little understood phenomenon and in this age of missiles and satellites a great deal of work has gone into its study. The ion concentration in a hydrocarbon flame is many times higher than can be accounted for by thermal ionisation alone. Stern (366) postulated a new species formed by stripping off the molecular skeleton to give a solid-carbon aggregate, the work function of carbon (ca 4 - 7 ev) being low enough to account for the high ionisation observed. The suggestion was widely accepted and when the flame ionisation detector was introduced Stern's theory was automatically assumed to apply.

Several objections to the carbon mechanism were raised by Calcote (367) who pointed out that at the same flame temperature the ion concentration is the same in both rich and lean flames. He worked out that there were roughly 200 times more ions than could be accounted for by carbon particles if every carbon atom were tied up in a carbon particle of radius 100 Å. Kinbara (368) has shown that the maximum electrical conductivity occurs in a relatively low temp-:erature portion of the flame. Calcote proposed a chemi-ionisation process in which the energy released in strongly exothermic chemical reactions is retain-:ed in the product molecules leading to ionisation before thermal dissipation of the energy occurs.

Sugden and his collaborators (369-370) using mass spectrometry found that a typical ion mass spectrum for a lean acetylene flame showed over 110 peaks from mass 19 to 150. Two peaks which persist in other flames corresponded to H_3O^+ and $C_2H_3O_2^+$. C_3 units are particularly favoured and might arise from the addition of CH^+ to C_2H_2, the CH^+ being formed by $C_2 + OH \longrightarrow CO + CH^+ + e$. Subse-:quent higher molecular weight ions can then beformed by a stepwise polymeris-:ation. Calcote selected for the probable basic mechanisms:

$$CO\ (^1\pi) + C_2\ (^1\textstyle\sum_u^+) \longrightarrow CO\ (^1\textstyle\sum^+) + C_2^+ + \ominus e \text{ (cumulative excitation)}$$

and $C_2\ (^3\pi_g) + O_2 \longrightarrow CO\ (^1\textstyle\sum^+) + CO^+ + \ominus e$ (chemi-ionisation)

and suggested for the formation of H_3O^+,

$$CO^+ + H_2O \longrightarrow (H_2O.\ CO^+) \xrightarrow{H_2O} H_3O^+ + (HOC = O)$$

$$\downarrow$$

$$OH + CO$$

or $OH^+ + H_2O \longrightarrow H_3O^+ + O$

The high molecular weight ions can then be formed by

$$H_3O^+ + C_nH_m \longrightarrow H_2O + C_nH_m^+ + 1$$

From a theoretical treatment, Eyring et al. (371) showed that it is the high free energy of formation of CO and CO_2 which couple with less favourable ionisation processes to produce the observed ions. Sternberg (129) has discussed the flame processes in detail.

The detector is normally operated as a diffusion flame, diffusion rather than chemical reaction being rate-determining. In the inner cone (see Figure 79) oxygen is essentially absent and free radical reactions are initiated by back diffusion of the mobile H atoms from the main reaction zone. Under these conditions, following the Rice-Herzfield scheme (372-3) rupture of the weakest bonds leads to dehydration, decarboxylation, de hydrohalogenation and some dehydrogenation processes. Very near the outer boundary of C cracking and stripping of fragments to give such reactive species as CH_2, CH and C atoms occurs. In the main reaction zone D the oxidising fragments consisting of oxygen atoms and molecules, OH and HO_2 radicals lead to highly exothermic oxidation reactions. The energy liberated in these reactions is retained by the product molecules formed in the form of electronic energy and is not readily converted to translational energy on collision; the 'hot' product molecules may thus retain their energy and undergo further exothermic reactions. A 'chemionisation' process results from direct utilisation of this energy before thermal ionisation has time to occur. The kinetics of the free radical processes occurring is the factor determining the extent of ionisation and not the flame temperature. The response thus varies directly with the rate of energy release in the reaction zone, the rates of the chemical reactions occurring and the burning velocity. Where a carbon is already oxidised in the starting sample, e.g. in carbon monoxide, an oxidised carbon fragment is split out in the endothermic cracking stage of the reactions and this oxidised carbon fragment is incapable of producing ionisation in the flame and there is no response from carbonyl carbon, etc.

The linearity of response down to very low carbon levels further refutes Stern's theory and indicates that response is not dependent upon C_2 or any other 2-carbon fragment. Though a detailed mechanism is still speculative, the close

equality of response per gram atom of carbon regardless of its source suggests that a single basic process contributes most of the ionisation in each case. Most of the steps proposed by Calcote require either 2-carbon fragments or electronic excitation on an already high energy CH fragment. Such steps are improbable in the hydrogen flame and correlations of response with rate of energy release in the reaction zone of the flame indicate steps utilising C, CH and CH_2 fragments in reaction with excited OH, O_2 or H_2O in the hydrogen flame to give firstly ions such as COH^+, $COOH^+$ which when struck by a H_2O molecule readily transfer a proton to form H_3O^+, $H_5O_2^+$, etc. H_3O^+ is the most common positive ion in uncontaminated hydrocarbon-air flames.

VI. List of Symbols

A	= Area of a peak
	Multipath term in the van Deemter equation
A'	= Giddings' coupled eddy diffusion coefficient
A_c	= Cross-sectional area of empty column
B	= Molecular diffusion term in the van Deemter equation
B_o	= Specific permeability
BC	= Background current
C	= Nonequilibrium coefficient
	Constriction
C_g, C_l	= Coefficients for resistance to mass transfer in gas and liquid phases
C_s	= Concentration on adsorbent
C_G	= Concentration in gas phase
CV	= Collector electrode voltage
c	= Concentration
	Velocity of light
c^*	= Concentration at equilibrium
c_1, c_2	= Constants
D_g, D_m	= Diffusivity in the gas and mobile phases
D_l	= Diffusivity in the liquid phase
D_{12}	= Diffusion coefficient of gas 1 in gas 2
D_{eff}	= Effective longitudinal diffusivity
D_g^o	= Gas diffusivity at column outlet pressure

d_c = Column diameter

d_p = Particle diameter

d_g = Gas film thickness

d = Distance

F_l, F_g = Volume fraction of column occupied by gas and liquid

F_o = Volume flow rate of carrier gas at column outlet

f_l = Gas compressibility factor

f_m = Mobile fraction of gas phase volume

GC = Gas chromatography

GLC = Gas-liquid chromatography

GSC = Gas-solid chromatography

H, HETP = Height equivalent to a theoretical plate

H_c = Mobile phase contribution to H apart from longitudinal diffusion

H_{tc} = Contribution to H from trans-column effects

H_g^o = Local gas plate height

H = Observed plate height

H_{min} = Minimum HETP

h = Reduced HETP

Planck's constant

i, I = Current

i_D = Discharge current

K = Partition coefficient

k = Column capacity coefficient = amount of solute per unit length in liquid phase divided by amount per unit length in gas phase

Boltzmann constant

L	= Column length
M, MW	= Molecular weight
N	= Number of theoretical plates
n	= Number of moles
p_i, p_o	= Column inlet and outlet pressure
p, p_m	= Average column pressure
$-p$	= Column pressure drop
R	= Fraction of solute in gas phase
	Gas constant
R_e	= Reynold's number
r	= Tube radius
s	= Rate of solute accumulation due to local non-equilibrium
T	= Temperature
	Tortuosity
t	= Time
t_R	= Retention time
u	= Linear gas velocity
u_o	= Linear gas velocity at column outlet
$\bar{u}$	= Average linear gas velocity
u_{opt}	= Linear gas velocity at H_{min}
u_b	= Peak or band velocity
v	= Voltage
ν	Reduced linear gas velocity
W	= Peak width
X	= Mole fraction

γ = Tortuosity factor

ϵ = Interparticle porosity

Force constant in Lennard-Jones function

η = Viscosity

λ = Packing irregularity factor

Mean free path

ρ = Density

d_c/d_p

σ = Standard Deviation

Force constant in Lennard-Jones function

Molecular diameter

σ^2 = Variance

$\sigma(x)$ = Standard deviation of a peak measured as a length

$\sigma(t)$ = Standard deviation of a peak measured in time units

ω = Coefficient indicating magnitude of H_c

Ω = Collision integral

Note: In addition to the above, there are symbols used in a particular discussion which apply to that discussion only.

References

1. Martin and Synge: Biochem. J. 35, 1358, 1941.
2. "Vapour Phase Chromatography" (Desty ed.), Academic Press, N.Y. 1957.
3. Tswett: Ber. dtsch. bot. Ges. 24, 316, 384, 1906.
4. Kvitka: Report to Baku Technical Committee 1900.
5. Day: Proc. Amer. Phil. Soc., 36, 112, 1897.
6. Kuhn et al: Hoppe-Seyl Z., 197, 141, 1931.
7. Ramsay: Proc. Roy. Soc., A76, 111, 1905.
8. Martin and James: Biochem. J., 50, 679, 1952.
9. Claesson: Arkiv. Kemi. Mineral Geol. 23A, 133, 1946; 24A, 7, 1946.
10. Claesson: Discussions Faraday Soc., 7, 34, 1949.
11. Clough: Petrol Engr., 27, 686, 1955.
12. Turner: Nat. Petrol. News, 35, 234, 1943.
13. Turkel 'taub: Zhur. Anal. Khim., 5, 200, 1950.
14. Phillips: Discussions Faraday Soc., 7, 241, 1949.
15. Tiselius: Arkiv. Kemi. Mineral Geol., 14B, 5, 1940; A16, 11, 1943.
16. Cremer and Mueller: Z. Electrochem., 55, 217, 1951.
17. Zhukhovitskii et al: Doklady Akad. Nauk. U.S.S.R., 77, 435, 1951.
18. Janak: Chem. Listy. 47, 464, 817, 1184, 1953.
    Ann. N.Y. Acad. Sci., 72, 606, 1959.
19. Ray: J. Appl. Chem., 4, 21, 82, 1954.
20. Patton et al: Anal. Chem., 27, 170, 1955.
21. James and Martin: Analyst, 77, 915, 1952.
22. James and Phillips: J. Chem. Soc., 1953, p.1600; 1954, p.3446.
23. Glueckauf: Trans. Faraday Soc., 51, 1540, 1955.
24. Knox and Purnell: Knox Ph.D. Thesis, Cambridge 1953.
25. Ettre in "Gas Chromatography", I.S.A. Symposium, June 1959 (Noebels, Wall and Brenner, eds.) p. 375, Academic Press, N.Y. 1961.

26. Bosanquet in "Gas Chromatography", (Desty ed.), p. 107, Butterworths, London, 1958.

27. Bosanquet and Morgan in "Vapour Phase Chromatography" (Desty ed.), p. 35, Academic Press, N.Y. 1957.

28. James and Phillips: J. Chem. Soc., 1954, p. 1066.

29. Bohemen et al: J. Chem. Soc., 1960, p. 2444.

30. Walter: J. Chem. Phys., 13, 229, 1945.

31. Thomas: Ann. N.Y. Acad. Sci., 49, 161, 1941.

32. Martin et al in "Gas Chromatography" (Desty ed.), Butterworths, London, 1958.

33. Jones and Kieselbach: Anal. Chem., 30, 1590, 1958.

34. Van Deemter et al: Chem. Eng. Sci., 5, 271, 1956.

35. Hardy and Pollard: J. Chromatog., 2, 1, 1959.

36. Martin: Endeavour 6, 22, 1947.

37. Wilson: J. Am. Chem. Soc., 62, 1583, 1940.

38. De Vault: J. Am. Chem. Soc., 65, 532, 1943.

39. Keulemans "Gas Chromatography", Reinhold, N.Y. 1957.

40. Klinkenberg and Sjenitzer: Chem. Eng. Sci., 5, 258, 1956.

41. Golay in "Gas Chromatography" (Desty ed.), p. 36, Butterworths, London, 1958.

42. Chmitov and Filatova in "Gas Chromatography" (Desty ed.), p. 99, Butterworths, London, 1958.

43. Mayer and Tompkins: J. Am. Chem., 69, 2866, 1947.

44. Glueckauf: Trans. Faraday Soc., 51, 34, 1955.

45. Lapidus and Amundsen: J. Phys. Chem., 56, 984, 1952.

46. Tunitskii: Doklady Akad. Nauk. U.S.S.R., 99, 577, 1954.

47. Glueckauf: Discussions Faraday Soc., 7, 12, 202, 1949.

48. Glueckauf: Analyst., 77, 903, 1952.
Ann. N.Y. Acad. Sci., 72, 562, 1959.

49. Glueckauf: "Ion-Exchange and its Applications", p. 34, Metcalfe and Cooper Ltd., London, 1955.

50. Keulemans and Kwantes in "Vapour Phase Chromatography", (Desty ed.), p. 15, Academic Press, N.Y. 1957.

51. Mysels: J. Chem. Phys., 24, 371, 1956.

52. Giddings: J. Chem. Phys., 26, 1755, 1957.

53. Giddings: J. Chem. Phys., 31, 1462, 1959.

54. Beynon et al: Trans. Faraday Soc., 54, 705, 1958.

55. Giddings and Eyring: J. Phys. Chem., 59, 416, 1955.

56. Giddings: J. Chem. Educ., 35, 588, 1958.

57. Uhlenbeck and Ornstein: Phys. Rev., 36, 93, 1930.

58. Le Rosen: J. Am. Chem. Soc., 67, 1693, 1945.

59. McQuarrie: J. Chem. Phys., 38, 437, 1963.

60. Giddings: J. Chromatog., 2, 44, 1959.

61. Giddings: J. Chem. Phys., 26, 1210, 1957.

62. Giddings: J. Chem. Phys., 26, 169, 1957.

63. Golay in "Gas Chromatography" I.S.A. Symposium, August, 1957. (Coates, Noebels, Fagerson eds.), p. 1, Academic Press, N.Y. 1958.

64. Golay: Anal. Chem., 29, 928, 1957.

65. Golay: Nature, 180, 435, 1957.

66. Golay: Nature, 182, 1146, 1958.

67. Aris: Proc. Roy. Soc., A.252, 538, 1959.

68. Taylor: Proc. Roy. Soc., A.219, 186, 1953.

69. Taylor: Proc. Roy. Soc., A. 223, 446, 1954.
A. 225, 473, 1954.

70. Aris: Proc. Roy. Soc., A. 235, 67, 1956.

71. Westhaver: Ind. Eng. Chem., 34, 146, 1942.

72. Desty et al in "Gas Chromatography" I.S.A. Symposium, June, 1961, (Brenner, Caller and Weiss eds.), p. 105, Academic Press, N.Y. 1962.

73. Desty et al: J. Inst. Petrol., 45, 287, 1959.

74. Desty et al: Nature, 183, 107, 1959.

75. Giddings et al: Anal. Chem., 32, 867, 1960.

76. Stewart et al: Anal. Chem., 31, 1738, 1958.

77. Haarhoff and Pretorius: J.S. Afr. Chem. Inst., 13, 87, 1960.

78. Martin: Anal. Chem., 33, 347, 1961.

79. Krige and Pretorius: Anal. Chem., 35, 2009, 1963.

80. Khan: Nature, 186, 800, 1960.

81. Khan in "Gas Chromatography: 1962" (M. van Swaay, ed.), p. 3, Butterworths, London, 1962.

82. Vivian and Peaceman: A.I.Ch.E.J., 2, 437, 1956.

83. Goodridge et al: Trans. Inst. Chem. Eng. (London), 40, 54, 1962.

84. Jones in Kieselbach Anal. Chem., 32, 880, 1960.

85. Giddings: Anal. Chem., 34, 458, 1962.

86. Zlatkis and Kaufman: Nature, 184, 2010, 1959.

87. Scott: Nature, 183, 1753, 1959.

88. Golay in "Gas Chromatography: 1960" (Scott, ed.), p. 139, Butterworths, London, 1960.

89. Purnell: Nature, 184, 2009, 1959.

90. Purnell: J. Chem. Soc., 1960, p. 1268.

91. Purnell: Anal. Chem., 32, 339, 1960.

92. Purnell and Quinn in "Gas Chromatography 1960" (Scott, ed.), p. 193, Butterworths, London, 1960.

93. Smith in "Gas Chromatography: 1962" (M. van Swaay, ed.), p. 204, Butterworths, London,1962.

94. Giddings: Hirshfelder: J. Phys. Chem., 61, 738, 1957.
6th Int. Symp. on Combustion, N.Y. 1957, p. 199.

95. Giddings: J. Chromatog., 3, 16, 444, 1964.

96. Giddings and Shin: Trans. Faraday Soc., 57, 468, 1961.
J. Phys. Chem., 65, 1164, 1961.

97. Littlewood et al: J. Chem. Soc., 1955, p. 1480.

98. Scott and Hazeldean: J. Inst. Petrol., 48, 380, 1960.

99. James et al: J. Phys. Chem., 68, 1725, 1964.

100. Giddings: J. Chromatog., 5, 61, 1961.

101. Giddings: J. Chromatog., 3, 443, 1960.

102. Giddings: J. Chromatog., 5, 46, 1961.

103. Giddings: Anal. Chem., 34, 1186, 1962.

104. Giddings: J. Chromatog., 3, 520, 1960.

105. Giddings: Anal. Chem., 34, 1026, 1962.

106. Giddings: J. Phys., Chem., 68, 184, 1964.

107. Giddings: Anal. Chem., 33, 962, 1961.

108. Giddings: Anal. Chem., 35, 439, 1963.

109. Giddings: Nature, 188, 847, 1960.

110. Giddings: Anal. Chem., 34, 722, 1962.

111. Giddings: J. Gas Chromatog., 1, 4, 38, 1963.

112. Giddings: "Dynamics of Chromatography: Principles and Theory", Marcel Dekker Inc. N.Y. Press.

113. Boyd et al: J. Am. Chem. Soc., 69, 2849, 1947.

114. Jones: A.C.S.-I.S.A. Conference, Memphis, Tenn., Dec. 1956.

115. Van Deemter: 2nd Informal Symp. G.C. Disc. Group, Cambridge, 1957.

116. Giddings: Nature, 184, 357, 1959.

117. Jones: Anal. Chem., 33, 829, 1961.

118. Bethea and Adams: Anal. Chem., 33, 832, 1961.

119. Loyd et al: Anal. Chem., 32, 618, 1960.

120. Golay in "Gas Chromatography", I.S.A. Symposium, June, 1959, (Noebels, Wall and Brenner, eds.), p. 11, Academic Press, N.Y. 1961.

121. Bohemen and Purnell: J. Chem. Soc., 1961, p. 2630.

122. Norem: Anal. Chem., 34, 40, 1962.

123. Dal Nogare and Chiu: Anal. Chem., 34, 890, 1962.

124. Perrett and Purnell: Anal. Chem., 35, 430, 1963.

125. Kramers and Alberda: Chem. Eng. Sci., 2, 173, 1953.

126. Carberry and Bretton: A.I.Ch.E.J., 4, 367, 1958.

127. Giddings and Robison: Anal. Chem., 34, 885, 1962.

128. Giddings: Anal. Chem., 35, 1338, 1963.

129. Bohemen and Purnell in "Gas Chromatography" (Desty ed.), p. 6, Butterworths, London, 1958.

130. Littlewood in "Gas Chromatography" (Desty ed.), p. 23, 35, Butterworths, London, 1958.

131. Ayers et al: Anal. Chem., 33, 987, 1961.

132. Brennan and Kemball: J. Inst. Petrol., 44, 14, 1958.
J. Chem. Educ.,33, 490, 1956.

133. Kieselbach: Anal. Chem., 33, 806, 1961.

134. Bohemen and Purnell: J. Chem. Soc., 1961, p. 360.

135. Desty et al in "Gas Chromatography" (Desty ed.), p. 200, Butterworths, London, 1958.

136. Glueckauf in "Gas Chromatography" (Desty ed.), p. 18, 29, Butterworths, London, 1958.

137. Rijnders in "Gas Chromatography" (Desty ed.), p. 18, Butterworths, London, 1958.

138. Glueckauf in "Gas Chromatography" (Desty ed.), p. 33, Butterworths, London, 1958.

139. Purnell: Ann. N.Y. Acad. Sci., 72, 592, 1959.

140. Kieselbach: Anal. Chem., 33, 23, 1961.

141. Glueckauf: Ann. N.Y. Acad., Sci., 72, 614, 1959.

142. Jones in "Gas Chromatography" I.S.A. Symposium, August, 1957, (Coates, Noebels, Fagerson, eds.), p. 13, Academic Press, N.Y. 1958.

143. Giddings: Nature, 187, 1023, 1960.

144. Glueckauf: Analyst, 77, 903, 1952.

145. Kieselbach: Anal. Chem., 35, 1342, 1963.

146. De Wet and Pretorius: Anal. Chem., 30, 325, 1958.

147. Scott in "Gas Chromatography" (Desty ed.), Butterworths, London, 1958.

148. Baker et al in "Gas Chromatography", I.S.A., Symposium, June, 1959, (Noebels, Wall and Brenner, eds.), p. 21, Academic Press, N.Y. 1961.

149. Martin: Anal. Chem., 33, 1143, 1961.

150. Hirshfelder, Curtis and Bird "Molecular Theory of Gases and Liquids", Wiley, New York (1954).

151. Houghton et al: J. Phys. Chem., 65, 649, 1961.

152. Giddings: Anal. Chem., 36, 1483, 1964.
Cvetanovic and Kutschke in "Vapour Phase Chromatography" (Desty ed.), p. 87, Academic Press, N.Y. 1957.

153. Hishta and Messerly: Anal. Chem., 32, 880, 1960.

154. Hornstein and Crowe: Anal. Chem., 33, 310, 1961.

155. Sternberg and Poulson: Anal. Chem., 36, 1492, 1964.

156. Johnson and Stross: Anal. Chem., 31, 357, 1959.

157. Guiochon: Anal. Chem., 35, 399, 1963.

158. Daniels: Chem. and Ind. (London) 1963. p.1078.

159. Reilley et al: Anal. Chem., 34, 1198, 1962.

160. Scott: Private communication to Knox.

161. Dal Nogare and Safranski in Organic Analysis Vol. IV:

162. Ryce and Bryce: Nature 179, 541, 1957.
Can. J. Chem., 35, 1293, 1957.

163. Lovelock: Nature, 181, 1460, 1958.

164. Pitkethly: Anal. Chem., 30, 1309, 1958.

165. Karmen and Bowman: Ann. N.Y. Acad. Sci., 72, 714, 1959.

166. Lovelock: J. Chromatog., 1, 35, 1958.

167. Lovelock and Lipsky: J. Am. Chem. Soc., 82, 431, 1960.

168. Evans and Willard: J. Am. Chem. Soc., 78, 2908, 1956.

169. Liberti and Cartoni in "Gas Chromatography" (Desty ed.), p. 321, Butterworths, London, 1958.

170. Martin and Smart: Nature, 175, 422, 1955.

171. Gohlke: Anal. Chem., 31, 535, 1959.

172. Scott: Nature, 176, 793, 1955.

173. Grant in "Gas Chromatography" (Desty ed.), p. 153, Butterworths, London, 1958.

174. McWilliam and Dewar in "Gas Chromatography" (Desty ed.), p. 142, Butterworths, London, 1958.
Nature, 181, 760, 1958.
Nature, 182, 1664, 1958.

175. McWilliam: 2nd Informal Symp. G.C. Disc. Group, 1957.

176. Harley et al: Nature, 181, 177, 1958.

177. Onkiehong in "Gas Chromatography 1960" (Scott ed.), p. 7, Butterworths, London, 1960.

178. Desty et al: in "Gas Chromatography 1960" (Scott ed.), p. 46, Butterworths, London, 1960.

179. Sternberg et al: in "Gas Chromatography" I.S.A. Symposium, June, 1961, (Brenner, Caller and Weiss eds.), p. 231, Academic Press, New York, 1962.

180. Lovelock: Anal. Chem. 33, 162, 1961.

181. Halasz in "Gas Chromatography" I.S.A. Symposium, June, 1961, (Brenner, Caller and Weiss eds.), p. 267, Academic Press, New York, 1962.

182. Jarrell: Ash Co. Gas Pipe Oct., 1963, No. 5.

183. Novak and Janak: J. Chromatog., 4, 249, 1960.

184. Condon et al in "Gas Chromatography 1960" (Scott ed.), p. 30, Butterworths, London, 1960.

185. Fowlis et al: J. Chromatog. 15, 1449, 1964.

186. Perkins et al in "Gas Chromatography" I.S.A. Symposium, June, 1961, (Brenner, Caller and Weiss eds.), p. 269, Academic Press, New York, 1962.

187. Ettre in "Gas Chromatography" I.S.A. Symposium, June, 1961, (Brenner, Caller and Weiss eds.), p. 307, Academic Press, N.Y. 1962.

188. De Ford et al: Anal. Chem., 35, 426, 1963.

189. Carman "Flow of Gases through Porous Media", Butterworths, London, 1956.

190. Ashley et al: Anal. Chem., 36, 1369, 1964.

191. Guiochon and Landault: Bull Soc. Chim, France, 1963, p. 2433.
5th Int. Symp. on Gas Chromatog., Brighton, 1964.

192. Halasz and Heine: Nature, 194, 971, 1962.

193. Collins "Flow of Fluids through Porous Materials", Reinhold, N.Y. 1961.

194. Perkins and Johnson: Soc. Pet. Engrs. J., March, 1963, p. 70.

195. Scheidegger "Physics of Flow through Porous Media", MacMillan, N.Y. 1957.

196. Muskat "Flow of Homogeneous Fluids", McGraw Hill, N.Y. 1937.

197. Knox and McLaren: Anal. Chem., 35, 449, 1963.

198. Klinkenberg and Sjenitzer: Nature, 187, 1023, 1960.

199. Giddings: Anal. Chem., 35, 2215, 1963.

200. Giddings: J. Chromatog., 13, 301, 1964.

201. Terry et al: Meeting Soc. Petrol Engrs. Houston, Oct., 1958.

202. Knox: unpublished work.

203. Giddings: Anal. Chem., 35, 1338, 1963.

204. Bayer et al: Anal. Chem., 35, 492, 1963.

205. Frisone: J. Chromatog., 6, 97, 1961.

206. Pypker in "Gas Chromatography 1960" (Scott ed.), p. 240, Butterworths, London, 1960.

207. Higgins and Smith: 5th Int. Symp. on Gas Chromatog., Brighton, Sept. 1964.

208. Giddings and Fuller: J. Chromatog., 7, 255, 1962.

209. Giddings: J. Gas Chromatog., 1, 12, 1963.

210. Colay in "Gas Chromatography" I.S.A. Symposium, June, 1961, (Brenner, Caller and Weiss eds.), Academic Press, N.Y. 1962.

211. Schwartz and Smith: Ind. Eng. Chem., 45, 1209, 1953.

212. Hupe in Bayer et al. see ref. 204.

213. Carle and Johns in "Gas Chromatography" I.S.A. Symposium, August, 1957, (Coates, Noebels, Fagerson eds.), Academic Press, New York, 1958.

214. Huyten et al in "Gas Chromatography 1960" (Scott ed.) p. 244, Butterworths, London, 1960.

215. Benenati and Brosilow: A.I.Ch.E.J., 8, 359, 1962.

216. Frisone in "Gas Chromatography" I.S.A. Symposium, June, 1961, (Brenner, Caller and Weiss eds.), p. 528, Academic Press, New York, 1962.

217. Norem in "Gas Chromatography" I.S.A. Symposium, June, 1961, (Brenner, Caller and Weiss eds.), p. 528, Academic Press, New York, 1962.

218. Hudy in "Gas Chromatography" I.S.A. Symposium, June, 1961, (Brenner, Caller and Weiss eds.), p. 528, Academic Press, New York, 1962.

219. Littlewood: 5th Int. Symp. Gas Chromatog., Brighton, Sept., 1964.

220. Priestley: Expts. and Obs. on Nat. Phil. Birmingham, 1786, 3, 390.

221. Dalton: Ann. Phys., 1803, 13, 25, 122, 197.

222. Berthollet: Mem. Soc. Arcueil, 2, 463, 1809.

223. Grahame: Ann. Phys., 17, 341, 1829.

224. Fick: Ann. Phys., 94, 59, 1855.

225. Purnell "Gas Chromatography" Wiley, New York, 1962.

226. Boyd et al: J. Chem. Phys., 19, 548, 1951.

227. Kimpton and Wall: J. Phys. Chem., 56, 715, 1952.

228. Wall and Kidder: J. Phys. Chem., 50, 235, 1946.

229. Westenberg and Walker: J. Chem. Phys., 29, 1139, 1958.

230. Boardman and Wild: Proc. Roy. Soc. (London), A.162, 511, 1937.

231. Coward and Georgeson: J. Chem. Soc., 1937, p. 1085.

232. Walker and Westenberg: J. Chem. Phys. 31, 519, 1959.
32, 1314, 1960.

233. Waldman: Z. Naturforsch 59, 327, 1950.
Naturwissenschafter 32, 222, 1944.

234. Stefan Stitzker: Akad. Wiss. Wien 63, 63, 1871.
Akad. Wiss. Wien 68, 385, 1873.

235. Carmichael et al: Ind. Eng. Chem., 47, 2205, 1955.

236. Fairbanks and Wilke: Ind. Eng. Chem., 42, 471, 1950.

237. Lee and Wilke: Ind. Eng. Chem., 46, 2381, 1954.

238. McCurtrie and Keyes: J. Am. Chem. Soc., 70, 3755, 1948.

239. Schwertz and Brow: J. Chem. Phys., 19, 640, 1951.

240. Winkelman: Ann. Phys., 22, 154, 1884.
33, 445, 1888.
36, 93, 1889.

241. Seager et al: J. Chem. Eng. Data 8, 168, 1963.

242. Giddings and Seager: Ind. Eng. Chem. Fund, 1, 277, 1962.

243. Giddings and Seager: J. Chem. Phys., 33, 1579, 1960.

244. Giddings and Seager: J. Chem. Phys., 35, 2242, 1961.

245. Fejes and Cjaran: Acta. Chimica. Acad. Scient. Hung., 29, 171, 1961.

246. Scott and Hazeldean in "Gas Chromatography 1960" (Scott ed.), p. 144,
Butterworths, London, 1960.

247. Carberry and Bretton: A.I.Ch.E.J., 4, 367, 1958.

248. Carberry and Bretton: J. Chem. Phys., 35, 2241, 1961.

249. Giddings and Fuller: Private communication to be published in J.Gas
Chromatography.

250. Johnson and Babb: Chem. Revs. 56, 387, 1956.

251. Reid and Sherwood "Properties of Gases and Liquids" McGraw-Hill,
New York, 1958.

252. Bird, Stewart and Lightfoot: "Transport Phenomena", John Wiley, New York, 1960.

253. Meyer: Frankel Phys. Rev., 57, 660, 1941.

254. Maxwell: Phil. Mag., 19, 19, 1860.
Phil. Trans., 157, 49, 1867.

255. Chapman and Cowling "Mathematical Theory of Nonuniform Gases" 2nd ed.,
Cambridge Univ. Press, London, 1952.

256. Gilliland: Ind. Eng. Chem., 26, 681, 1934.

257. Arnold: Ind. Eng. Chem., 22, 1091, 1930.

258. Sutherland: Phil. Mag., 36, 507, 1893.

259. Hirschfelder, Bird and Spotz: Chem. Rev., 44, 205, 1949.
J. Chem. Phys., 16, 968, 1948.

260. Bird: Adv. in Chem. Eng. Vol. 1, p. 156, Academic Press, New York, 1956.

261. Rowlinson: J. Chem. Phys., 17, 101, 1949.

262. Rowlinson and Townley: Trans. Faraday Soc., 49, 20, 1953.

263. Chen and Othmer: J. Chem. Eng. Data, 7, 37, 1962.

264. Wilke and Lee: Ind. Eng. Chem., 47, 1253, 1955.

265. Slattery and Bird: A.I.Ch.E.J., 4, 137, 1958.

266. Othmer and Chen: I.E.C.Proc. Desg. and Dev., 1, 249, 1962.

267. Clarke and Ubbelohde: J. Chem. Soc., 1957, p. 2050.

268. Cummings and Ubbelohde: J. Chem. Soc., 1953, p. 3751.

269. Bartell and Osterhof: J. Phys. Chem., 32, 1553, 1928.

270. Carmen: Trans. Instn. Chem. Engrs. Lond., 15, 150, 1937.

271. Fowler and Hertel: J. Appl. Phys., 11, 496, 1940.

272. Barrer in "Gas Chromatography" (Desty ed.), p. 35, Butterworths, London, 1958.

273. McDonald 'Ionography' Yearbook Publishers, 1955.

274. Kunkel and Tiselius: J. Gen. Physiol. 35, 89, 1951.

275. Tiselius: Discussions Faraday Soc., 13, 29, 1953.

276. Owen: Am. Inst. Mining Met. Engrs., 195, 169, 1950.

277. Boyack and Giddings: J. Biolog. Chem., 235, 1970, 1960.

278. Boyack and Giddings: J. Theoret. Biol., 2, 1, 1962.

279, Boyack and Giddings: Arch. Biochem. Biophys, 100, 16, 1963.

280. Kiselev: Quarterly Reviews, 15, 99, 1961.

281. Klein: Anal. Chem., 34, 733, 1962.

282. Lowen and Broge: J. Phys. Chem., 65, 16, 1961.

283. Conner in "Gas Chromatography" (Desty ed.), p. 214, Butterworths, London, 1958.

284. Scholz and Brandt in "Gas Chromatography" I.S.A. Symposium, June, 1961. (Brenner, Caller and Weiss eds.), p. 7, Academic Press, New York, 1962.

285. Shapiro and Kolthoff: J. Am. Chem. Soc., 72, 776, 1950.

286. Perrett and Purnell: J. Chromatog., 7, 455, 1962.

287. Liberti in "Gas Chromatography" (Desty ed.), p. 214, Butterworths, London, 1958.

288. Zlatkis et al: Anal. Chem., 31, 945, 1959.

289. Bens: Anal. Chem., 33, 178, 1961.

290. Averill in "Gas Chromatography" I.S.A. Symposium, June, 1961. (Brenner, Caller and Weiss eds.), p. 1, Academic Press, N.Y. 1962.

291. Knight: Anal. Chem., 30, 2030, 1958.

292. Ormerod and Scott: J. Chromatog., 2, 65, 1959.

293. Martin and Howard: Biochem. J., 46, 532, 1960.

294. Kwantes and Rijnders in "Gas Chromatography" (Desty ed.), p. 125, Butterworths, London, 1958.

295. Holmes and Stack: Biochem. Biophys. Acta., 56, 163, 1962.

296. Sawyer and Barr: Anal. Chem., 34, 1518, 1962.

297. Cieplinski: Anal. Chem., 35, 256, 1963.

298. Berge and Pretorius: Trans. Faraday Soc., 58, 2272, 1962.

299. Berge and Pretorius: Anal. Chem., 35, 1537, 1963.

300. Ottenstein: J. Gas Chromatog., 1, No. 4, 11, 1963.

301. Janak and Staszewski: J. Gas Chromatog., 2, No. 2, 47, 1964.

302. Janak in "Gas Chromatography: 1962" (M. van Swaay, ed.), p. 59, Butterworths, London, 1962.

303. Smith: Fifth Int. Symp. on Gas Chromatography: Brighton, 1964.

304. Giddings and Boyack: Anal. Chem., 36, 1229, 1964.

305. Scott: Nature, 185, 312, 1960.

306. Scott and Cumming in "Gas Chromatography 1960" (Scott ed.), p. 117, Butterworths, London, 1960.

307. "C-Scope" Handbook B.P. Ltd., Engrs., Edinburgh.

308. Guiochon and Farre-Rius: Nature, 196, 63, 1962.

309. Desty et al: Anal. Chem., 32, 302, 1960.

310. Condon: Anal. Chem., 31, 1717, 1959.

311. Zlatkis and Lovelock: Anal. Chem., 31, 620, 1959.

312. Dijkstra and De Goey in "Gas Chromatography" (Desty ed.), p. 56, Butterworths, London, 1958.

313. Kreyenbuhl: Bull. Soc. Chim., France, 2125, 1960.

314. Averill: Pittsburgh Conf. on Anal. Chem. and Appl. Spect., March, 1961.

315. Mohmke and Saffert in "Gas Chromatography: 1962" (M. van Swaay, ed.), p. 216, Butterworths, London, 1962.

316. Smith in "Gas Chromatography: 1962" (M. van Swaay, ed.), p. 99, Butterworths, London, 1962.

317. Miller: B.H.C. Ltd., Grangemouth, private communication.

318. Lovelock: Nature, 182, 1663, 1958.

319. Jesse and Sadauski's Phys. Rev., 100, 1755, 1955.

320. Lovelock et al: Ann. N.Y. Acad. Sci., 72, 720, 1959.

321. Lovelock in "Gas Chromatography 1960" (Scott ed.), p. 16, Butterworths, London, 1960.

322. Willis: Nature, 184, 894, 1959.

323. Lovelock: Nature, 181, 1460, 1958.

324. Smith: N.R.P.R.A. private communication.

325. Lipsky et al: Anal. Chem., 31, 852, 1959.

326. Lovelock: Nature, 188, 401, 1960.

327. Kaye: and Laby "Physical and Chemical Constants" Longmans, Green & Co., London, 1956.

328. Griffin and George Ltd.: private communication.

329. Fowlis and Scott: J. Chromatog., 11, 1, 1963.

330. Craggs, Liverpool: private communication.

331. U.S. Patent Office, 2,959,677. Nov. 8., 1960.

332. Yamane: J. Chromatog., 9, 162, 1962.

333. Yamane: J. Chromatog., 11, 158, 1963.

334. Yamane: J. Chromatog., 14, 355, 1964.

335. Hopfield: Astrophys. J., 72, 133, 1930.

336. Tanaka, Huffmann et al: J. Opt. Soc. Am., 48, 304, 1958.

337. Tanaka, Huffmann et al: J. Opt. Soc. Am., 52, 851, 1962.

338. Martin and Smart: Nature, 175, 422, 1955.

339. Franc and Jokl: Chem. Listy., 52, 276, 1958.

340. Liberti et al: Chim.e.ind.Milan., 38, 674, 1956.

341. Johnstone and Douglas: Chem. and Ind. 1959, p. 154.

342. Deal et al: Anal. Chem., 28, 1956, 1958.

343. Boer in "Vapour Phase Chromatography" (Desty ed.), p. 169, Academic Press, New York, 1957.

344. Lovelock and Gregory in "Gas Chromatography" I.S.A. Symposium, June, 1961, (Brenner, Caller and Weiss eds.) p. 219, Academic Press, New York, 1962.

345. Lovelock: Nature, 187, 49, 1960.

346. Willis: Nature 183, 1754, 1959.

347. Druyvesteyn and Penning: Revs. Mod. Phys., 12, 87, 1940.

348. Harley and Pretorius: Nature 178, 1244, 1956.

349. Pitkethly: Anal. Chem., 30, 1309, 1958.

350. Basson et al: J.S. African Chem. Inst., 12, 62, 1959.

351. Lovelock: Nature 181, 1460, 1958.

352. Thompson: J. Chromatog., 2, 148, 1959.

353. Arndt et al: J.S. African Chem. Inst., 12, 62, 1959.

354. Karmen and Bowman: Nature, 182, 1233, 1958.

355. Johnson and Stross: Anal. Chem., 31, 1206, 1959.

356. Mitchell: Submicogram Experimentation. (Cheronis ed.), Vol. I, p. 201.

357. Johnson: Pittsburgh Conf. on Anal. Chem and Appl. Spect., March, 1961.

358. Phillips "Gas Chromatography" Butterworths Scientific Publications, London 1956.

359. Margenau and Murphy "The Mathematics of Physics and Chemistry", 2nd ed. Van Nostrand, Princeton, New Jersey, 1956.

360. Ambrose and Ambrose "Gas Chromatography", Newnes, London, 1961.

361. Stewart et al: Anal. Chem., 31, 1738, 1959.

362. Giddings et al: Anal. Chem., 32, 867, 1960.

363. Giddings: Anal. Chem., 35, 353, 1963.

364. Sternberg and Poulson: Anal. Chem., 36, 58, 1964.

365. Littlewood "Gas Chromatography" Academic Press, London, 1962.

366. Stern: see Lewis and Von Elbe 'Combustion, Flames and Explosions', p.206, 1951.

367. Calcote: Combustion and Flame, 1, 392, 1957.

368. Kinbara and Nakamura: 5th Int. Symp. on Comb., p. 285, 1955.

369. Sugden and Knewstubb: Nature, 181, 475, 1261, 1958.

370. Sugden: Proc. Roy. Soc., A255, 520, 1960.

371. Eyring et al: 8th Int. Symp. on Comb., 1960.

372. Rice - Herzfield: J. Am. Chem. Soc., 56, 284, 1934.

373. Benson "Foundations of Chemical Kinetics", McGraw-Hill, New York, 1960, p.66.

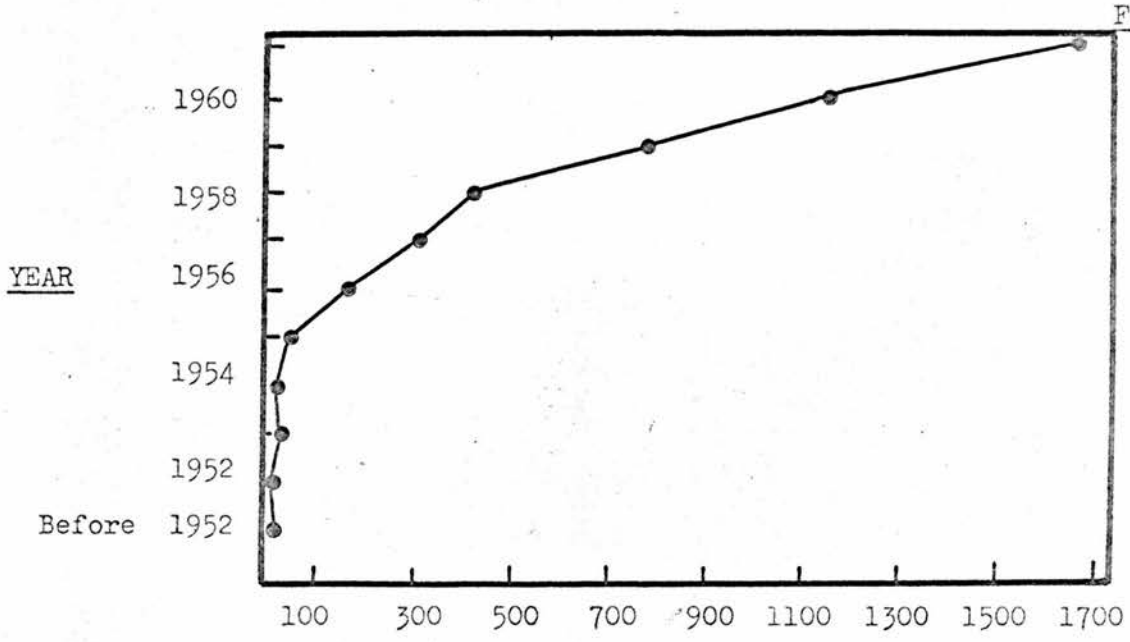

Figure 1 : Number of gas chromatography publications according to year.

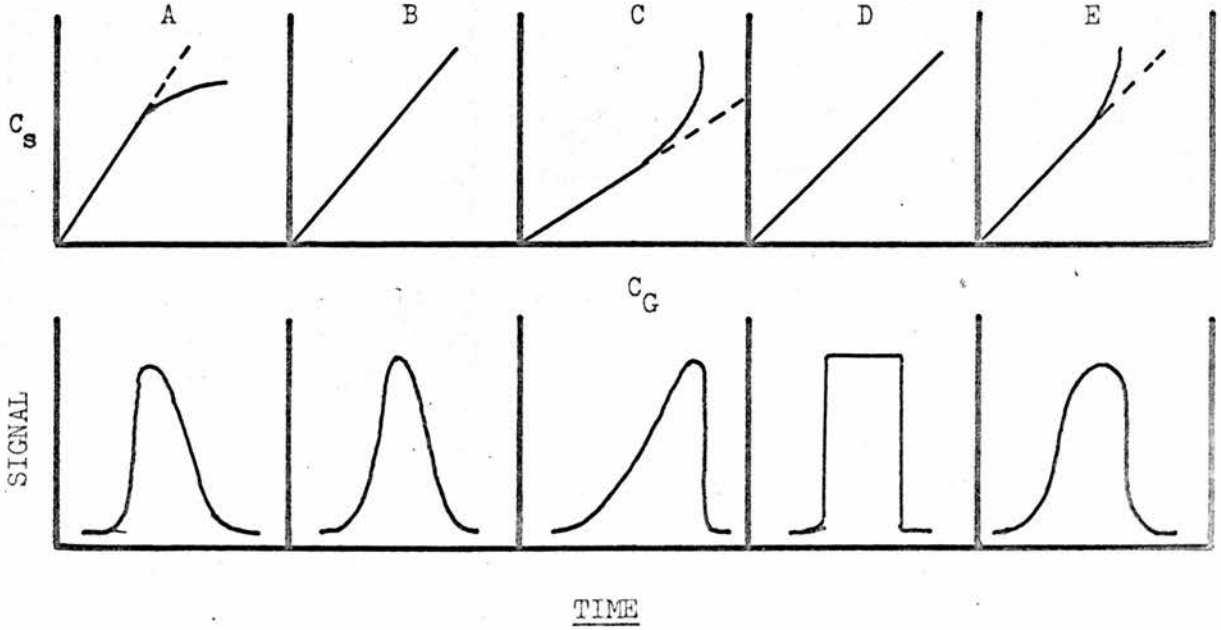

Figure 2 : Relationships between the distribution isotherms and the form of the peaks in the gas chromatogram by election analysis : non-linear ideal (A, C), linear non-ideal (B), linear-ideal (D) and non-linear non-ideal (E).

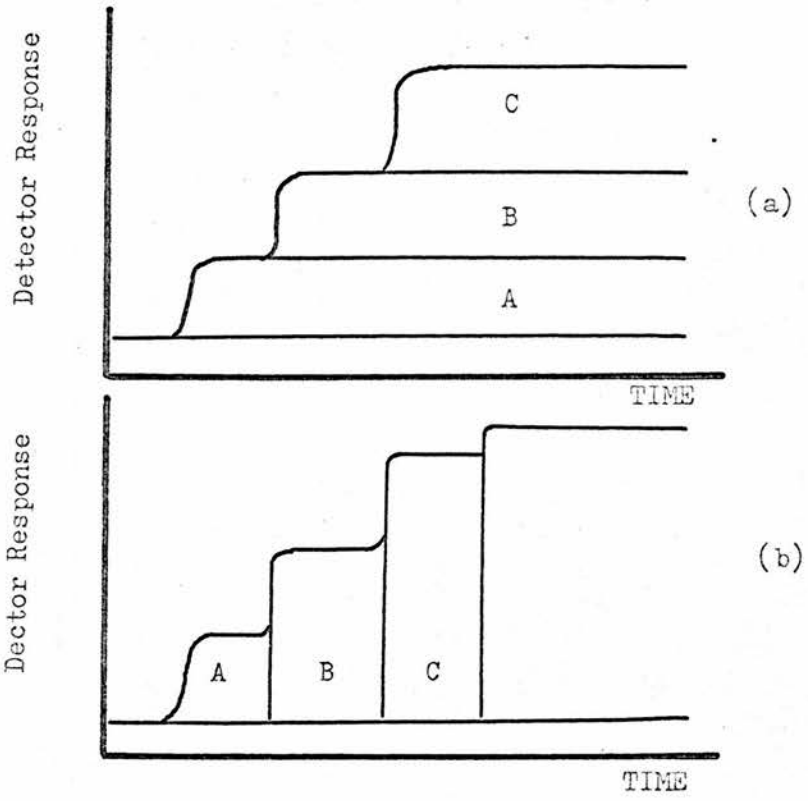

Figure 3 : Frontal analysis (a) and displacement development (b) of a 3 - component mixture.

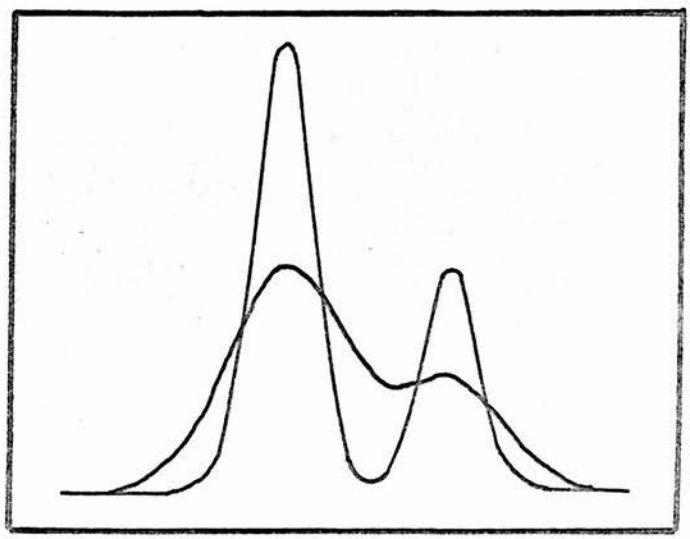

Figure 4 : The effect of peak width on component separation

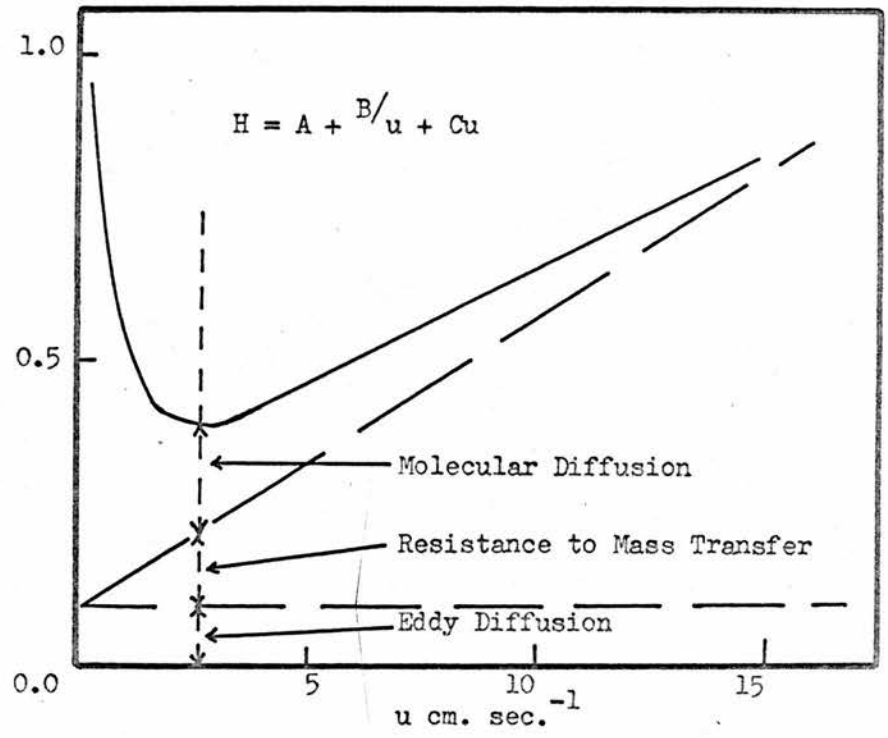

Figure 5 : Plot of H E T P against calculated linear gas velocity (after Keulemans)

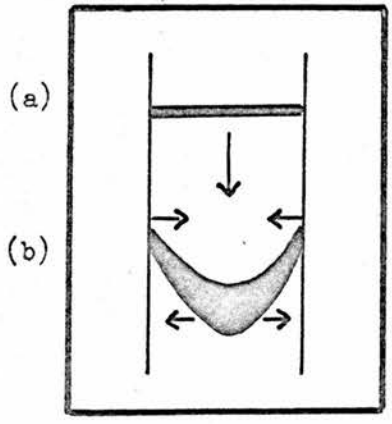

Figure 6 : Flow and Diffusion in an empty tube.

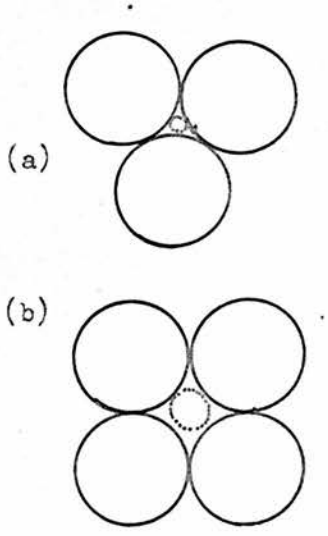

Figure 7 : Two packing structures of spheres.

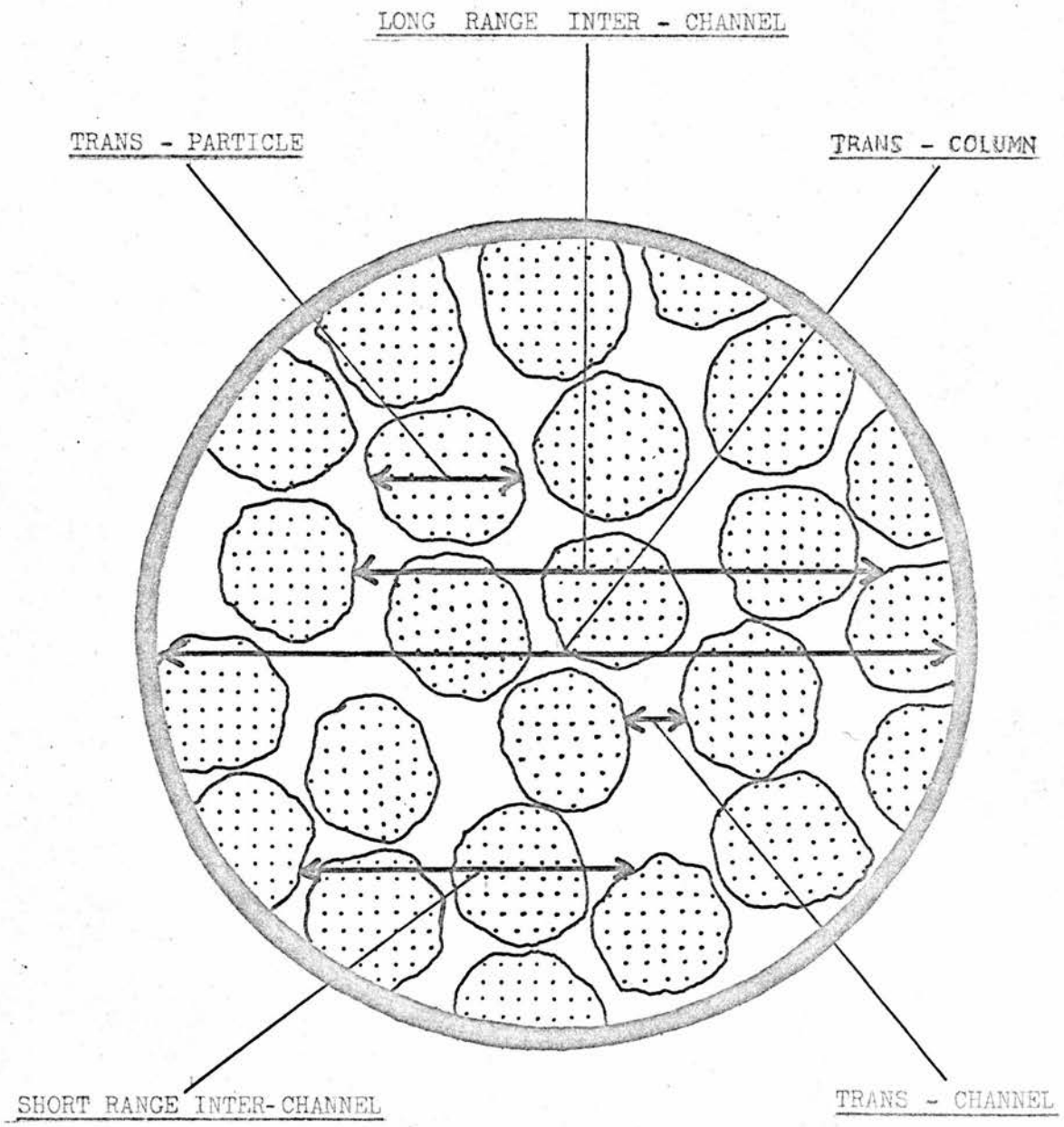

Figure 8 : The location and distance covered by the various exchange processes between velocity extremes in the mobile phase.

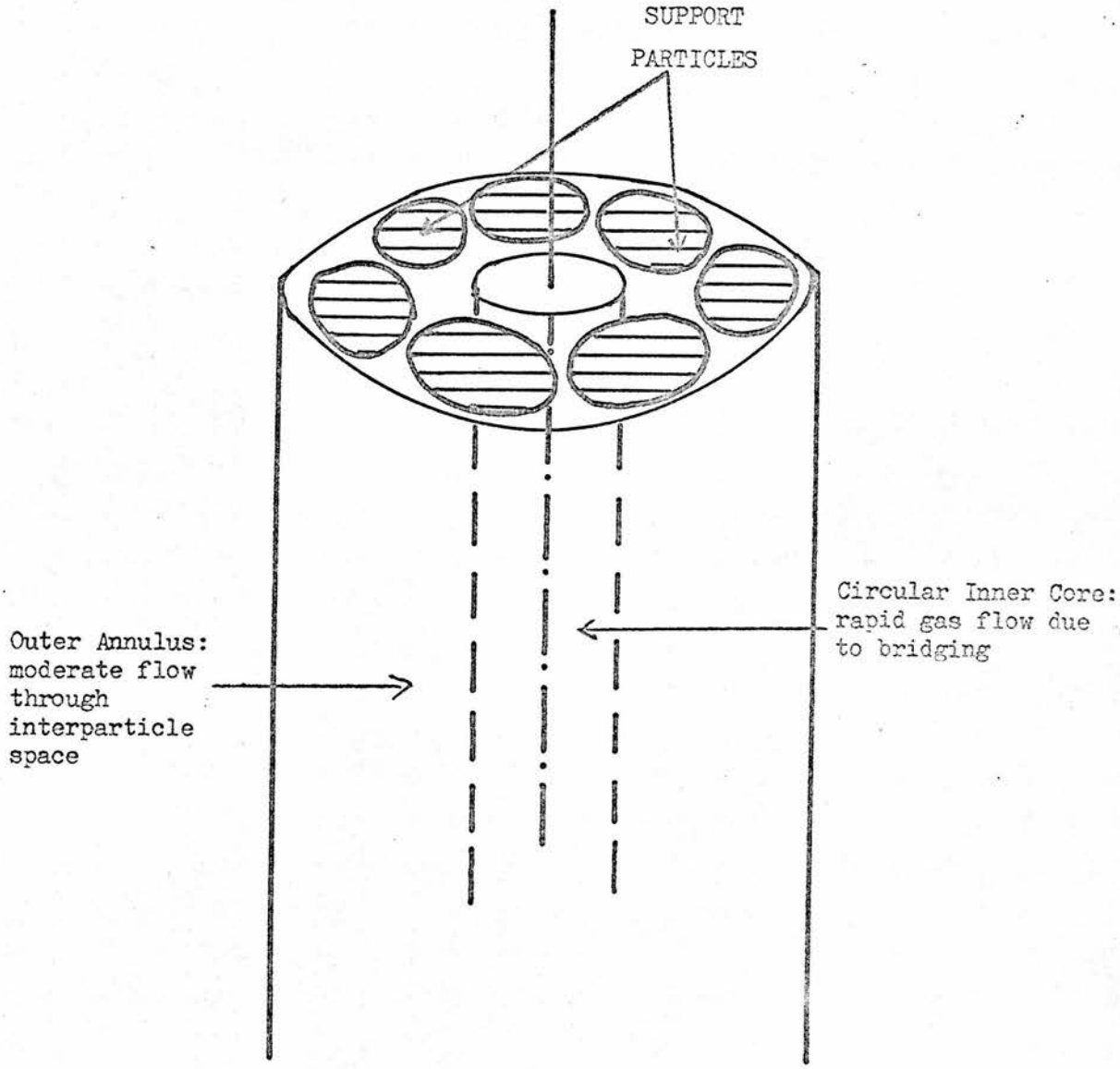

Figure 9: Model used by Giddings to approximate repeating flow unit in chromatographic packing.

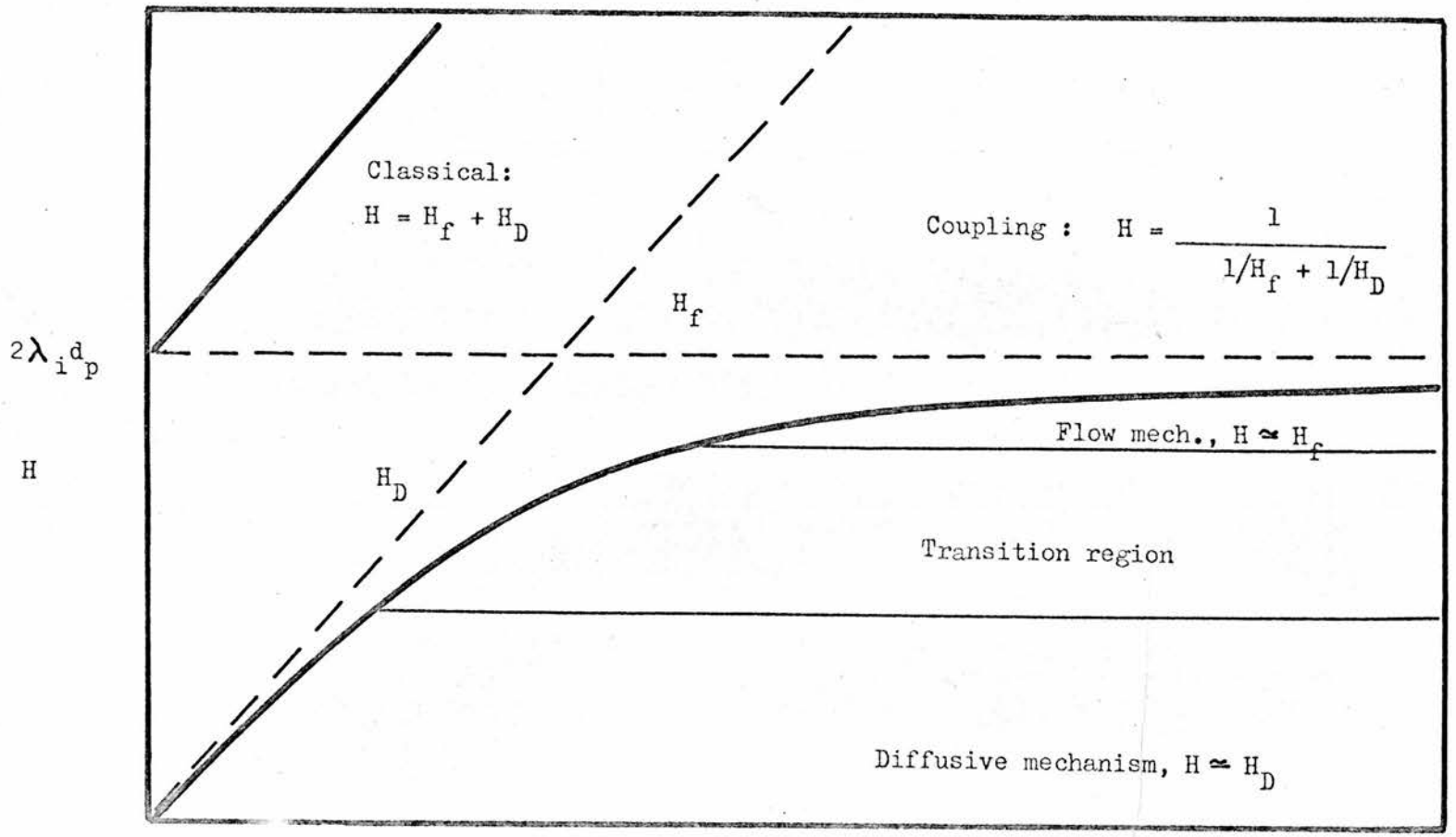

Figure 10 : Contrast between coupling and classical expressions for plate height as a function of velocity. The coupling H is always less than H_f and H_D while the classical H is always greater than either of these.

Fig. 10

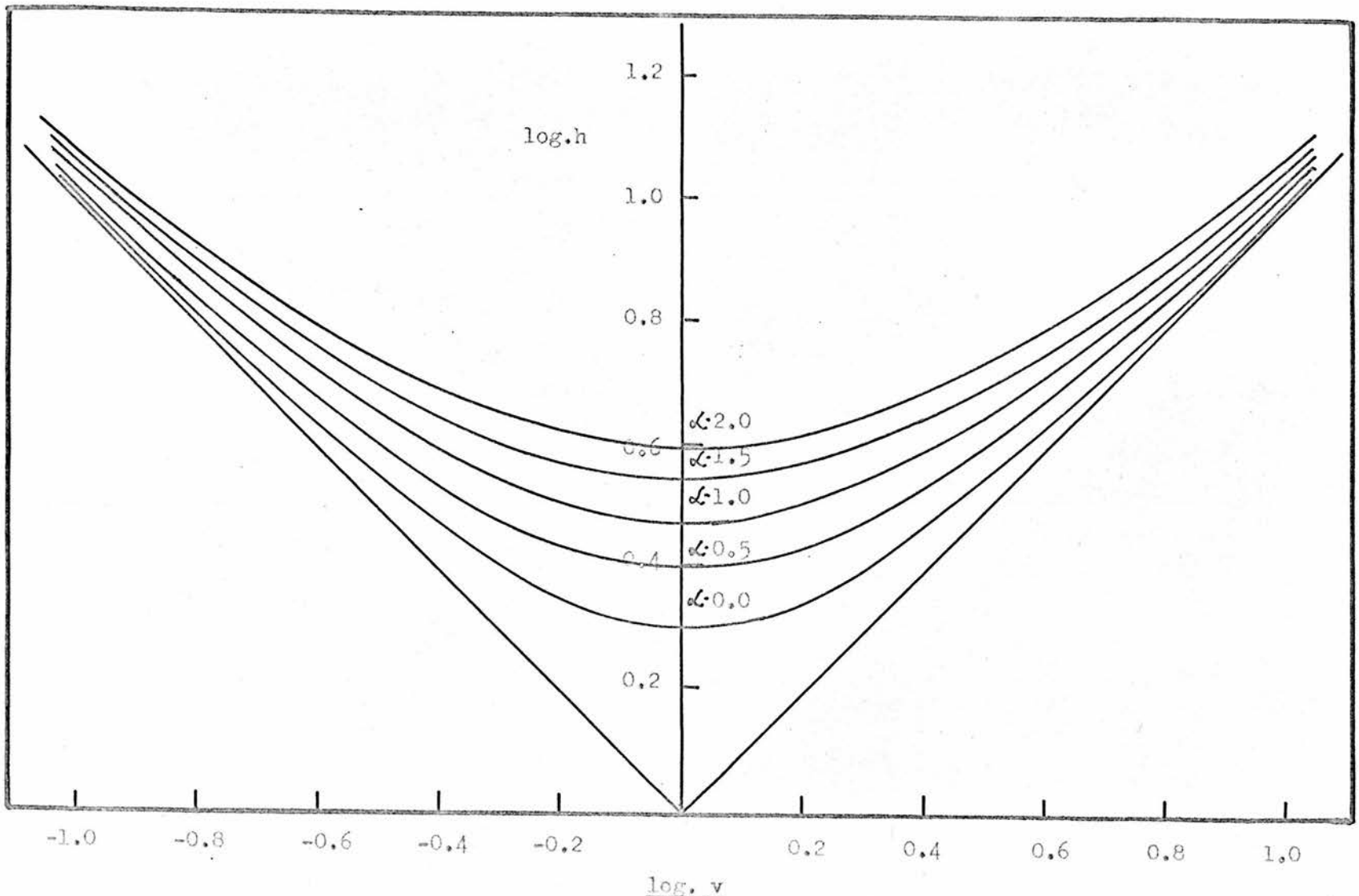

Figure 11 : Logarithmic plot of reduced H E T P against linear gas velocity, $h = v + \alpha + 1/v$ with various values of α.

Fig. 11

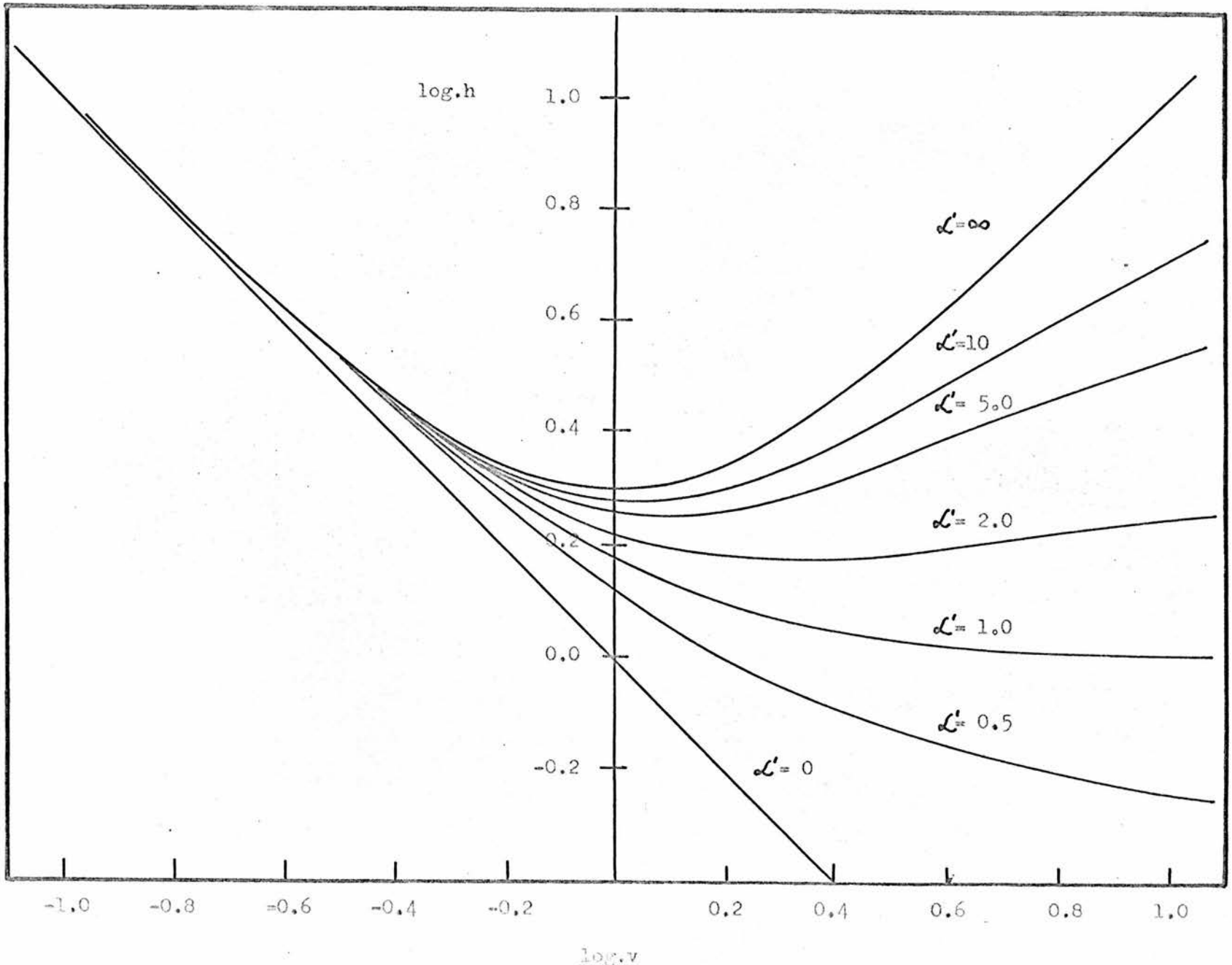

Fig. 12

Figure 12 : Logarithmic plot of reduced H E T P against reduced linear gas velocity, $h = 1/v + (1/\alpha' + 1/v)^{-1}$ with various values of α'

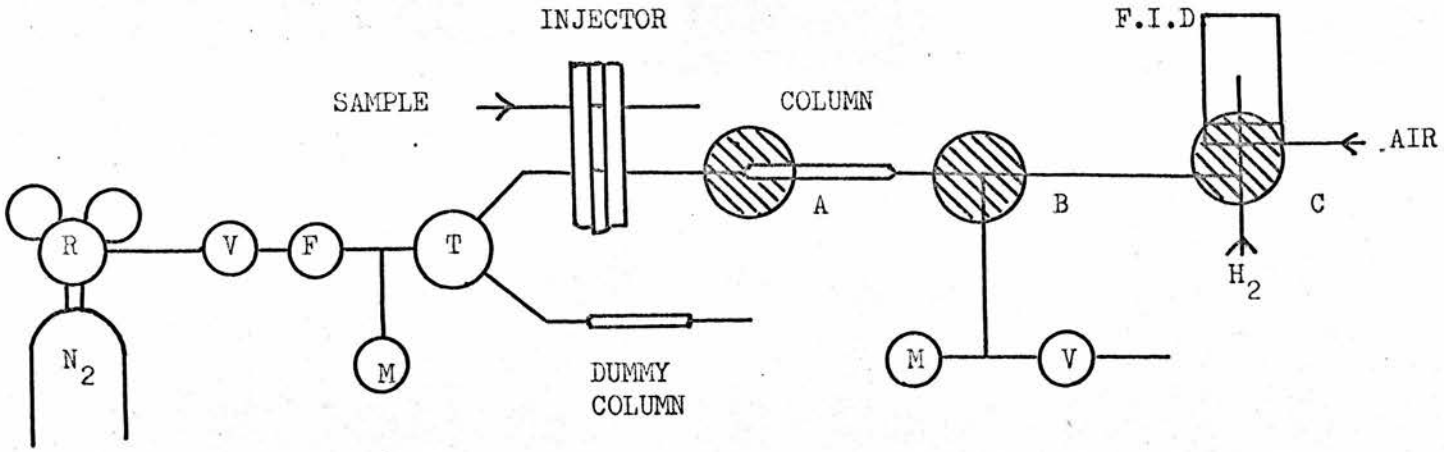

Figure 13 : Gas Line.

R : two-stage reducing valve and pressure regulator, V = needle valve, F = flow meter, M = manometer, T = two-way tap, F.I.D. = flame ionization detector. The dummy column was used in Section II work. A, B and C are described in figure 16.

Fig. 13

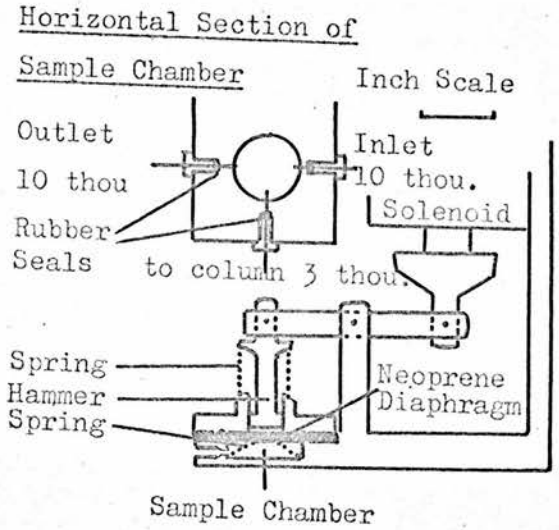

Figure: 14 Hammer Injector.

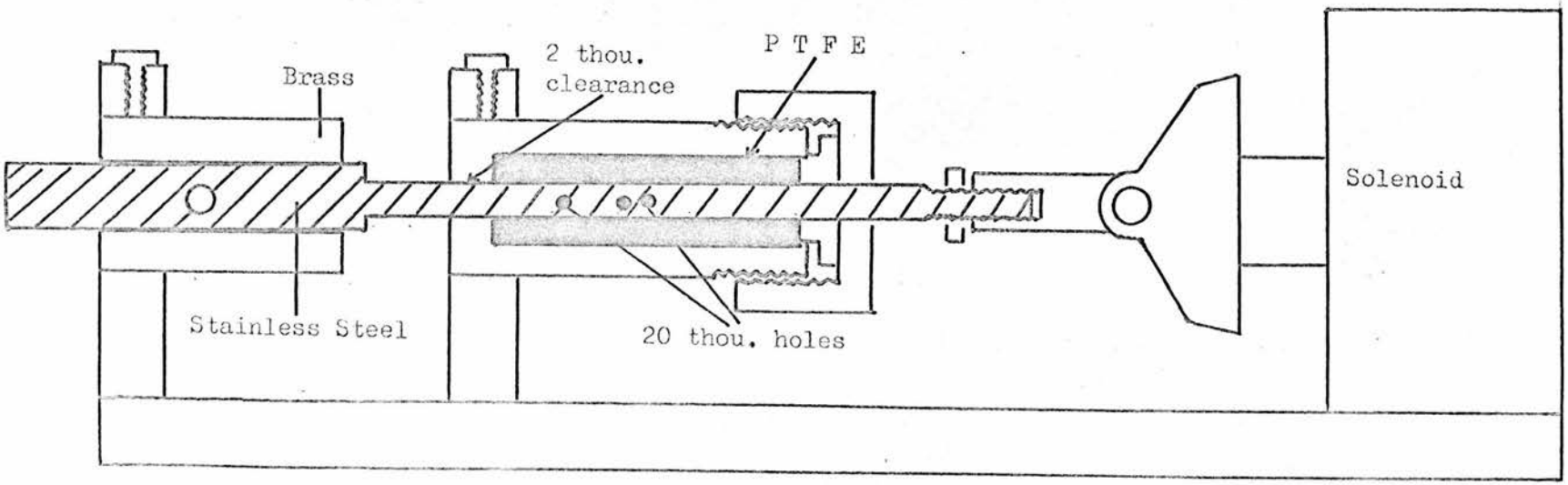

Figure 15 : Piston Injector (full scale)

Fig. 14 and 15

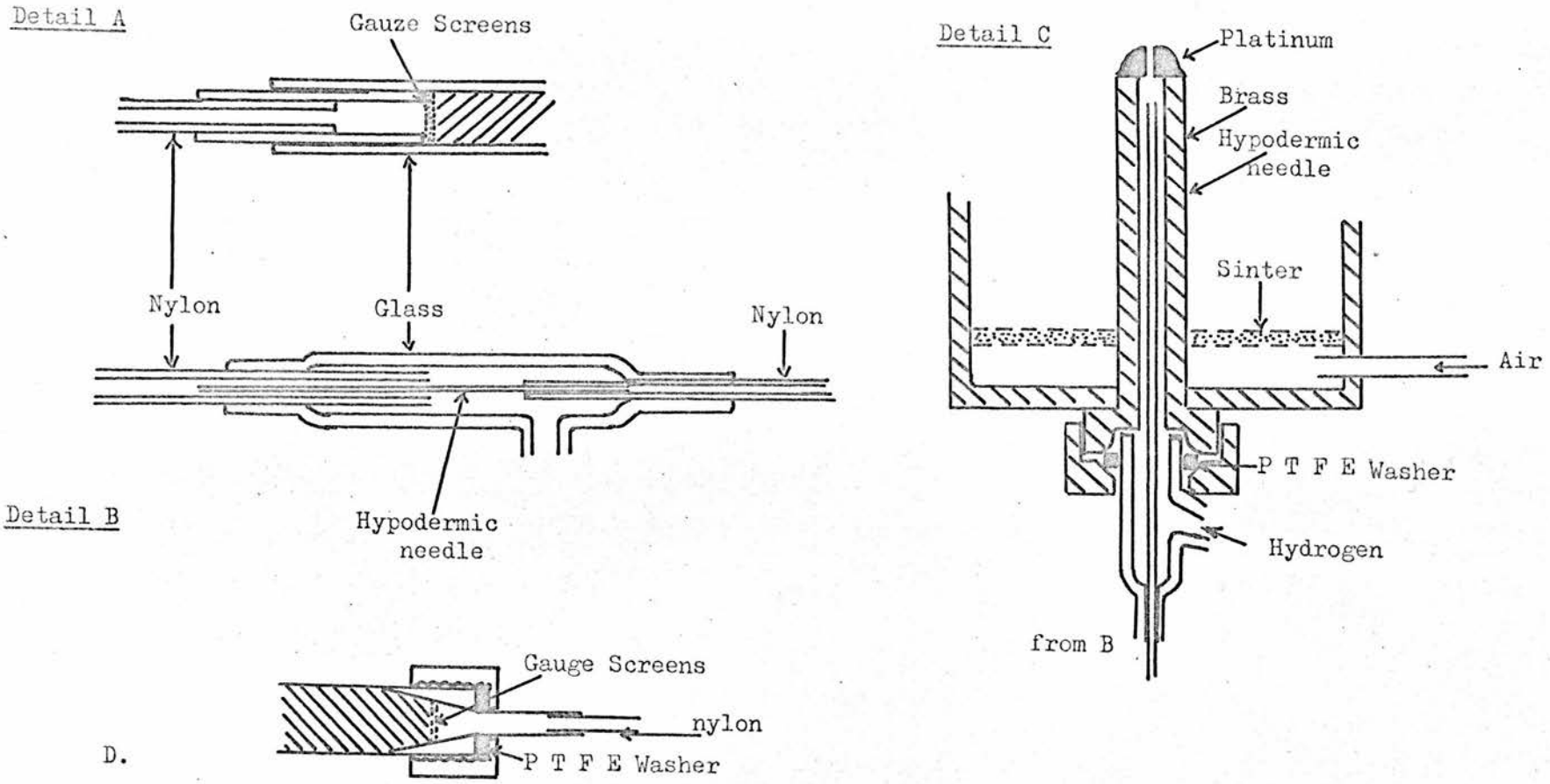

Figure 16 : Details of connections : Locations of A, B and C are shown on figure 13. Connection to stainless steel column is illustrated in D.

Fig. 16

Fig.17

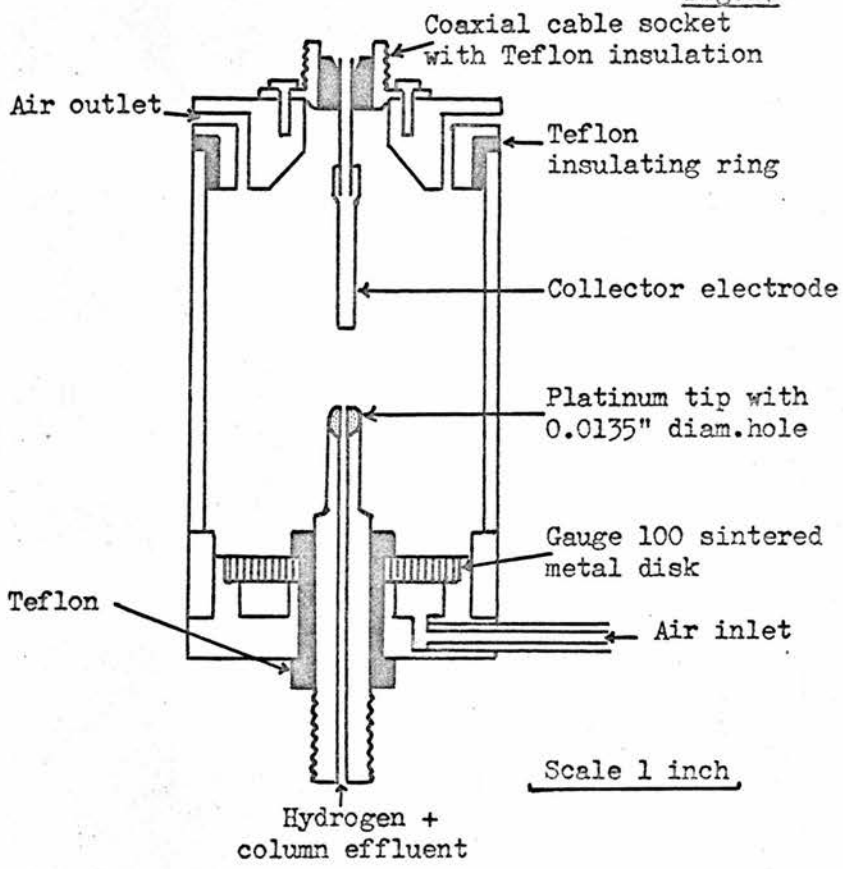

Flame Ionisation Detector

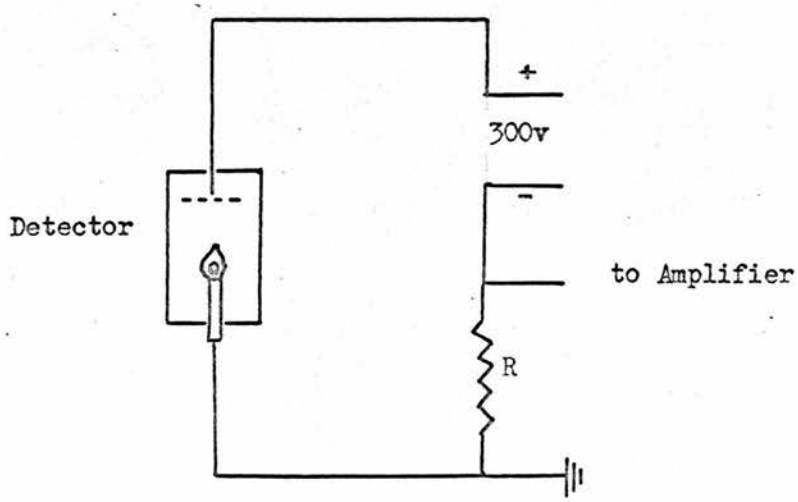

Figure 17 : The Flame Ionisation Detector and basic circuitry.

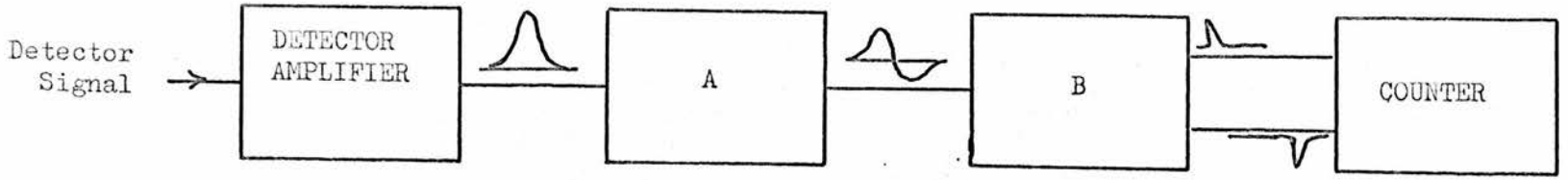

Figure 18 a :

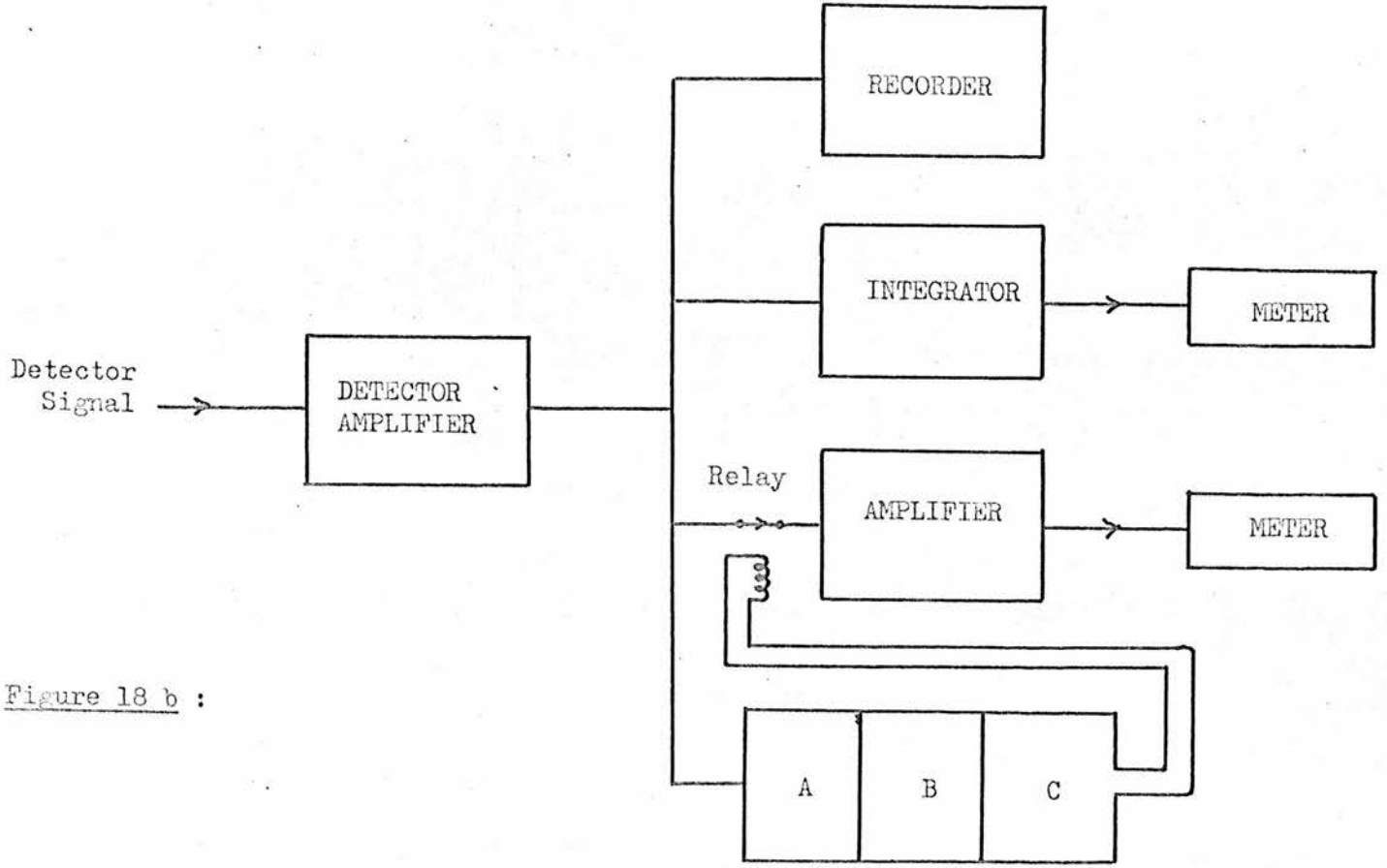

Figure 18 b :

Figure 18 : Block diagram of electronics : measurement of retention time (18a) and peak height and integral (18b)

Fig.18

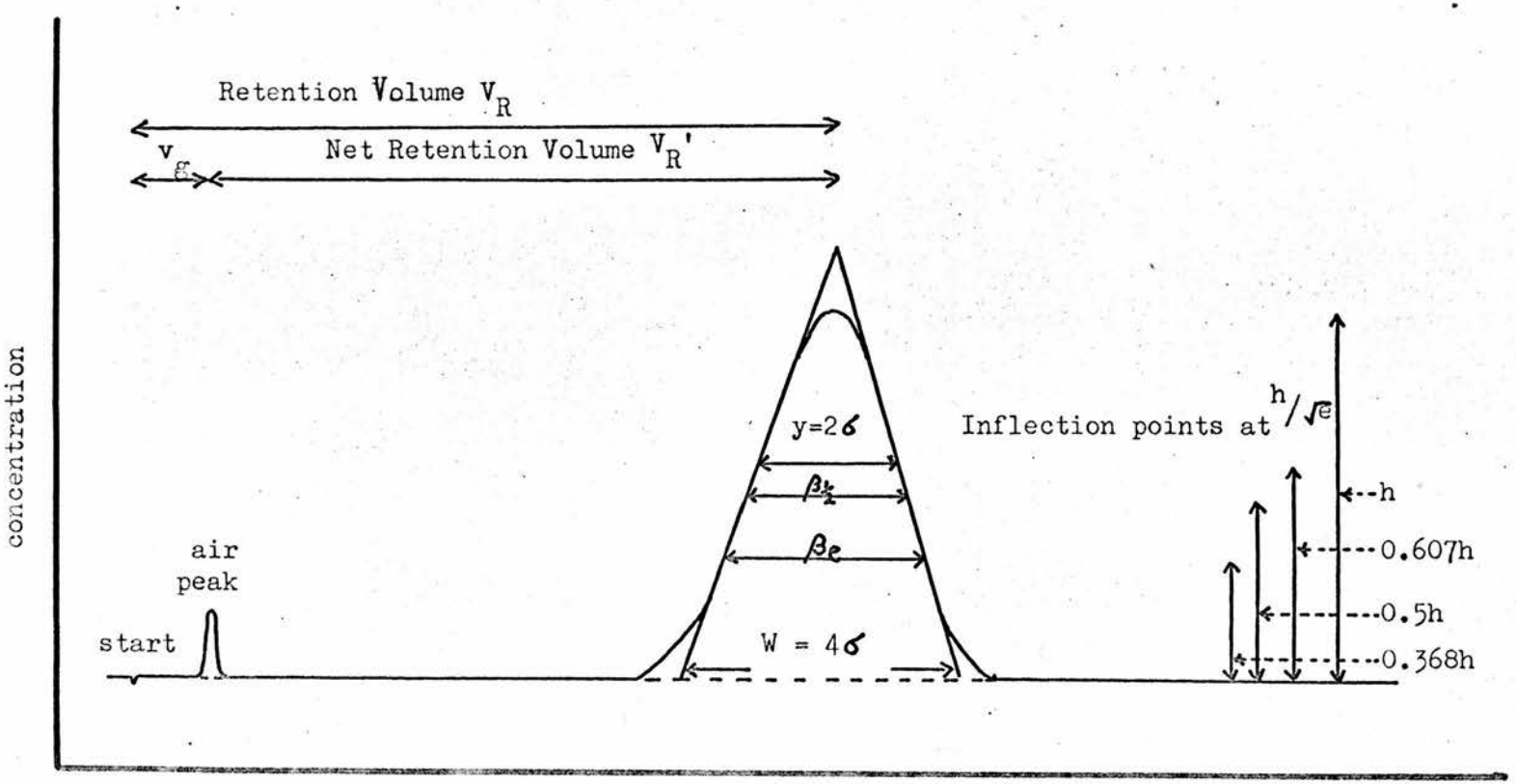

Volume of carrier gas passed (at column temperature and average pressure)

Figure 19: A typical air peak illustrating the main parameters of a chromatogram

Fig. 19

Fig. 20

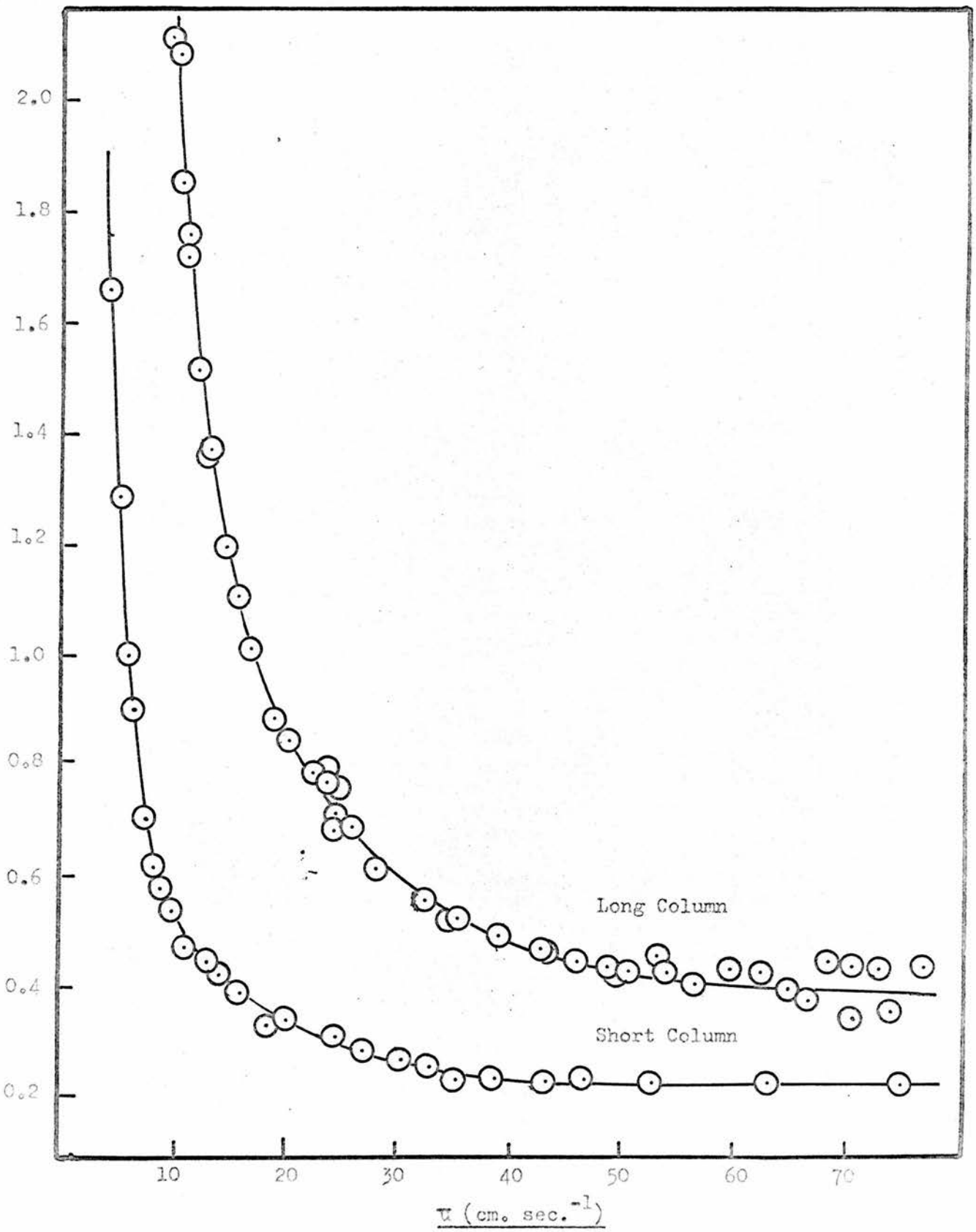

Figure 20 : Variation of peak width with average linear gas velocity for long and short capillary columns.

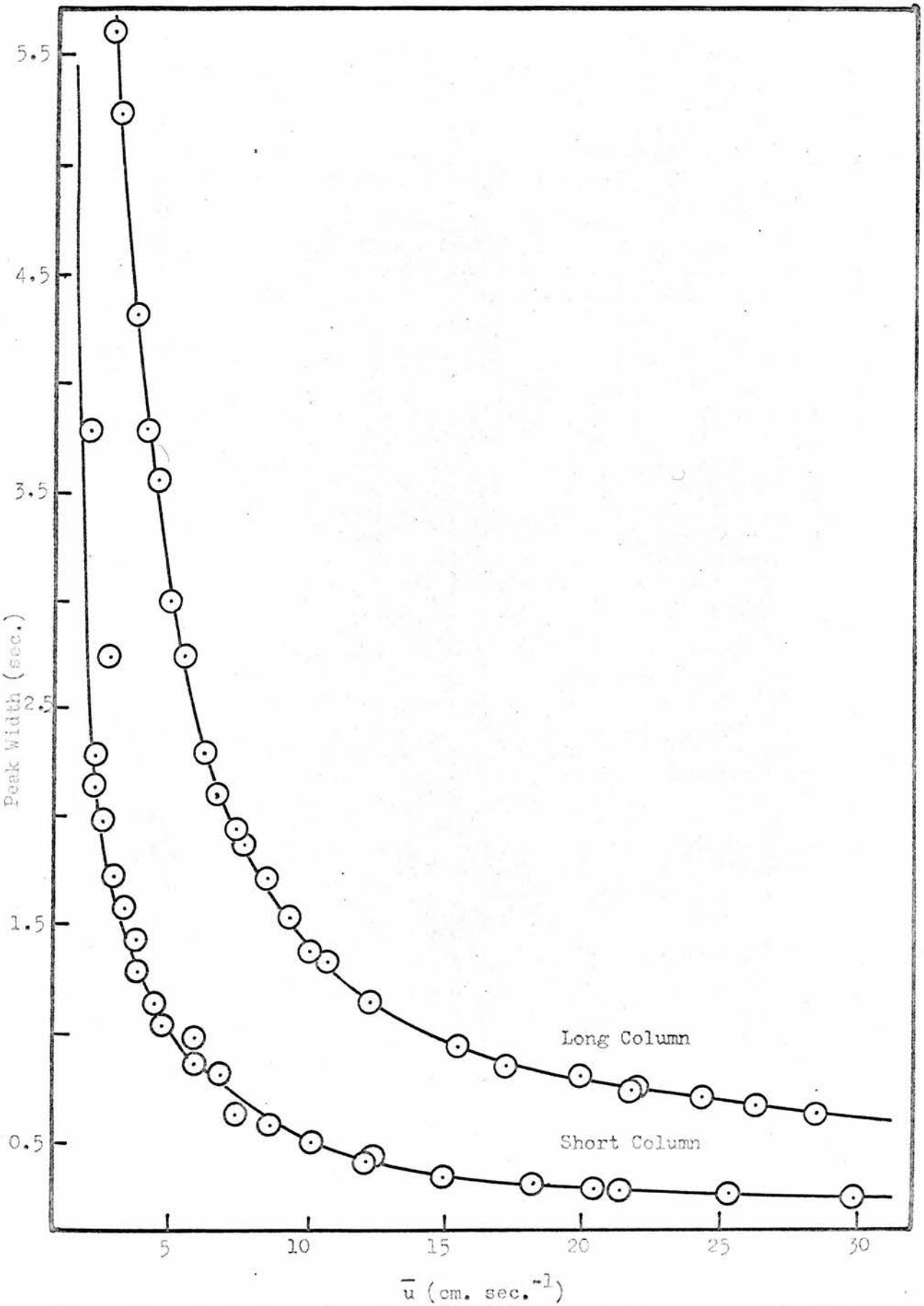

Figure 21 : Variation of peak width with average linear gas velocity for long and short packed columns.

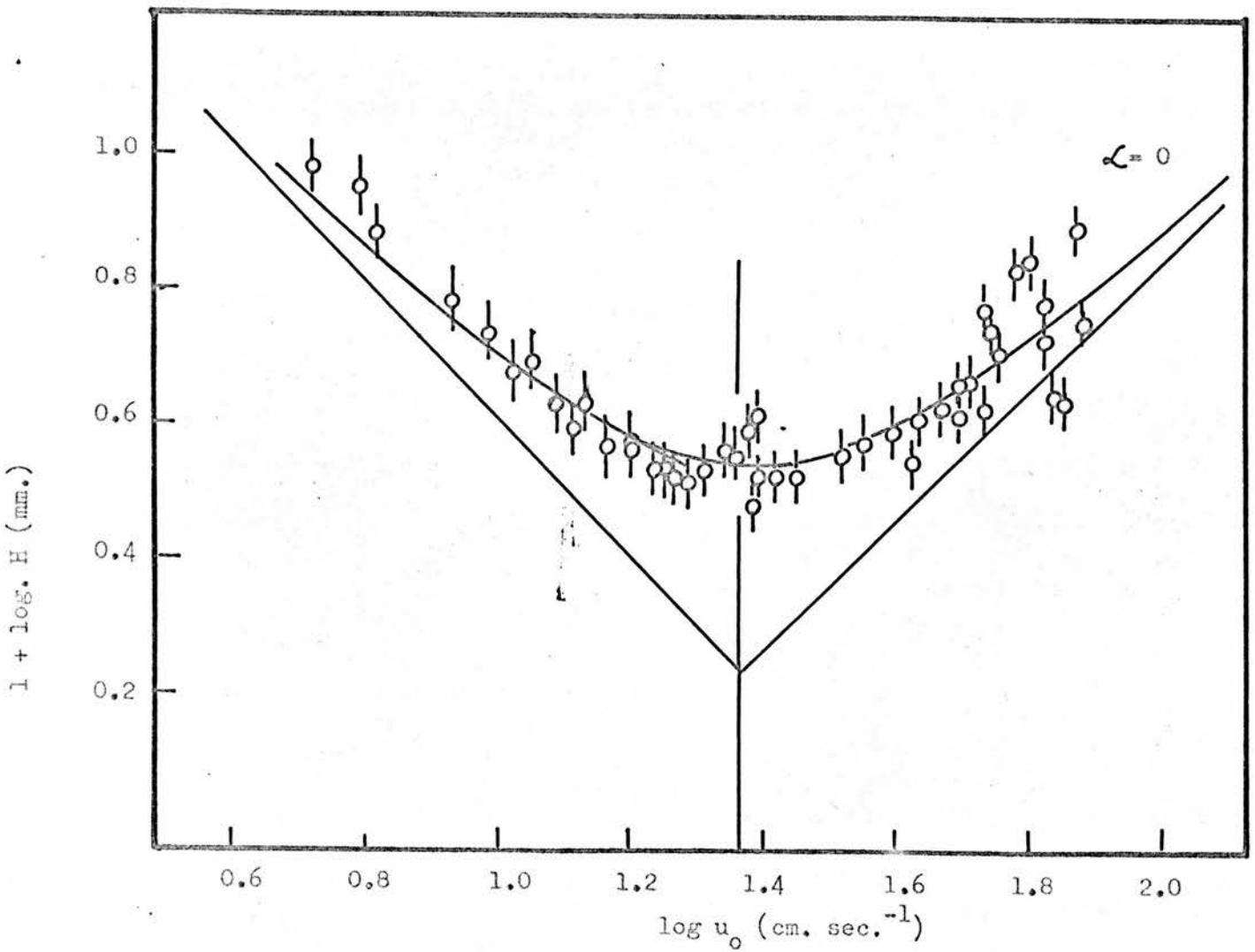

Figure 22 : Logarithmic plot of H E T P against u_o for capillary column.

Fig. 22

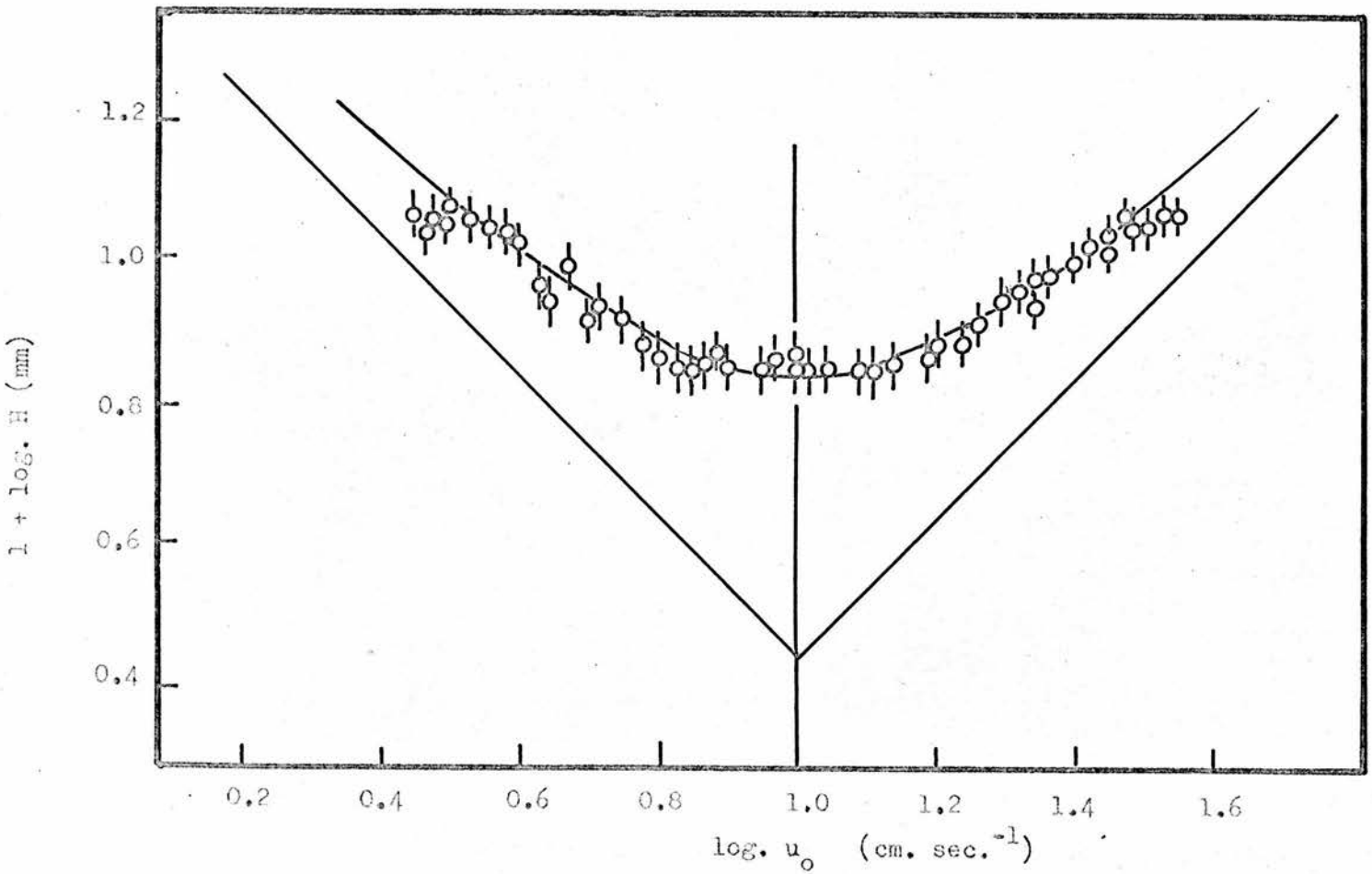

Figure 23 : Logarithmic plot of H E T P against u_o for packed column.

Fig. 23

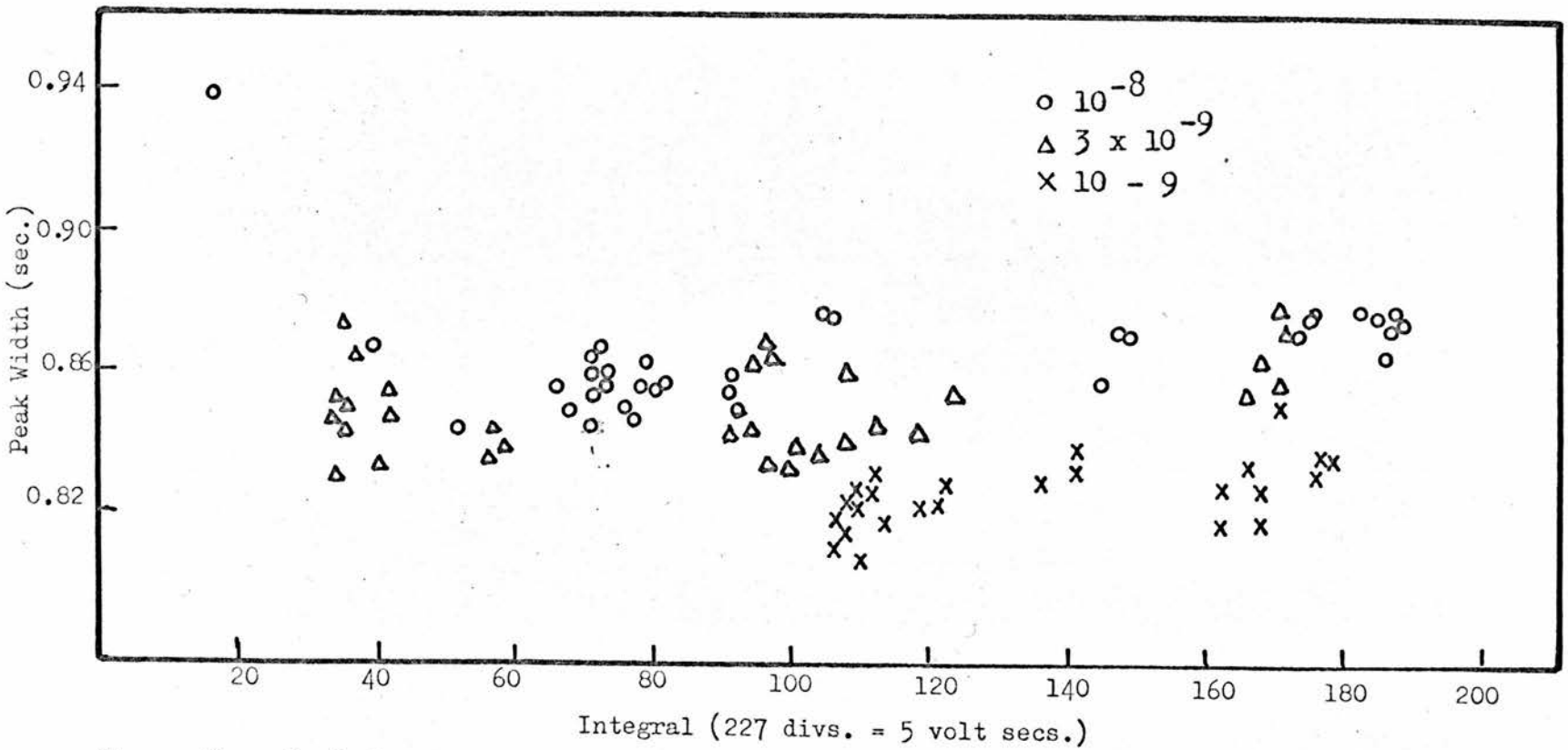

Figure 24 : Variation of peak width with integral on three amplifier ranges.

Fig 24.

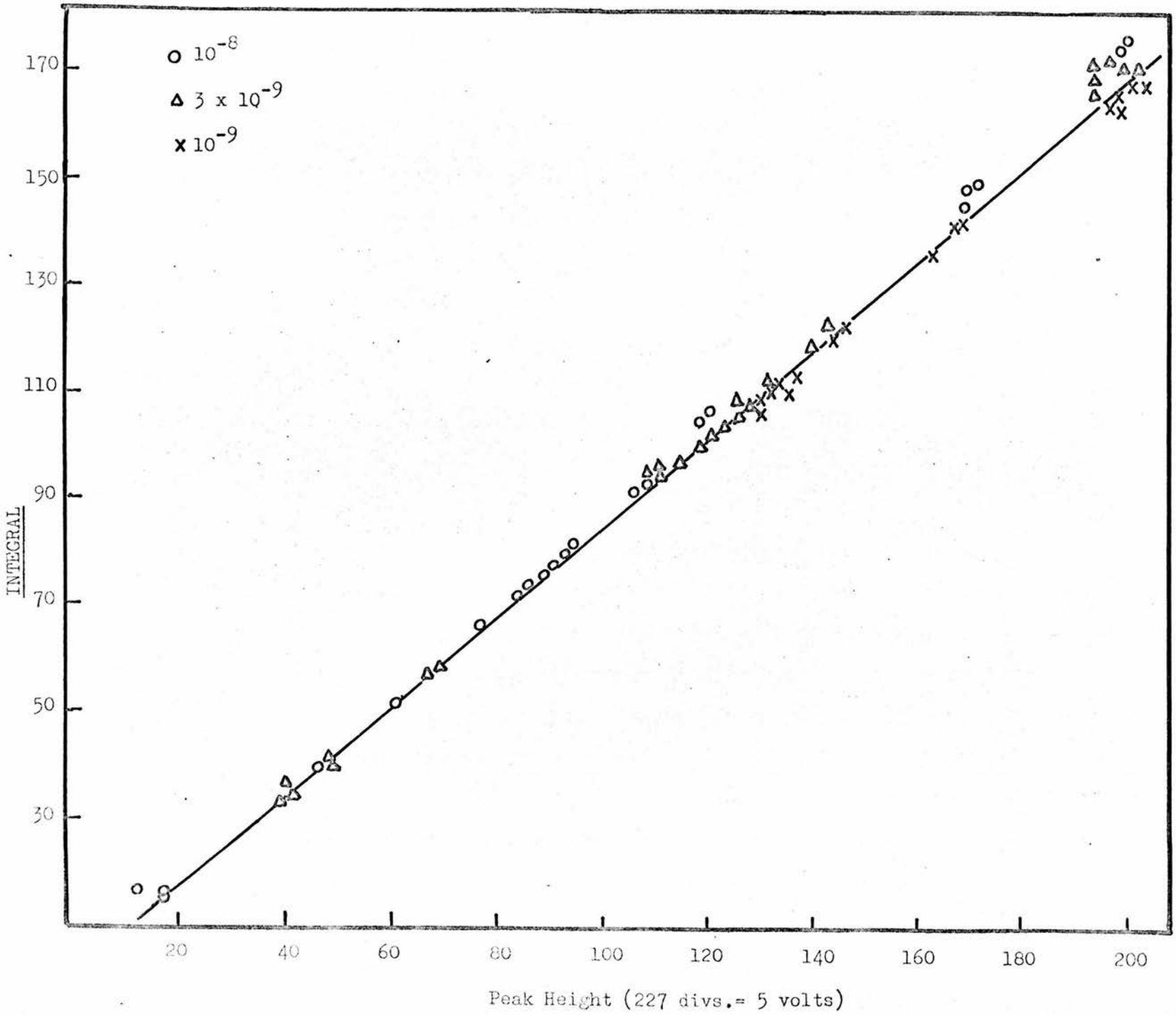

Figure 25: Variation of Integral with peak height on 3 ranges of the amplifier

Fig. 25

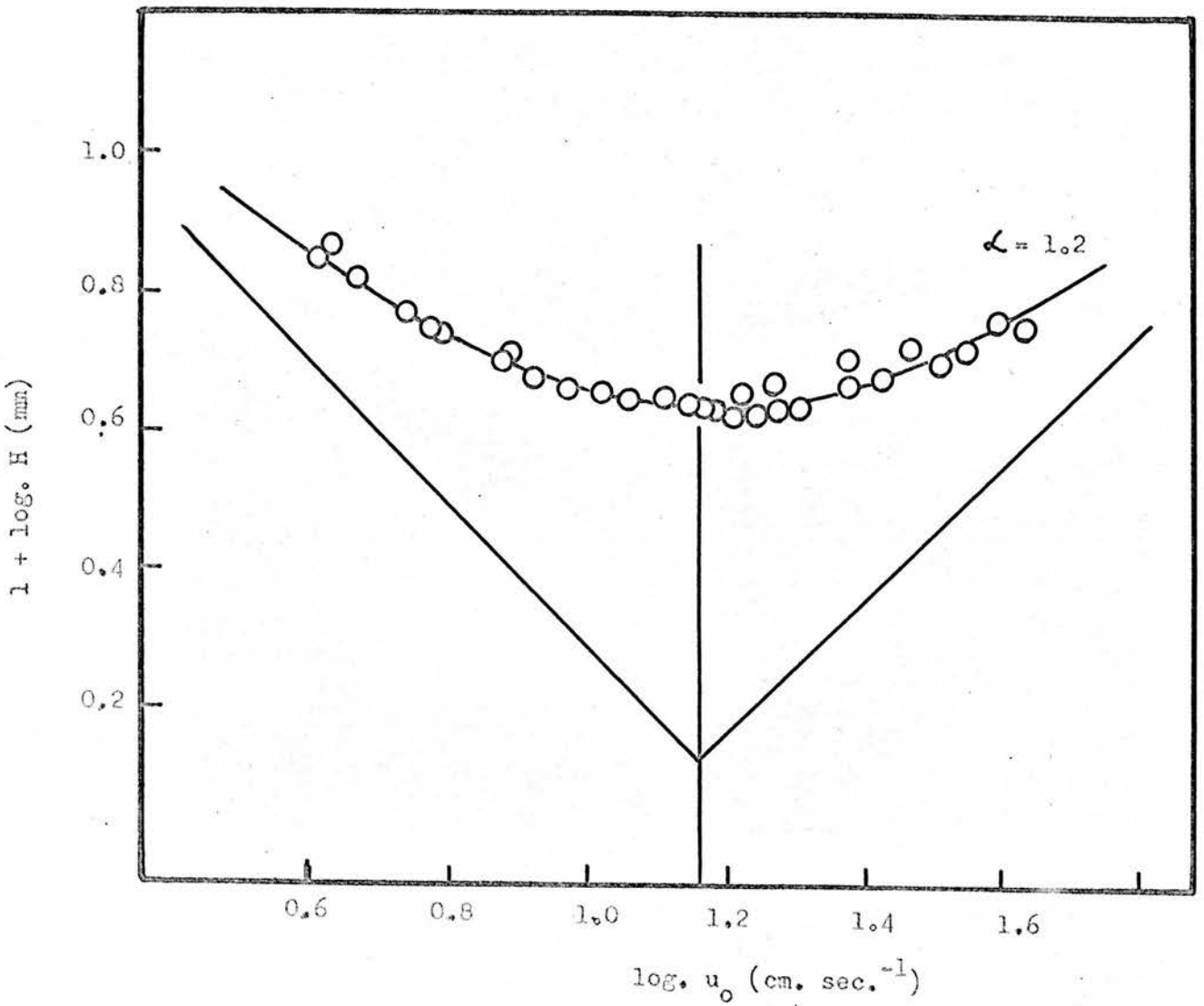

Figure 26 : Logarithmic plot of H E T P against u_o for packed column.

Fig. 26

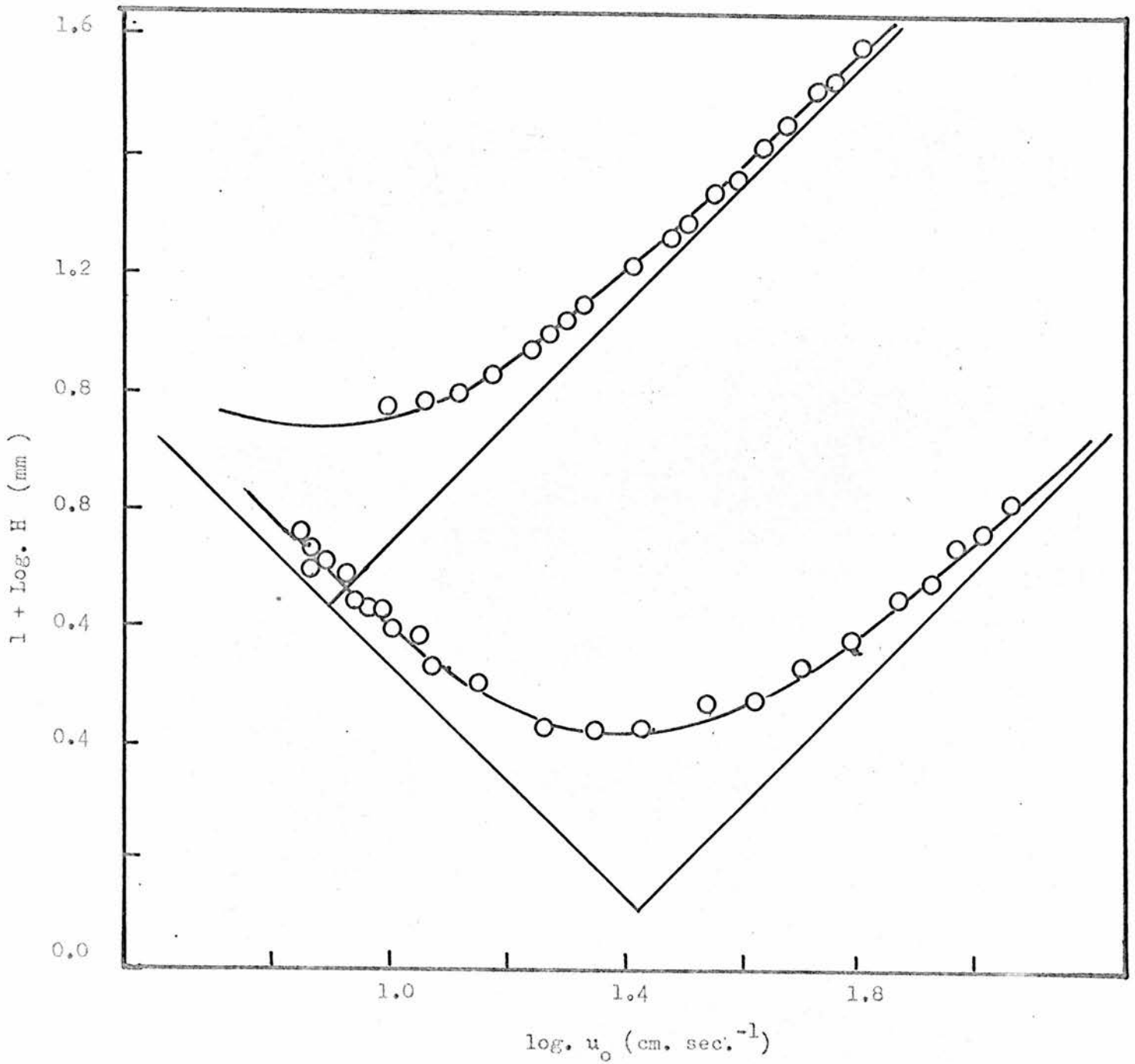

Figure 27 : Logarithmic plot of H E T P against u_o for open, tubular columns.

Fig. 27

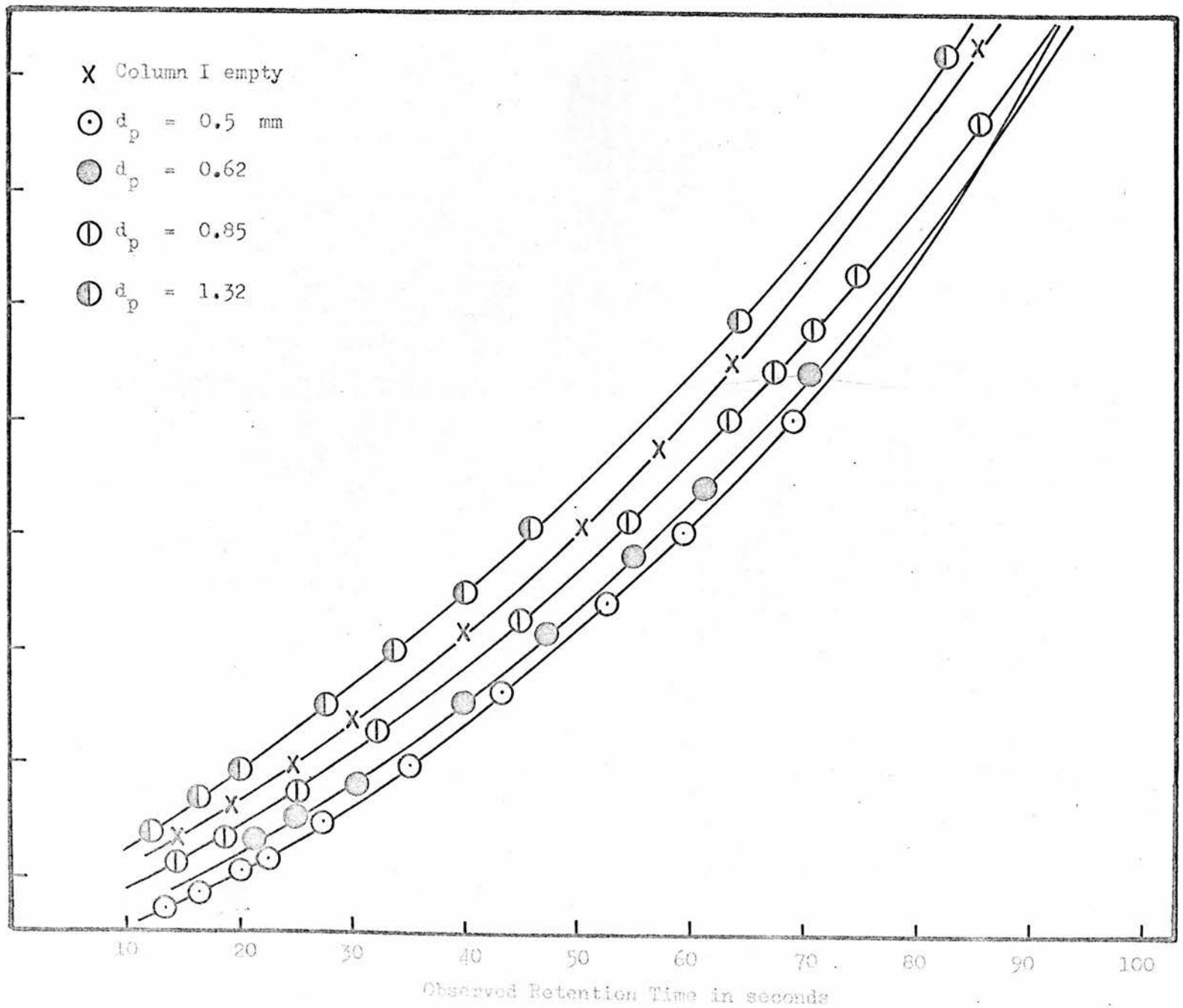

Fig. 28

Figure 28 : Plot of peak width against retention time for column I for different d_p values.

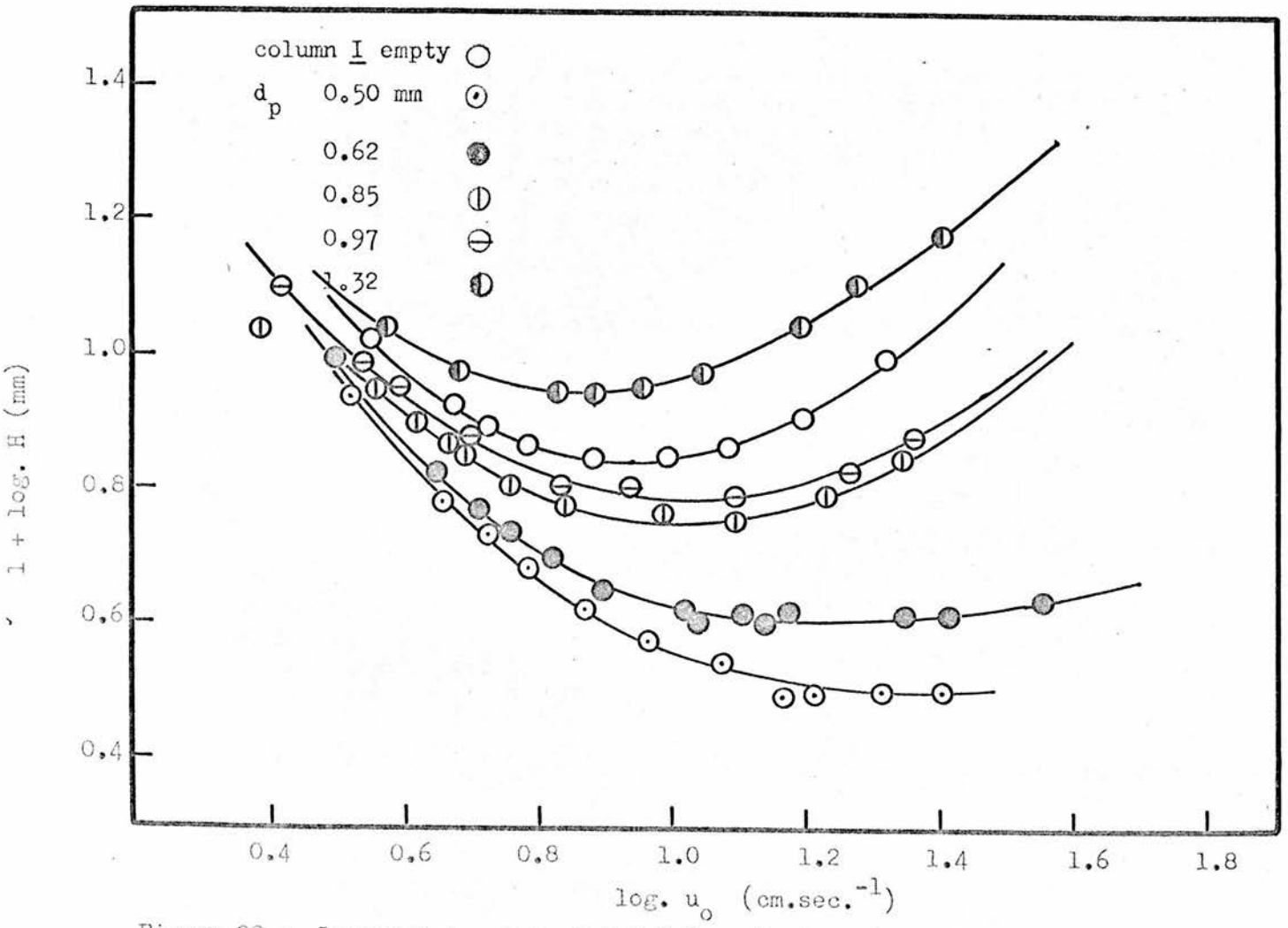

Figure 29 : Logarithmic plot of H E T P against u_o for column I for different particle diameters.

Fig. 29

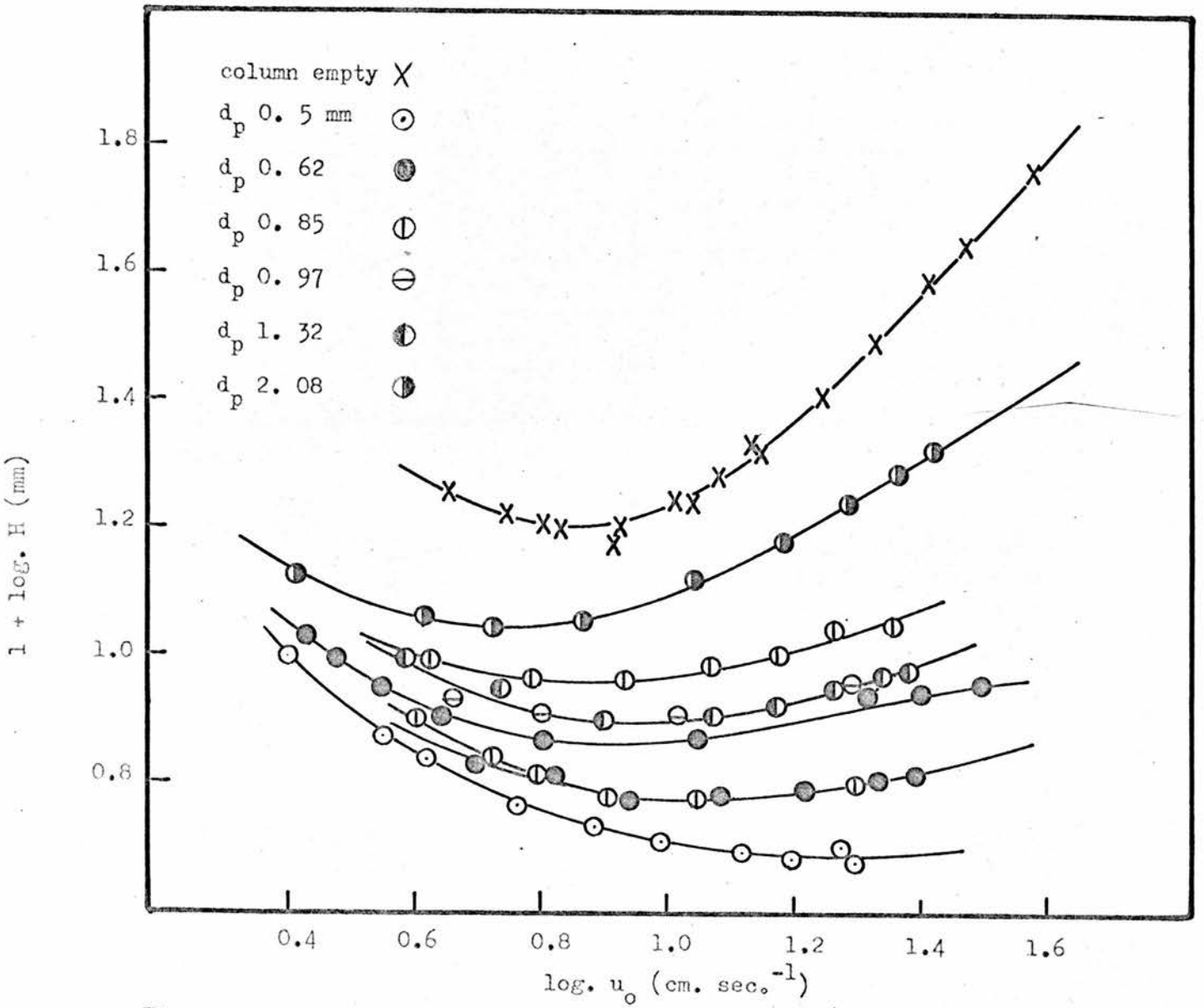

Figure 30 : Logarithmic plot of H E T P against outlet linear gas velocity for column II for different particle diameters.

Fig. 30

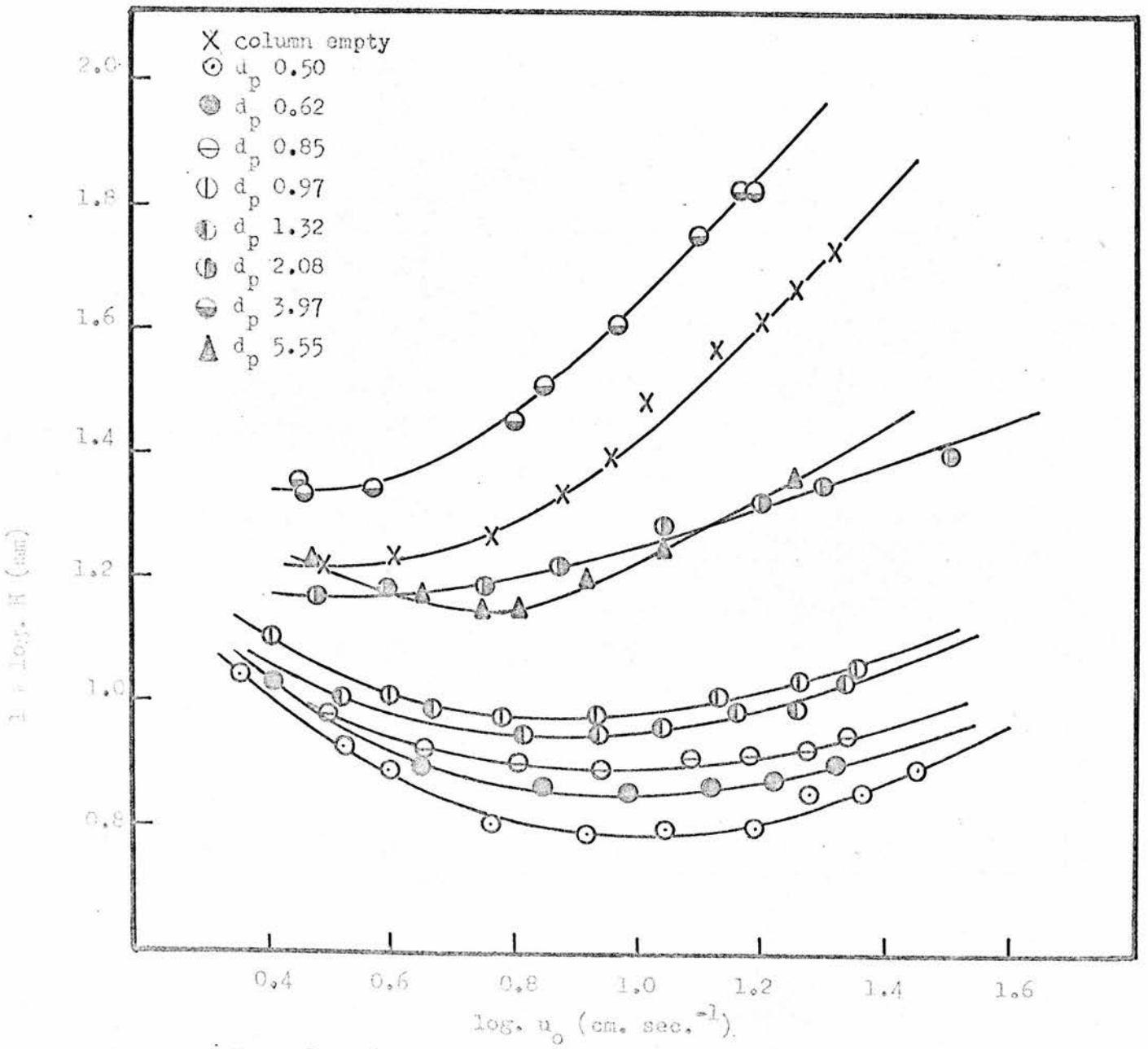

Figure 31 : Logarithmic plot of H E T P against outlet linear gas velocity for column III for different particle diameters.

Fig. 31

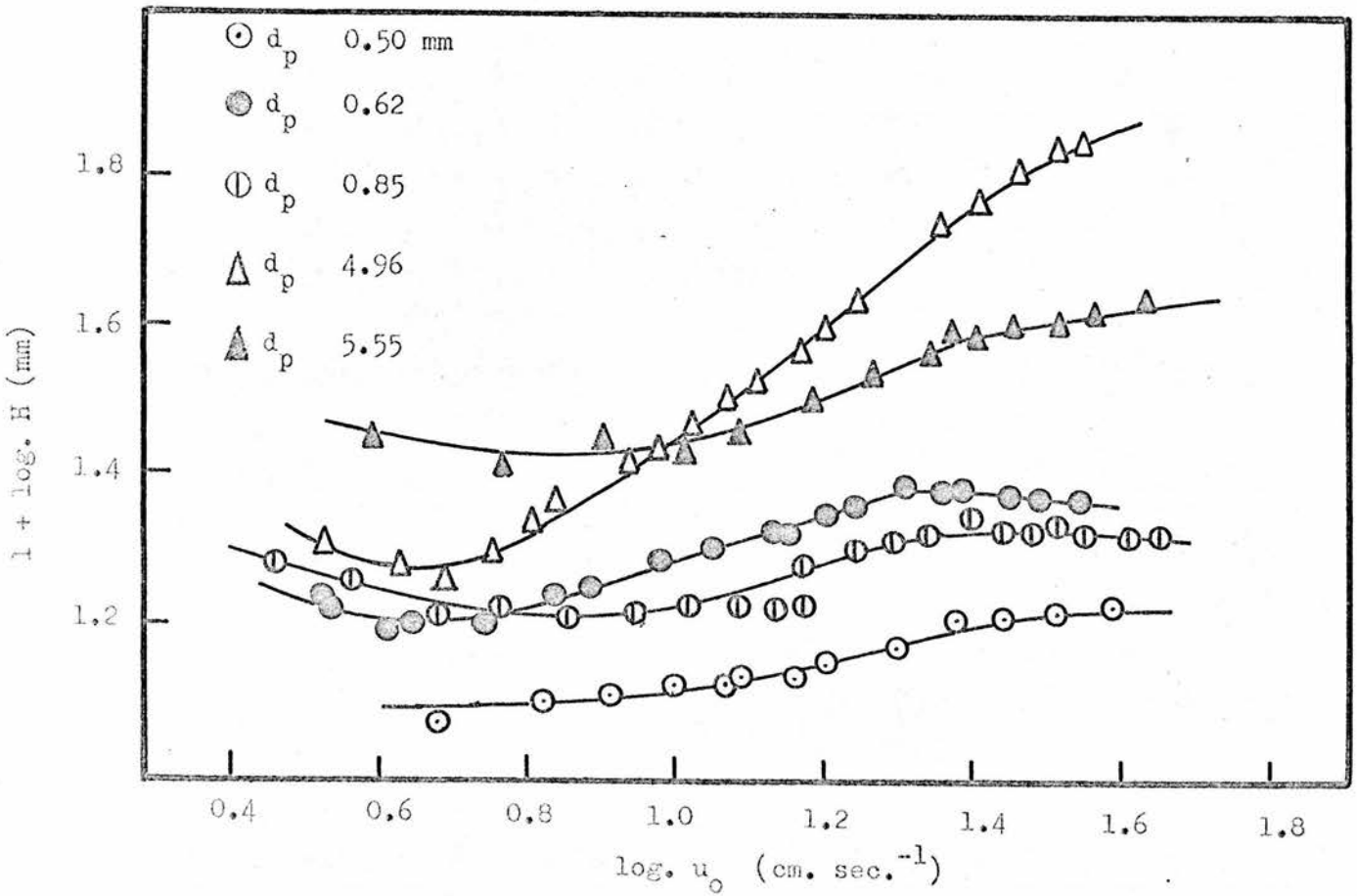

Figure 32 : Logarithmic plot of H E T P against u_o for column IV for different particle diameters.

Fig. 32

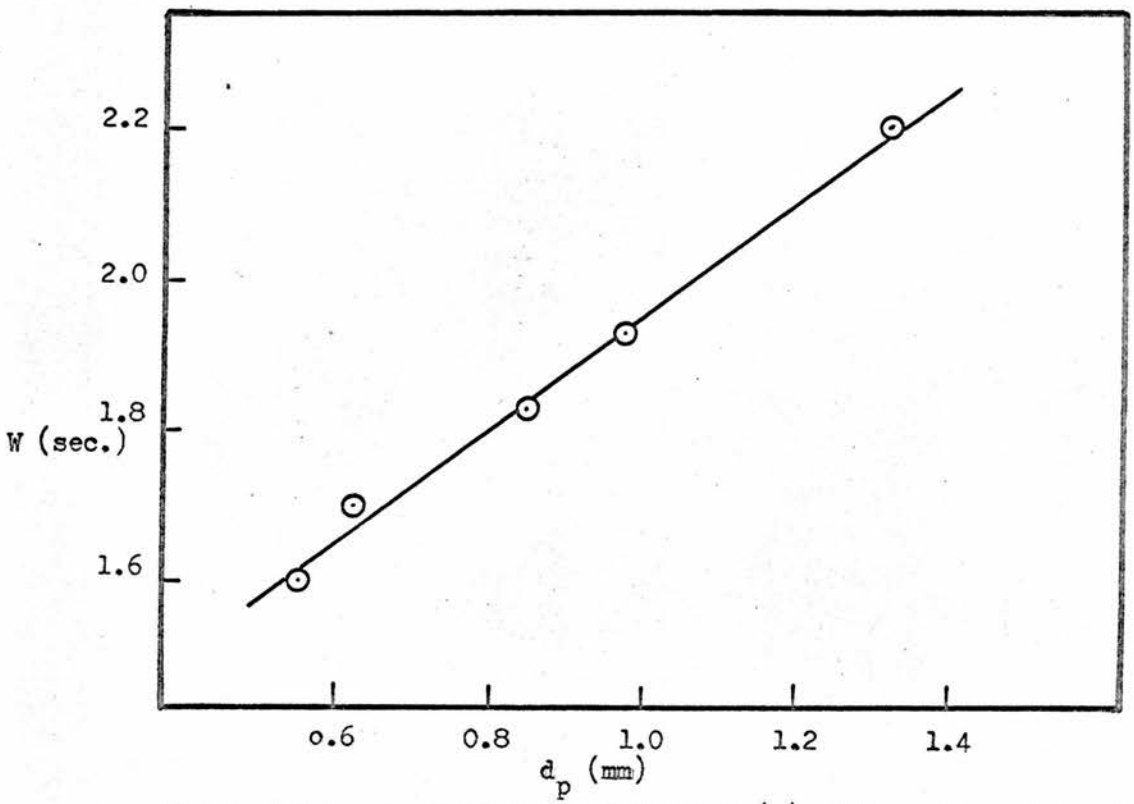

Figure 33a : Variation of peak width (W) with particle diameter for column I at a fixed retention time (50 secs.)

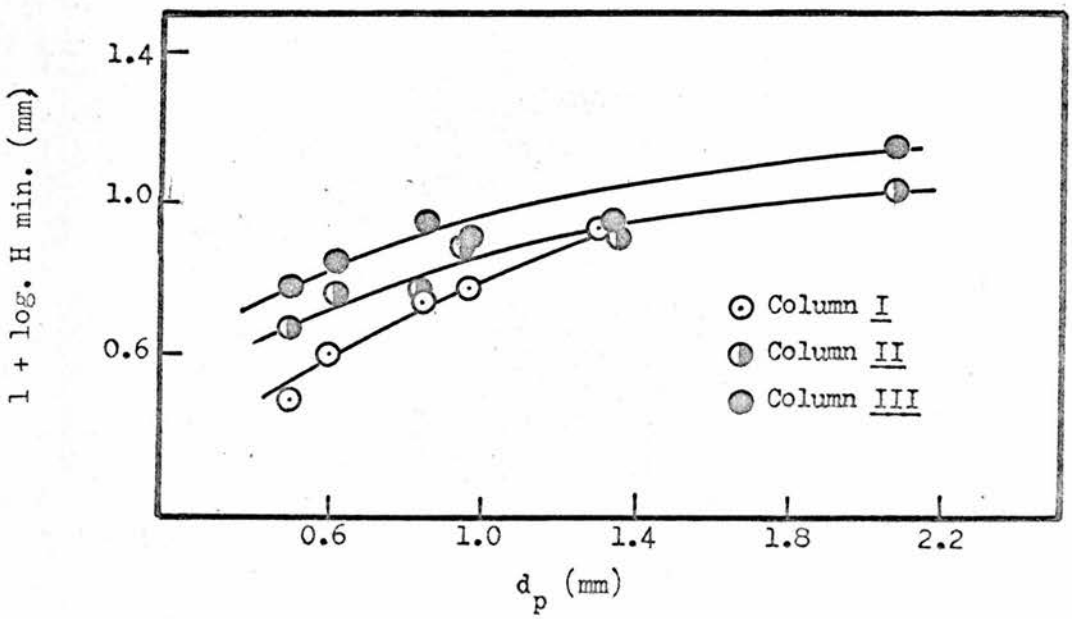

Figure 33b : Dependence of log. H min. on particle diameter.

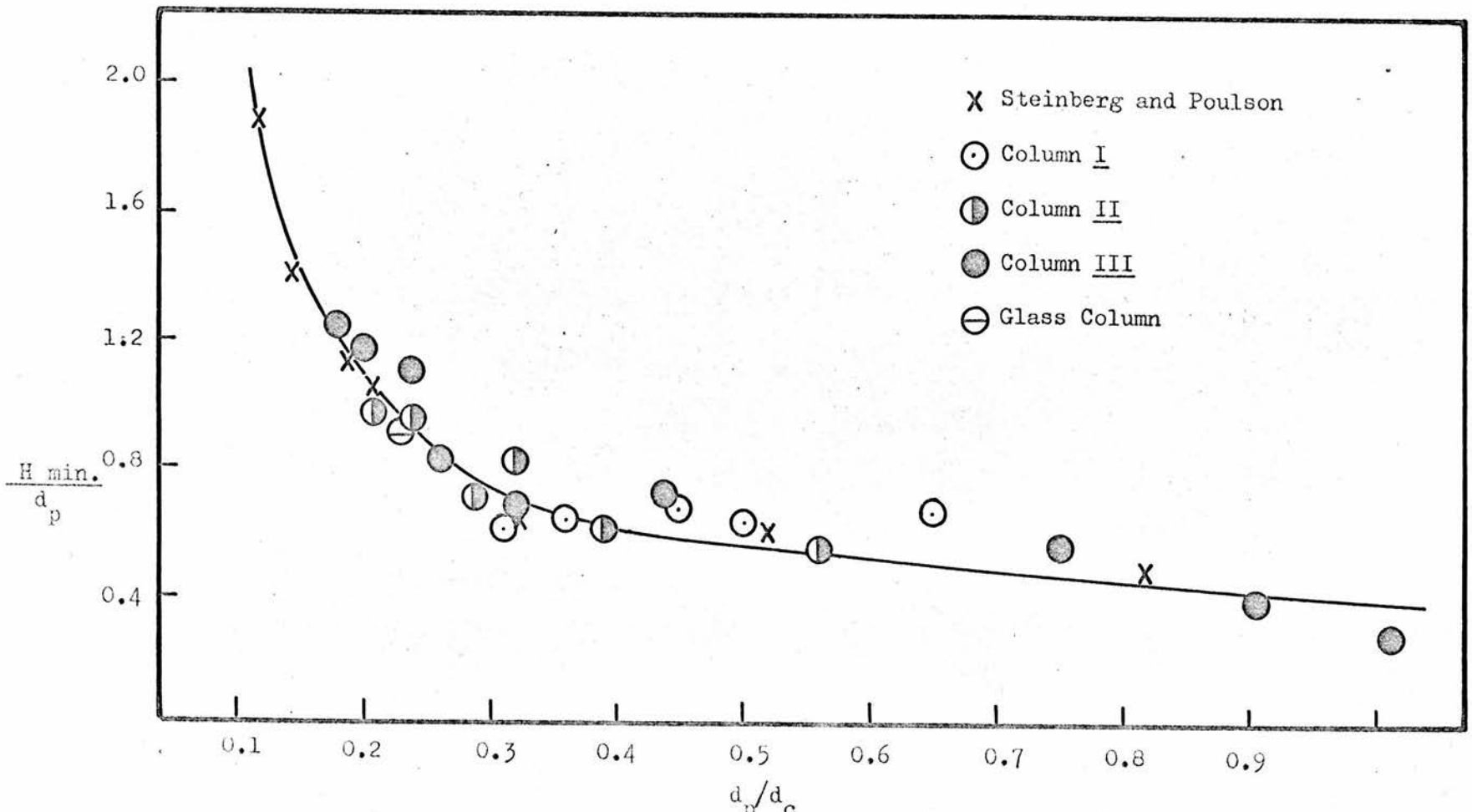

Figure 34 : Dependence of plate height upon particle - to - column diameter ratio.

Fig. 34

Fig. 35

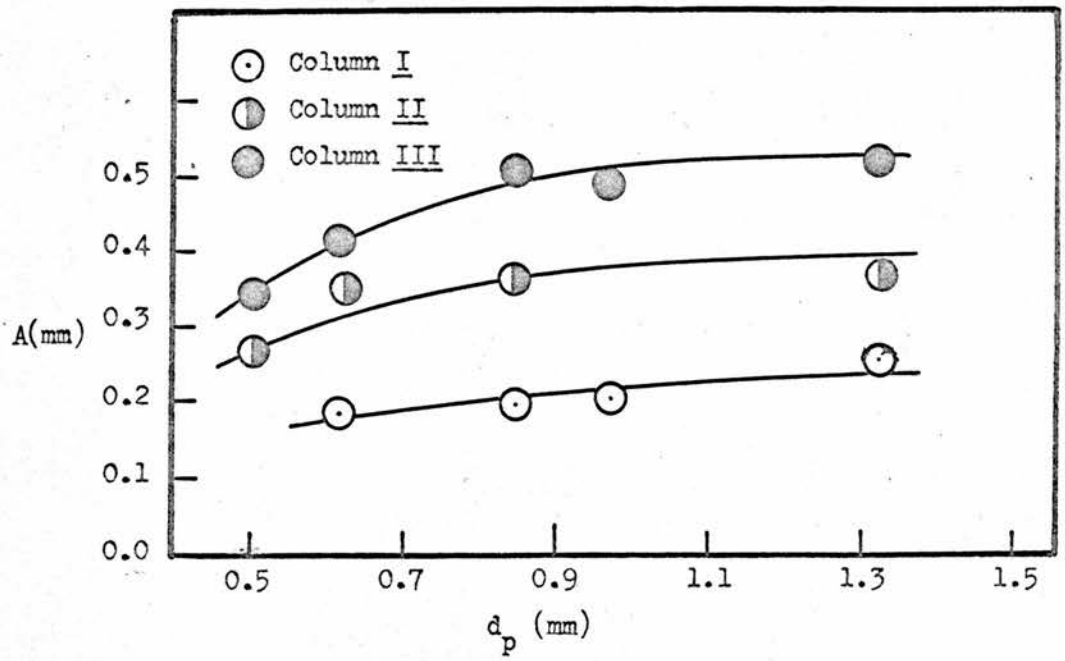

Figure 35a

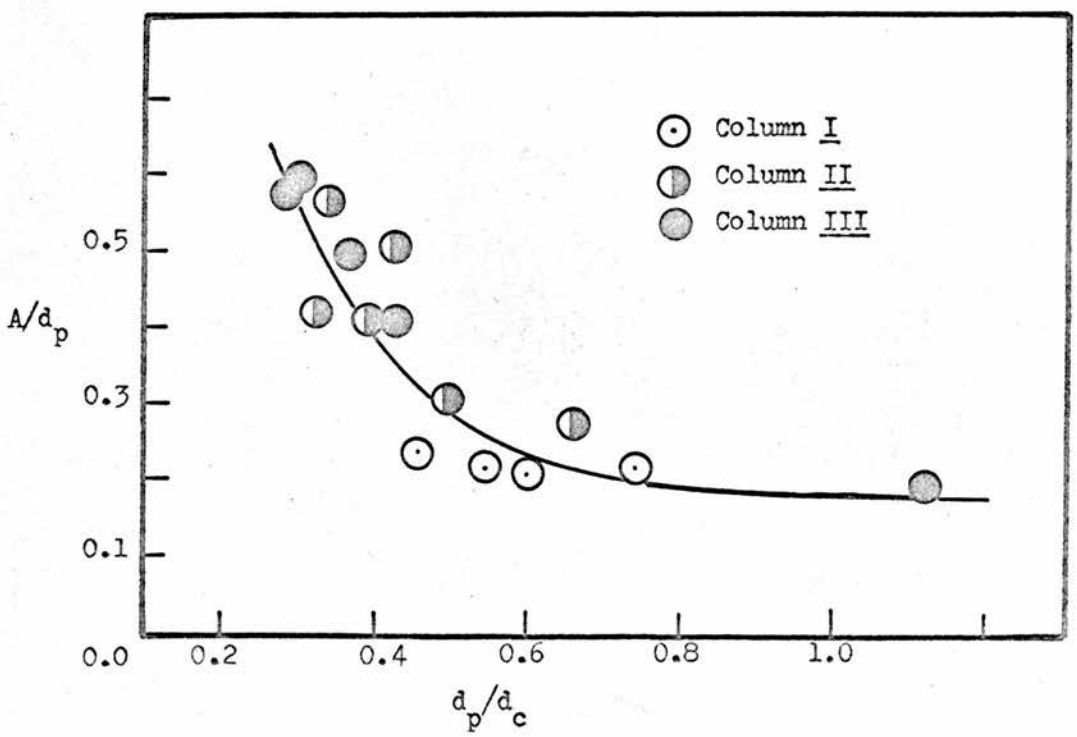

Figure 35b

Figure 35 : Variation of eddy diffusion with particle diameter (35a) and particle - to - column diameter ratio (35b).

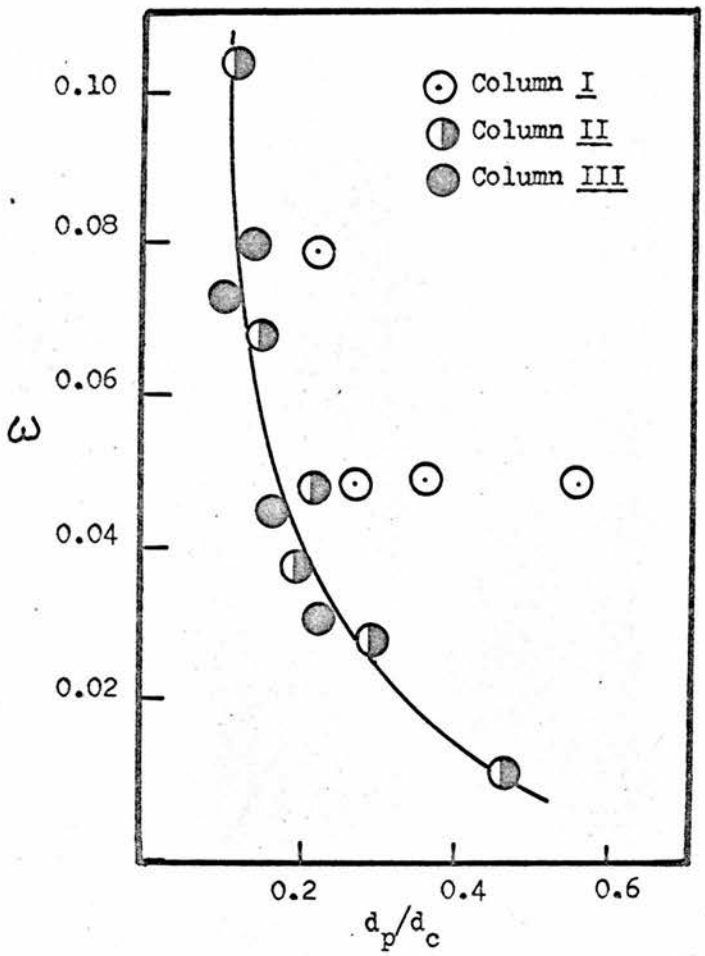

Figure 36 : Effect of particle - to - column diameter ratio on gas phase mass transfer.

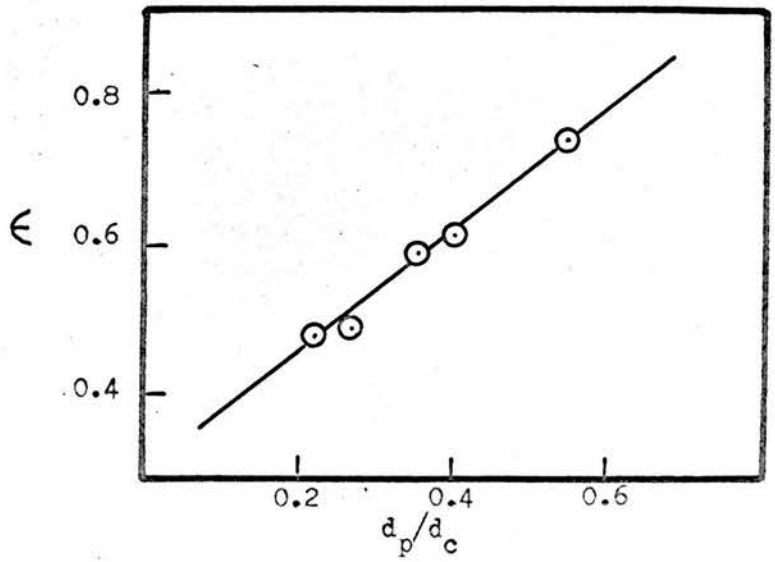

Figure 37 : Dependence of porosity on particle - to - column diameter ratio.

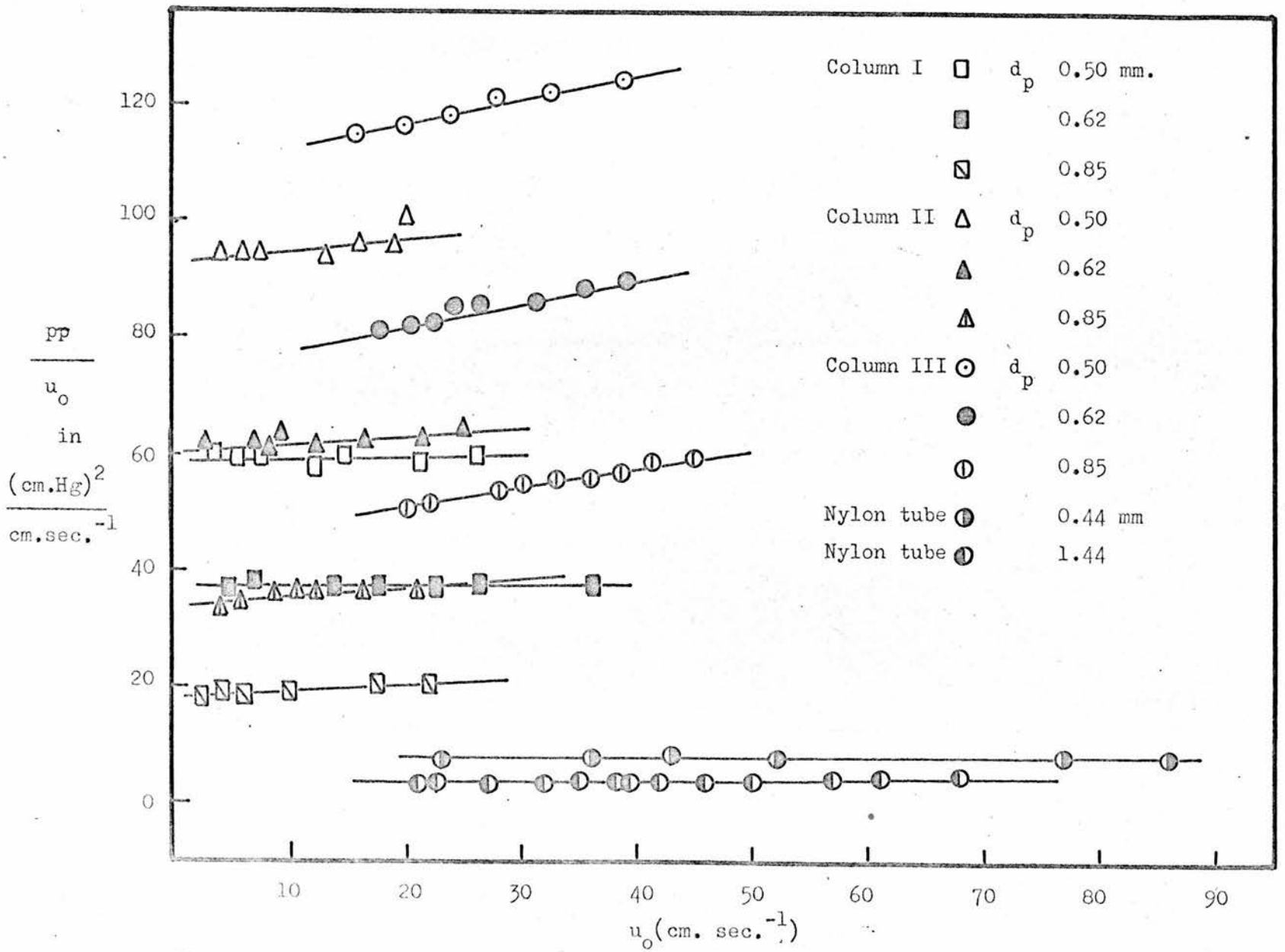

Figure 38 : Evidence for turbulence from flow data.

Fig. 38

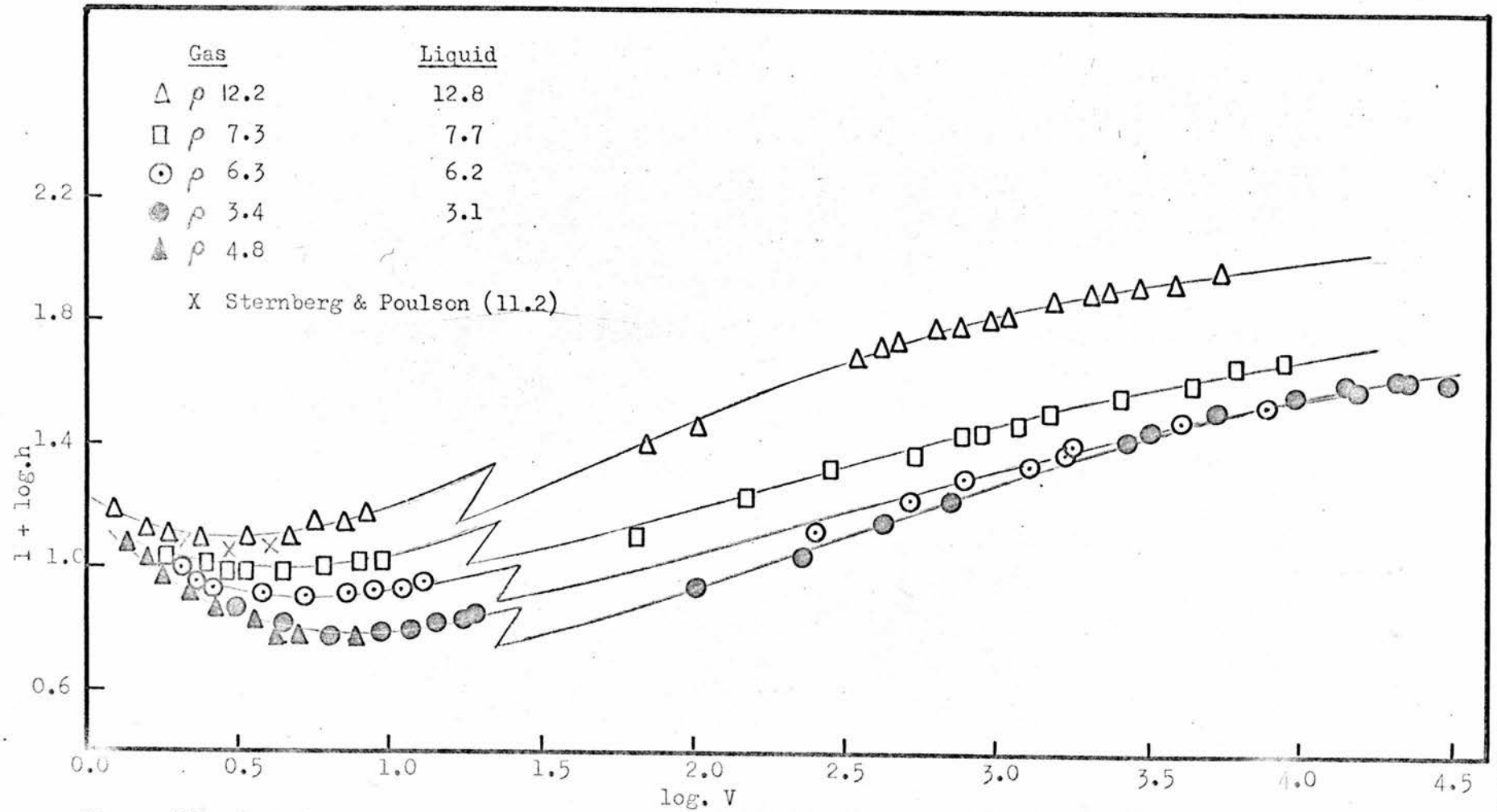

Fig. 39

Figure 39 : Logarithmic plot of reduced plate height against reduced gas velocity for gas and liquid systems: effect of column - to - particle diameter ratio.

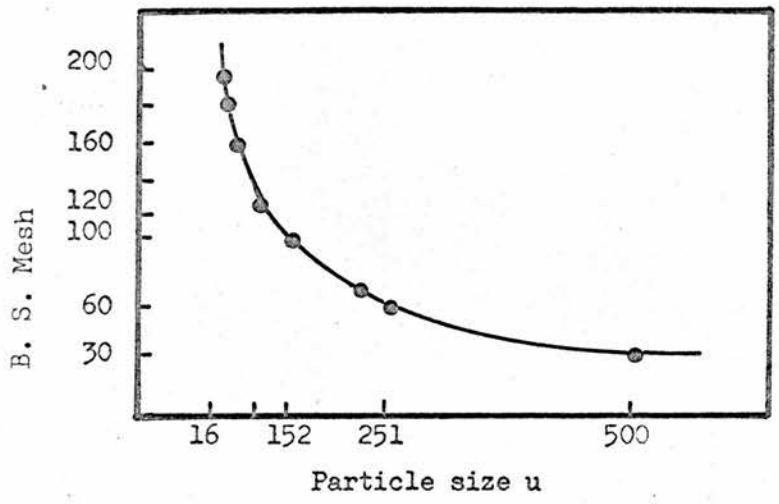

Figure 40 : B.S. mesh values and metric measurements (mm^{-3})

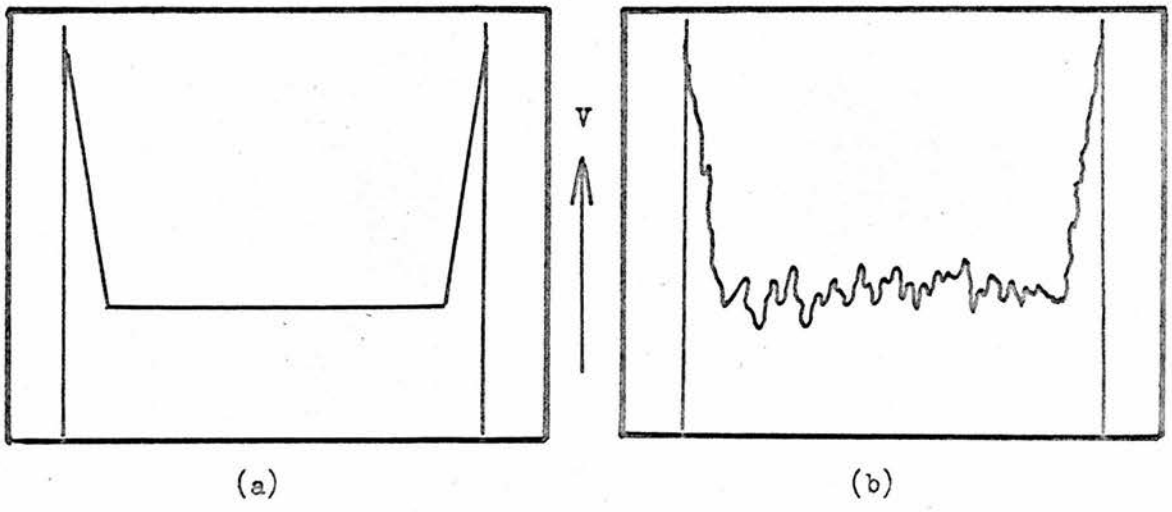

Figure 41 : Velocity profile as a result of the wall effect
(a) is the ideal case, (b) shows the effect of long range inhomogeneity.

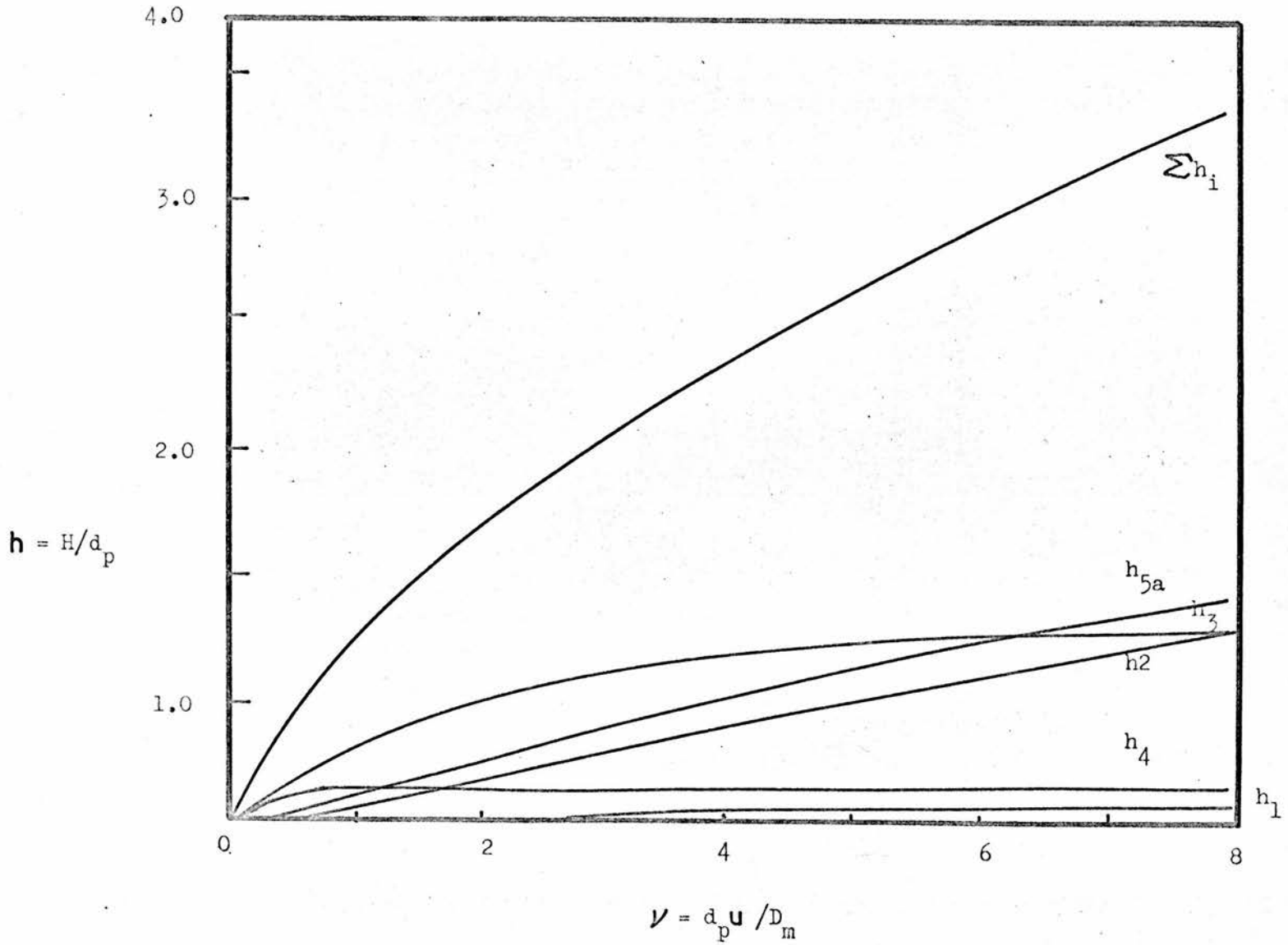

Figure 42 : A plate height vs. flow velocity plot, using the reduced co-ordinates h and v, for the various categories of velocity inequalities in the mobile phase.

Fig. 42

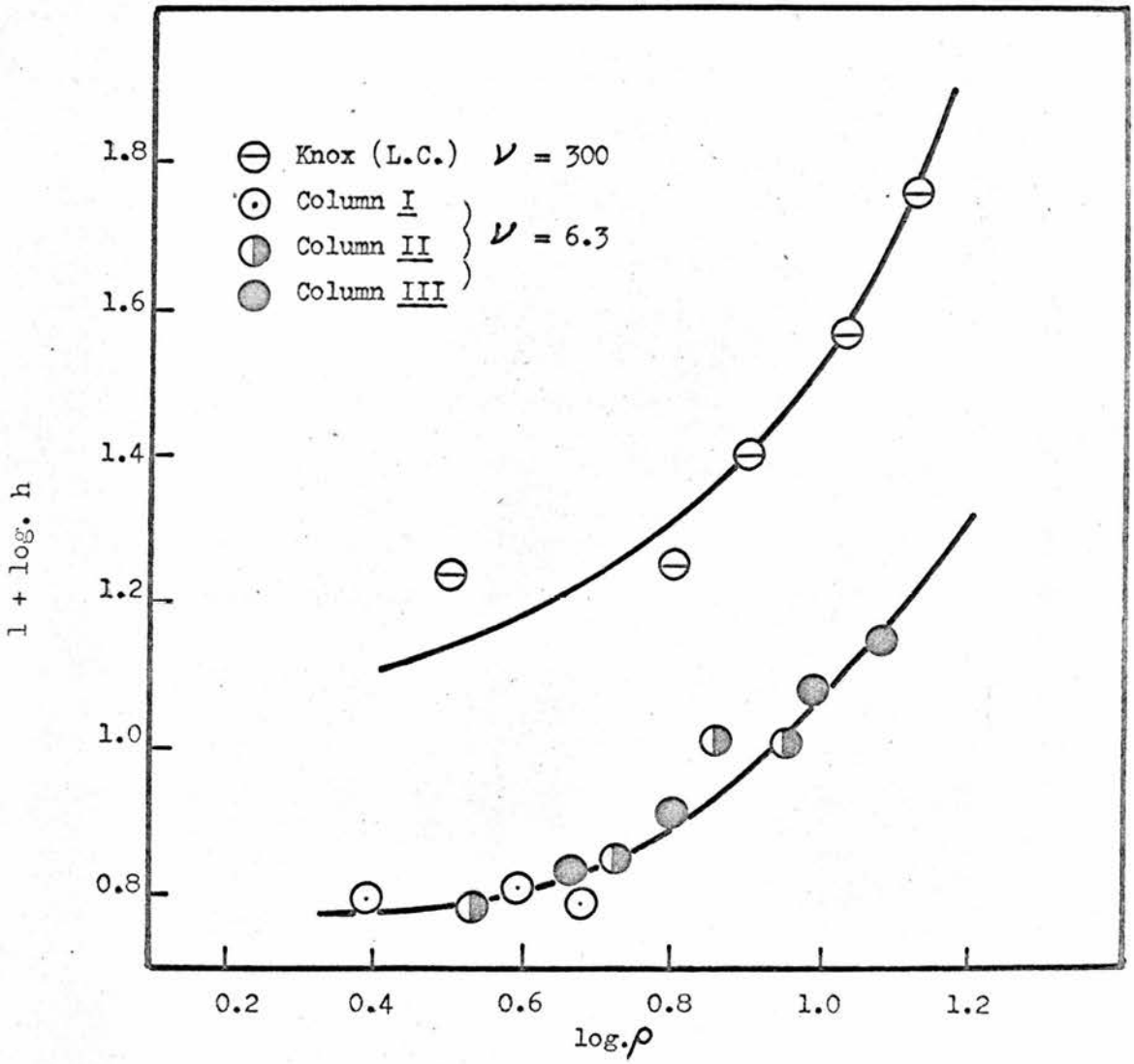

Figure 43 : Logarithmic plot of reduced plate height against column - to - particle diameter ratio : comparison between gas and liquid systems.

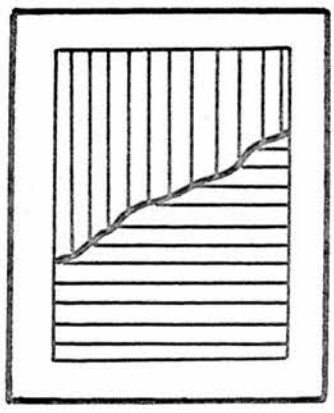

Figure 44 : Contour of colour change (after Littlewood).

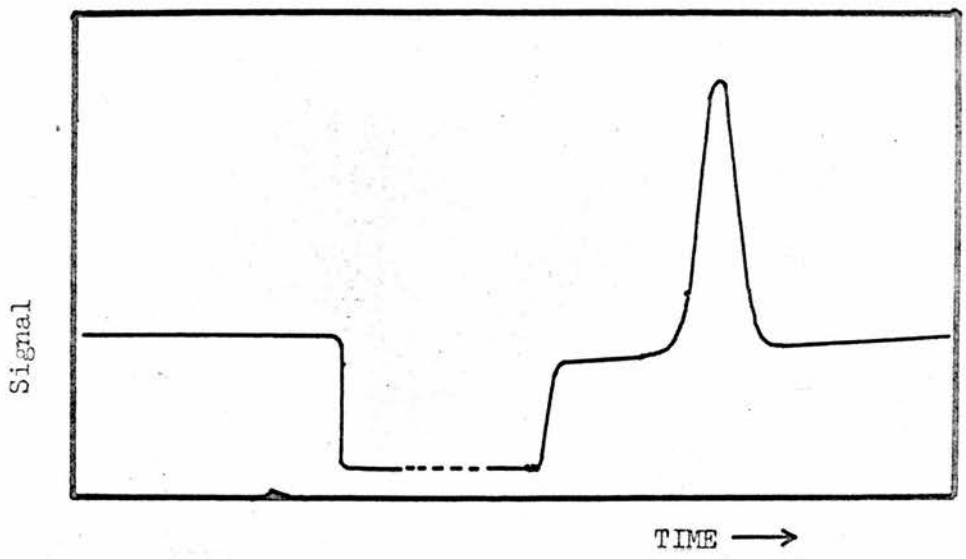

Figure 45a : (Column Inlet Pressure = 15 cm. Hg)

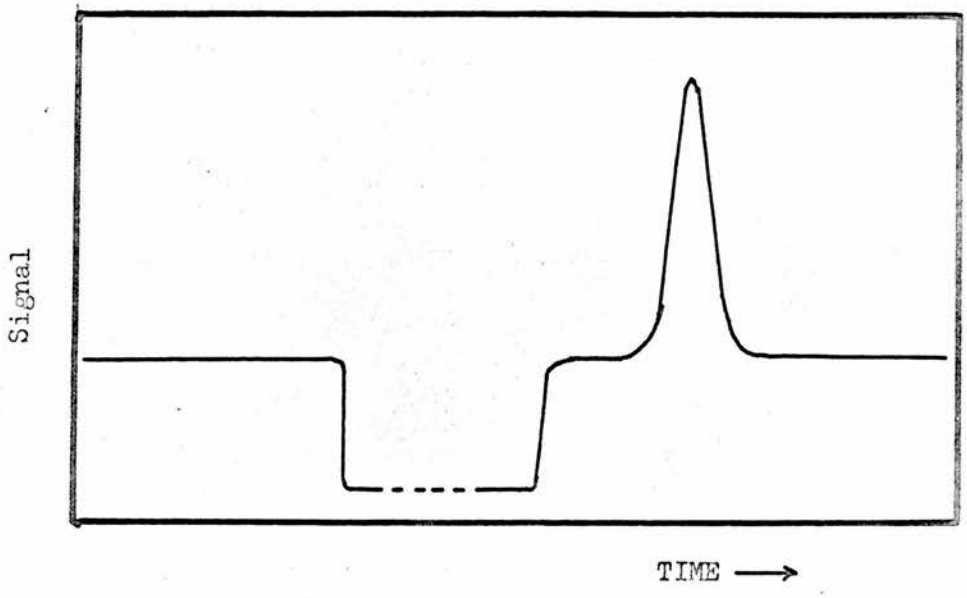

Figure 45b : (Column Inlet Pressure = 2 cm. Hg)

Figure 45 : Effect of column inlet pressure on rate of attainment of velocity. The signal is a measure of the gas velocity.

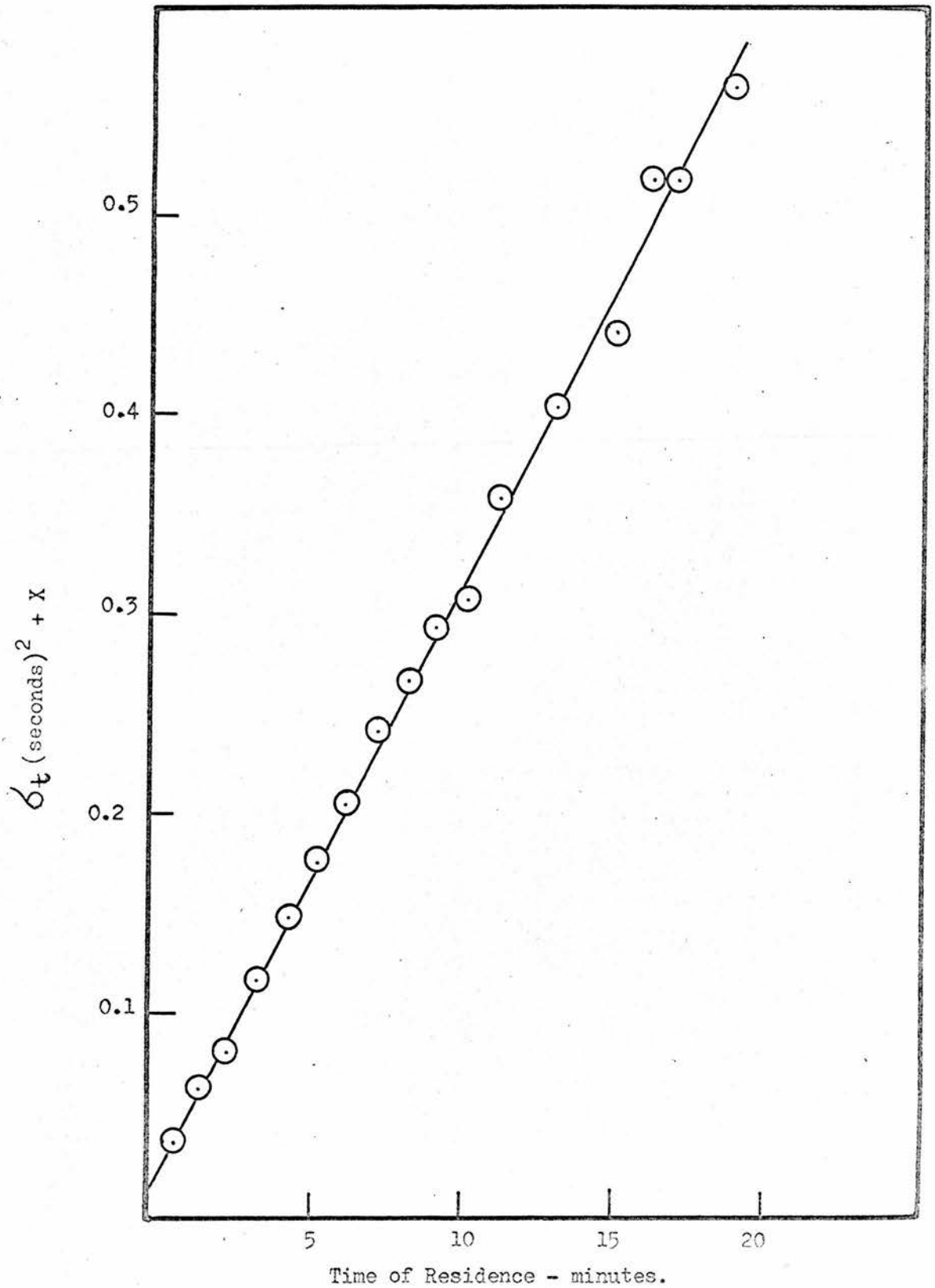

Figure 46 : Change of (variance)^2 with residence time for ethylene in nylon tube II.

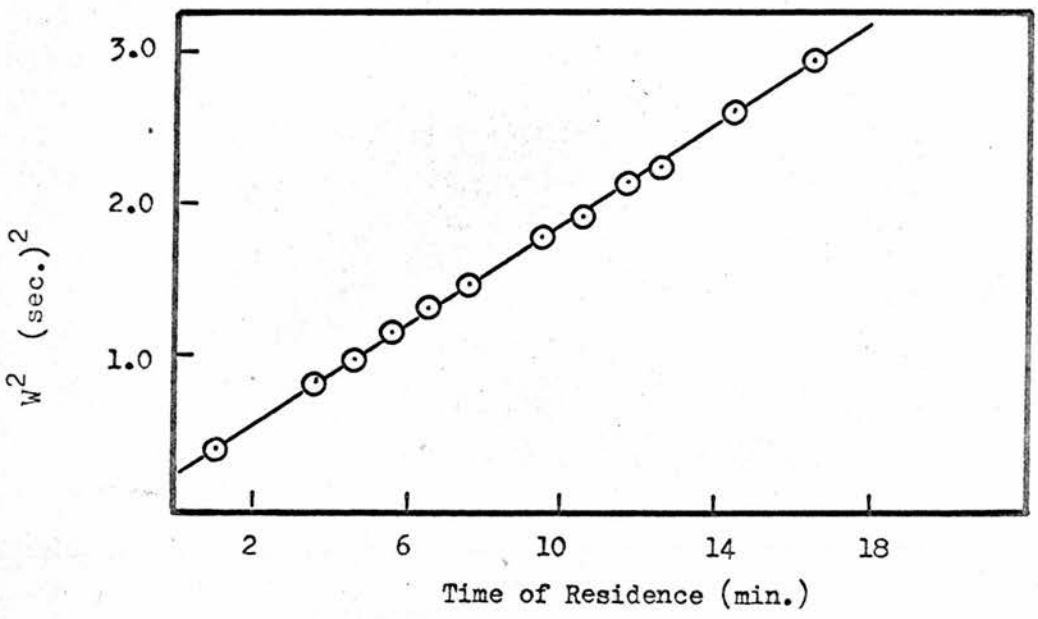

Figure 47 (a)

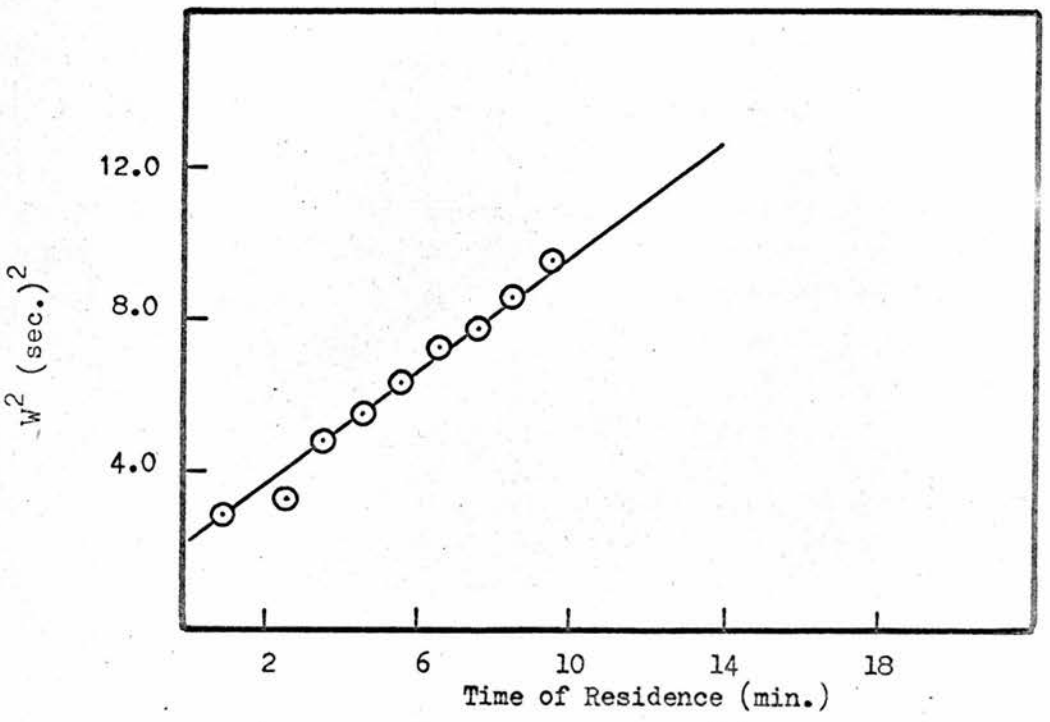

Figure 47 (b)

Figure 47 : Change of (peak width)^2 with residence time for nylon tubes I (47a) and III (47b).

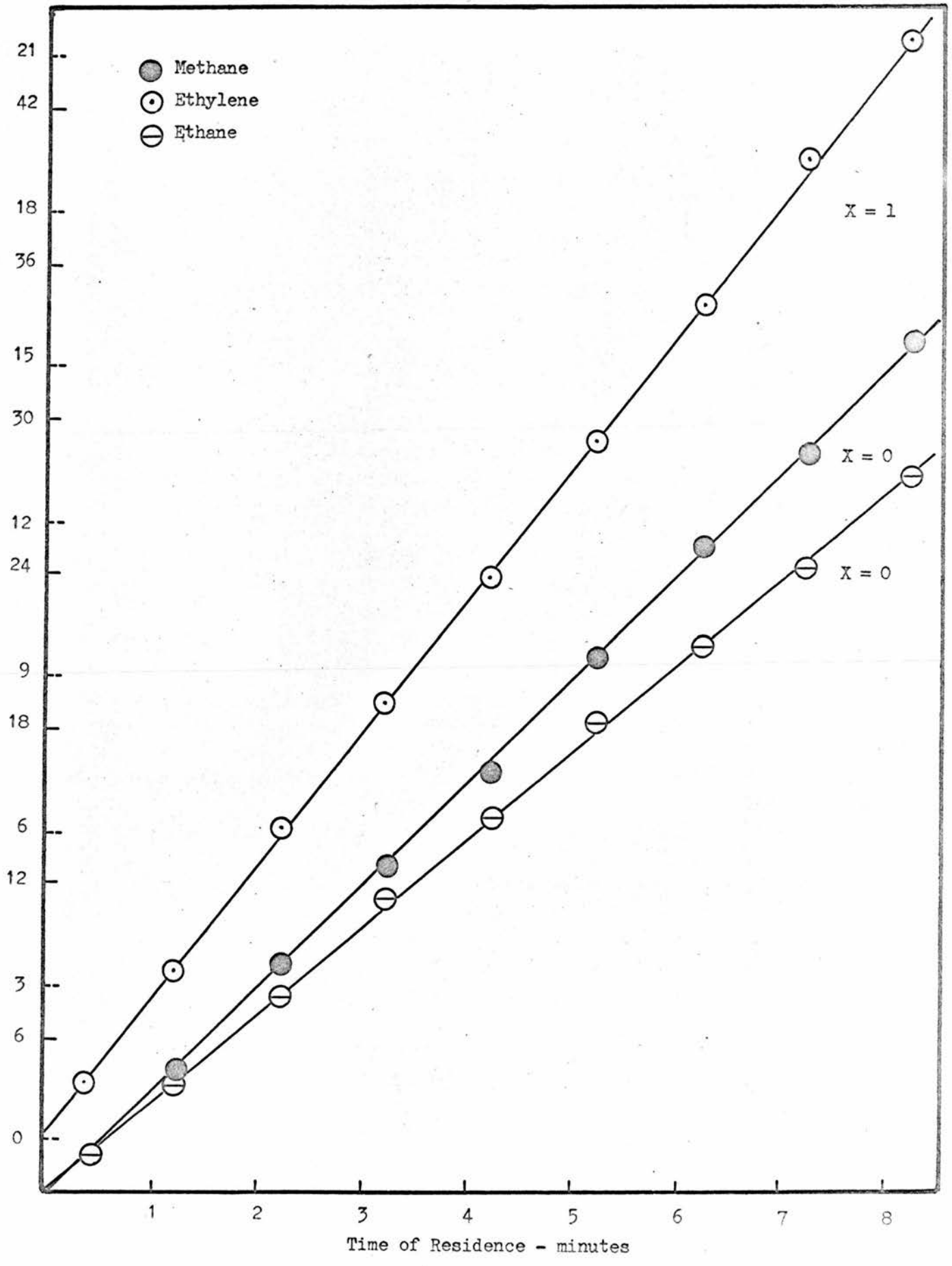

Figure 48 : Change of (peak width)^2 with residence time for methane, ethylene and ethane.

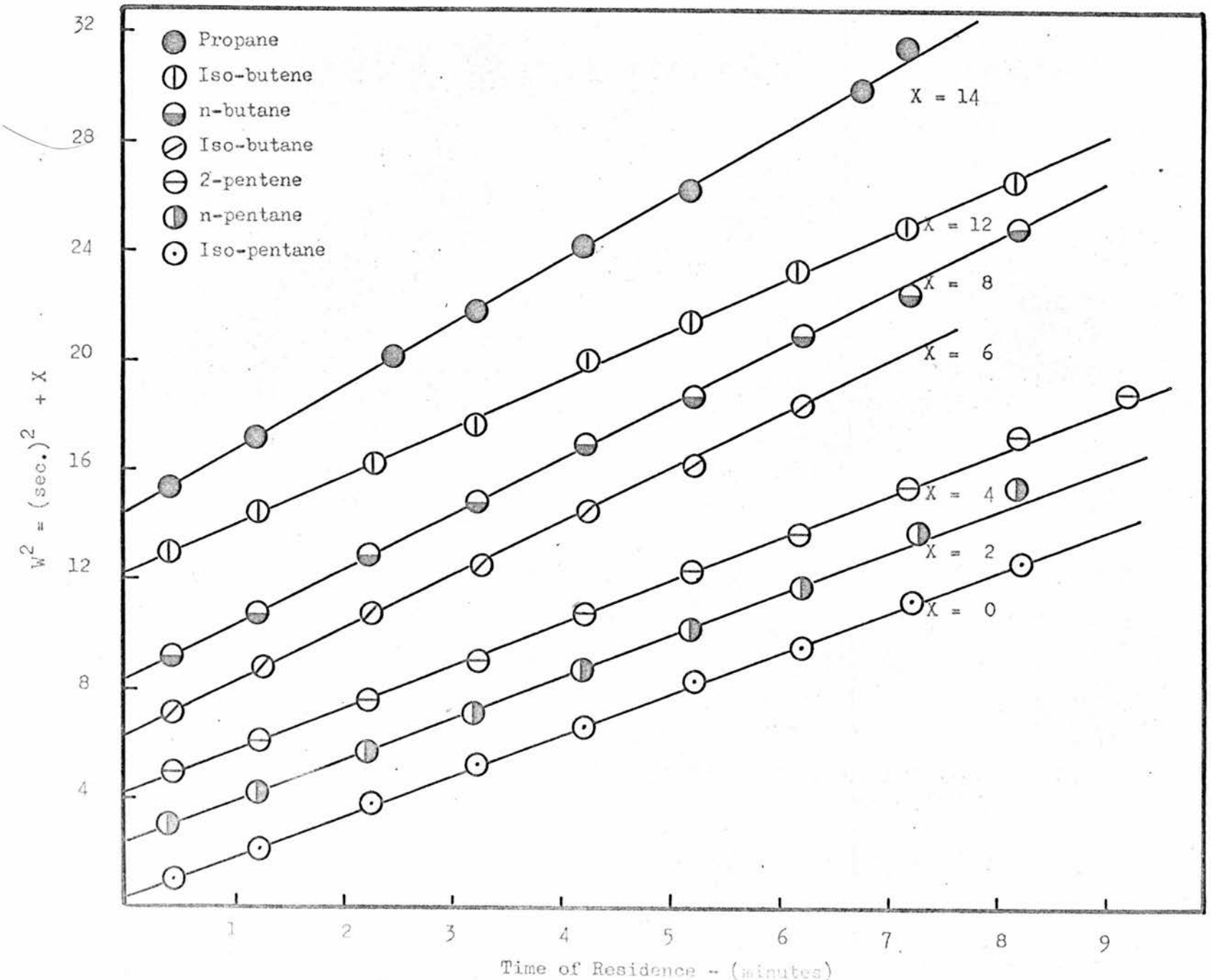

Figure 49 : Change of (peak width)^2 with residence time for different gases.

Fig. 49

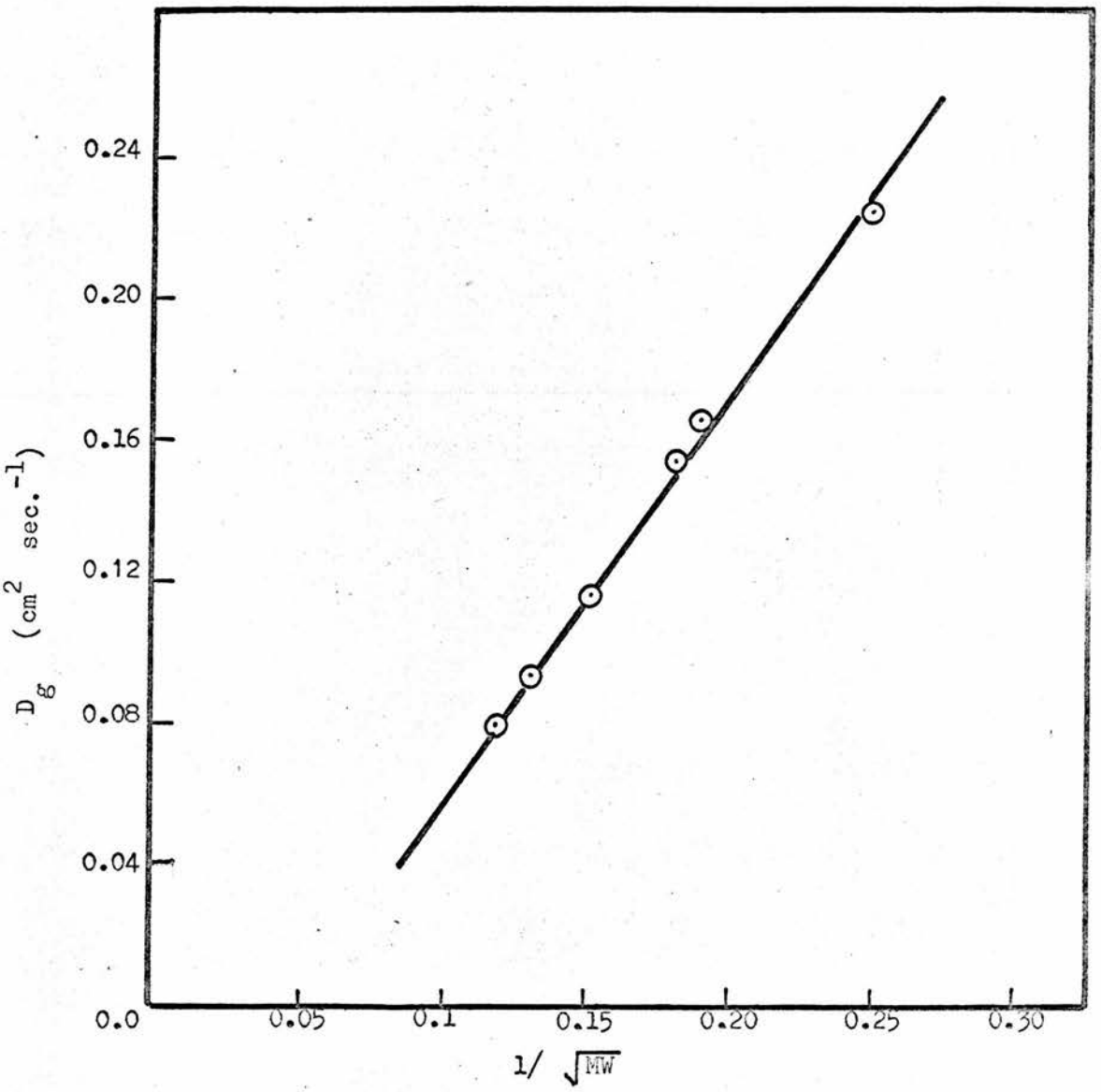

Figure 50 : Variation of diffusion coefficient with inverse square root of molecular weight.

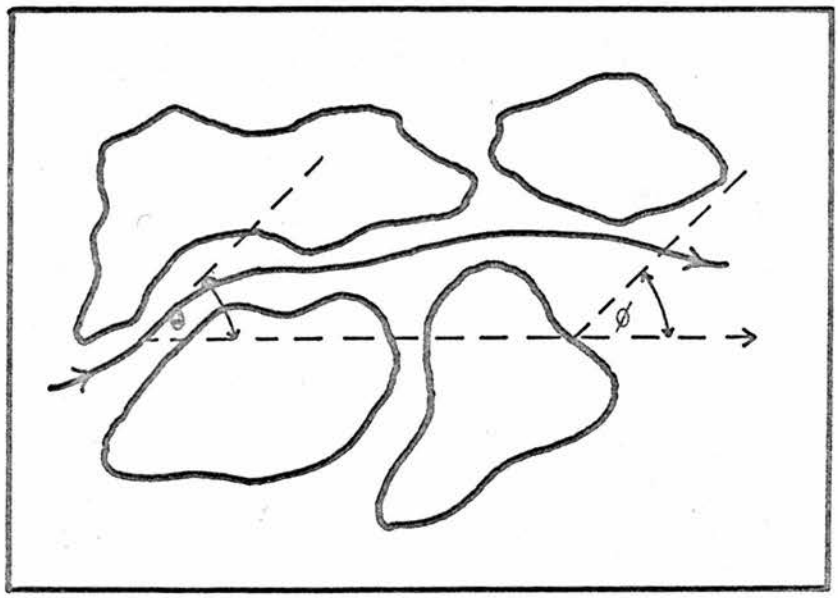

Figure 51 : Illustration of θ and ø .

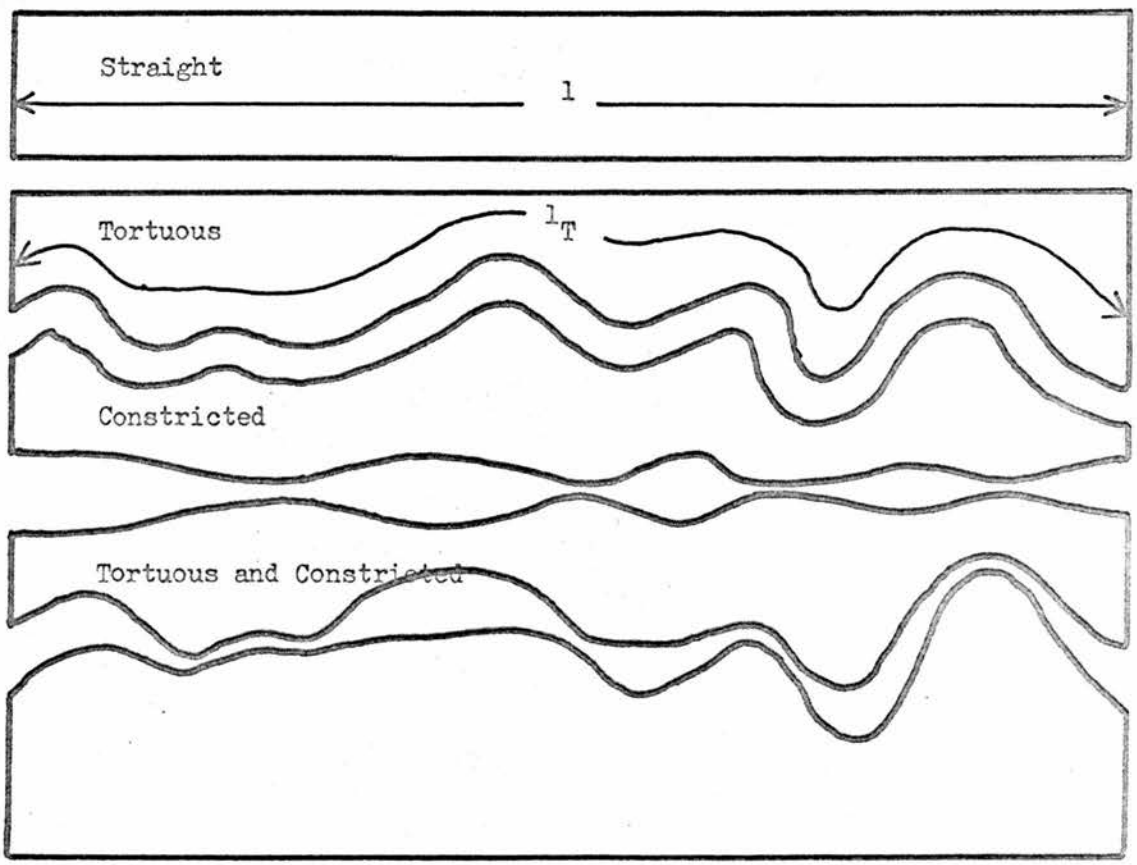

Figure 52 : Illustration of various types of paths.

A

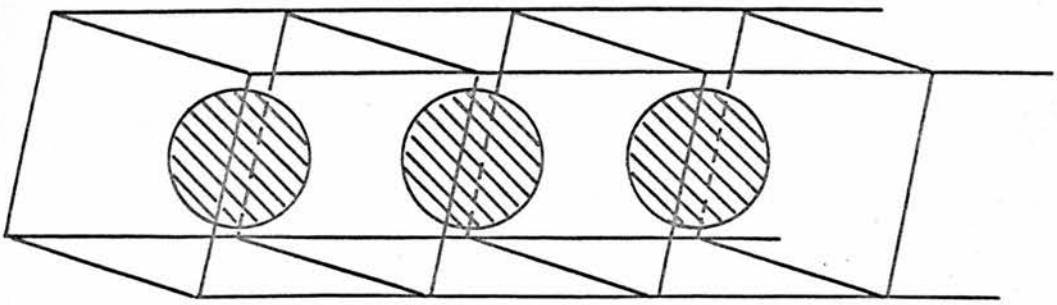

B

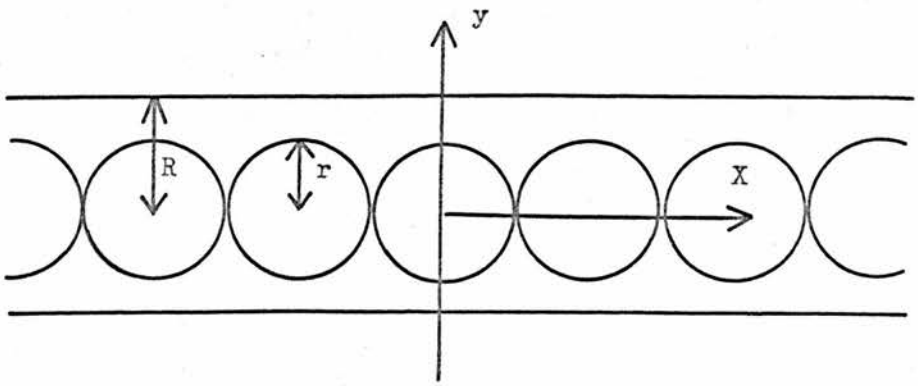

C.

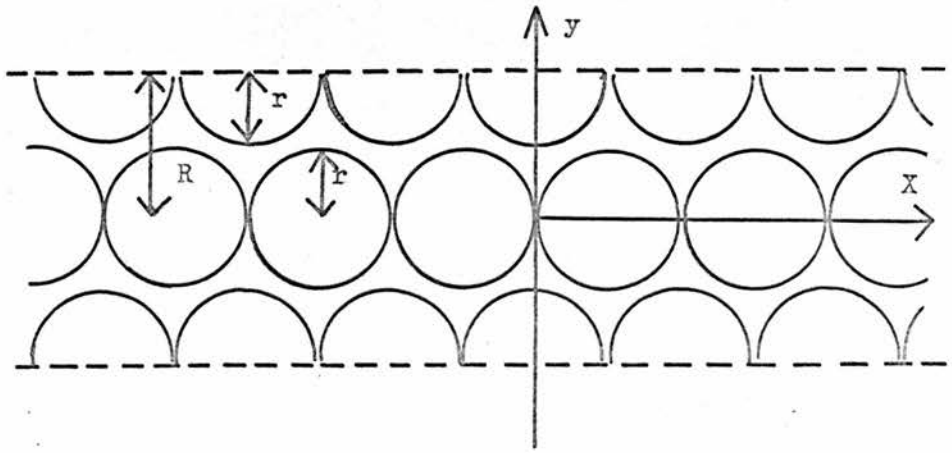

Figure 53 : Models for packed columns.

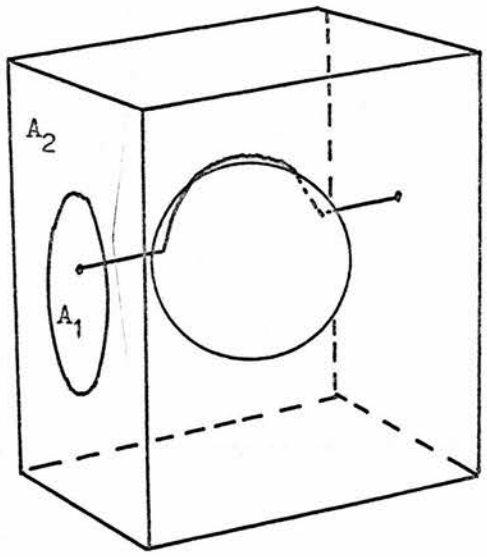

Figure 54 : Model used by Giddings and Boyack in the calculation of tortuosity.

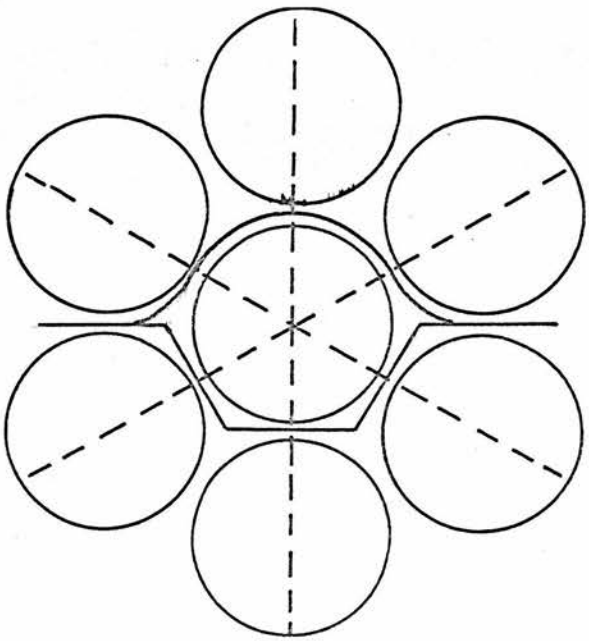

Figure 55 : Illustration of tortuosity for a model of close packed spheres.

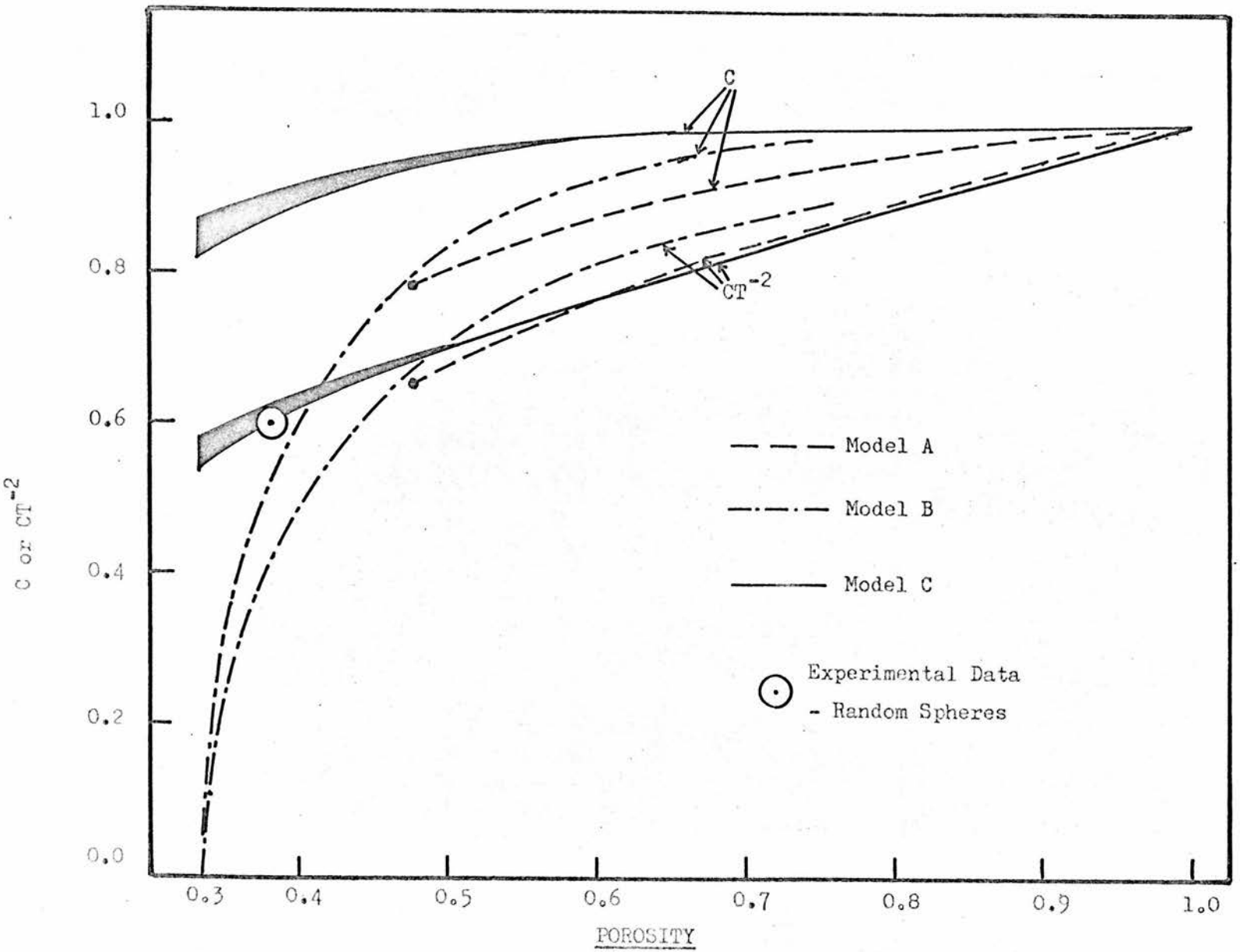

Fig. 56

Figure 56 : Variation of constriction and obstructive factors with porosity for different models of packed columns.

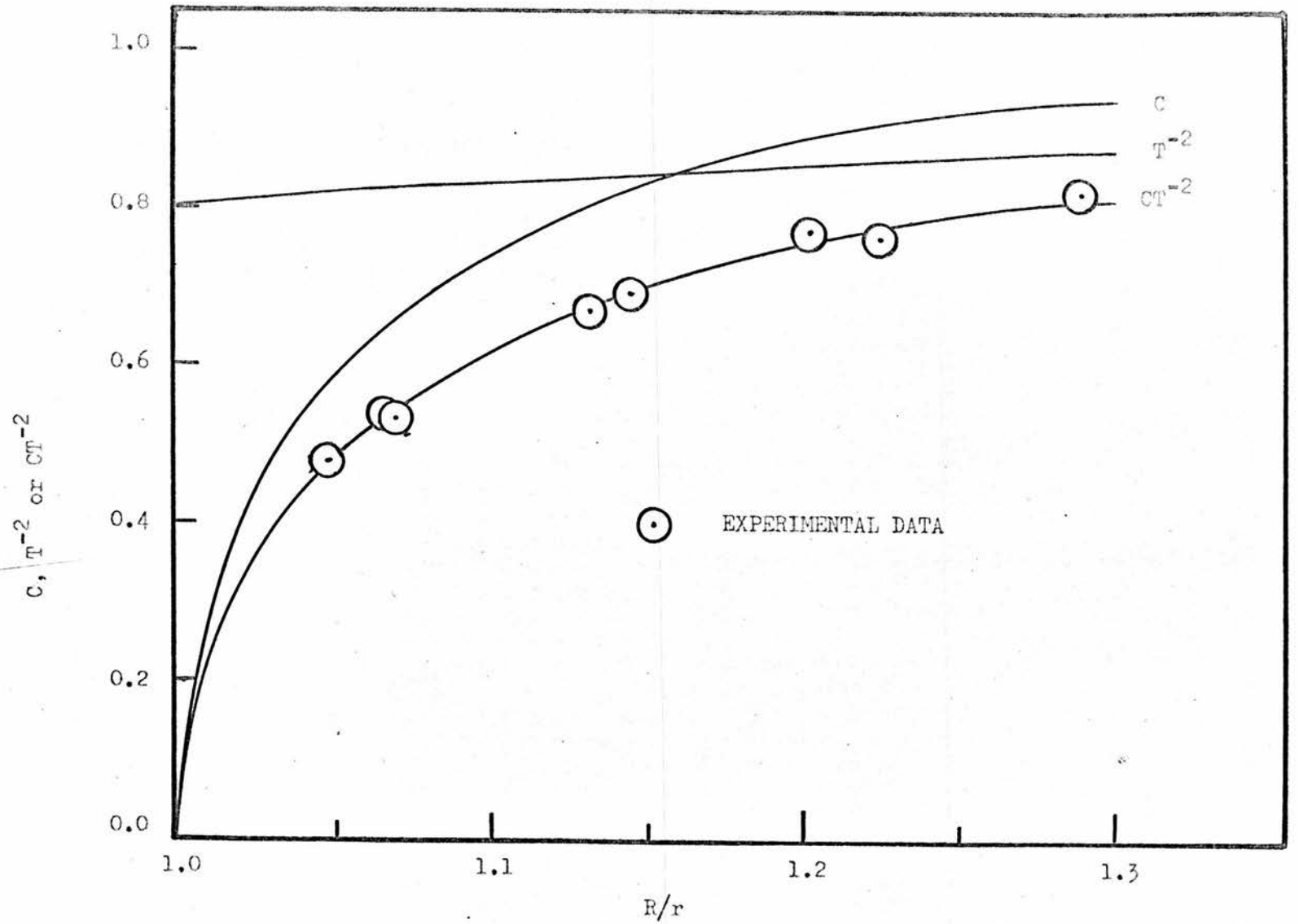

Fig. 57

Figure 57 : Variation of obstructive parameters for model B in figure 53: comparison with experimental data.

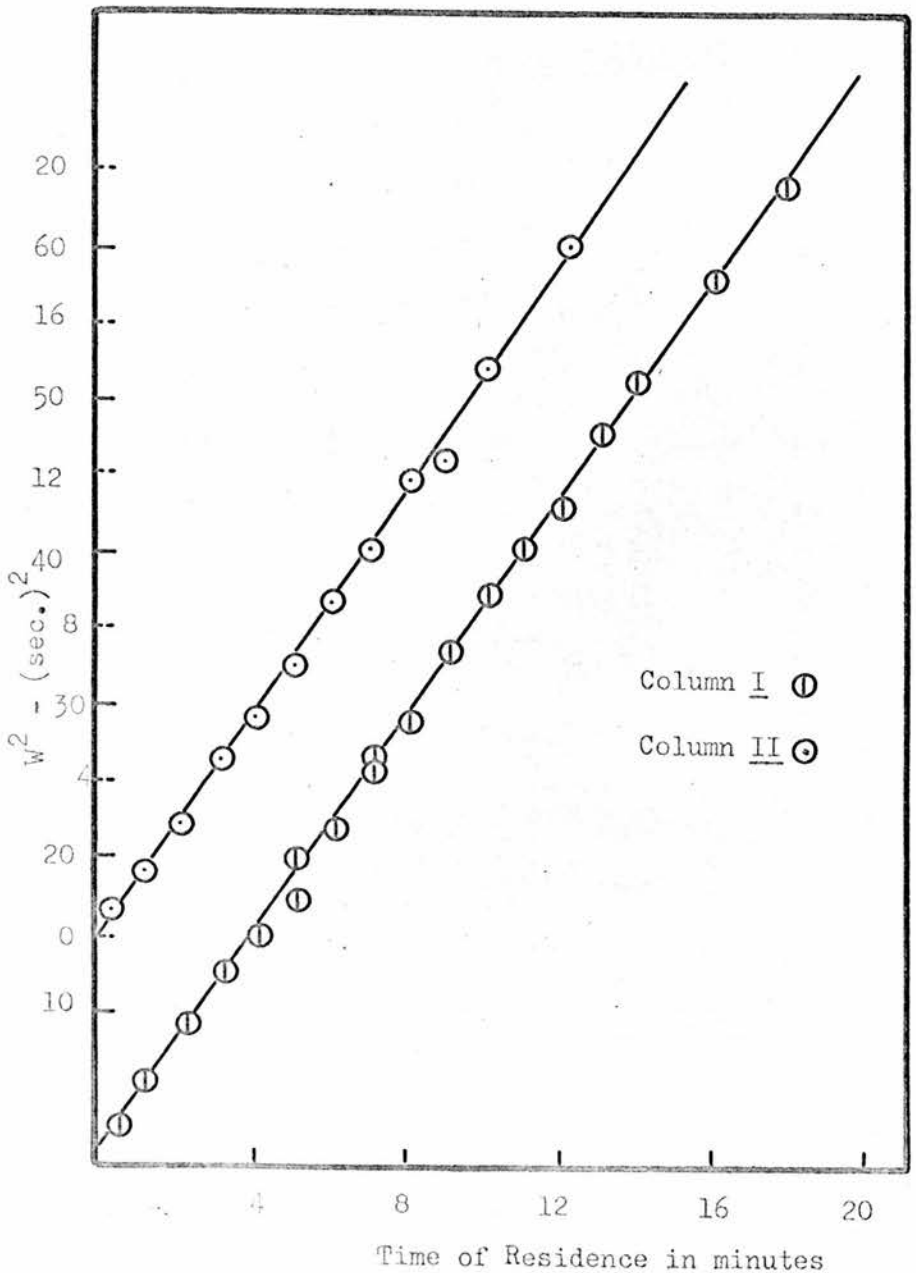

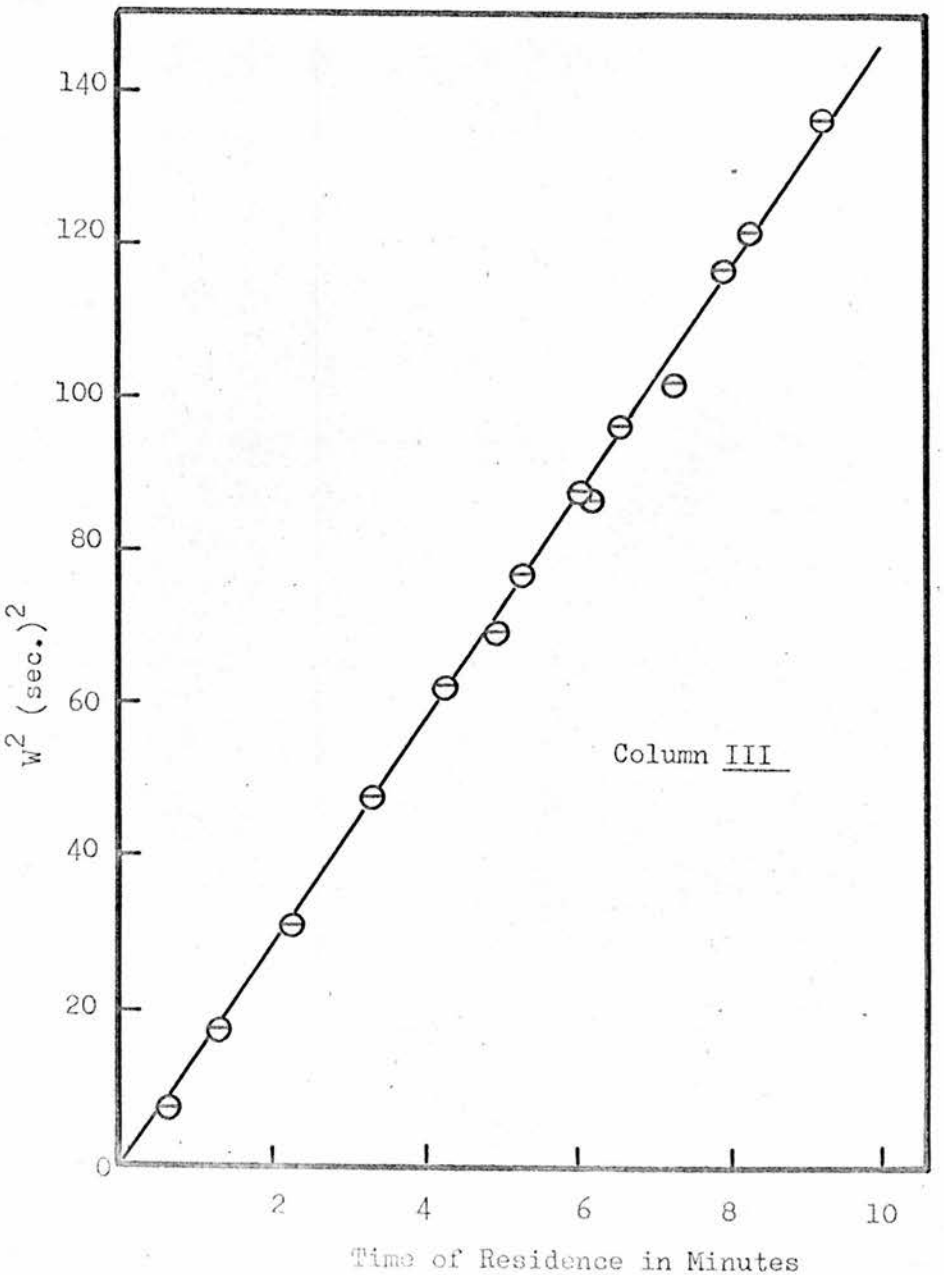

Fig. 58

Figure 58 : Change of (peak width)^2 with residence time for glass bead columns.

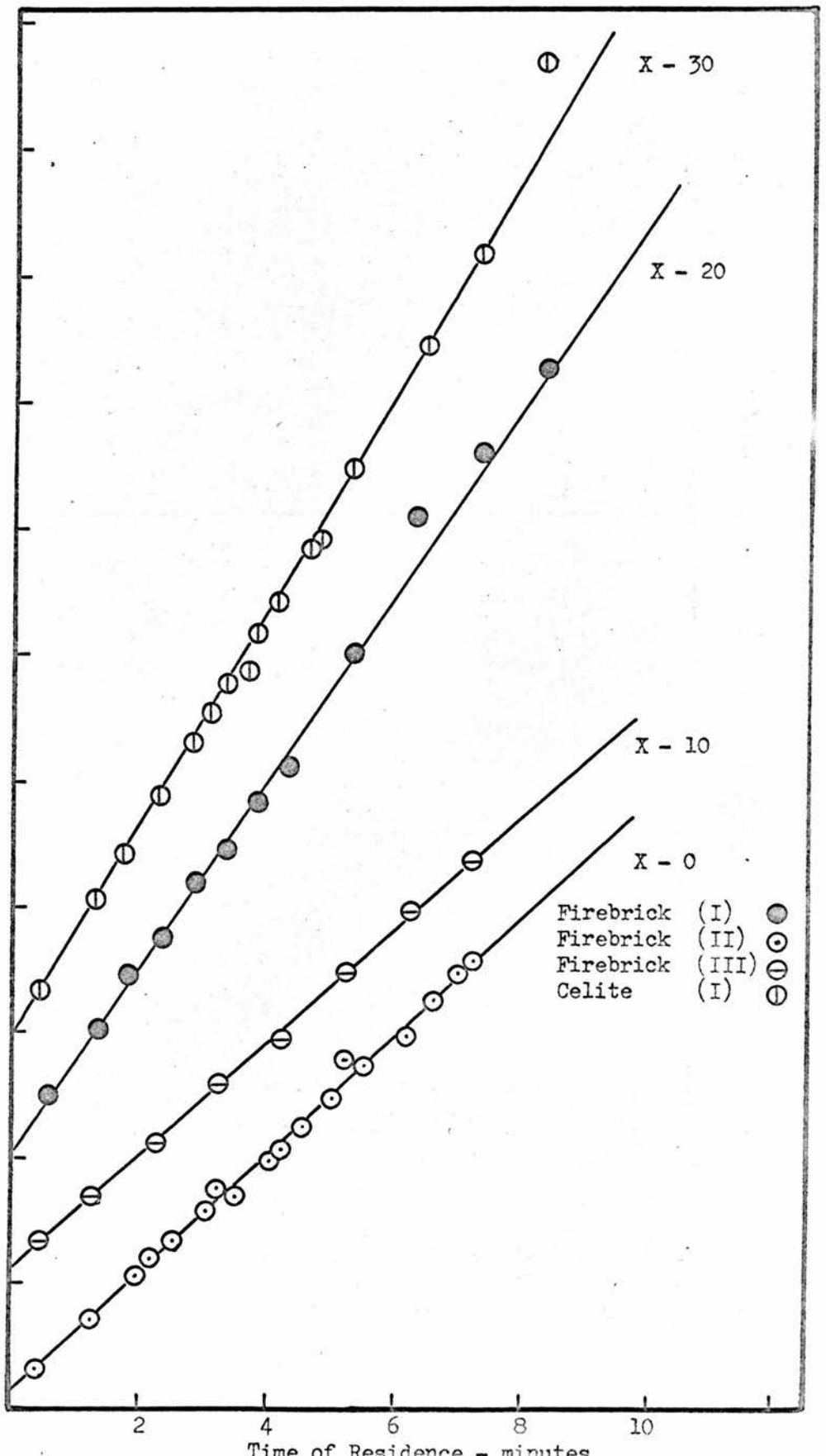

Figure 59 : Change of (peak width)^2 with residence time for firebrick and celite columns.

Fig. 60

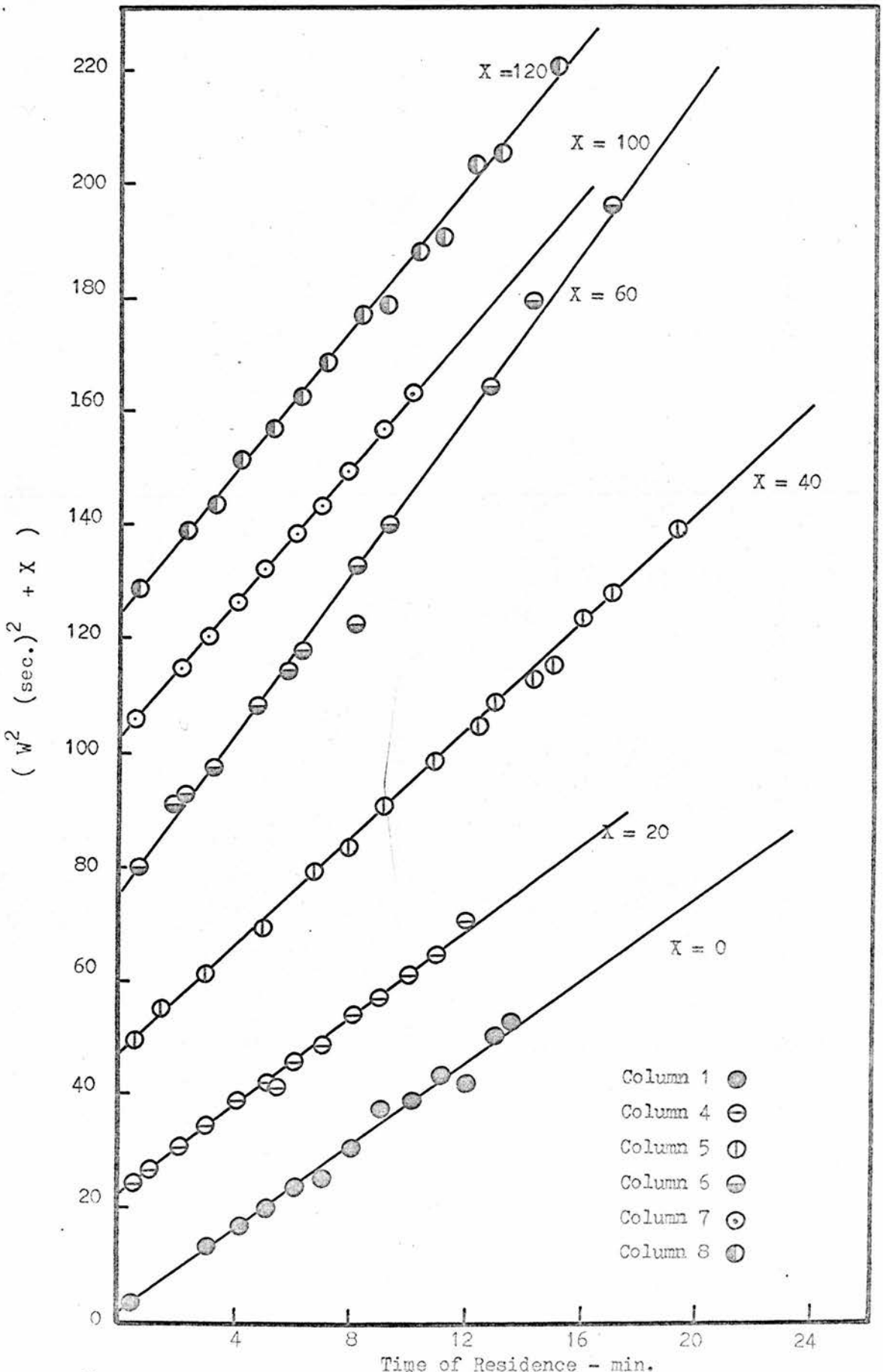

Figure 60 : Change of (peak width)^2 with residence time for model B in figure 53.

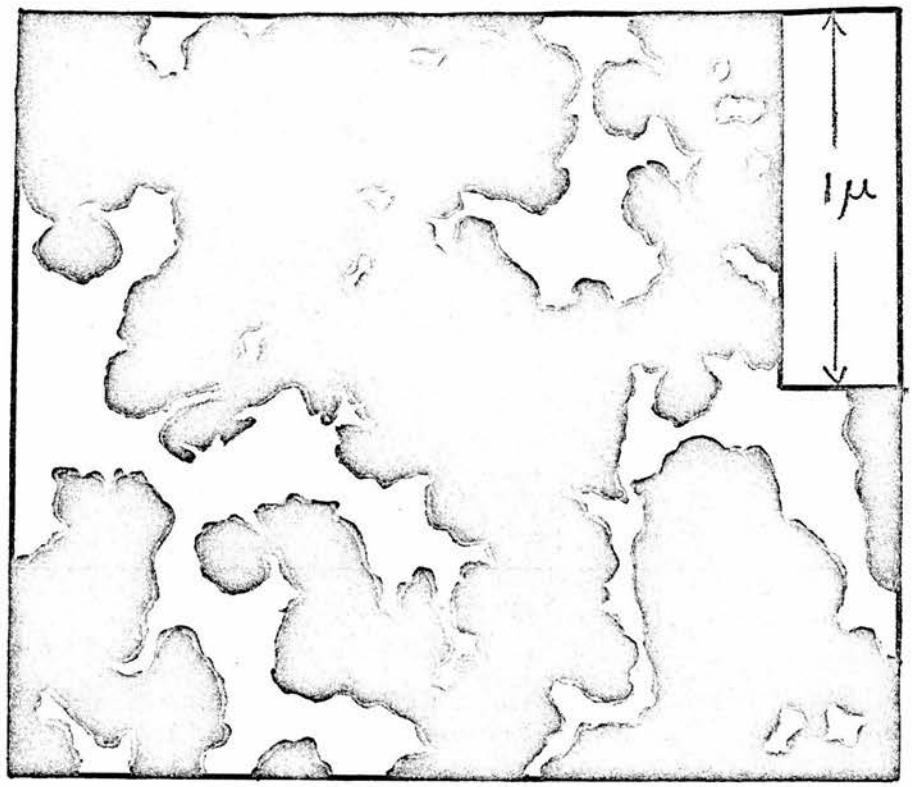

(a)

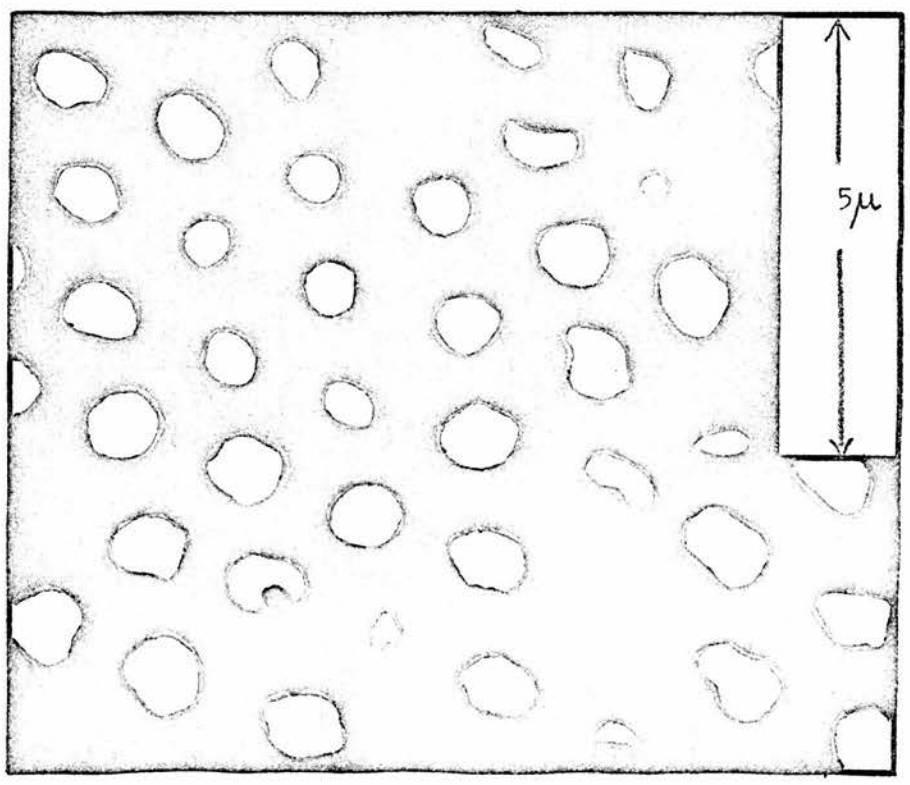

(b)

Figure 61: Typical electron microscope photographs of (a) firebrick of the sterchamol type and (b) celite showing pore structure.

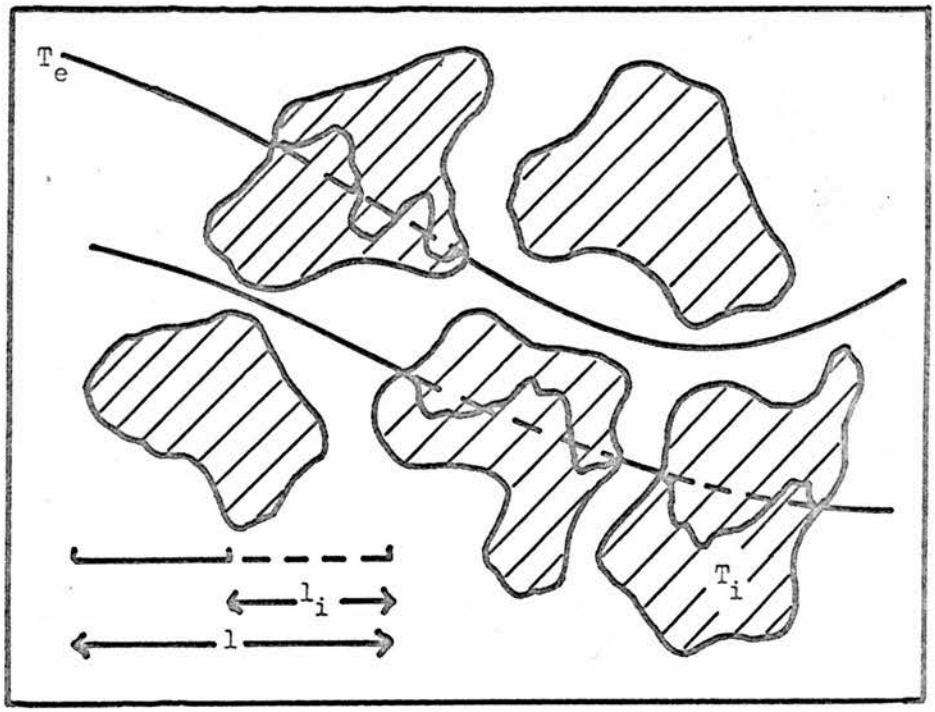

Figure 62 : Illustration of interstitial and intraparticle tortuosity.

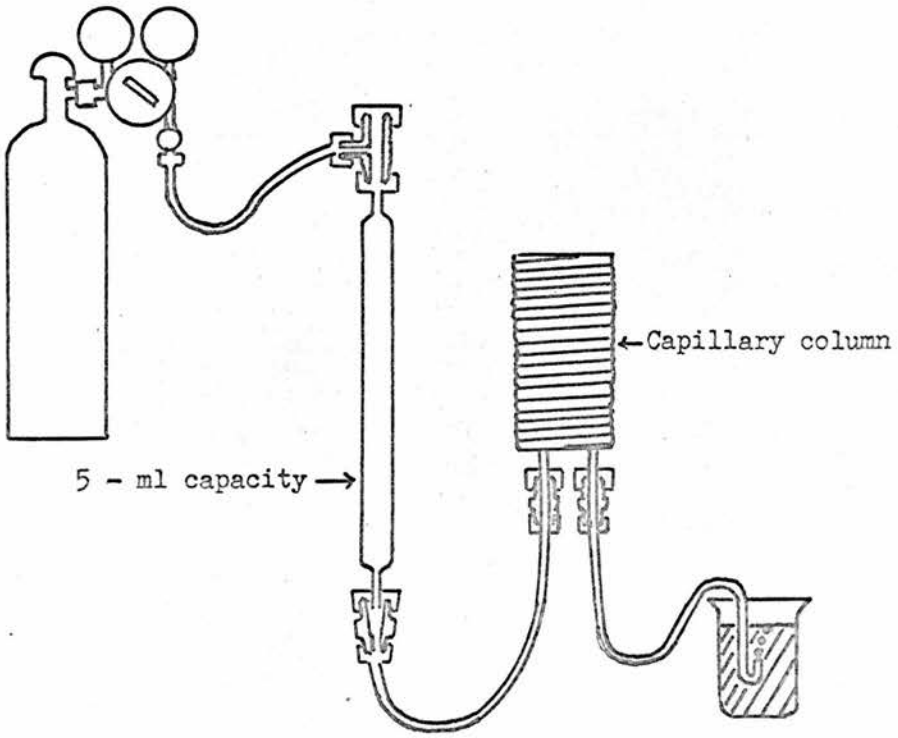

Figure 63 : Apparatus for preparation of capillary column.

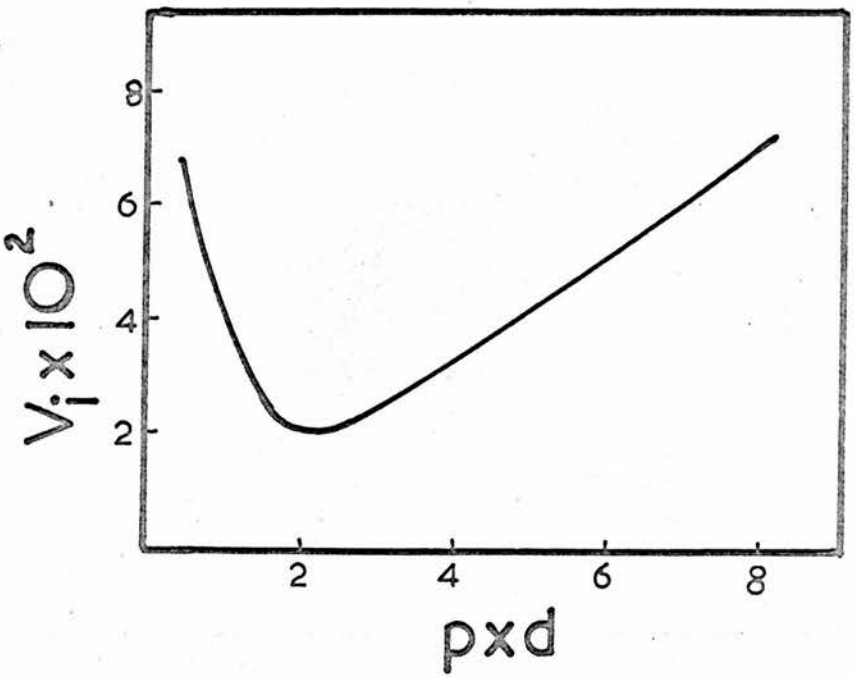

Figure 64 : Variation of breakdown voltage with pxd.

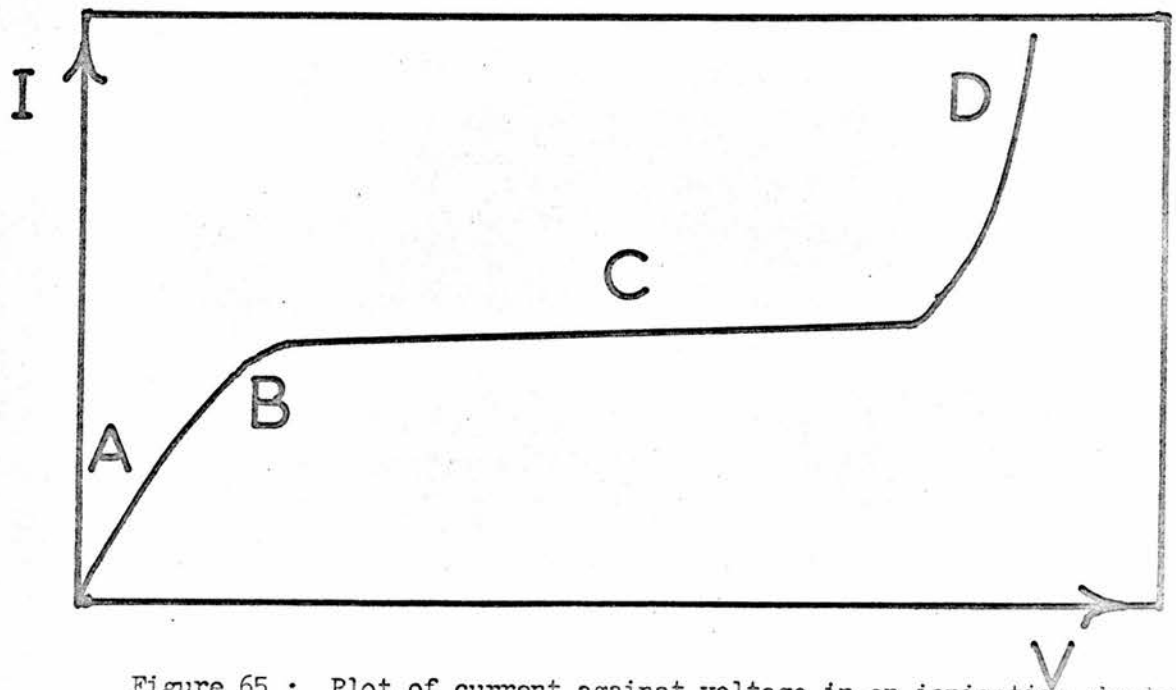

Figure 65 : Plot of current against voltage in an ionisation chamber.

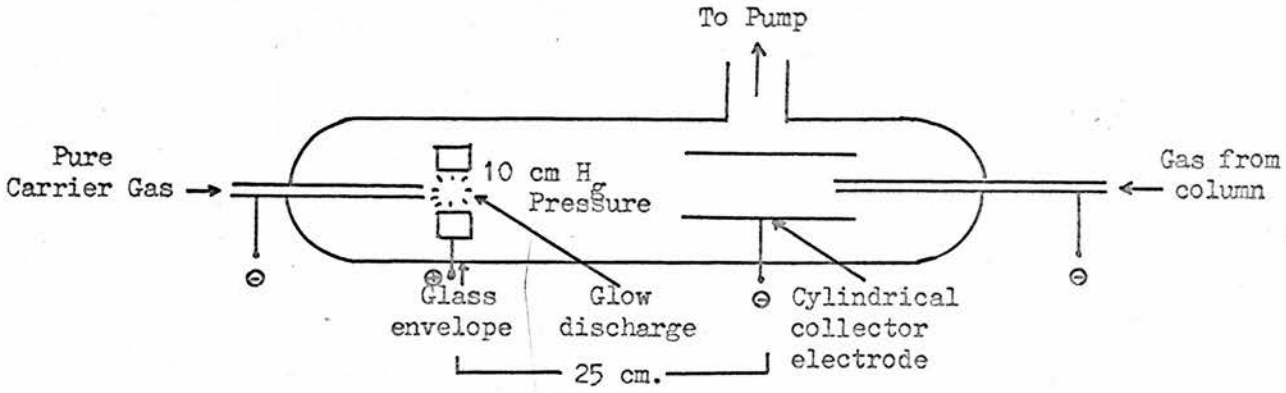

Figure 66 : Photo - Ionisation Detector (after Lovelock).

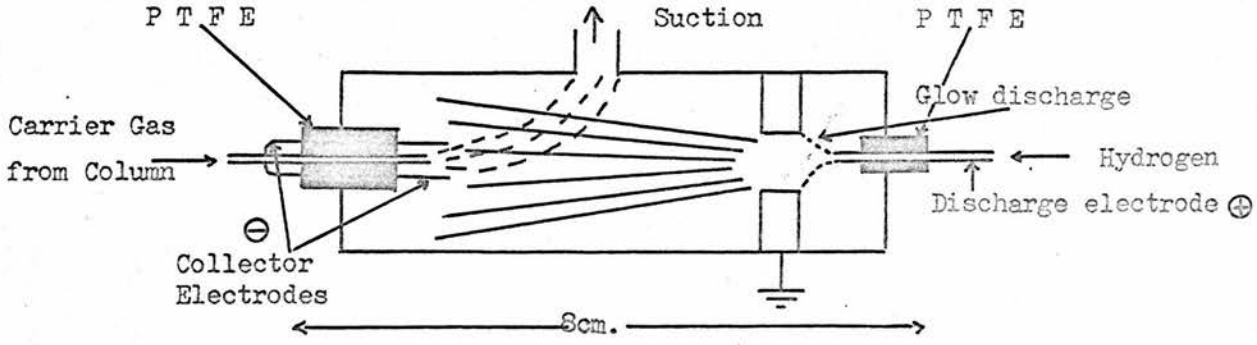

Figure 67 : The Griffin & George design of the photo - ionisation detector.

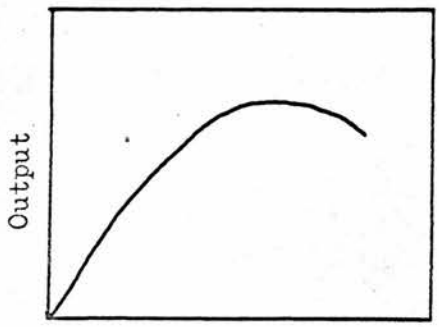

Figure 68 (a)

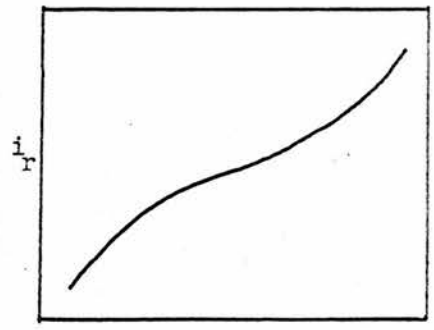

Figure 69

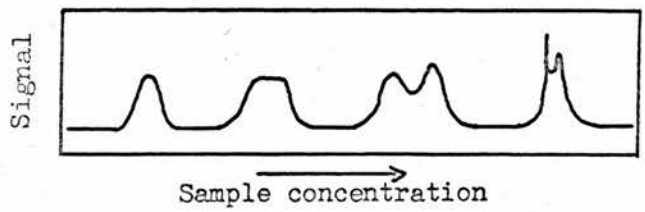

Figure 68 (b)

Figure 68 : Illustration of detector non - linearity.

Figure 69 : Variation of current with voltage : absence of plateau.

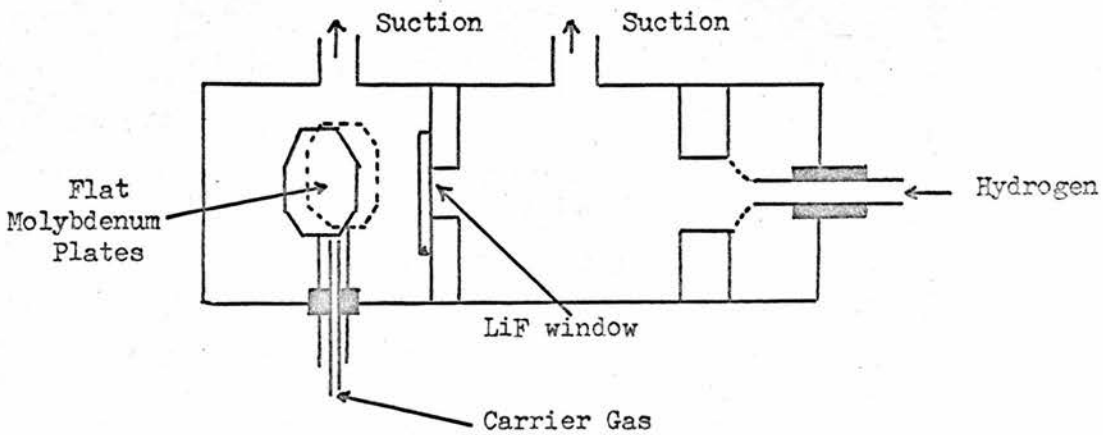

Figure 70 : Smith modification of the photo-ionisation detector.

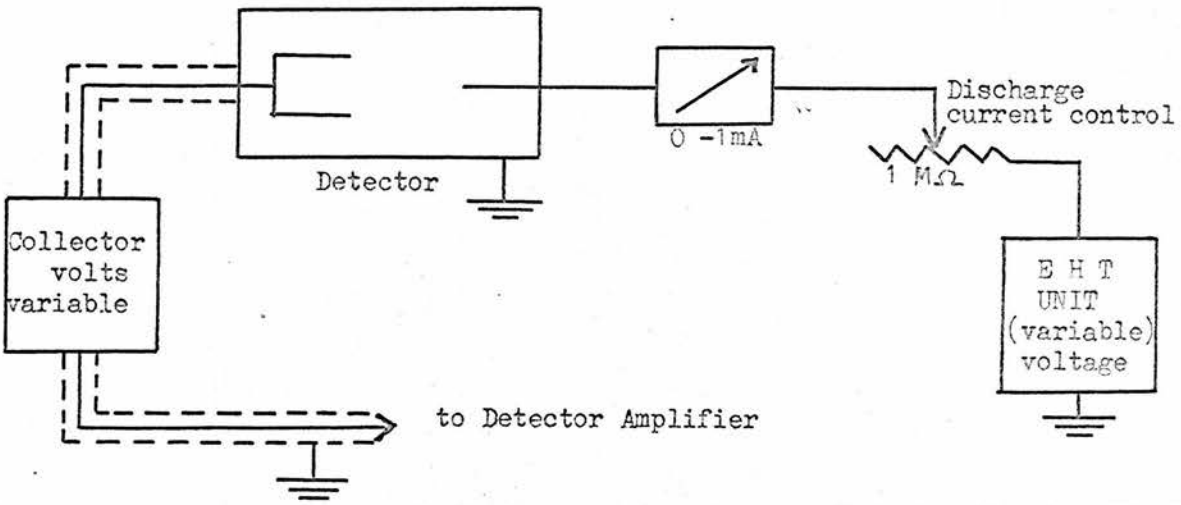

Figure 71 (a) : Block diagram of apparatus

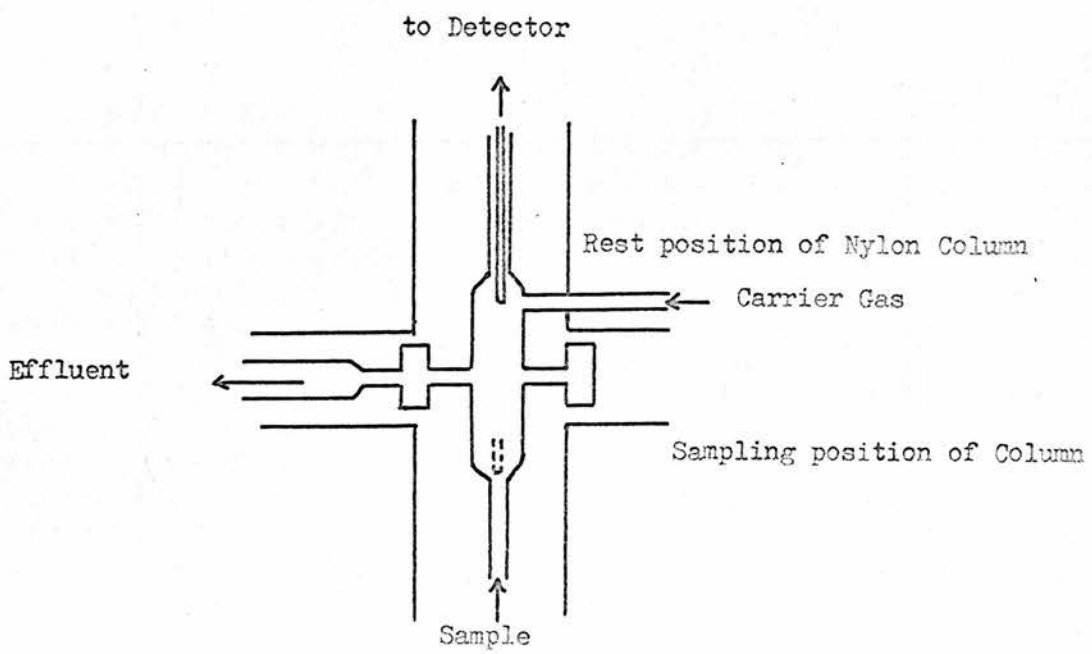

Figure 71 (b): The Injector

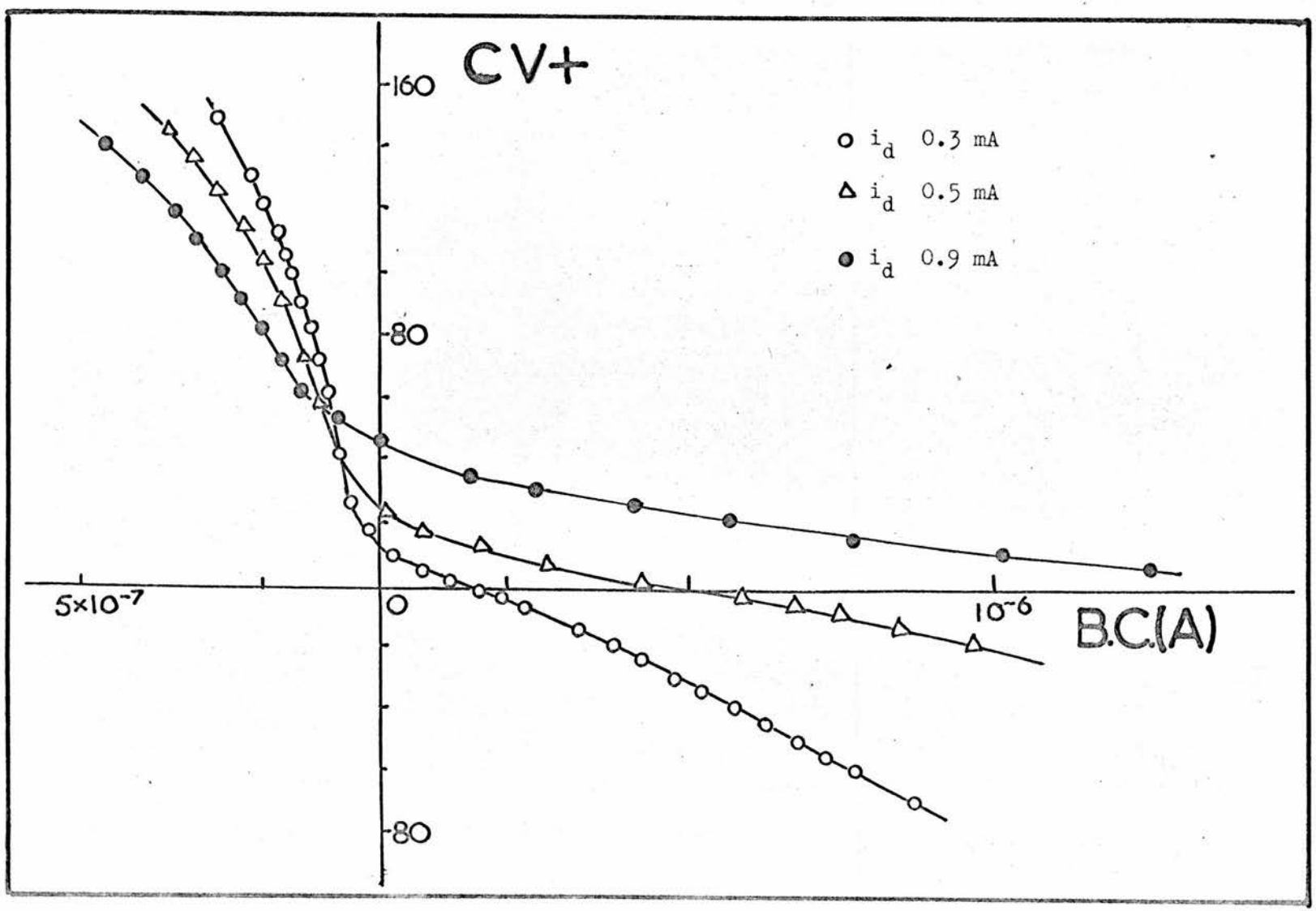

Fig. 72

Figure 72 : Plot of collector volts (CV) against background current (BC) for the Griffin and George design of the P.I.D.

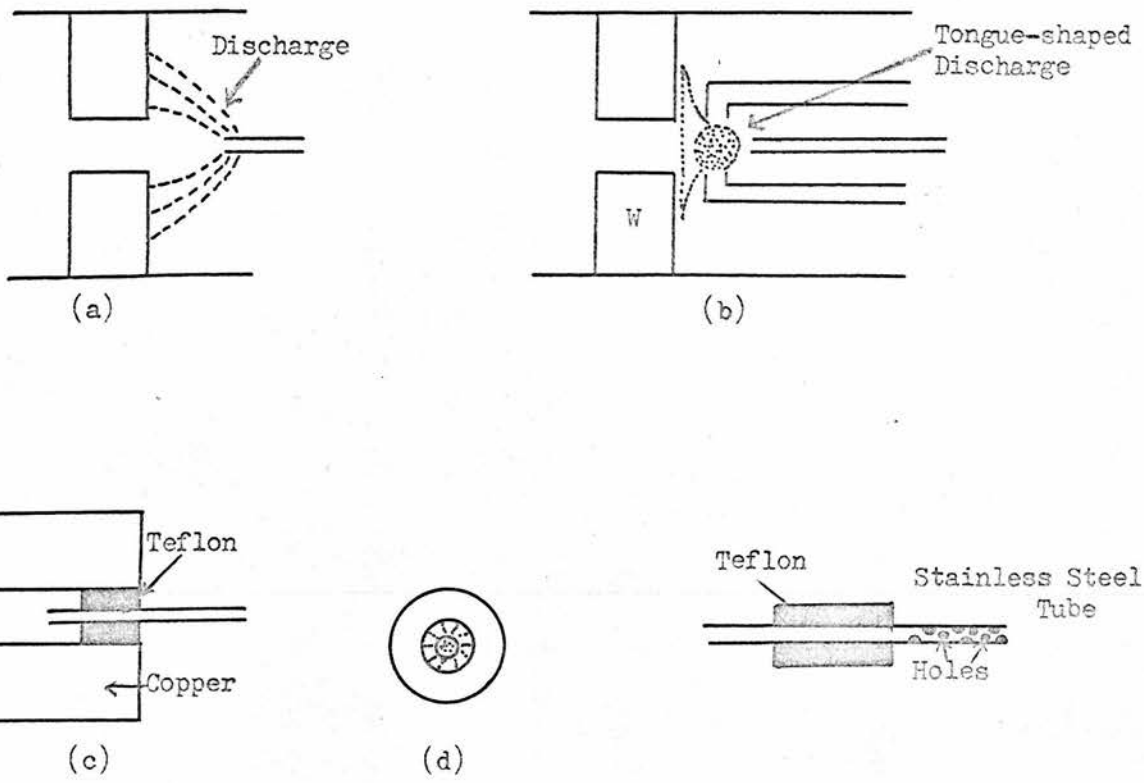

Figure 73: (a) Original discharge electrode
(b), (c): Modifications.
(d) End-on View of model (c).

Figure 74: Collector Electrode

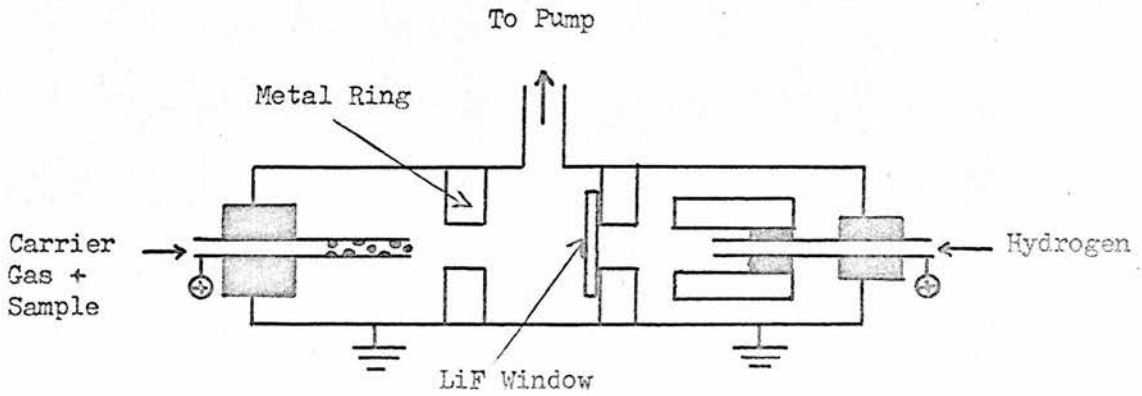

Figure 75: Final design of the photo-ionisation detector.

Fig. 76

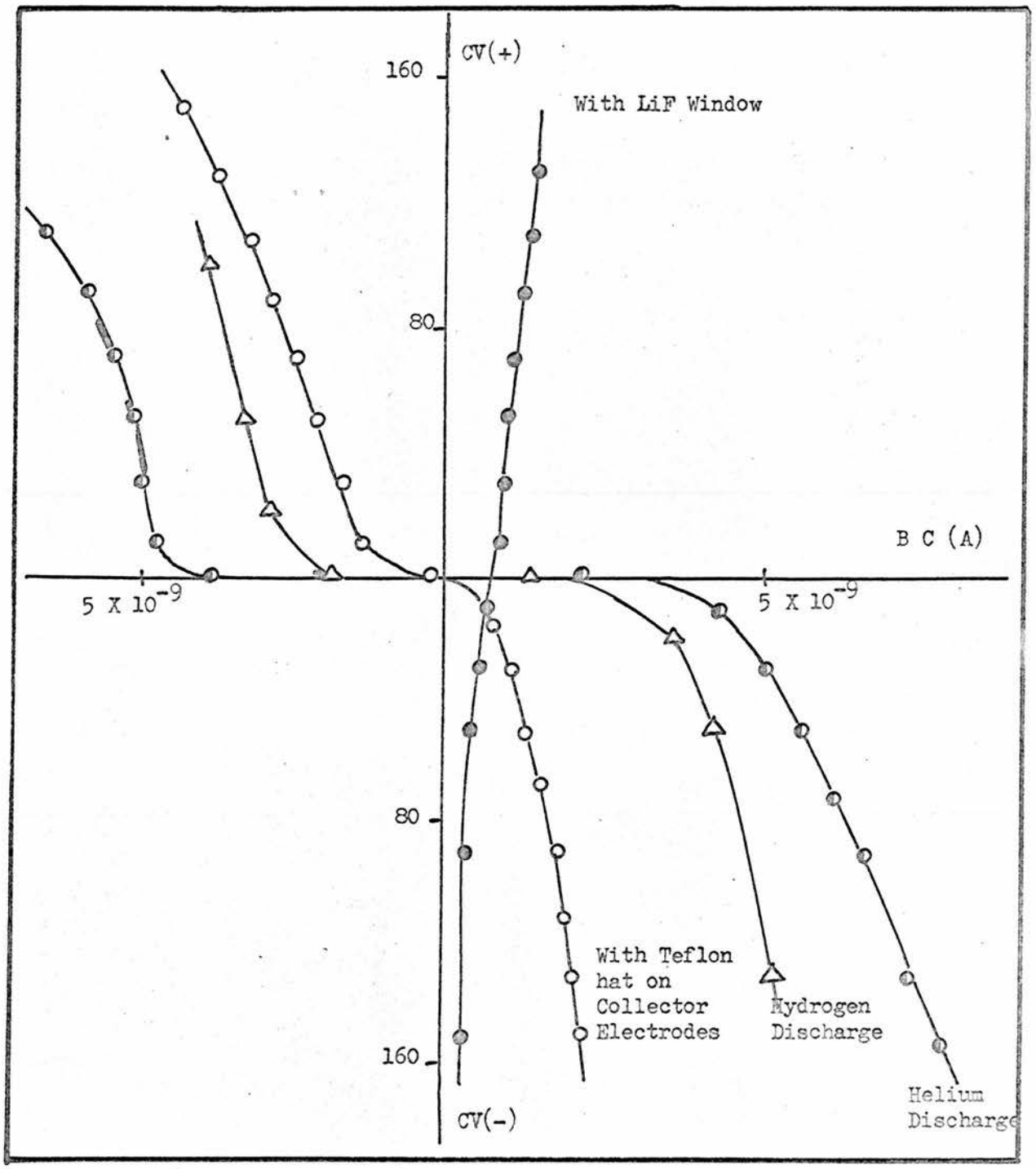

Figure 76 : Plot of collector volts against background current for the final design of the photo-ionisation detector.

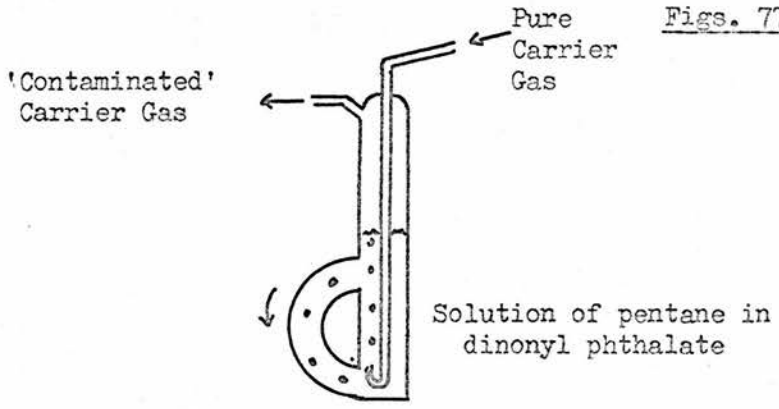

Figure 77: Mixing vessel for detector linearity studies ; provision of contaminated gas stream.

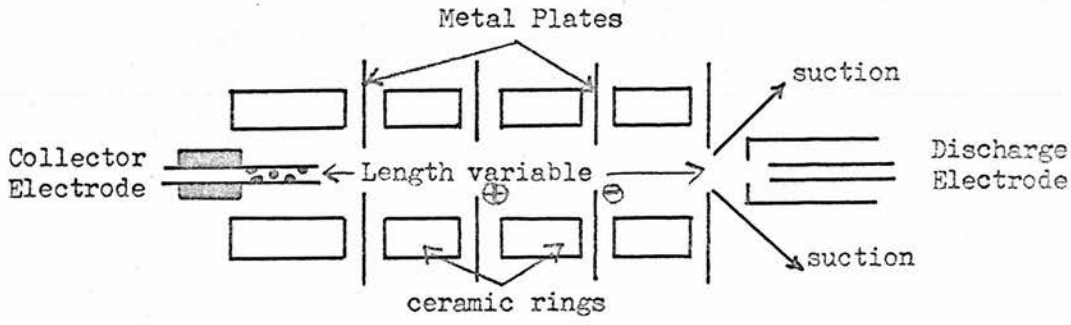

Figure 78: Schematic illustration of photo-ionisation detector (after Nicholls)

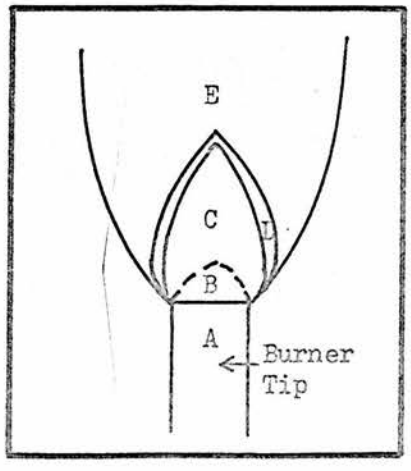

Figure 79: Flame zones schematic.

Reprinted from **ANALYTICAL CHEMISTRY**, Vol. 35, Page 449, April 1963

The Spreading of Air Peaks in Capillary and Packed Gas Chromatographic Columns

J. H. KNOX and LILIAN McLAREN

Department of Chemistry, University of Edinburgh, Scotland

▶ Current theories for the spreading of packets of unsorbed substances in gas chromatographic columns are considered. It is shown that the usual *HETP* equations can be cast into reduced forms and that various column parameters, in particular the geometrical parameters A and A', can be found by curve fitting. The method is applied to the data from a capillary and a packed column. It is shown that within experimental error the Golay equation is obeyed quantitatively. The diffusion coefficient for ethylene in nitrogen is found to be 0.16 cm.^{2} sec.$^{-1}$ Comparison of the *HETP*'s for the capillary and packed column show that the tortuosity factor for glass beads is about 0.8. There is little evidence for eddy diffusion or coupled eddy diffusion as envisaged by Giddings. The eddy diffusion parameter λ is less than 0.15. The gas phase mass transfer coefficient is $C_g = 0.3 \times d_p^2/D_g = 0.0045$ second.

THE SPREADING of bands in gas chromatographic columns is usually considered in relation to an *HETP* equation. The commonest form of such equation can be written

$$H = L(\sigma/l_R)^2 = A + B/u + Cu \quad (1)$$

where u is the linear gas velocity in the column. A is the contribution to the *HETP* from the structural inhomogeneity of the column and is purely geometrical in nature. For open tubes A is zero. B/u results from longitudinal diffusion in the gas phase and Cu from the failure to attain complete equilibrium in and between the gas and liquid phases. The factor C is usually made up of several terms, one for each slow process contributing to the nonequilibrium. In the original van Deemter equation (*5*) only resistance to mass transfer in the liquid phase was considered to be important in making up C. However, Golay (*15*) in his treatment of open tubes showed that resistance to mass transfer in the gas phase should also be considered. Its practical importance for open tubes or capillaries has been established by Desty (*8*) and Scott (*22*). Golay pointed out that contrary to general belief resistance to mass transfer in the gas phase should be much more important in packed columns than in open tubes because of the irregularity of the packing. Recent work has supported this. C_g is often comparable with C_l and in certain cases considerably greater. Dal Nogare and Chiu (*4*) for example have established that C is definitely nonzero for both weakly and strongly sorbed substances. For both types C_l should theoretically be zero and C is therefore due entirely to slow processes in the gas phase. Norem (*20*) has shown that there is a distinct upward trend in the *HETP vs.* u curves for unsorbed peaks and hence C_g must have a significantly positive value. This is supported by the results of Kieselbach (*17*) although his curves for air peaks show only a flattening at high gas velocities.

Several attempts have been made to treat gas phase mass transfer in packed columns quantitatively, but the problem is difficult because of the complex geometry of a randomly packed bed. Nevertheless substantial progress has been made by Jones (*16*), van Deemter (*6*), and Giddings (*9*, *10*) although all treatments leave undetermined a number of geometrical constants.

Giddings (*11*) has criticized Equation 1 on the grounds that it misinterprets the role of the structural factors. He points out that the tortuosity of the

stream lines in a packed column will tend to assist mass transfer. Thus a molecule in any stream will wander (even in the absence of lateral diffusion) from low to high velocity regions and will from time to time approach the surfaces of particles quite closely. There are thus two alternative ways in which a molecule may move across the gas stream and so encourage mixing of the gas, or approach closely to a particle surface so encouraging mass transfer. These are diffusion across the gas stream and movement along a tortuous stream line. Since the two effects are complementary they should be compounded like resistances in parallel rather than resistances in series, and their combined contribution to H should be written

$$H_g = (1/A' + 1/C_g u)^{-1} \qquad (2)$$

This value is of course less than $C_g u$. Whereas the classical eddy diffusion term A was expected to be of the order of the particle diameter, Giddings' parameter A' should be much larger, possibly some 10 particle diameters. The effect responsible for A' has been called coupled eddy diffusion (*11*). The process envisaged by Giddings which aids mass transfer in the gas phase appears to us to differ from the classical eddy diffusion as envisaged by van Deemter although it still derives from the geometry of the packing. Giddings (*12*) describes classical eddy diffusion as follows: "It arises from the nonequivalence in velocity of various flow paths which a fluid and solute follow in migrating through a porous support. The less tortuous higher velocity paths lead some solute to a position in advance of the bulk solute and vice versa. Because a random distribution of flow paths exists the resulting band spreading is random and the subsequent concentration profile Gaussian." The process so described does not assist mass transfer in the gas phase. Nevertheless, as the molecules of solute follow these tortuous paths they also move from regions of high to regions of low gas velocity which will aid mixing, and from time to time approach so closely to the surface of particles that the diffusional path thereto is substantially reduced which assists mass transfer. It therefore appears to us that both types of structural effect should be considered in a complete equation for the *HETP*, at least for purposes of discussion. Such an equation would read:

$$H = A + B/u + (1/A' + 1/C_g u)^{-1} + C_l u \qquad (3)$$

This equation is unfortunately too complex for a simple experimental test because of the different effects of column pressure drop on C_g and C_l (*13*), and the necessity for covering a wide range of u to isolate the different parameters. However, the equation is much simplified if consideration is restricted to unsorbed substances. C_l is now zero and both the second and third terms are pressure invariant since the pressure dependent quantities u and D_g appear only as the pressure independent ratio u/D_g. D_g and u can thus be taken to have constant values equal to those at the outlet of the column. The *HETP* equation now takes the simplified form

$$H = A + 2\gamma D_g^o/u^o + (1/A' + D_g^o/(\omega d_p^2 u^o))^{-1} \qquad (4)$$

The parameter ω introduced by Giddings (*9*) represents the square of the average distance in particle diameters that a solute molecule diffuses during the period of the gas phase equilibration process. According to Giddings ω is expected to be about unity for a packed column. This has been confirmed by the experiments of Norem (*20*) and Dal Nogare and Chiu (*4*). It is of interest to consider what value ω would take if a packed column could indeed be regarded as equivalent to a bundle of capillaries with the same linear flow resistance. The Kozeny-Carman equation (*1*) shows that a column of randomly packed spheres has the same linear flow resistance as a capillary whose radius is 0.135 times the particle diameter. If r in the Golay equation is replaced by 0.135 d_p, the factor C_g for $k = 0$ becomes $C_g = r^2/24D_g = d_p^2/1300D_g$ hence $\omega = 1/1300$. This comparison illustrates the enormous difference in performance between a packed and capillary column as far as gas phase mass transfer is concerned, and it encourages the hope that there is room for substantial improvement in the design of the former.

In the present work we have attempted to obtain information on the magnitudes of A, A' and ω for a packed column with unsorbed gas samples, and to verify the Golay equation quantitatively. The capillary column was 1664 cm. of 0.88-mm. i.d. nylon tubing and the packed column was four 150-cm. lengths of 3.8-mm. tubing packed with 0.50-mm. diameter glass beads.

When $A' = \infty$ Equation 4 reduces to the van Deemter form, Equation 1. This equation is symmetrical in u and $1/u$ and can be cast into a reduced form

$$h = v^{-1} + \alpha + v \qquad (5)$$

where $h = H/(BC)^{1/2}$; $v = u(C/B)^{1/2}$; and $\alpha = A/(BC)^{1/2}$. Plots of log h against log v are therefore symmetrical about the log v axis and show minima at $h = 2 + \alpha$ and $v = 1$. A series of such plots for different values of α is given in Figure 1. The asymptotes to all curves are the same, and it is worth noting that the critical region for determining α is that around the minimum. Plots of Log H against Log u^o for any set of experimental data obeying Equation 1 must fit one of the theoretical curves apart from a displacement of the origin. It should therefore be a relatively simple matter in practice to show whether or not Equation 1 is obeyed and if it is to determine α by curve fitting. This method of determination is superior to methods such as extrapolation of the "straight" parts of H *vs.* u^o or H *vs.* $1/u^o$ plots since these place undue emphasis on values of H obtained at high or low gas velocities while ignoring the most important points which are those in the vicinity of the minimum H. A logarithmic plot is also more satisfactory for the determination of the probable error in A or α since the proportional error in u^o or H can readily be accommodated by making the points of a representative size. Generally the percentage error in H and u^o will be the same for all readings, and all points can be made the same size in plotting the experimental data on a logarithmic scale.

For an accurate determination of the eddy diffusion parameter A or α, two requirements should be met. Firstly the region around the minimum H should be carefully mapped so that both H_{min} and u_{opt} are accurately determinable. Secondly the position of the asymptotes on both sides of the minimum should be reasonably clear. Ideally it is desirable to cover a hundredfold range of gas velocity so that at both high and low gas velocities eddy diffusion can be assumed to play an insignificant part in peak spreading. This is some 10 times the range usually covered and a really effective experiment will put a considerable strain on the experimental technique.

When $A = 0$ Equation 4 reduces to that suggested by Giddings (*11*):

$$H = B/u + (1/A' + 1/C_g u)^{-1} \qquad (6)$$

The reduced form of this equation is written

$$h = v^{-1} + (1/\alpha' + 1/v)^{-1} \qquad (7)$$

where h and v have the same meaning as before and $\alpha' = A'/(BC)^{1/2}$ This equation is no longer symmetrical in v and $1/v$ and shows a minimum h only when $\alpha' > 1$. The minimum is then at $h = 2 - 1/\alpha', v = (1 - 1/\alpha')^{-1}$. Plots of log h against log v for different values of α' are given in Figure 2. The left-hand asymptote is the same for all curves and indeed on the low velocity side there is little difference between curves for different values of α'. The right-hand asymptotes on the other hand differ and are horizontal at $h = \alpha'$. All curves for $\alpha' > 1$ show inflection points. The effect represented by A' can therefore be observed only in experiments carried out at gas velocities

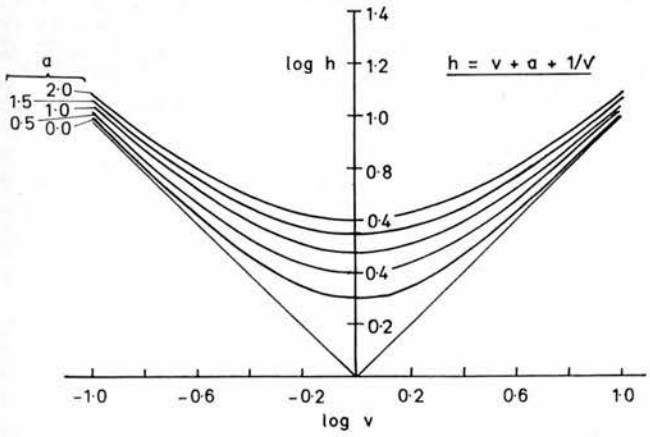

Figure 1. Logarithmic plot of reduced *HETP* against reduced linear gas velocity, $h = v + \alpha + 1/v$ with various values of α

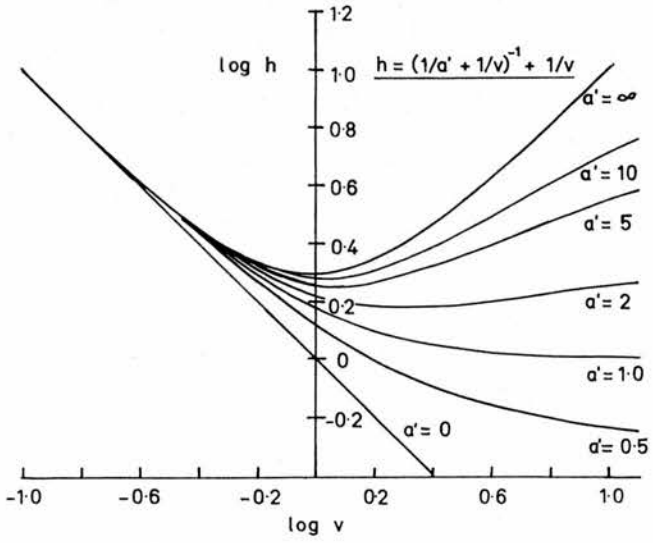

Figure 2. Logarithmic plot of reduced *HETP* against reduced linear gas velocity, $h = 1/v + (1/\alpha' + 1/v)^{-1}$ with various values of α'

considerably above those for minimum H. The curve fitting method clearly provides a general method for determining both A and A'. For the general case it would be necessary to provide theoretical curves for all possible combinations of α and α'. However a reasonable estimate of α and α' can be made by using the low velocity part of the curve to determine α and the asymmetry of the curve to determine α'.

Experimental work on the determination of A has been reviewed by Giddings (*12*). The main features of the data are their irreproducibility, the appearance of values of A much less than d_p, and the appearance of negative values of A. The view is now becoming general that A is probably close to zero for well constructed columns and that nonzero values result from imperfections in the rest of the apparatus. Littlewood (*19*) and Kieselbach (*18*) have for example shown that positive values of A can arise from a finite sample volume and from bad geometry of the column inlet and outlet. Other features which are likely to contribute to spurious eddy diffusion terms are dead volumes throughout the apparatus. Such dead volumes will normally result in tailed peaks. Both effects are likely to be more important with substances which have low retention times. In this connection it is significant that the early peaks in chromatograms are usually less symmetrical than later peaks. Negative values of A which have been reported several times (*3, 8, 19*) resulted in one case (*3*) from the use of average instead of outlet gas velocity but may also be explained by supposing a finite time constant for the injector or detector. The effect of this would be to add a finite width to any peak such that at high gas velocities an increasing proportion of the total peak width would be due to the time constant of the apparatus. Values of H at high flow rates would be too large and the dependence of H upon u too steep. Any method of analysis which laid emphasis on the points for high gas velocities (for example the extrapolation method) and assumed an *HETP* equation of form 1 would be likely to give negative values of A. In our own experiments this effect was significant. As with a finite sample volume this effect would be most serious for early peaks.

There is almost no experimental work on the possible magnitude of A'. Norem (*20*) has shown that there is a definite minimum in the *HETP vs. u* curve for air peaks in a packed column. Thus α' is likely to be at least two and probably greater than five (see Figure 2). Since $(BC)^{1/2}$ is generally of the order of d_p [Bohemen and Purnell's data (*3*) give $(BC)^{1/2}/d_p$ between 0.8 and 2.5 and values for air peaks are likely to be in the lower range], A' is probably at least five particle diameters. Unfortunately, to determine A' it is necessary to work in the high velocity region where any inadequacy in technique is likely to make the experimentally determined H too large to an increasing degree as u increases. Until the value of A' is clearly established by a number of different workers any published values must be regarded as upper limits.

EXPERIMENTAL

The main experimental difficulties in determining the spreading of air peaks in a gas chromatographic column have been noted by Norem (*20*). They are first, the difficulty of measuring peak widths accurately when they may be only some 100 mseconds, and second, the difficulty of isolating the spreading due to the column alone and eliminating that caused by external factors (injector, detector, etc.). Considerable care has to be taken to devise fast injectors and column arrangements which minimize dead space. Even so it is advisable to carry out experiments with long and short columns (*12*) and to subtract out the spreading due to the apparatus. Since the total spreading due to a number of independent or consecutive processes is given by

$$\sigma^2 = \sigma_1^2 + \sigma_2^2 + \sigma_3^2 + \ldots \qquad (8)$$

the spreading due to the column alone may be obtained from the total spreading and that due to the apparatus from the formula

$$w^2_{\text{column}} = w^2_{\text{total}} - w^2_{\text{apparatus}} \qquad (9)$$

In the present work, in spite of all precautions it was necessary to make this correction to the observed peak widths. At the highest gas velocities $w_{\text{apparatus}} = 0.44\ w_{\text{total}}$ and $w^2_{\text{column}} = 0.80\ w^2_{\text{total}}$.

We have evaluated the peak width by electronic measurement of the peak area and peak height. For this method to be reliable the peaks must be highly symmetrical. This was checked for peaks wider than 2 seconds by a $^1/_4$-second Brown recorder at a chart speed of 12 inches min.$^{-1}$ If the peaks are Gaussian the peak width is

$$w = \text{area}/\text{height} = \sqrt{2\pi}.\sigma = 2.51\sigma \qquad (10)$$

(it should be noted that w defined here differs from the usual "base width" equal to 4σ) and the number of plates in the column is

$$N = (t_R/\sigma)^2 = 2\pi(t_R/w)^2 \qquad (11)$$

Ethylene was used as solute and nitrogen was used as the carrier gas. A flame ionization detector was used because of its low detection volume and time constant. Hydrogen was added after the column at a rate of 30 ml. per min.$^{-1}$ and air was supplied at about 1000 ml. per min.$^{-1}$ The detector design was essentially that of Desty (*7*) except that a gauze basket was attached to the jet which served as the negative electrode. This increased the

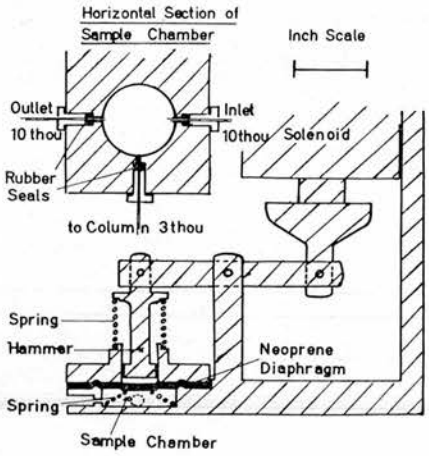

Figure 3. Details of hammer injector

(1 thou = 0.001 inch)

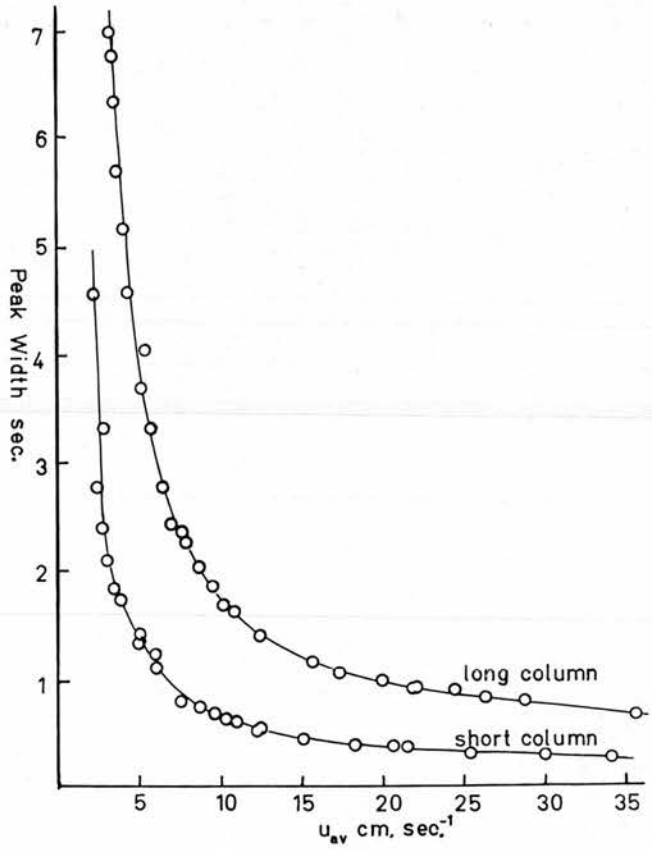

Figure 4. Variation of peak width with average linear gas velocity for long and short packed columns

linear range of the detector. The signal from the detector was supplied to an amplifier with a time constant of 10 mseconds and a most sensitive range of 5 volts per 10^{-9} amp. input. The signal was fed to an integrator and peak holding unit which stopped an electronic timer when the peak maximum was reached. The switch which started the timer also triggered the injector. Thus for each injection three parameters were recorded: retention time (seconds), peak height (volts), and peak area (volt seconds).

The injector was of the "hammer" type described by Scott (*21*). The original injector was redesigned for use with gases and details are shown in Figure 3. Ethylene was passed continuously through the injector chamber at a pressure slightly below that of the inlet to the column. This pressure was maintained by a rubber bladder containing ethylene which was mounted inside a glass bulb, itself held at a pressure slightly below that of the column by a slow leak through it from the column inlet to atmosphere. The line leading from the bladder to the injector was a piece of 0.25 mm. i.d. nylon and that from the injector to the column a 15-cm. length of 0.08 mm. i.d. nylon tubing. Because of the pressure drop between the column inlet and the injector chamber this piece of fine nylon tubing was continually purged by pure carrier gas. A small sample could be injected into the column (about 1 mm.^{3}) by energizing the solenoid which worked the hammer and momentarily compressed the gas in the chamber. The tube from the injector was led directly into the column to eliminate dead space. It was hoped that this type of injector would have a very small time constant but our results indicate that it may actually be as high as 0.2 second.

The connection of the columns to the detector was as direct as possible. With the capillary column (1664 cm. of 0.88-mm. i.d. nylon) the end was drawn down slightly and pushed well into the 1.6-mm. diameter hole leading to the 0.32-mm. diameter jet. With the packed column a piece of 0.88-mm. diameter nylon took part of the emergent gas stream to the detector while the remainder continually purged the inlet to this tube and so eliminated any stagnant backwaters. The proportion which passed to the detector could be varied by a needle valve on the rejected stream and was usually arranged so that a convenient size of sample passed to the detector. Under the best operating conditions the detector was slightly overloaded and therefore nonlinear. The effect was not great but to obtain the most reproducible results it was necessary to work to a constant peak height.

The packed column consisted of four 150-cm. lengths of 3.8-mm. diameter tubing packed with 0.50-mm. diameter glass beads. The packing was retained by 200-mesh gauze screens (*18*) held in position with glass tubing which just fitted inside the tube used for the column. The four lengths were connected together by short lengths of the 2-mm. i.d. tubing used to retain the screens.

To eliminate apparatus errors experiments were carried out with short columns, a 40-cm. length of capillary and a packed column consisting of 4- × 10-cm. lengths joined together in the same way as the 4- × 150-cm. lengths. Experiments with these columns showed that a significant part of the peak spreading was caused by factors outside the main columns. This is illustrated in Figure 4 for the packed column.

The peak widths for the short columns tend to a constant value as the velocity is increased. This suggests that the time constant of either the injector or detector was not as low as had been hoped. It is most probable that the delay occurred in the injector.

RESULTS AND DISCUSSION

The *HETP*'s derived from the corrected peak widths are plotted logarithmically in Figures 5 and 6 for the capillary and the packed columns. Values of various parameters derived from the plots are listed in Table I.

The points for the capillary column fit the theoretical curve $\alpha = 0$, $\alpha' = \infty$ within experimental error as expected for the Golay equation. The minimum *HETP* is 0.34 mm. compared with the theoretical value of $r/1.732 = 0.26$ mm. predicted by Golay. The somewhat higher experimental value may be due to overloading the detector. This point is being investigated. The linear gas velocity, u_{opt}, for minimum *HETP* is 11 cm. sec.$^{-1}$ From the Golay equation $u_{opt} = \sqrt{48} \times D_g/r$. Hence $D_g = 0.16$ cm.^{2} sec.$^{-1}$ This value compares with that derived from measurements on open tubes by Bohemen and

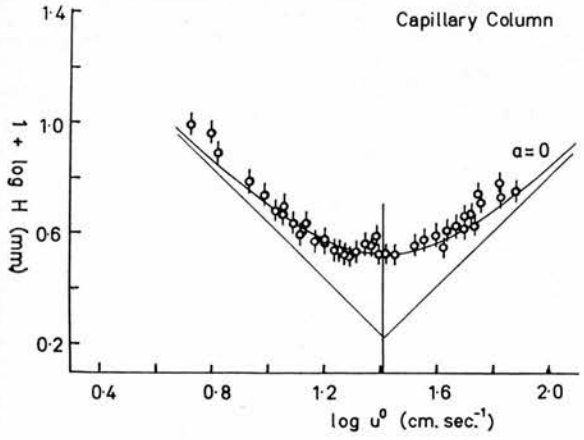

Figure 5. Logarithmic plot of *HETP* against u^0 for capillary column

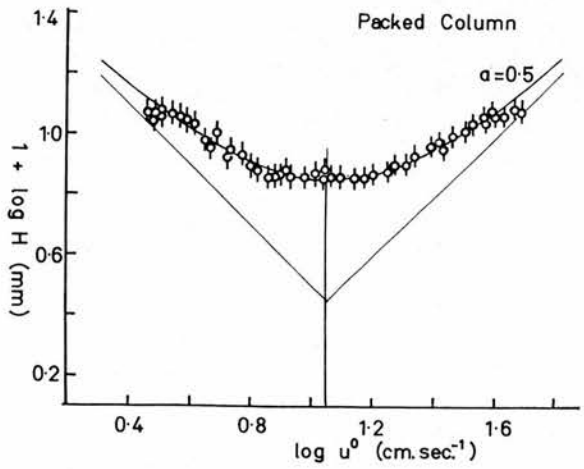

Figure 6. Logarithmic plot of *HETP* against u^0 for packed column

Purnell (*2*) for carbon dioxide in nitrogen (0.19 cm.^{2} sec.$^{-1}$). For CO_2 and C_2H_4 in N_2 the Gilliland equation (*14*) gives 0.13 and 0.12 cm.^{2} sec.$^{-1}$, respectively.

The plot for the packed column shows a higher degree of consistency than that for the capillary, the maximum error being about 5% in H or 2% in w. There is no evidence of asymmetry in the plot from which we may deduce that Giddings' geometrical parameter $\alpha' > 10$, and may be infinite. The classical eddy diffusion parameter α is certainly small. The best fit between the theoretical curves and the experimental data is with $\alpha = 0.5$. However, the points around the minimum are better fitted by $\alpha = 0$. There is therefore little evidence that structural inhomogeneity contributes to the *HETP* in a relatively narrow packed column (column diameter/particle diameter = 7.5). The minimum *HETP* is 0.71 mm. or $1.4 \times d_p$. Thus $A < 0.14$ mm. or $0.3 \times d_p$ and λ in the van Deemter equation is less than 0.14; $A' > 3.5$ mm. or $7 \times d_p$. The small value of A is in agreement with the results of Giddings and Robinson (*12*) and the prevailing evidence is that the eddy diffusion parameter is zero. The tortuosity factor γ in the van Deemter equation is readily determined by comparing the positions of the low velocity asymptotes for the capillary and packed columns. The value of γ depends somewhat on the values taken for α and α'. For the various reasonable combinations we obtain $\alpha = 0$, $\alpha' = \infty$, $\gamma = 0.85$; $\alpha = 0.5$, $\alpha' = \infty$, $\gamma = 0.70$; $\alpha = 0$, $\alpha' = 10$, $\gamma = 0.75$. Any of these values are acceptable and are in general agreement with previous estimates (*2*, *19*). Using the value of D_g obtained from the capillary the parameter ω (Equation 4) may be evaluated for each set of α and α'. If $\alpha' = \infty$, $H_{mix} = (2 + \alpha)(2\gamma\omega)^{1/2}.d_p$; if $\alpha = 0$, $H_{min} = (2 - 1/\alpha')(2\gamma\omega)^{1/2}.d_p$.

The value of ω like γ depends on the values taken for α and α': for $\alpha = 0$, $\alpha' = \infty$, $\omega = 0.30$; $\alpha = 0.5$, $\alpha' = \infty$, $\omega = 0.23$; $\alpha = 0$, $\alpha' = 10$, $\omega = 0.36$. These values agree well with that deduced from Norem's results (*9*, *20*). They indicate that a solute molecule must on the average diffuse about half a particle diameter within the time constant of the equilibration process. This compares with about one tenth of the tube diameter in a round capillary. Since the particle diameter in a packed column is about four times the diameter of the capillary which has the same linear flow resistance the solute molecule must have to diffuse about 20 times as far in the packed column as in the equivalent capillary. The whole process of gas phase mass transfer is thus about 400 times as slow. This difference emphasizes the great difference in the speed of analysis possible with the present types of packed columns when compared with capillaries and fully substantiates Golay's original suggestion. One of the present challenges in gas chromatography is to produce a packed column structure which has a higher permeability than the conventional packed column and a lower gas phase mass transfer coefficient.

LIST OF SYMBOLS

- A = eddy diffusion coefficient
- A' = Giddings' coupled eddy diffusion coefficient
- α, α' = reduced eddy diffusion terms (Equation 5)
- B = longitudinal diffusion coefficient
- C = nonequilibrium coefficient
- C_g, C_l = coefficients for resistance to mass transfer in gas and liquid phases
- γ = tortuosity factor, $B = 2\gamma D_g$
- D_g = gas phase diffusion coefficient of solute in carrier gas
- D_g^o = value of D_g at column outlet
- d_p = particle diameter in packed column

Table I. Column Operating Conditions and Experimental Parameters

	Packed	Capillary
Length	593 cm.	1664 cm.
Diameter of tube	0.38 cm.	0.088 cm.
Diameter of beads	0.050 cm.	...
Carrier gas	Nitrogen	Nitrogen
Solute	Ethylene	Ethylene
Temperature	18° C.	18° C.
Outlet pressure	Atmospheric	Atmospheric
H_{min}	0.071 cm.	0.034 cm.
u_{opt}	11 cm. sec.$^{-1}$	26 cm. sec.$^{-1}$
α	<0.5	Zero
α'	>10	Infinite
D_g (C_2H_4 in N_2)		0.16 cm.^{2} sec.$^{-1}$
Tortuosity, γ	$\alpha = 0$ $\alpha' = \infty$ 0.85	
	$\alpha = 0.5$ $\alpha' = \infty$ 0.70	
	$\alpha = 0$ $\alpha' = 10$ 0.75	
ω	$\alpha = 0$ $\alpha' = \infty$ 0.30	
	$\alpha = 0.5$ $\alpha' = \infty$ 0.23	
	$\alpha = 0$ $\alpha' = 10$ 0.36	
A and A'	<0.014 cm. >0.35 cm.	
A/d_p and A'/d_p	<0.28 >7	
$(BC)^{1/2}$	0.035 cm.	0.017 cm.
$(BC)^{1/2}/d_p$ and $(BC)^{1/2}/2r$	0.71	0.19
H_{min}/d_p and $H_{min}/2r$	1.42	0.39

H = height of a theoretical plate (*HETP*)
H_{min} = minimum *HETP*
h = reduced *HETP* (Equation 5)
k = column capacity coefficient = amount of solute per unit length in liquid phase divided by amount per unit length in gas phase
L = column length
λ = eddy diffusion parameter, $A = 2\lambda d_p$
N = number of theoretical plates in column
r = radius of capillary
σ = standard deviation
t_R = retention time
u = linear gas velocity
u^o = value of u at column outlet
u_{opt} = linear gas velocity at minimum *HETP*
v = reduced linear gas velocity (Equation 5)
w = peak width (Equation 10)
ω = parameter in gas phase mass transfer coefficient (Equation 4)

ACKNOWLEDGMENT

The authors are very much indebted to Bruce Peebles Ltd., Edinburgh, for designing and providing the integration and peak height measuring unit, and to the British Petroleum Co. Ltd., for a gift in aid of the research. Without this assistance the work could not have been carried out.

LITERATURE CITED

(1) Carman, P. C., "Flow of Gases through Porous Media," Butterworths, London, 1956.
(2) Bohemen, J., Purnell, J. H., *J. Chem. Soc.* **1961,** 360.
(3) Bohemen, J., Purnell, J. H. "Gas Chromatography 1958," Ed. Desty, p. 6, Butterworths, London, 1958.
(4) Dal Nogare, S., Chiu, J., ANAL. CHEM. **34,** 890 (1962).
(5) Deemter, J. J. van, Zuiderweg, F. J., Klinkenberg, A., *Chem. Eng. Sci.* **5,** 271 (1956).
(6) Deemter, J. J. van, *Gas Chromatography Symposium,* U. S. Public Health Service, Cincinnati, Ohio, 1957.
(7) Desty, D. H., Geach, C. J., Goldup, A., "Gas Chromatography 1960," Ed. Scott, p. 46, Butterworths, London, 1960.
(8) Desty, D. H., Goldup, A., "Gas Chromatography 1960," Ed. Scott, p. 162, Butterworths, London, 1960.
(9) Giddings, J. C., ANAL. CHEM. **34,** 1186 (1962).
(10) Giddings, J. C., *J. Chromatog.* **2,** 44 (1959).
(11) Giddings, J. C., *Nature* **184,** 357 (1959). *J. Chromatog.* **5,** 61 (1961).
(12) Giddings, J. C., Robison, R. A., ANAL. CHEM. **34,** 885 (1962).
(13) Giddings, J. C., Seager, S. L., Stucki, L. R., Stewart, G. H., *Ibid.,* **32,** 867 (1960).
(14) Gilliland, E. R., *Ind. Eng. Chem.* **26,** 681 (1934).
(15) Golay, M. J. E., "Gas Chromatography 1958," Ed. Desty, p. 36, Butterworths, London, 1958.
(16) Jones, W. L., ANAL. CHEM. **33,** 829 (1961).
(17) Kieselbach, R., *Ibid.,* **33,** 23 (1961).
(18) Kieselbach, R., *Ibid.,* **33,** 806 (1961).
(19) Littlewood, A. B., "Gas Chromatography 1958," Ed. Desty, p. 23, Butterworths, London, 1958.
(20) Norem, S. D., ANAL. CHEM. **34,** 40 (1962). (See also Dal Nogare, S., Juvet, R. S., "Gas-liquid Chromatography," p. 140, Interscience, New York, 1962.)
(21) Scott, R. P. W., Private communication.
(22) Scott, R. P. W., Hazeldean, G. S. F., "Gas Chromatography 1960," Ed. Scott, p. 144, Butterworths, London, 1960.

RECEIVED for review December 11, 1962. Accepted February 5, 1963. Presented at the International Symposium on Advances in Gas Chromatography, University of Houston, Houston, Texas, January 21–24, 1963.

PRINTED IN U. S. A.

Reprinted from **ANALYTICAL CHEMISTRY**, Vol. 36, Page 1477, July 1964

A New Gas Chromatographic Method for Measuring Gaseous Diffusion Coefficients and Obstructive Factors

JOHN H. KNOX[1] and LILIAN McLAREN

Department of Chemistry, University of Edinburgh, Edinburgh, Scotland

▶ A new elution method is described for the determination of gaseous diffusion coefficients and obstructive factors (D_g and γ). It has a standard deviation of about 2%. A narrow band of an unsorbed solute is injected into a column and eluted part way down. The flow is arrested and the band is allowed to spread by diffusion for different times. The band is then eluted from the column at a precisely known velocity and its concentration profile is determined by a suitable gas chromatographic detector. D_g or γD_g is determined from the gradient of a plot of (peak width)^2 against time of residence in the column. Experiments with open tubes gave D_g = 0.165 sq. cm. second^{-1} for ethylene in nitrogen at 18° C. and 750 mm. of Hg. Experiments with conventionally packed columns gave the following values of γ for glass beads, firebrick, and Celite, respectively: 0.60, 0.46, and 0.74. These values are interpreted in terms of the tortuosity and constriction of the diffusion paths. The reality of the two factors contributing to the obstructive parameter is verified by comparison of the calculated and measured values of γ for a series of columns composed of a single row of spherical beads in a closely fitting glass tube. Agreement is within 2% for all columns studied.

When an infinitely thin slice of a gas B spreads by diffusion into another gas A the concentration profile of B in A after a finite time t is gaussian and the rate of spreading is given by the equation

$$d\sigma_x^2/dt = 2D_g \quad (1)$$

where σ_x is the standard deviation of the gaussian concentration profile measured as a distance, and D_g is the diffusion coefficient of B in A. Equation 1 holds for axial diffusion in a uniform empty tube, but if the tube contains obstructing, but not sorbing, material, diffusion is hindered and

$$d\sigma_x^2/dt = 2\gamma D_g \quad (2)$$

where γ is less than unity and in gas chromatography has usually been called the "tortuosity factor". The term is unfortunate since the tortuosity of paths through a packed bed is only one factor contributing to the obstruction. In this paper, following Giddings (*8*), we shall call γ the "obstructive factor."

D_g could evidently be determined by inserting a slice of B into a tube containing A and measuring σ_x^2 as a function of time, but this is not generally possible in practice and an elution method must be used where the time variance, σ_t^2, of the eluted band rather than the length variance, σ_x^2, is measured. If the spreading band moves slowly down the column at a constant linear velocity, u, longitudinal diffusion will occur at the same rate as if the band were static. In an empty tube, if u is sufficiently low, other sources of spreading may be made insignificant. Since $\sigma_x/\sigma_t = u$, diffusional spreading is given by

$$d\sigma_t^2/dt = 2D_g/u^2 \quad \text{(empty tube)} \quad (3)$$

$$d\sigma_t^2/dt = 2\gamma D_g/u^2 \quad \text{(packed tube)} \quad (4)$$

The speed of movement of the band along the column is $u = f/A_o e$, where f = volume flow rate (cc. second^{-1}), A_o = area of tube when empty (sq. cm.), and e = total porosity of the packing = (volume of gas in packed column)/(volume of gas in empty column). If the gas B were sorbed by the column the apparent diffusion coefficient would be $\gamma D_g/(1 + k)$ where k is the column capacity ratio; u would still be the band velocity but would be $(1 + k)$ times lower than velocity of an unsorbed band.

There are two elution methods for determining D_g and γ, the continuous elution method hitherto used and the arrested elution method now described.

The continuous elution method has a number of distinct variants. In experiments specifically designed to determine D_g or γD_g, a band (*3*, *7*) or front (*12*) of an unsorbed gas is driven slowly down a column at a series of sufficiently low gas velocities that spreading from slowness of mass transfer in the gas phase is either negligible or can easily be allowed for. An interesting modification is the pulsed flow method of Carberry and Bretton (*5*) in which the rate of degeneration of a sinusoidal concentration profile is measured.

These methods are applicable to both

[1] Corresponding author. Address until September 30, 1964, Department of Chemistry, University of Utah, Salt Lake City, Utah.

open and packed tubes but suffer from the disadvantages inherent in operation at low flow rates; from the difficulty of correctly allowing for instrumental spreading outside the column; and with packed columns, from the uncertainty as to the role of "eddy diffusion," which may interact in a complex way with gas phase mass transfer processes (*8*).

More generally γD_g has been determined from *HETP* measurements of either sorbed or unsorbed solutes in packed columns (*1*, *14–18*) the measurements covering a range of velocities around u_{opt}—i.e., the velocity giving the minimum *HETP*. The measurements are not made specifically in the low velocity region and do not usually extend far into this region. By obtaining the best fit between the experimental data and an assumed *HETP* equation, such as the van Deemter equation, the parameter $B = 2\gamma D_g$ is obtained; γ is generally found by assuming a theoretical value of D_g. This method suffers from a disadvantage, additional to those mentioned above, that the assumed form of the *HETP* equation may be incorrect.

Neither of these variants is of very high precision and the best values of γ cannot be considered to be accurate to better than about 10%. Published values range from 0.5 to 0.75 with a concentration of values around 0.6: it is not clear whether γ is dependent upon the nature of the packing material.

The continuous elution method for the determination of D_g has been much improved by Giddings and Seager (*9–11*, *20*), who have employed the full potentialities of the open tube. They use a gas velocity which differs from that required for minimum *HETP* by a factor of at least two, either higher or lower. D_g may then be derived by solving the Taylor-Golay equation (*21*). Values obtained by this method have standard deviations of about 2%. The difficulties associated with the use of very low flow rates can thus be avoided. Unfortunately the method is not applicable to the determination of γ since the magnitude and functional dependence of the gas phase mass transfer coefficient in packed columns is not yet established.

The arrested elution method bypasses most of the experimental and theoretical difficulties met with in the continuous elution method. It is applicable equally to open or packed tubes and it is of intrinsically higher precision than the continuous methods based upon *HETP* measurements. The method is as follows. A sharp band of an unsorbed gas B is injected into the column and eluted at a controlled and measurable velocity. When the band is about half way down the column

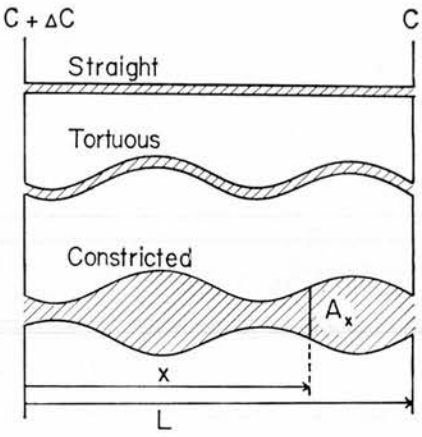

Figure 1. Various idealized types of paths

the gas flow is arrested for a time, t, during which spreading can occur only by diffusion. Finally the band is eluted from the column and its concentration profile and standard deviation determined by the detector. Provided that B is not sorbed by the column, Equations 3 and 4 hold for the additional variance produced by diffusion during the delay period if u is taken as the outlet elution velocity, u_o. The variance produced by the injector, column connections, detector, and elution along the column are now the same whatever the delay and can accordingly be subtracted out. Thus a plot of σ_t^2 against delay should be a straight line of gradient $2D_g/u_o^2$ or $2\gamma D_g/u_o^2$. The intercept at zero delay is the variance introduced by the standard procedure.

Since u_o occurs to the second power in Equations 3 and 4, its accurate measurement is vital to the precision of the method. In the examples given later an overall reproducibility of about $\pm 2\%$ is achieved.

THE INTERPRETATION OF γ

Boyack and Giddings (*4*) have given a theoretical treatment of electrophoresis in stabilized media which Giddings (*8*) has suggested can be applied with minor modifications to longitudinal diffusion in gas chromatography. Boyack and Giddings suggest that obstruction to electrophoresis can arise from two effects: (1) the tortuosity of the paths through the medium, and (2) the alternating constriction and widening of the paths along which typical particles move and along which a varying potential gradient is inevitably established.

As applied to gas chromatography these two factors may be illustrated as follows:

(1) Tortuosity. If a concentration difference Δc is established between two planes a distance l apart (Figure 1), the time taken for the average molecule to diffuse along a tortuous path S, of length s, is greater than that along a straight path L. There are two reasons for this: (a) the distance along S is greater by the factor $T = s/l$, and (b) the concentration gradient along S is lower in the same ratio. Thus the average time for diffusion along S is greater than along L by a factor T^2 and the apparent axial diffusion coefficient along S is

$$D_g(\text{apparent}) = T^{-2}D_g$$

Thus tortuosity contributes a factor T^{-2} to the obstructive factor.

(2) Constriction. Figure 1 also shows a tube of variable cross section, A_x. If a concentration difference, Δc, is set up between two planes a distance l apart, an equal number of molecules must diffuse per second across every section of the tube when a steady state is reached. This implies that the concentration gradient along the tube is not uniform but is greater in the narrow sections than in the wide sections. The rate of passage, R, of molecules across any section of the tube is

$$R = \text{constant} = D_g A_x(dc/dx) \quad (6)$$

The average time of diffusion of a molecule along the tube is

$$t = \int_o^l A_x c R^{-1}\, dx \quad (7)$$

If $c >> \Delta c$ the average time of passage is

$$t = cR^{-1}\int_o^l A_x dx = cR^{-1}\bar{A}l \quad (8)$$

where $\bar{A}$ is the mean cross-sectional area of the column. Since

$$\Delta c = \int_o^l dc = RD_g^{-1}\int_o^l dx/A_x \quad (9)$$

R may be eliminated from Equation 8 to give

$$t = (c\bar{A}l/\Delta c\, D_g)\int_o^l dx/A_x \quad (10)$$

If the tube is uniform, the time for diffusion, t_o, is

$$t_o = cl^2/\Delta c\, D_g \quad (11)$$

hence the constriction factor, C, is

$$C = t_o/t = l\left[\bar{A}\int_o^l dx/A_x\right]^{-1} \quad (12)$$

Thus C can be calculated for any specifiable geometry. The complete obstructive factor is then

$$\gamma = CT^{-2} \quad (13)$$

In a packed bed the situation at first appears more complex than that illustrated formally in Figure 1 since there

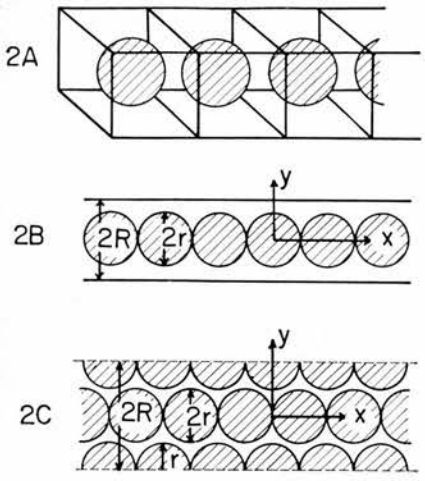

Figure 2. Models for packed columns

are no channels with clearly defined walls. However the concepts of tortuosity and constriction as applied to diffusion are still relevant if we define a diffusion path in an analogous way to a stream line in a flowing fluid. We define a "diffusion path" as a path through the column which is always in the direction of the maximum concentration gradient and consequently normal to successive surfaces of equal concentration. Such diffusion paths give the direction of bulk diffusion although any given molecule will not follow such a path. These diffusion paths are analogous to stream lines, which are normal to isobaric surfaces, but they do not coincide with them. Whereas stream lines will generally pass around porous particles, diffusion paths may pass through them as well as around them (*2*). The diffusion paths in a packed bed will inevitably be tortuous and any bundle of such paths will be successively constricted and expanded so that their envelope will, in broad terms, be similar to the tube shown in Figure 1.

CALCULATION OF γ—MODELS

To calculate γ simple regular models must be devised and we confine ourselves here to models based upon spheres of equal size. Boyack and Giddings (*4*) consider, among other models, a regular array of spheres in cubical boxes, each box containing a single sphere. This arrangement (Figure 2*A*) has a minimum porosity of 0.477 when the spheres are touching. This compares with a porosity of 0.26 for closest packing and 0.38 for random packing of spheres. Although the model is probably adequate for very porous media it is inadequate for the closely packed structures used in gas chromatography.

A model bearing more resemblance to a packed column is a round tube of radius R containing a single row of touching spheres of radius r (Figure 2*B*); this has a minimum porosity of 0.333 when $r = R$. However, in this configuration the model is impervious to gas, and for $e \approx 0.4$ it can bear little resemblance to a randomly packed column. Nevertheless this model has the merit that it can be precisely constructed and can be used to test predictions quantitatively.

A more realistic model (Figure 2*C*) may be constructed from 2*B* by imagining slightly deformable hemispheres to be attached to the walls of the tube in circles around the points of contact of the central row. In the porosity range 0.35 to 0.45, this arrangement probably gives a reasonable approximation to a randomly packed bed when 5 or 6 hemispheres are arranged around the central row.

CALCULATIONS

(1) Tortuosity. The tortuosity is difficult to calculate precisely. Boyack and Giddings (*4*) used an approximate method illustrated in Figure 3*A*. Molecules starting inside the area A, which is the axial projection of the particle profile on the end wall of the box, first move axially to the surface of the particle, then find the shortest way around the particle to rejoin the original axial line along which they then proceed out of the box. Molecules initially outside A go straight through the box. The authors point out that this approximation probably gives quite a good measure of T since paths starting inside A are assumed too long while those starting outside A are assumed too short. The treatment leads to a linear relation between tortuosity and occupancy (occupancy, $\theta = 1 -$ porosity), and for models 2*A* and 2*B* gives

$$T = 1 + 0.178\theta \qquad (14)$$

However both arrangements are unduly ordered since there are straight paths through the bed. In a randomly packed bed all paths are more or less tortuous and the factor 0.178 is almost certainly too small.

For the more highly packed arrangements the tortuosity may be considered by reference to Figure 3*B* representing close packed spheres through which there are no straight paths. The shortest and longest paths have tortuosities of 1.19 and 1.33, respectively. The occupancy of the arrangement is 0.74 and if a linear relationship between tortuosity and occupancy is assumed we obtain the two extreme equations

$$T = 1 + 0.26\theta \text{ and } T = 1 + 0.45\theta \qquad (15)$$

It seems likely that the majority of paths will be closer to the first than the second and on equation

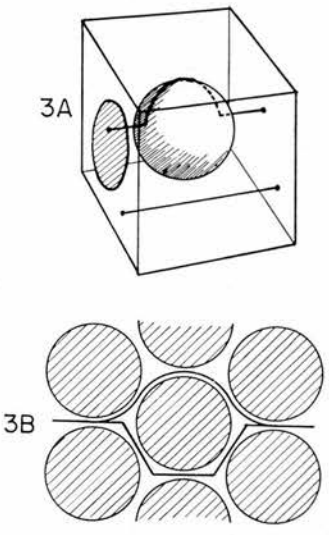

Figure 3. Illustration of tortuosity for different models of packed columns

$$T = 1 + 0.33\theta \qquad (16)$$

has been arbitrarily selected.

(2) Constriction. The constriction factor for model 2*A* has been worked out (*4*) and the dependence of C on porosity is shown along with other data in Figure 4.

In model 2*B* the unoccupied cross-sectional area a distance x from the center of any sphere in the central row is

$$A_x = \pi(R^2 - y^2) = \pi(R^2 - r^2 + x^2) \qquad (17)$$

and the mean area is

$$\bar{A} = \pi(R^2 - 2r^2/3) \qquad (18)$$

Insertion of Equations 17 into 12 and integration from 0 to r gives

$$C = \frac{\sqrt{\rho^2 - 1}}{(\rho^2 - \frac{2}{3}) \tan^{-1}\sqrt{\rho^2 - 1}} \qquad (19)$$

where $\rho = R/r$. The values of C, T^{-2} and $\gamma = CT^{-2}$ for various values of ρ are shown in Figure 5; values as a function of porosity are shown in Figure 4.

For model 2*C* with n hemispheres around the central row the free cross-sectional area a distance x from any point of contact on the axis, and the average area are, respectively,

$$A_x = \pi\left[R^2 - \frac{n}{2}r^2 + \frac{1}{2}(n+2)x^2 - 2rx\right] \qquad (20)$$

$$\bar{A} = \pi\left[R^2 - \frac{1}{3}(n+2)r^2\right] \qquad (21)$$

The integrated expressions for C are cumbersome but of a similar form to Equation 19, and for porosities above

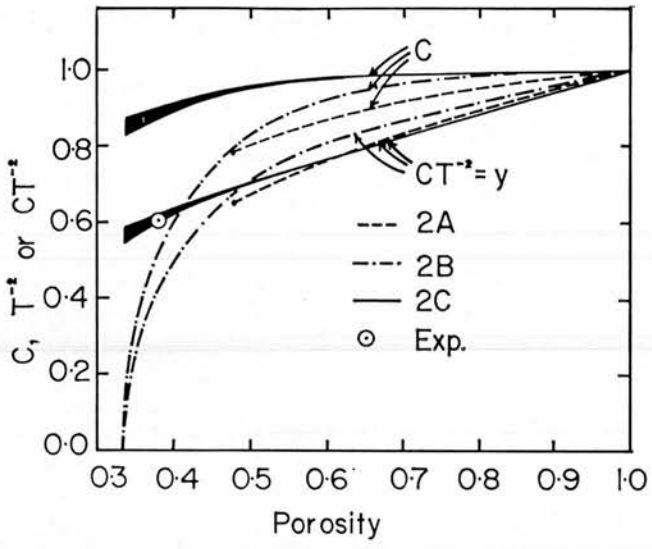

Figure 4. Variation of constriction and obstructive factors with porosity for different models of packed columns

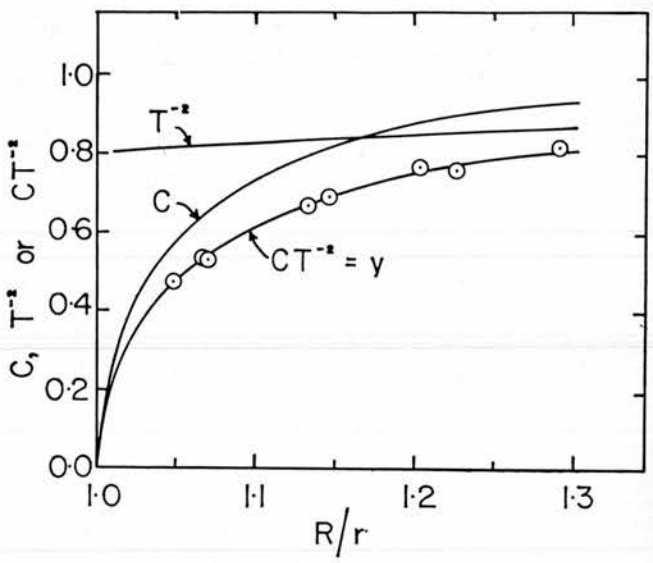

Figure 5. Variation of obstructive parameters for model 2B: comparison with experimental data

0.36 there is little to choose between the calculated values for five and six hemispheres around the central row. Values of C, and CT^{-2} are plotted against e in Figure 4; for $e = 0.38$ it is predicted that $\gamma = 0.63$. It is interesting to note that for high porosities all models give roughly the same value of γ, in spite of the fact that the constriction factor is much more important for the more regular models $2A$ and $2B$ than for the more random model $2C$.

EXPERIMENTAL

In all experiments 0.002-ml. samples of ethylene were eluted in nitrogen from nonsorbing columns at 18° C. and 750 mm. of Hg pressure. The injector was designed to be as free as possible from unswept dead volumes so as to ensure sharp injection. It consisted of a $^3/_{16}$-inch diameter steel rod with two transversely drilled holes about $^1/_2$ inch apart. The rod could move inside a closely fitting Teflon sleeve which was itself held in a tightly fitting steel tube. The two holes in the rod were positioned opposite holes in the sleeve so that sample gas could be passed through one hole while carrier gas passed through the other. On activating a solenoid by depressing the inject switch, the sample hole was brought into the carrier gas line and a sample injected.

The concentration profiles of the peaks could be observed on a $^1/_4$-second Brown recorder, which could be run at a speed of 12 inches per minute. Within the limits of the recorder the peaks were always symmetrical. Peak widths were obtained by dividing the peak areas measured with an electronic integrator, by the peak heights measured with the recorder. Both instruments were linear to better than 1%. The standard deviation was calculated from the formula $\sigma_t = \sqrt{(2\pi)}$ (area/height). The time of passage of the peak from injector to detector was measured by a timer which started when the inject switch was depressed and stopped at peak maximum. Detection was by a flame ionization detector of the Desty design (*6*). Its output was fed to an electrometer which had a time constant of 0.01 second and current ranges from 10^{-10} to 10^{-8} ampere; within this range the detector was linear.

The gas line connections are shown in Figure 6. Particular care was taken to eliminate any unswept dead volumes in the direct line between the injection and detector. In agreement with Kieselbach (*14*) we found it essential to terminate the packed columns with gauze screens not glass wool plugs to avoid an undesirably large instrumental spread and peak asymmetry. Details of the more important connections are shown in the insets to Figure 6. To avoid residual adsorption by the supports, the firebrick (Molar Products, Colchester, Fosalsil No. 6) and Celite (Gas Chromatography Ltd.) were silanized either with dichlorodimethylsilane or hexamethyldisilazane.

A typical experiment was carried out as follows. An ethylene sample was injected into the column and eluted in

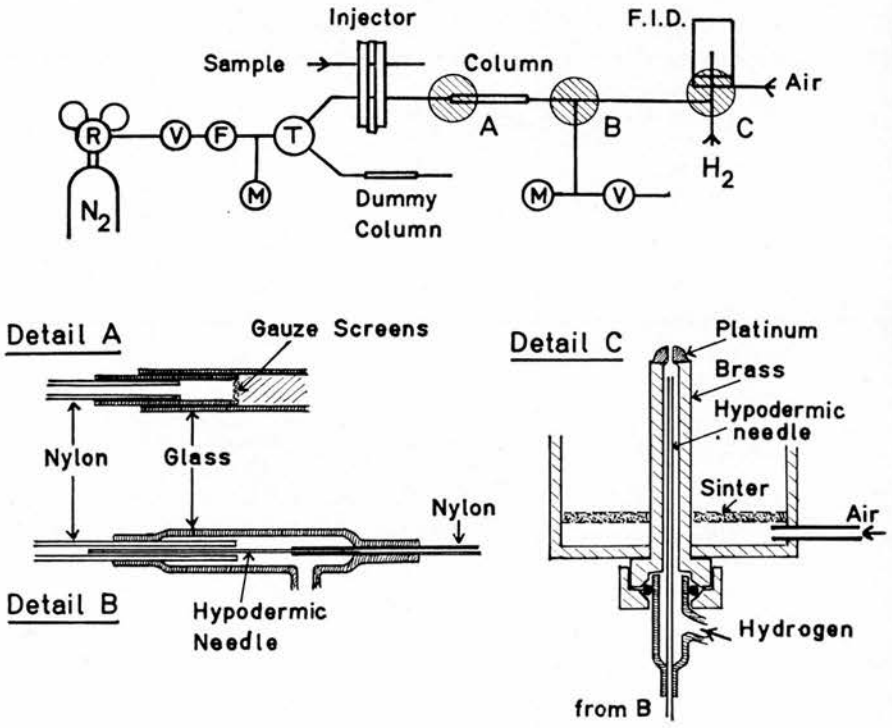

Figure 6. Gas line and details of important connections

R = two-stage reducing valve and pressure regulator, *V* = needle valve, *F* = flow meter, *M* = manometer, *T* = two-way tap, F.I.D. = flame ionization detector
A, *B*, and *C* refer to detailed connections shown in lower part of figure

the normal way without arresting the gas flow. The time of passage along the column, t_a, was calculated from the total time elapsing between injection and detection and from the volumes of the column and the ancillary tubing. The latter was always less than 3% of the column volume. The outlet velocity, u_o, was obtained from $u_{av} = l/t_o$ by applying the James-Martin pressure correction factor, knowing the pressure drop across the column. For all results reported here the pressure corrections were less than 2%. The values of u_o and t_a were checked by direct measurement of the volume flow rates and the gas phase volumes of the columns.

The volumes of the empty tubes were determined by filling them with water or mercury and weighing the liquid. The total porosities, e, of the packed columns were determined with a Toepler pump using ethylene and nitrogen; identical values of e with the two gases were taken to indicate absence of residual adsorption. The total porosities obtained for glass beads, firebrick, and Celite were, respectively, 0.38, 0.80, and 0.88. On treating the firebrick with 20% w./w. of urea formaldehyde resin polymerized in situ, the porosity was reduced to 0.73. The high total porosities of firebrick and Celite indicate that the particles themselves are highly porous since the interstitial porosity (measured say with mercury) is about 0.4 for both supports. Microscopic examination of thin sections of the supports mounted in synthetic resin confirmed this and showed that the Celite possessed a very open structure. The bulk densities of packed Celite and firebrick are, respectively, 0.25 and 0.45. Hence the density of the solid matter in the supports is about 2.2 which compares well with 2.6, the density of quartz, the main component of diatomaceous earths. These results agree with those of Bohemen and Purnell (*3*).

To study static spreading in a particular column a band of ethylene was eluted about half way along the column at the linear flow rate used in the continuous elution experiment. The flow was then switched to a dummy column of equal resistance (Figure 6) by turning the two way tap, T, placed upstream of the injector. After a delay of 1 to 20 minutes the flow was reconnected to the column and the peak eluted. From the data so obtained a plot of σ_t^2 against t could be drawn up and the real or apparent diffusion coefficient derived.

The procedure was satisfactory provided that the pressure drop, Δp, across the column during elution was low. With large pressure drops the gas velocity did not reach its stationary value before the peak was eluted; thus σ_t was overestimated and an excessively high value of the diffusion coefficient was obtained. The effect was demonstrated directly by using nitrogen slightly contaminated with an organic vapor as the carrier gas. The recorder deflection then measured the flow rate directly. With Δp = 2 cm. of Hg the deflection reached at least 99% of its stationary value before the peak was eluted, but with larger pressures this was not so and erroneous results were obtained.

RESULTS AND DISCUSSION

According to Equations 3 and 4, plots of σ_t^2 against t should be straight lines whose gradients give real or apparent diffusion coefficients. A typical plot is shown in Figure 7 for an empty nylon tube. Equally reproducible data were obtained with the other columns studied and the values of D_g and γ quoted in Table I are probably accurate to about 2%.

Three sets of experiments were carried out with open tubes of two different diameters and at different flow rates. They yielded a mean value of D_g = 0.165 sq. cm second^{-1} for ethylene in nitrogen with a spread of 0.002 sq. cm. second^{-1}. This value agrees well with the value of D_g = 0.16 ± 0.01 sq. cm. second^{-1} obtained from *HETP* measurements on unsorbed peaks in open tubes (*15*), and with the value of 0.163 sq. cm. second^{-1} quoted by Reid and Sherwood (*19*).

Using glass beads 0.50 mm. in diameter in two tubes of different diameters the obstructive factor was 0.60 ± 0.02. This value was confirmed using beads 0.275 mm. in diameter and is in agreement with a value of 0.7 ± 0.1 obtained from *HETP* measurements on unsorbed peaks in glass bead columns (*15*). With firebrick and Celite the values were, respectively, 0.46 ± 0.01 and 0.74 ± 0.02. These values for typical ga

Table I. Values of D_g and γ for Various Columns

Columns at 18° C. and 750 mm. of Hg Pressure

Column No.	Material or packing	Length, cm.	Tube diam., mm.	Particle diam., mm.	Mesh ASTM	Tube diam. / Particle diam.,	Total porosity	u_o, cm./sec.	D_g or γD_g, sq. cm./sec.	γ
				OPEN TUBES						
1	Nylon	1640	0.88					28.8	0.164	Unity
2	Nylon	693	1.48					13.4	0.164	Unity
3	Nylon	834	0.88					26.2	0.166	Unity
				PACKED TUBES						
4	Glass beads	152	5.7	0.50		11.4	0.38	4.9	0.102	0.62
5	Glass beads	152	3.0	0.50		6.0	0.38	7.4	0.096	0.58
6	Glass beads	79	6.4	0.275		23.3	0.38	2.40	0.102	0.62
7[a]	Firebrick	79	6.4		25–35	11[g]	0.80	3.63	0.077	0.47
8[a]	Firebrick	79	6.4		35–45	15	0.80	2.87	0.075	0.46
9[b]	FB + UFR	79	6.4		25–35	11	0.73	3.65	0.073	0.45
10[c]	Celite	72	5.6		35–45	13	0.88	3.46	0.125	0.76
11[d]	Celite	74	5.7		80–100	35	0.88	1.80	0.119	0.72
				MODEL 2B						
12	BB[e]	74	4.16	3.97		1.047	0.392	4.20	0.078	0.48
13	PVC[f]	144	6.28	5.90		1.065	0.413	5.82	0.088	0.54
14	PVC[f]	151	5.20	4.87		1.070	0.417	8.50	0.088	0.54
15	BB	106	6.28	5.55		1.132	0.479	4.90	0.110	0.67
16	PVC	148	6.75	5.90		1.145	0.491	4.41	0.113	0.69
17	PVC	152	5.90	4.87		1.210	0.537	7.80	0.126	0.77
18	PVC	144	6.28	4.87		1.290	0.598	4.25	0.134	0.82

[a] Firebrick silanized with dichlorodimethylsilane.
[b] Firebrick coated with 20% (w./w.) of urea–formaldehyde resin polymerized in situ.
[c] Celite silanized with dichlorodimethylsilane.
[d] Celite silanized with hexamethyldisilazane.
[e] BB are steel ball bearings.
[f] PVC are polyvinylchloride spheres of 2% diameter range.
[g] Tube diameter/mesh opening.

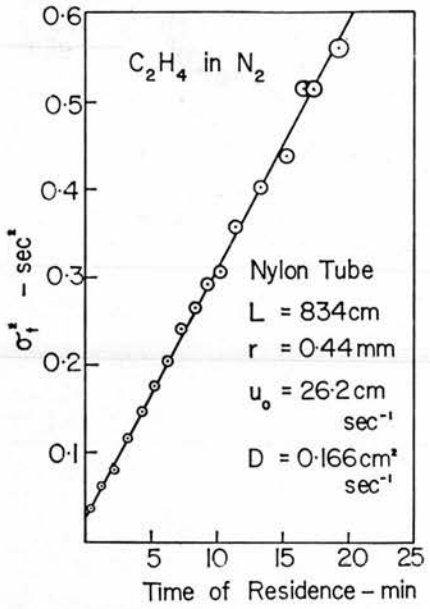

Figure 7. Change of variance with residence time

chromatographic packings show that γ is well below unity and is not the same for all supports. These results agree with previous experimental values determined by continuous elution experiments (*1*, *3*, *12–18*).

The value of γ for glass beads is plotted in Figure 4 and agrees excellently with that predicted from model 2*C*. This agreement is, however, largely fortuitous because the calculated value rests heavily on the value assumed for the tortuosity. It nevertheless appears necessary to consider both tortuosity and constriction to explain a value as low as 0.60. More convincing evidence of the reality of the constriction effect comes from the experiments carried out with model 2*B*. The values of γ obtained for columns containing a single row of spheres in a round tube are listed in Table I and plotted in Figure 5. The agreement between the experimental and the calculated values is most satisfactory. Since the tortuosity varies only slightly with ρ, it is clear that with this model the major reason for the change in obstructive factor is the variation in the constriction.

The values of γ for firebrick columns are lower than those for the glass bead columns although the porosity of firebrick is much higher. It is clear that none of the models considered predict such low values in the porosity range near 0.8.

The situation with porous supports might resemble that in a sorbing column, for which the rate of spreading would be

$$d\sigma_t^2/dt = 2\gamma D_g/(1 + k)u_o^2 \qquad (24)$$

where u_o is the band velocity, $u_o = f/[A_o e(1 + k)]$, and k = column capacity ratio. If the molecules of the gas within the particles are effectively immobile and exchange only slowly with those in the interstitial gas space—i.e., D_g within the particles is much lower than D_g in free gas—the rate of spreading would be given by Equation 24 with k equal to the ratio of gas within the particles to gas in the interstitial space, that is $k = 1$ for firebrick or Celite. The apparent obstructive factor, as measured by the arrested elution method, would then be $\gamma' = \gamma/(1 + k)$, and might be expected to be about 0.3. This is lower than the value of 0.45 obtained for firebrick and much lower than 0.74 obtained for Celite. Hence the hypothesis that D_g within the particles is very low must be unsound. There is indeed no reason to believe that the diffusion coefficient within porous particles differs from that outside, since diffusion, unlike flow, is not restricted by the narrowness of the channels within which it occurs (*2*).

It is therefore necessary to consider the construction and tortuosity of the average diffusional paths within and without the particles. The parts of the paths through the interstitial gas are tortuous, and if the particles were nonporous, T would be about 1.20. Superimposed upon this tortuosity is the tortuosity of the paths through the particles themselves which will wind much more sharply than those through the interstitial gas (Figure 8). Thus the overall tortuosity might be increased above that expected for solid particles, and given by

$$T = T_e[(l - l_i) + T_i l_i]/l \qquad (25)$$

where T_e = tortuosity of smooth paths through the bed, T_i = tortuosity of the paths within the particles, l_i = length of that part of a smooth path which passes through the particles (broken line) and l = total length of a smooth path (broken line + full line in interstitial gas).

Since the interstitial porosity is about 0.4 and the total porosity about 0.8, the porosity of the particles themselves is about $^2/_3$. Thus $T_i = 1.11$ (Equation 16). If we assume that 60% of the total length of a diffusion path is through the particles and 40% outside then $T = 1.20 \times 1.07 = 1.28$. If the constriction is unaltered, $\gamma = 0.55$. Thus the net effect of the particles being porous is to reduce γ by about 15%. This is not quite sufficient to account for the difference between the obstructive factor in glass beads and firebrick but it is of the correct order.

Celite on the other hand gives $\gamma = 0.74$ and here it seems that the smooth diffusion paths through the bed must be almost straight and that the main source of obstruction arises in the porous particles themselves. This is in accord with the extremely high porosity of Celite, the occupancy being only 0.12 compared to 0.20 for firebrick.

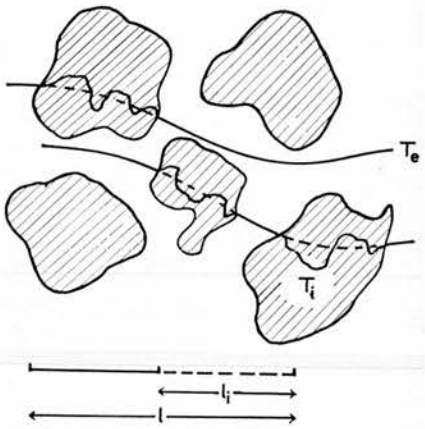

Figure 8. Illustration of interstitial and intraparticle tortuosity

ACKNOWLEDGMENT

The authors thank the British Petroleum Co., Ltd. for a maintenance grant to L. M., and Bruce Peebles Ltd. (Edinburgh) for the provision of the electronic equipment.

LITERATURE CITED

(1) Berge, P. C., Haarhoff, P. C., Pretorius, V., *Trans. Faraday Soc.* **58,** 2272 (1962).
(2) Berge, P. C., Pretorius, V., ANAL. CHEM. **36,** 693 (1964).
(3) Bohemen, J., Purnell, J. H., *J. Chem. Soc.* **1961,** p. 360.
(4) Boyack, J. R., Giddings, J. C., *Arch. Biochem. Biophys.* **100,** 16 (1963).
(5) Carberry, J. J., Bretton, R. H., *J. Chem. Phys.* **35,** 2241 (1961).
(6) Desty, D. H., Geach, C. J., Goldup, A., "Gas Chromatography," R. P. W. Scott, ed., p. 46, Butterworths, London, 1960.
(7) Fejes, P., Czaran, L., *Acta Chim. Acad. Sci. Hung.* **29,** 171 (1961).
(8) Giddings, J. C., ANAL. CHEM. **35,** 439 (1963).
(9) Giddings, J. C., Seager, S. L., *Ind. Eng. Chem. Fundamentals* **1,** 277 (1962).
(10) Giddings, J. C., Seager, S. L., *J. Chem. Phys.* **33,** 1579 (1960).
(11) *Ibid.*, **35,** 2242 (1961).
(12) Glueckauf, E., "Gas Chromatography," D. H. Desty, ed., p. 33, Butterworths, London, 1958.
(13) Kieselbach, R., ANAL. CHEM. **33,** 23 (1961).
(14) *Ibid.*, p. 806.
(15) Knox, J. H., McLaren, L., *Ibid.*, **35,** 449 (1963).
(16) Littlewood, A. B., "Gas Chromatography," D. H. Desty, ed., p. 23, Butterworths, London, 1958.
(17) Norem, S. D., ANAL. CHEM. **34,** 40 (1962).
(18) Perrett, R. H., Purnell, J. H., *Ibid.*, **35,** 430 (1963).
(19) Reid, R. C., Sherwood, T. K., "Properties of Gases and Liquids," p. 275, McGraw-Hill, New York, 1958.
(20) Seager, S. L., Geertson, L. R., Giddings, J. C., *J. Chem. Eng. Data* **8,** 168 (1963).
(21) Taylor, Sir G., *Proc. Roy. Soc.* (*London*) **A219,** 186 (1953).

RECEIVED for review February 3, 1964. Accepted April 24, 1964. Presented at 2nd International Symposium on Advances in Gas Chromatography, University of Houston, Houston, Texas, March 23–6, 1964.

PRINTED IN U. S. A.